공학박사학위논문

Theory of Disturbance Observers: A New Perspective on Inverse Model-based Design

외란 관측기 이론 : 역동역학 기반 설계에 대한 새로운 관점

2018년 2월

서울대학교 대학원

전기컴퓨터공학부

박 경 훈

ABSTRACT

Theory of Disturbance Observers: A New Perspective on Inverse Model-based Design

by

Gyunghoon Park

Department of Electrical and Computer Engineering
College of Engineering
Seoul National University

February 2018

The problem of compensating model uncertainty and external disturbance in control systems is one of long-standing and critical issues in academia and industry. Among several promising solutions to the problem, the disturbance observer approach has gained a particular attraction in the literature, due to its structural simplicity and powerful ability. This dissertation presents new theoretical results on the inverse-model based disturbance observers, in order to overcome the limitation of the existing disturbance observer approaches and to address several problems which modern control systems have encountered. Specific subjects dealt with in the dissertation are listed as follows:

- The recovery of nominal performance is a key feature of the inverse model-based disturbance observers. It is remarkable that this property is generically an approximation, mainly because structural information of disturbance is not explicitly employed in the disturbance observer design. Motivated by the internal model principle, in the first part of this dissertation we propose a new disturbance observer into which a generating model of disturbance is embedded. Unlike those in the existing works, the proposed disturbance observer achieves "asymptotic" (rather than approximate) recovery of nominal performance in a sense of input-to-state stability. As a further research in this direction, we also find out that the asymptotic recovery of nominal performance is still possible even without exact knowledge on the frequencies of the sinusoidal disturbance, by realizing the internal model to be embedded in an adaptive fashion with a frequency identifier.

- Modern control systems have often experienced not only persistent disturbances and model uncertainty, but also sudden faults of systems and actuators. Even though various fault-tolerant control schemes have been proposed to tackle the problem, guaranteeing satisfactory tracking performance under faults has been not fully studied yet. As another contribution of the dissertation, we propose a disturbance observer-based fault-tolerant controller that guarantees a "fault-free" tracking performance for the entire period (including the moment when an actuator fault occurs). By reminding that the disturbance observer approach is commonly applied to minimum phase systems, the underlying idea is to redefine a virtual input from the redundant control inputs such that the composite system from the virtual input to the output remains of minimum phase under any actuator faults. This work is in fact an extension of the disturbance observer for a larger class of systems that have more inputs than outputs, while the conventional disturbance observer scheme is mostly designed for "square" systems (that is, systems that have the same numbers of inputs and outputs).

- While a physical plant is a continuous-time system, control schemes are usually implemented in discrete time. The mixture of continuous- and discrete-

time components introduces some distinctive characteristics of the sampled-data systems, which possibly incurs unexpected situations when a discrete-time disturbance observer is employed for the sampled-data system. In the dissertation, a theoretical analysis of the discrete-time disturbance observer is newly provided in the sampled-data setting. In particular, by focusing on the limiting behavior of the overall system as the sampling period goes to zero, we obtain a "necessary and sufficient condition" for the robust stability under fast sampling. One important finding from our approach is that the discrete-time "sampling zeros" of the sampled-data model may hamper stability (even regardless of model uncertainty) when these zeros are not carefully taken into account in the disturbance observer design. Based on the stability analysis, we also present systematic design guidelines of the discrete-time disturbance observer to satisfy the stability constraint under arbitrarily large (but bounded) model uncertainty, and at the same time to embed a disturbance model (if available) into the discrete-time disturbance observer structure.

- With increased interests in these days, the security of cyber-physical systems has been dealt with in the literature from a control-theoretical point of view. In the last part of this dissertation, we address the problem of constructing a "robust stealthy attack" that compromises uncertain cyber-physical systems having unstable zeros. It has been well known that the conventional zero-dynamics attack, a systematic stealthy attack to non-minimum phase systems, is easily detected as long as (even small) model uncertainty exists. Different from the conventional approach, our key idea is to isolate the real zero-dynamics from the plant's input-output relation and to replace it with an auxiliary nominal zero-dynamics; as a result, this alternative attack does not require the exact model knowledge anymore. We show in this dissertation that all this can be realized by the disturbance observer, which now serves as an attack generator. This work explains the underlying principle of destabilizing phenomenon when the inverse model-based disturbance observer is applied to the non-minimum phase plants carelessly.

Keywords: disturbance observer, internal model principle, nominal performance recovery, robust control, sampled-data system, cyber-physical system
Student Number: 2013–30235

격려와 사랑으로 응원해주신 모든 분들께
본 논문을 바칩니다.

Contents

List of Tables

List of Figures

Symbols and Acronyms

$\mathbb{R}$	field of real numbers
$\mathbb{C}$	field of complex numbers
$\mathbb{R}^n$	Euclidean space of dimension n
$\mathbb{R}^{m\times n}$	space of $m \times n$ matrices with real entries
$\mathrm{Re}(s)$	real part of a complex number s
$\mathrm{Im}(s)$	imaginary part of a complex number s
$[m]$	$:= \{1, 2, \ldots, m\}$
$\mathbb{R}_{>0}$	set of positive real numbers
I_n	$n \times n$ identity matrix
0_n	$n \times 1$ column vector having all elements equal to 0
$O_{m\times n}$	$m \times n$ matrix having all elements equal to 0
$\mathrm{diag}(a_1, \ldots, a_k)$	diagonal matrix whose i-th diagonal is a_i
$\mathrm{blockdiag}(A_1, \ldots, A_k)$	block diagonal matrix whose i-th block diagonal is A_i
$2^{\mathcal{A}}$	power set of a set $\mathcal{A}$
$\overline{\lambda}(A)$	the maximum eigenvalue of the matrix $A \in \mathbb{R}^{n\times n}$
$\underline{\lambda}(A)$	the minimum eigenvalue of the matrix $A \in \mathbb{R}^{n\times n}$
$[a; b]$	$:= [a^\top, b^\top]^\top$ for two column vectors a and b
$\|a\|$	$:= \sqrt{a^\top a}$ for a vector $a \in \mathbb{R}^n$

$\|A\|$	$:= \sqrt{\overline{\lambda}(A^\top A)}$ for a matrix $A \in \mathbb{R}^{m\times n}$
$\mathfrak{C}^i$	i-th times continuously differentiable
$\mathcal{L}(x(t))$	Laplace transform of $x(t)$
$\mathcal{F}(x(t))$	Fourier transform of $x(t)$
$\mathcal{Z}(x[k])$	$\mathcal{Z}$-transform of $x[k]$
$\mathrm{dist}(\mathcal{A}, \mathcal{B})$	$:= \inf_{a\in\mathcal{A}, b\in\mathcal{B}} \|a - b\|$ for two sets $\mathcal{A} \subset \mathbb{R}^n$ and $\mathcal{B} \subset \mathbb{R}^n$
$\mathcal{E}(a, b)$	line segment in the complex plane connecting the points $-(1/a) + j0$ and $-(1/b) + j0$ (for two real numbers a and b)
$\mathcal{D}(a, b)$	closed disk in the complex plane whose diameter is $\mathcal{E}(a, b)$ (for two real numbers a and b)
$\partial\mathcal{A}$	boundary of a set $\mathcal{A}$
$\forall$	for all
$\Diamond$	end of theorems, lemmas, propositions, assumptions, remarks, and so on
$\square$	end of proof

- A square matrix A is said to be Hurwitz (matrix) if every eigenvalue λ of A has strictly negative real parts, i.e., $\mathrm{Re}(\lambda) < 0$.
- For any state variable $x(t)$, its initial condition will be denoted by $x(0)$.
- In order to messy notation, the time symbol t is omitted when there in no confusion.
- For two sets $\mathcal{A} \subset \mathbb{R}^n$ and $\mathcal{B} \subset \mathbb{R}^n$ and a positive real number ϵ, we use $\mathcal{A} \overset{\epsilon}{\sqsubset} \mathcal{B}$ if $\mathcal{A} \subset \mathcal{B}$ and $\inf_{a\in\partial\mathcal{A}, b\in\partial\mathcal{B}}\{\|a - b\|\} > \epsilon$ where $\partial\mathcal{A}$ and $\partial\mathcal{B}$ indicate the boundary of $\mathcal{A}$ and $\mathcal{B}$, respectively, and $\mathcal{A} \sqsubset \mathcal{B}$ if there exists $\epsilon > 0$ such that $\mathcal{A} \overset{\epsilon}{\sqsubset} \mathcal{B}$.
- For simplicity, we often use I_n, 0_n, and $O_{m\times n}$ without subscripts if their dimensions are obvious.

Acronyms

LTI	Linear time-invariant
SISO	Single-input single-output
MISO	Multi-input single-output
DOB	Disturbance observer
CT	Continuous-time
DT	Discrete-time
CT-DOB	Continuous-time disturbance observer
DT-DOB	Discrete-time disturbance observer
CPS	Cyber-physical system

Chapter 1

Introduction

1.1 Research Background

1.1.1 Overview of Researches on Disturbance Observers

As Brockett says in his essay [Bro01], "If there is no uncertainty in the system, the control or the environment, feedback control is largely unnecessary". The problem of compensating internal model uncertainty and external disturbance would be one of the central and long-standing issues in the control theory. Moreover, this is an ongoing challenge in our era where modern control systems become more complicated and thus introduce a variety of sources of uncertainty and disturbance. In this context, a tremendous amount of research efforts have been paid during the last several decades to resolve the problem of robust control design [PT14, Saf12, Kwa93], including $\mathcal{H}_2/\mathcal{H}_\infty$ controller [Kwa93, ZD96], sliding mode controller [SEFL14, Utk92], robust output regulator [SI00, Hua04], to name just a few.

As a possible direction of research for ensuring the robustness of the control system, the disturbance observer (DOB) scheme has gained a lot of interest in these days [LYCC14, SPJ$^+$16, CYGL15]. The underlying philosophy of the DOB approach is, as the name implies, to "explicitly" estimate the effect of the uncertain quantities using the measurement signals and the (maybe imperfect) structural information on the plant. Compared with other existing solutions, this idea offers a quite intuitive way of disturbance attenuation; e.g., to simply subtract the estimate of uncertain quantities into the original control input (Figure 1.1).

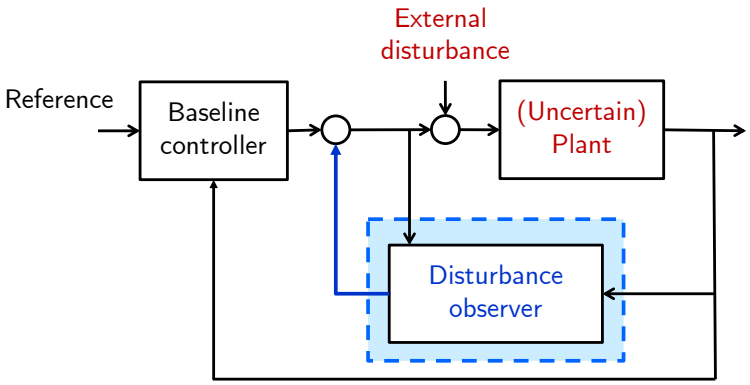

Figure 1.1: General concept of DOB approach

The inherent advantages have motivated researchers to develop several types of DOBs, a large part of which can be classified into the following three categories:

- **Internal model-based design**:

  Provided that the external disturbance is generated by a certain "exogenous" system, a natural method for its estimation (from the viewpoint of the internal model principle [FW76]) would be to utilize the knowledge on the disturbance model into the DOB design. As a pioneering work in this direction, Johnson [Joh71, Joh76, Joh08] introduced a solution of the robust output regulation based on the estimation of the modeled disturbance, named *disturbance accommodation control*. The central idea of his work is to augment the disturbance model into the system model, upon which classical observer techniques can be employed (with some modification). This in turn led to the invention of the *unknown input disturbance observer* [PVM90, SvD02], a variant of the traditional unknown input observer with disturbance model. More recently, Chen and his colleagues proposed yet another nonlinear DOB to deal with a class of nonlinear systems under a polynomial-in-time disturbance (i.e., $d(t) = \mathsf{d}_0 + \mathsf{d}_1 t + \cdots + \mathsf{d}_k t^k$ with constants d_i) [CBGO00, CYGL15, GC05, Che04, YLC12]. While the exact expression on the disturbance must be dependent of high-order time derivatives of the plant state, the authors in [CBGO00] employed an alternative

observer for an auxiliary variable (rather than the disturbance itself) whose dynamics is implementable only with state variables. This technique was initially proposed by assuming that the full state variables are available, and in turn an extension to the output feedback case was introduced in [Che04]. Another work on the internal model-based design can be found in [KRK10, KR13] where a reduced order DOB was constructed based on the frictional observer scheme. It is important to note that most of the previous works in this category were interested in the "asymptotic" estimation and compensation of the disturbance, at the cost of using the "full" structural information on both disturbance and plant models.

- **Inverse model-based design**:

  Without using exact model knowledge on the disturbance, an alternative way of estimating the disturbance is to compare the control input (generated by a baseline controller) with its "estimate", where the latter is obtained by passing the plant output through the "inverse dynamics of a nominal plant model". Roughly speaking, the disparity can be interpreted as a "quantitative expression" of model uncertainty and disturbance, in the sense that the signal will be vanished as long as there is no uncertain factor in the environment. (From this standpoint, we call this lumped signal as *total disturbance*). This is the main philosophy of the inverse model-based designs in the literature. A basic configuration of the inverse model-based DOB is depicted in Figure 1.2. It is seen in the figure that a low-pass filter $\mathrm{Q}(s;\tau)$ (called *Q-filter*) is additionally attached in the DOB loop. This is mainly for the realization of the idea, and the Q-filter plays an essential role in the stability and performance of the closed-loop system.

  Since the first report on the inverse model-based DOB design in [NOM87], several theoretical results on the robust stability analysis and design guidelines have been presented for the last three decades. When it comes to the stability analysis, the small gain theorem has been widely used as a mathematical tool [WT04, YCC05, KC03, UH91]. Yet since the small gain theorem takes into account only the amplitude of the system response, it

may provide a conservative consequence in a sense. In this context, alternative approaches have been performed in the literature. As an example, the authors of the works [SO12, GG01] employed the concept of the structured singular value in their analysis, by focusing mainly on the structural uncertainty of the plant. This allows to avoid a conservative design of the Q-filter. On the other hand, the equivalence between the DOB structure and the other control schemes, such as the unknown input disturbance observer and the adaptive observer, was exploited in [SvD02, BT99], by which the stability of the DOB structure is analyzed indirectly. In [CCY96], Choi et al. presented a $\mathcal{H}_\infty$ framework for the stability analysis of the DOB structure, based on the factorization approach. Moving away from the frequency domain analysis, Shim and Joo [SJ07] proposed a state space approach from the viewpoint of the singular perturbation theory. In particular, the work [SJ07] pointed out that enlarging the bandwidth of the Q-filter incurs the time separation of the overall closed-loop system so that the stability of the overall system is decomposed into that of the slow and fast subsystems. As a frequency domain counterpart of this approach, an almost necessary and sufficient condition for robust stability under large bandwidth of Q-filter was derived in [SJ09, JJS14]. On the other hand, it has been reported in [KPSJ16, SO13a] that the stability margin, a notion in the classical control theory, of the DOB controlled system is possibly increased as the bandwidth of the Q-filter gets larger.

In addition to the stability analysis, several design procedures of the Q-filter have been proposed based on the $\mathcal{H}_\infty$ framework [SWY14], the Bode and Poison integral formulas [SO13b], and the internal model principle [YKIH97, CT12, JPBS16]. Moreover, a particular attention was paid to the selection of the nominal model [KT13, CCKH16].

- **State extension-based design**:

  The works in this category follow the same philosophy of the inverse model-based designs above; that is, to estimate the total disturbance (instead of the disturbance itself) with no requirement on the disturbance model.

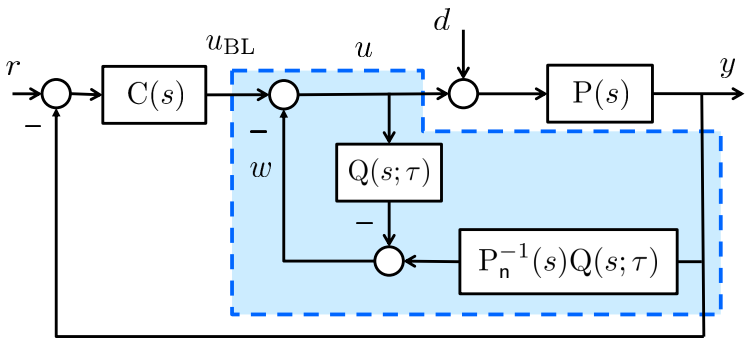

Figure 1.2: Basic configuration of inverse model-based DOB controlled systems: $\mathrm{P}(s)$, $\mathrm{P_n}(s)$, $\mathrm{C}(s)$, and $\mathrm{Q}(s;\tau)$ indicate the plant and its nominal model, baseline controller, and the Q-filter, respectively.

However, rather than utilizing the inverse model of the nominal plant in its structure, the strategy here is to "extend" the system dynamics by taking the time derivative of order larger than the relative degree of the plant as an "auxiliary" state variable. Then the problem of estimating the total disturbance can be recast to that of estimating the auxiliary state of the extended system dynamics, which can be solved by employing a high-gain observer (in an approximate fashion). This idea was originated from Han's work [Han09] under the name of *extended state observer*, and then inspires Khalil and his colleague to develop the control via *extended high-gain observer* [FK08, LMK16] At the same time, another composite control law on basis of this idea, called *active disturbance rejection controller*, has been also widely employed in these days [XH15, Gao14].

Based on the theoretical results, the DOB-based control techniques have been widely employed in industrial problems. Some remarkable applications of the DOB schemes include (but are not limited to): optical disk drives ([YCC05, RDC04, OMI+06, OSM96]), hard disk drives ([Xie10, Ats10]), position and force control of mechanical systems ([KC03, WT04, CLTT17, SO15, KKO07]), robot manipulators ([OC99, CBGO00, BT99, MMT17]), motor drives ([YCL+17]), autopilot design ([LY13]), and air-breathing hypersonic vehicles ([ALWW16])

1.1.2 Motivating Questions on Inverse Model-based Designs

In this dissertation, we are mainly interested in developing the theory of the inverse model-based DOB designs. In particular, our ultimate goal is to answer the questions listed below, which motivate the work of this dissertation.

- The ability of compensating the total disturbance allows the DOBs to recover the nominal tracking performance. Yet at the same time, this recovery is approximate in general. If so, can we recover nominal performance "asymptotically"?

- Most of the previous works on the inverse model-based design focused only on the square systems (i.e., the systems having the same number of inputs and outputs), while redundancy of the control input may exist in various control problems. In this situation, what benefits can we achieve by the DOB?

- As most of the modern control systems consist of physical plant and digital controller, the DOB scheme is often implemented in the DT domain with the help of sampler and zero-order holder. However, as reported in several experimental results, applying a discretization of a CT-DOB to the sampled-data system directly may not guarantee the stability of the closed-loop system in general. Then, what is a necessary and sufficient condition for robust stability of DT-DOB controlled system in the sampled-data framework?

- It has been investigated that the inverse model-based DOB under large bandwidth of the Q-filter must destabilize the closed-loop system when applied to non-minimum phase systems. In this case, is the recovery of nominal performance in the first bullet immediately broken (so that the instability of the system can be captured directly from the measurement output)?

1.2 Contributions and Outline of Dissertation

Chapter 2. Recovery of Nominal Performance in Asymptotic Sense: Part I - Embedding Internal Model into Disturbance Observer

In this chapter, we address the problem of recovering the nominal performance in "asymptotic" sense for uncertain minimum phase systems, provided that a part of the external inputs are generated by an exogenous system. As a solution for the problem, this work presents a new design methodology for the inverse model-based DOB based on the singular perturbation theory and internal model principle. The contents of this chapter is based on [PSJ] and the main contributions of this work is listed as follows:

- We propose a reduced-order type DOB in the state space, into which the generating model of the external inputs is embedded. The proposed DOB structure generalizes those in the relevant works [BS14, JPBS16].
- To the best of our knowledge, this is the first in the literature to handle the arbitrarily accurate recovery in transient period and the complete recovery in steady-state period at once.
- The asymptotic recovery of the nominal performance via the proposed DOB is analyzed by the Lyapunov analysis from the viewpoint of the singular perturbation theory. In particular, since the standard singular perturbation theory cannot capture the effect of the modeled inputs appropriately, we newly present a modified notion of the quasi-steady-state for the analysis.
- Systematic design guidelines for the DOB design that deals with (bounded but) arbitrarily large model uncertainty is presented.
- To verify the validity of the proposed scheme, we perform the simulation for the mechanical positioning system.

Chapter 3. Recovery of Nominal Performance in Asymptotic Sense: Part II - An Extension with Adaptive Internal Model

As an extension of the result in the previous chapter, in this chapter we tackle the same problem for linear mechanical systems, under a relaxed assumption that the frequency of the sinusoidal inputs is not exactly known. The contents of this work are presented in [PK17] and the main contributions of this work is listed as follows:

- To deal with the uncertain frequency of the sinusoidal input, we propose a new inner-loop controller by combining the DOB in Chapter 2 with a frequency identifier.

- Noting that the use of the frequency identifier introduces one additional time scale separation in the overall system, we analyze the performance recovery by transforming the overall system into a "multiple-time scaled" singular perturbation form.

- The proposed DOB-based controller is applied to track-following problem of the optical disk drives. Both simulation and experimental results are presented.

Chapter 4. Guaranteeing Almost Fault-free Performance from Transient to Steady-state: Disturbance Observer-based Fault Tolerant Control

The main purpose of this chapter is to construct an output feedback fault tolerant controller that guarantees almost "fault-free" tracking performance for the entire time period by following the DOB approach. A standing assumption for the controller design is that the plant has redundant inputs and they are possibly under floating or lock-in-place faults. The contents of this chapter are contained in [PS]. The contribution of this chapter is as follows:

- This work covers the problem of ensuring the satisfactory "transient" performance at the moment of actuator faults, which is still an ongoing research topic in the field of the fault tolerant control.

- We propose a new inverse model-based DOB design method when the number of inputs is larger than that of outputs, while only few works have dealt with this situation explicitly [CT14].

- Simulation for the fault tolerant control of Boeing 747 is performed.

Chapter 5. Stability, Performance, and Design of Discrete-time Disturbance Observer for Sampled-data Systems: A Fast Sampling Approach

In this chapter, we provide an analysis and design guidelines for the DT-DOB controlled sampled-data systems in the frequency domain. Particularly, an almost "necessary and sufficient condition" for robust internal stability of the DT-DOB closed-loop system is carried out, under a mild assumption that the sampling period is sufficiently small. It is briefly seen that the recovery of the nominal performance is still valid in the sampled-data framework. Some part of this chapter is based on [PJLS15, PS15]. The contribution of this work is:

- The result theoretically reveals that the sampling process indeed may hamper the stability of the overall system, while such an obstacle can be handled by constructing the DT-DOB appropriately.
- This work presents a "generalized" framework for the stability analysis, in the sense that linear systems with general order and a large class of discretized components are dealt with.
- Some rule-of-thumbs widely used in the DT-DOB designs are reinterpreted by the present analysis.
- Based on the analysis part, new design procedures for the DT-DOB with and without considering the disturbance model are proposed.

Chapter 6. Robust Zero-dynamics Attack on Uncertain Cyber-physical Systems: Malicious Use of Disturbance Observer

In this chapter, we address the problem of constructing a "robustly stealthy attack" policy (on the side of malicious adversary) when a cyber-physical system (CPS) is of non-minimum phase and is uncertain. While a traditional stealthy attack mimics the unstable zero dynamics of the plant and thus utilizes the full model knowledge, this work shows that another "robust" attack is enabled when the adversary employs the inverse model-based DOB as an attack generator. The main contents of this chapter are based on [PLS$^+$, PSL$^+$16], and its contribution is listed as follows:

- We reveal that the recovery of the nominal performance in the conventional DOB is maintained for a while even if the plant is of non-minimum phase

(and thus the system is internally unstable), which allows the new attack to remain stealthy robustly.

- A remarkable observation is that fatal attacks on CPS are possible without exact system knowledge, particularly when the adversary employs robust control techniques.

Chapter 2

Recovery of Nominal Performance in Asymptotic Sense: Part I - Embedding Internal Model into Disturbance Observer

Guaranteeing robust performance against model uncertainty and external disturbance is one of the long-standing issues on control systems. Nowadays, as of particular importance for precise control is the robust "transient" performance, the problem of recovering a (pre-defined) nominal output trajectory for the entire time period is gaining considerable attentions in the literature. Several promising approaches to achieving this nominal performance recovery (NPR), including extended high-gain observers [FK08, LMK16], disturbance observers (DOB) [BS08, BS14], active disturbance rejection controllers [XH15], and $\mathcal{L}_1$ adaptive controllers [CH08] have been concurrently developed just over a decade.

It is interesting that all these approaches, even though they were invented independently, share a common methodology for the NPR. In the previous works, the effect of external inputs (i.e., disturbances and references) and model uncertainty on the controlled system is represented as a lumped signal, so-called *total disturbance*, for whose estimation and compensation high-gain techniques are usually employed. Thus a standing assumption on the external inputs is only that they are bounded and slowly varying, whereas their structural information has not been explicitly used in the controller designs. This enables the resulting

controllers applicable to a wide range of control systems that unmodeled disturbances dominantly enter, yet at the same time, as the internal model principle [FW76] interprets clearly, the NPR studied so far was restricted to an approximation; in other words, the real output may persistently remain around the nominal trajectory, but in the end it may not converge to.

In this chapter, we present an extended notion of the NPR in an "asymptotic" sense from the perspective of the internal model principle [FW76]. In addition to keeping the distance of the actual and nominal outputs as close as desired (as the traditional notion aimed at), this new NPR means that, as long as the disturbance and reference signals are generated by an exogenous system, the actual output "asymptotically" converges to the nominal trajectory. Moreover, it is also desired that the asymptotic NPR is maintained in an input-to-output stable sense in terms of additional unmodeled part of the external input. To the best of author's knowledge, this is the first time in the literature to extend the NPR in view of the internal model principle, which is one of the main contributions in this work.

To tackle this problem, the DOB approach is adopted in the controller design. As is pointed out in [SJ07], the principle behind the robustness of the DOB is the compensating action of the total disturbance. This observation motivates the authors of [BS08, BS14] to employ the DOB (with some refinements) as a tool for recovering nominal performance in an approximate fashion. On top of that, we develop a new DOB structure into which the internal model of the external inputs is embedded. Unlike other robust controllers that achieve the approximate NPR only, with the help of the internal model, the proposed DOB also "perfectly" estimates and compensates the modeled part of the total disturbance in the steady-state. This allows to carry out the asymptotic NPR from the new DOB scheme.

The way of embedding the internal model into a DOB structure is inherently motivated by the recent researches [JPBS16, CT12], yet there are several significant contributions of this work beyond them. First, whereas only the disturbance model was taken into account in [JPBS16, CT12] for its rejection, we highlight that the reference model should be considered when it comes to the asymptotic NPR. Another improvement is that the order of the proposed DOB is reduced, since its construction is based on a reduced-order implementation of

the conventional DOB. In addition, a systematic design method for dealing with arbitrarily large (but bounded) parametric uncertainty is provided in this work. Finally, the refined DOB structure in this paper makes the NPR guaranteed from the transient period, whereas this is often not the case for the linear DOBs in [JPBS16, CT12] because unavoidable initial peak of control input may exist (as described in [BS08]).

2.1 Problem Formulation

In this chapter, we consider a single-input single-output (SISO) linear plant written in the Byrnes-Isidori normal form [Kha96, Chapter 13]:

$$\dot{z} = Sz + GC_\nu x, \tag{2.1.1a}$$

$$\dot{x} = A_\nu x + B_\nu\big(\psi^\top z + \phi^\top x + g(u+d)\big), \qquad y = C_\nu x \tag{2.1.1b}$$

where $z \in \mathbb{R}^{n-\nu}$ and $x \in \mathbb{R}^\nu$ are the states, $u \in \mathbb{R}$ is the input, $y \in \mathbb{R}$ is the output, $d \in \mathbb{R}$ is the external disturbance, and $\nu \geq 1$ and $n \geq \nu$ are integers. For an integer $i \geq 1$, the matrices A_i, B_i, and C_i are defined as

$$A_i := \begin{bmatrix} 0_{i-1} & I_{i-1} \\ 0 & 0_{i-1}^\top \end{bmatrix} \in \mathbb{R}^{i\times i}, \quad B_i := \begin{bmatrix} 0_{i-1} \\ 1 \end{bmatrix} \in \mathbb{R}^{i\times 1}, \quad C_i := \begin{bmatrix} 1 & 0_{i-1}^\top \end{bmatrix} \in \mathbb{R}^{1\times i}. \tag{2.1.2}$$

The scalar g and the matrices S, G, ψ, and ϕ are constants. The initial conditions $z(0)$ and $x(0)$ of the plant (2.1.1) belong in compact sets $\mathcal{Z}^0 \subset \mathbb{R}^{n-\nu}$ and $\mathcal{X}^0 \subset \mathbb{R}^\nu$, respectively.

Remark 2.1.1. It is well known that for any linear system, there always exists a suitable coordinate change with which the system is rewritten in the Byrnes-Isidori normal form as in (2.1.1). ♢

Throughout this chapter, we suppose that the plant (2.1.1) under consideration has (possibly large but) bounded parametric uncertainty, as stated below.

Assumption 2.1.1. The components g, S, G, ψ, and ϕ in (2.1.1) are uncertain but bounded, and the bounds of the uncertain quantities are known. Specifically,

there exist positive constants $\underline{g}$ and $\overline{g}$ such that $0 < \underline{g} \le g \le \overline{g}$. ◊

Moreover, the internal dynamics (2.1.1a) of the plant is assumed to be stable.

Assumption 2.1.2. The plant (2.1.1) is of minimum phase (that is, S in (2.1.1a) is Hurwitz). ◊

As a counterpart of the uncertain plant (2.1.1), the following *nominal* system without any uncertainty and disturbance is taken into account:

$$\dot{z}_{\mathsf{n}} = S_{\mathsf{n}} z_{\mathsf{n}} + G_{\mathsf{n}} C_\nu x_{\mathsf{n}}, \tag{2.1.3a}$$

$$\dot{x}_{\mathsf{n}} = A_\nu x_{\mathsf{n}} + B_\nu \big(\psi_{\mathsf{n}}^\top z_{\mathsf{n}} + \phi_{\mathsf{n}}^\top x_{\mathsf{n}} + g_{\mathsf{n}} u_{\mathsf{n}}\big), \qquad y_{\mathsf{n}} = C_\nu x_{\mathsf{n}} \tag{2.1.3b}$$

where $z_{\mathsf{n}} \in \mathbb{R}^{n_{\mathsf{n}}-\nu}$ and $x_{\mathsf{n}} \in \mathbb{R}^\nu$ are the states, $u_{\mathsf{n}} \in \mathbb{R}$ is the control input, $y_{\mathsf{n}} \in \mathbb{R}$ is the output. It is noted that the dimension $n_{\mathsf{n}} \ge \nu$ of the nominal model (2.1.3) is not necessarily the same as n of the actual one (2.1.1), so that structural uncertainty of the internal dynamics (2.1.1a), whose dimension is $n - \nu$, also can be considered. The parameters S_{n}, G_{n}, ψ_{n}, ϕ_{n}, and $g_{\mathsf{n}} > 0$ are some nominal counterparts of S, G, ψ, ϕ, and g, respectively. The nominal control input u_{n} in (2.1.3) is supposed to be generated by an output feedback nominal controller

$$\dot{c}_{\mathsf{n}} = E c_{\mathsf{n}} + F(r - y_{\mathsf{n}}), \qquad u_{\mathsf{n}} = J c_{\mathsf{n}} + K(r - y_{\mathsf{n}}) \tag{2.1.4}$$

designed *a priori* for the nominal system. Here $c_{\mathsf{n}} \in \mathbb{R}^{n_{\mathsf{c}}}$ is the controller state with a nonnegative integer n_{c} (and thus (2.1.4) can be either static or dynamic), $r \in \mathbb{R}$ is a $\mathfrak{C}^1$ reference command for y_{n}, and E, F, J, and K are constant matrices with appropriate dimensions. The controller (2.1.4) is supposed be designed such that the nominal closed-loop system (2.1.3) and (2.1.4) is internally stable, as well as its (nominal) tracking performance is satisfactory.

Assumption 2.1.3. The system matrix of the nominal closed-loop system (2.1.3) and (2.1.4)

$$\mathsf{A}_{\mathsf{n}} := \begin{bmatrix} S_{\mathsf{n}} & G_{\mathsf{n}} C_\nu & O \\ B_\nu \psi_{\mathsf{n}}^\top & A_\nu + B_\nu \phi_{\mathsf{n}}^\top - g_{\mathsf{n}} B_\nu K C_\nu & g_{\mathsf{n}} B_\nu J \\ O & -F C_\nu & E \end{bmatrix} \tag{2.1.5}$$

is Hurwitz. ◊

Roughly speaking, we in this chapter are interested in recovering the tracking performance of the nominal closed-loop system (2.1.3) and (2.1.4), in the sense that the actual output $y(t)$ is forced to behave as the nominal one $y_{\mathsf{n}}(t)$. Since the two trajectories will be compared "from the beginning" of system operation, it is natural to assume that $x_{\mathsf{n}}(0) = x(0) \in \mathcal{X}^0$, or equivalently, $y_{\mathsf{n}}(t)$ and its time derivatives up to $\nu - 1$ are initiated by those of $y(t)$. On the other hand, we arbitrarily select some compact sets $\mathcal{Z}_{\mathsf{n}}^0 \subset \mathbb{R}^{n_{\mathsf{n}}-\nu}$ and $\mathcal{C}_{\mathsf{n}}^0 \subset \mathbb{R}^{n_{\mathsf{c}}}$ and pick the remaining initial conditions $z_{\mathsf{n}}(0)$ and $c_{\mathsf{n}}(0)$ of the nominal closed-loop system in $\mathcal{Z}_{\mathsf{n}}^0$ and $\mathcal{C}_{\mathsf{n}}^0$, respectively.

We further assume that the external inputs $r(t)$ and $d(t)$ in the plant (2.1.1) and the nominal closed-loop system (2.1.3) and (2.1.4) are bounded and partially generated by an "internal model".

Assumption 2.1.4. The external inputs $r(t)$ and $d(t)$ are decomposed by

$$r(t) = r_{\mathsf{u}}(t) + r_{\mathsf{m}}(t), \qquad d(t) = d_{\mathsf{u}}(t) + d_{\mathsf{m}}(t) \tag{2.1.6}$$

where

(a) $r_{\mathsf{m}}(t)$ and $d_{\mathsf{m}}(t)$ are biased sinusoidal signals

$$r_{\mathsf{m}}(t) = M_{\mathsf{rm},0} + \sum_{i=1}^{n_{\mathsf{m}}} M_{\mathsf{rm},i} \sin\big(\sigma_i t + \varphi_{\mathsf{rm},i}\big), \tag{2.1.7a}$$

$$d_{\mathsf{m}}(t) = M_{\mathsf{dm},0} + \sum_{i=1}^{n_{\mathsf{m}}} M_{\mathsf{dm},i} \sin\big(\sigma_i t + \varphi_{\mathsf{dm},i}\big) \tag{2.1.7b}$$

where n_{m} is the known nonnegative integer, the frequencies $\sigma_i > 0$ of the sinusoids are known and distinct (i.e., $\sigma_i \neq \sigma_j$ for $i \neq j$), and the magnitudes $M_{\mathsf{rm},i} \in \mathbb{R}$ and $M_{\mathsf{dm},i} \in \mathbb{R}$, and the phases $\varphi_{\mathsf{rm},i} \in [0, 2\pi)$ and $\varphi_{\mathsf{dm},i} \in [0, 2\pi)$ are uncertain but bounded with known bounds.

(b) The unmodeled parts $r_{\mathsf{u}}(t)$ and $d_{\mathsf{u}}(t)$ are of $\mathfrak{C}^1$ and bounded, whose time derivatives are also bounded.

◊

Under the assumption, it is clear that there exist some constants $\overline{r} \geq 0$ and $\overline{d} \geq 0$ such that $\|[r(t); \dot{r}(t)]\| \leq \overline{r}$ and $\|[d(t); \dot{d}(t)]\| \leq \overline{d}$ for all $t \geq 0$.

Now, we are ready to introduce the notions of the nominal performance recovery (NPR).

Definition 2.1.1. For a given $\epsilon > 0$, an output feedback controller

$$\dot{\varrho} = f(\varrho, y, r), \qquad u = h(\varrho, y, r) \tag{2.1.8}$$

is said to *recover nominal performance within ϵ-bound* if for each initial condition $[z(0); x(0)] \in \mathcal{Z}^0 \times \mathcal{X}^0$ of (2.1.1) and for each nominal output $y_{\mathsf{n}}(t)$ of (2.1.3) and (2.1.4) initiated at $[z_{\mathsf{n}}(0); x(0); c_{\mathsf{n}}(0)] \in \mathcal{Z}_{\mathsf{n}}^0 \times \mathcal{X}^0 \times \mathcal{C}_{\mathsf{n}}^0$, the output $y(t)$ of the closed-loop system (2.1.1) and (2.1.8) satisfies

$$\|y(t) - y_{\mathsf{n}}(t)\| \leq \epsilon, \quad \forall t \geq 0 \tag{2.1.9}$$

where $\varrho(0)$ is a bounded function of $[z_{\mathsf{n}}(0); c_{\mathsf{n}}(0)] \in \mathcal{Z}_{\mathsf{n}}^0 \times \mathcal{C}_{\mathsf{n}}^0$. Furthermore, if

$$\begin{aligned} \|y(t) - y_{\mathsf{n}}(t)\| \leq{}& \mathsf{k}_{\mathrm{NPR},1} e^{-\mathsf{h}_{\mathrm{NPR}} t} \\ &+ \mathsf{k}_{\mathrm{NPR},2} \left(\sup_{0 \leq \rho \leq t} \|[r_{\mathsf{u}}(\rho); \dot{r}_{\mathsf{u}}(\rho); d_{\mathsf{u}}(\rho); \dot{d}_{\mathsf{u}}(\rho)]\| \right), \quad \forall t \geq 0 \end{aligned} \tag{2.1.10}$$

additionally holds for some constants $\mathsf{k}_{\mathrm{NPR},i} > 0$ and $\mathsf{h}_{\mathrm{NPR}} > 0$, then the output feedback controller (2.1.8) is said to *recover nominal performance in an asymptotic sense* within ϵ-bound. $\lozenge$

Notice that the nominal output trajectory $y_{\mathsf{n}}(t)$ considered in Definition 2.1.1 is not uniquely determined, because there is no restriction on $[z_{\mathsf{n}}(0); c_{\mathsf{n}}(0)] \in \mathcal{Z}_{\mathsf{n}}^0 \times \mathcal{C}_{\mathsf{n}}^0$. In fact, one can pick up any certain $y_{\mathsf{n}}(t)$ among several candidates, by selecting $\varrho(0)$ (which is a function of $[z_{\mathsf{n}}(0); c_{\mathsf{n}}(0)] \in \mathcal{Z}_{\mathsf{n}}^0 \times \mathcal{C}_{\mathsf{n}}^0$) suitably.

Throughout this chapter, our attention will be paid to:

Problem of Chapter 2. Given the plant (2.1.1), the nominal closed-loop system (2.1.3) and (2.1.4), and a threshold $\epsilon > 0$, to construct an output feedback controller (2.1.8) that recovers nominal performance in an asymptotic sense within ϵ-bound in the sense of Definition 2.1.1 under Assumptions 2.1.1–2.1.4. $\lozenge$

Remark 2.1.2. We point out that most relevant works in literature were mainly interested in recovering the nominal performance "just approximately" (similar to the former notion of Definition 2.1.1); that is to say, the two output trajectories $y(t)$ and $y_{\mathsf{n}}(t)$ may be close to each other but cannot converge to in the end. On the other hand, by relying on the structural information of the external inputs (Assumption 2.1.4), the purpose of this chapter is to go beyond such an approximation and to recover nominal performance in "asymptotic" sense in Definition 2.1.1. To interpret this new notion intuitively, for now assume that the external inputs $r(t)$ and $d(t)$ are fully modeled (i.e., $r(t) = r_{\mathsf{m}}(t)$ and $d(t) = d_{\mathsf{m}}(t)$). Then the additional requirement (2.1.10) is simplified to

$$\lim_{t\to\infty} \|y(t) - y_{\mathsf{n}}(t)\| = 0; \tag{2.1.11}$$

or equivalently, the actual output $y(t)$ asymptotically converges to the (ideal) nominal output $y_{\mathsf{n}}(t)$. (This is why we put the term "in an asymptotic sense" in the definition.) In Definition 3.1.3, we generalized this concept in an input-to-state stability (ISS) sense, with respect to the unmodeled inputs $r_{\mathsf{u}}(t)$ and $d_{\mathsf{u}}(t)$. ◊

2.2 Controller Design

As a solution to the problem of interest, we will construct the output feedback controller (2.1.8) based on the DOB approach. Motivated by the internal model principle [FW76], our key idea for the asymptotic recovery is to embed the generating model of $[r_{\mathsf{m}}(t); d_{\mathsf{m}}(t)]$ into the DOB structure. To provide further insight into this embedding, in the following subsection we briefly look again at the conventional DOB in the frequency domain, with particular interest on the modeled external inputs.

2.2.1 Motivating Idea from Frequency Domain Analysis

We revisit the conventional DOB controlled system in Figure 1.2 where the Q-filter has the form of

$$\mathrm{Q}(s;\tau) = \frac{\mathsf{c}_{l_\mathsf{q}}(\tau s)^{l_\mathsf{q}} + \cdots + \mathsf{c}_0}{(\tau s)^{n_\mathsf{q}} + \mathsf{a}_{n_\mathsf{q}-1}(\tau s)^{n_\mathsf{q}-1} + \cdots + \mathsf{a}_0} =: \frac{\mathrm{N}_\mathsf{q}(s;\tau)}{\mathrm{D}_\mathsf{q}(s;\tau)}. \tag{2.2.1}$$

In the figure, the actual output $\mathrm{y}(s)$ is represented with the external inputs $\mathrm{d}(s)$ and $\mathrm{r}(s)$ as

$$\mathrm{y}(s) = \mathrm{T}_{\mathsf{yr}}(s)\mathrm{r}(s) + \mathrm{T}_{\mathsf{yd}}(s)\mathrm{d}(s) \tag{2.2.2}$$

where

$$\mathrm{T}_{\mathsf{yr}}(s) := \frac{\mathrm{P}(s)\mathrm{P}_\mathsf{n}(s)\mathrm{C}(s)}{\mathrm{Q}(s;\tau)\big(\mathrm{P}(s)-\mathrm{P}_\mathsf{n}(s)\big)+\mathrm{P}_\mathsf{n}(s)\big(1+\mathrm{P}(s)\mathrm{C}(s)\big)}, \tag{2.2.3a}$$

$$\mathrm{T}_{\mathsf{yd}}(s) := \frac{\mathrm{P}(s)\mathrm{P}_\mathsf{n}(s)\big(1-\mathrm{Q}(s;\tau)\big)}{\mathrm{Q}(s;\tau)\big(\mathrm{P}(s)-\mathrm{P}_\mathsf{n}(s)\big)+\mathrm{P}_\mathsf{n}(s)\big(1+\mathrm{P}(s)\mathrm{C}(s)\big)}. \tag{2.2.3b}$$

In addition, we also write the nominal output $\mathrm{y}_\mathsf{n}(s)$ as

$$\mathrm{y}_\mathsf{n}(s) = \frac{\mathrm{P}_\mathsf{n}(s)\mathrm{C}(s)}{1+\mathrm{P}_\mathsf{n}(s)\mathrm{C}(s)}\mathrm{r}(s) =: \mathrm{T}_\mathsf{n}(s)\mathrm{r}(s). \tag{2.2.4}$$

Using these expressions, one can compute the difference between $\mathrm{y}(s)$ and $\mathrm{y}_\mathsf{n}(s)$ in the frequency domain as

$$\begin{aligned}
&\mathrm{y}(s) - \mathrm{y}_\mathsf{n}(s) \\
&= \big(\mathrm{T}_{\mathsf{yr}}(s) - \mathrm{T}_\mathsf{n}(s)\big)\,\mathrm{r}(s) + \mathrm{T}_{\mathsf{yd}}(s)\mathrm{d}(s) \\
&= \left(\frac{\mathrm{P}(s)\mathrm{P}_\mathsf{n}(s)\mathrm{C}(s)}{\mathrm{Q}(s;\tau)\big(\mathrm{P}(s)-\mathrm{P}_\mathsf{n}(s)\big)+\mathrm{P}_\mathsf{n}(s)\big(1+\mathrm{P}(s)\mathrm{C}(s)\big)} - \frac{\mathrm{P}_\mathsf{n}(s)\mathrm{C}(s)}{1+\mathrm{P}_\mathsf{n}(s)\mathrm{C}(s)}\right)\mathrm{r}(s) \\
&\quad + \frac{\mathrm{P}(s)\mathrm{P}_\mathsf{n}(s)\big(1-\mathrm{Q}(s;\tau)\big)}{\mathrm{Q}(s;\tau)\big(\mathrm{P}(s)-\mathrm{P}_\mathsf{n}(s)\big)+\mathrm{P}_\mathsf{n}(s)\big(1+\mathrm{P}(s)\mathrm{C}(s)\big)}\mathrm{d}(s) \\
&= \frac{\big(\mathrm{P}(s)-\mathrm{P}_\mathsf{n}(s)\big)\mathrm{P}(s)\mathrm{P}_\mathsf{n}(s)\big(1-\mathrm{Q}(s;\tau)\big)}{\big(\mathrm{Q}(s;\tau)\big(\mathrm{P}(s)-\mathrm{P}_\mathsf{n}(s)\big)+\mathrm{P}_\mathsf{n}(s)\big(1+\mathrm{P}(s)\mathrm{C}(s)\big)\big)\big(1+\mathrm{P}_\mathsf{n}(s)\mathrm{C}(s)\big)}\mathrm{r}(s) \\
&\quad + \frac{\mathrm{P}(s)\mathrm{P}_\mathsf{n}(s)\big(1-\mathrm{Q}(s;\tau)\big)}{\mathrm{Q}(s;\tau)\big(\mathrm{P}(s)-\mathrm{P}_\mathsf{n}(s)\big)+\mathrm{P}_\mathsf{n}(s)\big(1+\mathrm{P}(s)\mathrm{C}(s)\big)}\mathrm{d}(s).
\end{aligned}$$

It is noted that all the effects of the external inputs $\mathrm{d}(s)$ and $\mathrm{r}(s)$ on the error $\mathrm{y}(s) - \mathrm{y}_{\mathsf{n}}(s)$ are filtered by $1 - \mathrm{Q}(s;\tau)$.

Even though a typical conclusion with an arbitrary low-pass filter $\mathrm{Q}(s;\tau)$ is the approximation

$$\mathrm{y}(j\omega) \approx \frac{\mathrm{P}_{\mathsf{n}}(j\omega)\mathrm{C}(j\omega)}{1 + \mathrm{P}_{\mathsf{n}}(j\omega)\mathrm{C}(j\omega)}\mathrm{r}(j\omega) \tag{2.2.5}$$

in the low frequency range where $\mathrm{Q}(j\omega;\tau) \approx 1$, one can go further by relying more on the internal model of the external inputs. For this, we assume for now that $d(t) = d_{\mathsf{m}}(t)$ and $r(t) = r_{\mathsf{m}}(t)$. Under the hypothesis, the Laplace transforms $\mathrm{d}(s)$ and $\mathrm{r}(s)$ of these signals turn out to be

$$\mathrm{r}(s) = \frac{\mathsf{r}_{\mathsf{m},0}}{s} + \sum_{i=1}^{n_{\mathsf{m}}} \frac{\mathsf{r}_{\mathsf{m},i}}{s^2 + \sigma_i^2}, \qquad \mathrm{d}(s) = \frac{\mathsf{d}_{\mathsf{m},0}}{s} + \sum_{i=1}^{n_{\mathsf{m}}} \frac{\mathsf{d}_{\mathsf{m},i}}{s^2 + \sigma_i^2} \tag{2.2.6}$$

in which $\mathrm{r}_{\mathsf{m},i}$ and $\mathrm{d}_{\mathsf{m},i}$ are some uncertain constants. In turn, it readily follows from the final value theorem that, if the Q-filter $\mathrm{Q}(s;\tau) = \mathrm{N}_{\mathsf{q}}(s;\tau)/\mathrm{D}_{\mathsf{q}}(s;\tau)$ in (2.2.1) is properly designed to satisfy an additional constraint

$$\mathrm{D}_{\mathsf{q}}(s;\tau) - \mathrm{N}_{\mathsf{q}}(s;\tau) = s\prod_{i=1}^{n_{\mathsf{m}}}(s^2 + \sigma_i^2)\mathrm{R}_{\mathsf{q}}(s;\tau) \tag{2.2.7}$$

with a polynomial $\mathrm{R}_{\mathsf{q}}(s;\tau)$,

$$\lim_{t\to\infty}\big(y(t) - y_{\mathsf{n}}(t)\big) = \lim_{s\to 0} s\big(\mathrm{y}(s) - \mathrm{y}_{\mathsf{n}}(s)\big) = 0 \tag{2.2.8}$$

and thus, the nominal performance is not approximately but completely recovered in the steady state (as long as the closed-loop system is stable). It is surprising that (2.2.8) (with exponential rate of convergence by the linear system theory) is exactly the same as (2.1.10) in Definition 2.1.1 for the limited situation $r_{\mathsf{u}}(t) \equiv 0$ and $d_{\mathsf{u}}(t) \equiv 0$ (as described in (2.1.2)) and moreover, all this can be done with a specific Q-filter satisfying (2.2.7). In the remainder of this subsection, we will extend this idea to the state space domain in order to deal with the transient behavior and unmodeled external inputs, keeping the constraint (2.2.7) on the Q-filter's coefficients in mind.

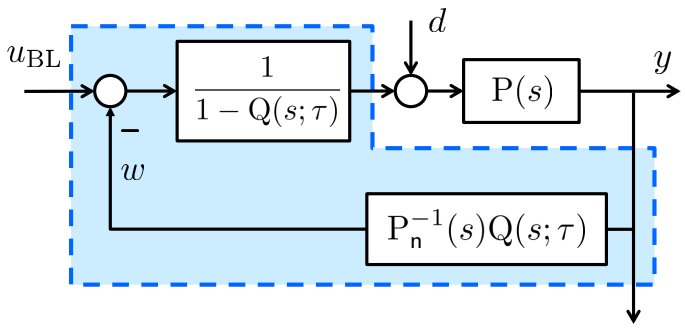

Figure 2.1: An equivalent block diagram of conventional DOB

Remark 2.2.1. It should be noted that to derive the asymptotic behavior (2.2.8), the reference model (as well as the disturbance model) should be taken into account in the constraint (2.2.7). Intuitively, this requirement is because the total disturbance to be compensated consists of not only the disturbance but also uncertain quantities where the latter may be multiplied by a reference signal. ◊

In the meanwhile, another way of interpreting this phenomenon might be to take a closer look at the equivalent block diagram of the linear DOB in Figure 2.1. In the figure, a hidden block $1/(1-\mathrm{Q}(s;\tau))$ explicitly comes out, which is computed under the constraint (2.2.7) as follows:

$$\frac{1}{1-\mathrm{Q}(s;\tau)} = \frac{\mathrm{D}_{\mathsf{q}}(s;\tau)}{\mathrm{D}_{\mathsf{q}}(s;\tau)-\mathrm{N}_{\mathsf{q}}(s;\tau)} = \frac{1}{s\prod_{i=1}^{n_{\mathsf{m}}}(s^2+\sigma_i^2)} \times \frac{\mathrm{D}_{\mathsf{q}}(s;\tau)}{\mathrm{R}_{\mathsf{q}}(s;\tau)}.$$

In this regard, it can be said that by the constraint (2.2.7), the internal model of the external modeled inputs $r_{\mathsf{m}}(t)$ and $d_{\mathsf{m}}(t)$ is "embedded" into the DOB structure (in view of the input-to-output relation).

Remark 2.2.2. The first attempt to embed an internal model into the DOB structure was found in [YKIH97]. In [YKIH97, PJSB12], multiple integrators were taken into account as a disturbance model, under the philosophy that any analytic disturbance can be approximated by a "polynomial-in-time" signal (i.e., $d_{\mathsf{m}}(t) = \mathsf{d}_0 + \mathsf{d}_1 t + \cdots + \mathsf{d}_k t^k$). It has been seen that the resulting DOB with multiple integrators, called "high-order DOB (or type-k DOB)", could present a

better disturbance rejection ability than the conventional DOB. More recently, the authors of [CT12, JPBS16] proposed linear DOB structures that contain the generating model of the sinusoidal disturbances (in continuous- and discrete-time domains, respectively), whose goal is to eliminate the modeled disturbance "exactly" in the steady state. All these studies shared the common idea for embedding the disturbance model (while the details are different) as described in the above paragraph, which partially motivates the work of this chapter. ◊

2.2.2 Reduced-order Implementation of Disturbance Observer with Higher Order Numerator of Q-filter

As an intermediate step for the DOB design, in this subsection we implement the conventional DOB in Figure 1.2 into the state space. In particular, while a traditional way is to realize the two components $\mathrm{P}_{\mathsf{n}}^{-1}(s)\mathrm{Q}(s;\tau)$ and $\mathrm{Q}(s;\tau)$ in the figure directly (as in [SJ07]), we here present another realization of the DOB by transforming the DOB into an equivalent structure. This alternative method allows to reduce the total order of the controller and to simplify its performance analysis, as clarified later.

We begin with the typical expression of the DOB output $\mathrm{w}(s)$ in the frequency domain

$$\mathrm{w}(s) = -\mathrm{Q}(s;\tau)\mathrm{u}(s) + \mathrm{P}_{\mathsf{n}}^{-1}(s)\mathrm{Q}(s;\tau)\mathrm{y}(s) \tag{2.2.9}$$

and with the Q-filter

$$\mathrm{Q}(s;\tau) = \frac{\mathsf{c}_{l_{\mathsf{q}}}(\tau s)^{l_{\mathsf{q}}} + \cdots + \mathsf{c}_0}{(\tau s)^{\nu+l_{\mathsf{q}}} + \mathsf{a}_{\nu+l_{\mathsf{q}}-1}(\tau s)^{\nu+l_{\mathsf{q}}-1} + \cdots + \mathsf{a}_0} \tag{2.2.10}$$

so that its relative degree $n_{\mathsf{q}} - l_{\mathsf{q}}$ is the same as that of the nominal model $\mathrm{P}_{\mathsf{n}}(s)$. By transforming the Byrnes-Isidori normal form (2.1.4) of $\mathrm{P}_{\mathsf{n}}(s)$ into the s-domain, one can rewrite the inverse dynamics $\mathrm{P}_{\mathsf{n}}^{-1}(s)\mathrm{y}(s)$ of the nominal plant as follows:

$$\begin{aligned}\mathrm{P}_{\mathsf{n}}^{-1}(s)\mathrm{y}(s) &= \frac{1}{g_{\mathsf{n}}}\Big(s^{\nu}\mathrm{y}(s) - \psi_{\mathsf{n}}^{\top}\mathrm{z}_{\mathsf{n}}^{\dagger}(s) - \phi_{\mathsf{n}}^{\top}[1; s; \ldots; s^{\nu-1}]\mathrm{y}(s)\Big) \\ &= -\frac{1}{g_{\mathsf{n}}}\psi_{\mathsf{n}}^{\top}\mathrm{z}_{\mathsf{n}}^{\dagger}(s) + \frac{1}{g_{\mathsf{n}}}\big(s^{\nu} - \phi_{\mathsf{n},1} - \cdots - \phi_{\mathsf{n},\nu}s^{\nu-1}\big)\mathrm{y}(s)\end{aligned} \tag{2.2.11}$$

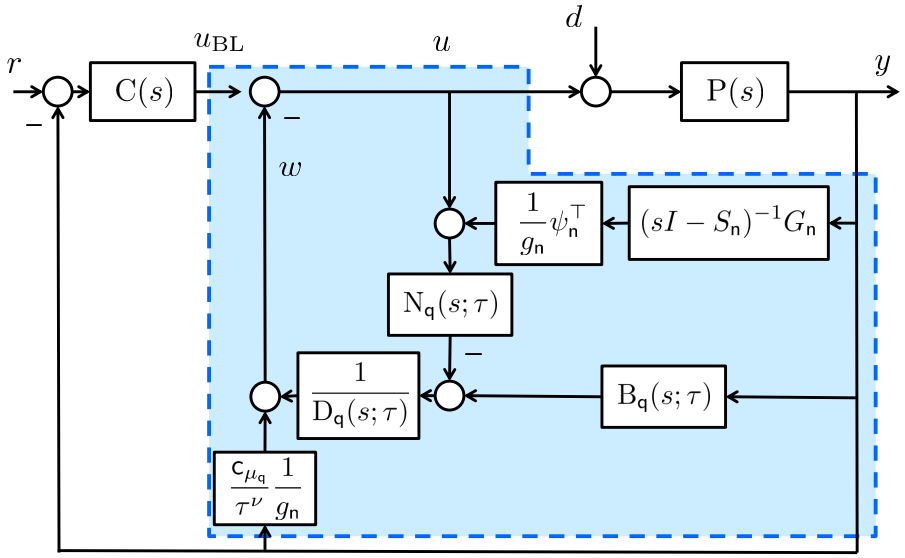

Figure 2.2: Equivalent representation (2.2.13) of conventional DOB based on Byrnes-Isidori normal form of $\mathrm{P}_{\mathsf{n}}(s)$

where

$$\mathrm{z}_{\mathsf{n}}^{\dagger}(s) = (sI - S_{\mathsf{n}})^{-1} G_{\mathsf{n}} \mathrm{y}(s). \tag{2.2.12}$$

Applying (2.2.11) into (2.2.9) then brings an equivalent representation of $\mathrm{w}(s)$

$$\begin{aligned} \mathrm{w}(s) = -\mathrm{Q}(s;\tau) \left(\mathrm{u}(s) + \frac{1}{g_{\mathsf{n}}} \psi_{\mathsf{n}}^{\top} \mathrm{z}_{\mathsf{n}}^{\dagger}(s) \right) \\ + \mathrm{Q}(s;\tau) \big(s^{\nu} - \phi_{\mathsf{n},1} - \cdots - \phi_{\mathsf{n},\nu} s^{\nu-1} \big) \frac{1}{g_{\mathsf{n}}} \mathrm{y}(s) \end{aligned} \tag{2.2.13}$$

with (2.2.12), whose configuration is shown in Figure 2.2.

Based on this finding, from now on we realize (2.2.13) instead of (2.2.9) in the state space. Note that for the polynomial $\mathrm{N}_{\mathsf{q}}(s;\tau)\big(s^{\nu} - \phi_{\mathsf{n},1} - \cdots - \phi_{\mathsf{n},\nu} s^{\nu-1}\big)$, its coefficient of s^i, $k = 0, \ldots, \nu + l_{\mathsf{q}}$, is computed by

$$-\sum_{j=0}^{i} \phi_{\mathsf{n},j+1} \mathsf{c}_{i-j} \tau^{i-j}$$

(for simplicity, let $\phi_{\mathsf{n},\nu+1} = -1$, $\phi_{\mathsf{n},\nu+2} = \cdots = \phi_{\mathsf{n},\nu+l_{\mathsf{q}}+1} = 0$, and $\mathsf{c}_{l_{\mathsf{q}}+1} = \cdots =$

$\mathsf{c}_{\nu+l_\mathsf{q}} = 0$). From this fact, one can rewrite the transfer function $\mathrm{Q}(s;\tau)\big(s^\nu - \phi_{\mathsf{n},1} - \cdots - \phi_{\mathsf{n},\nu}s^{\nu-1}\big)$ in (2.2.13), which is biproper and has the high-frequency gain as $\mathsf{c}_{l_\mathsf{q}}/\tau^\nu$, as

$$\begin{aligned}
&\mathrm{Q}(s;\tau)\big(s^\nu - \phi_{\mathsf{n},1} - \cdots - \phi_{\mathsf{n},\nu}s^{\nu-1}\big)\\
&= \frac{\mathsf{c}_{l_\mathsf{q}}}{\tau^\nu} + \frac{\mathrm{N}_\mathsf{q}(s;\tau)\big(s^\nu - \phi_{\mathsf{n},1} - \cdots - \phi_{\mathsf{n},\nu}s^{\nu-1}\big) - (\mathsf{c}_{l_\mathsf{q}}/\tau^\nu)\mathrm{D}_\mathsf{q}(s;\tau)}{\mathrm{D}_\mathsf{q}(s;\tau)}\\
&= \frac{\mathsf{c}_{l_\mathsf{q}}}{\tau^\nu} + \frac{\mathsf{b}_{\nu+l_\mathsf{q}-1}(\tau s)^{\nu+l_\mathsf{q}-1} + \cdots + \mathsf{b}_0}{(\tau s)^{\nu+l_\mathsf{q}} + \mathsf{a}_{\nu+l_\mathsf{q}-1}(\tau s)^{\nu+l_\mathsf{q}-1} + \cdots + \mathsf{a}_0} =: \frac{\mathsf{c}_{l_\mathsf{q}}}{\tau^\nu} + \frac{\mathsf{B}_\mathsf{q}(s;\tau)}{\mathrm{D}_\mathsf{q}(s;\tau)}
\end{aligned} \tag{2.2.14}$$

where the coefficients b_i, $i = 0, \ldots, \nu + l_\mathsf{q} - 1$, are given by

$$\mathsf{b}_i := \frac{1}{\tau^i}\bigg(- \sum_{j=0}^{i} \phi_{\mathsf{n},j+1}\mathsf{c}_{i-j}\tau^{i-j} - \mathsf{c}_{l_\mathsf{q}}\tau^{i-\nu}\mathsf{a}_i\bigg). \tag{2.2.15}$$

In short, another representation of $\mathrm{w}(s)$ is given by

$$\begin{aligned}
\mathrm{w}(s) = \frac{1}{\mathrm{D}_\mathsf{q}(s;\tau)}\bigg(&- \mathrm{N}_\mathsf{q}(s;\tau)\Big(\mathrm{u}(s) + \frac{1}{g_\mathsf{n}}\psi_\mathsf{n}^\top \mathrm{z}_\mathsf{n}^\dagger(s)\Big) + \mathsf{B}_\mathsf{q}(s;\tau)\frac{1}{g_\mathsf{n}}\mathrm{y}(s)\bigg)\\
&+ \frac{\mathsf{c}_{l_\mathsf{q}}}{\tau^\nu}\frac{1}{g_\mathsf{n}}\mathrm{y}(s).
\end{aligned} \tag{2.2.16}$$

Now, by implementing (2.2.12) and the dual-input single-output system (2.2.16) with respect to the inputs $\mathrm{u}(s) + (1/g_\mathsf{n})\psi_\mathsf{n}^\top \mathrm{z}_\mathsf{n}^\dagger(s)$ and $(1/g_\mathsf{n})\mathrm{y}(s)$ in the state space (particularly in the observable canonical form for the latter), we obtain a new state-space representation of the DOB as follows:

$$\dot{z}_\mathsf{n}^\dagger = S_\mathsf{n} z_\mathsf{n}^\dagger + G_\mathsf{n} y, \tag{2.2.17a}$$

$$\begin{aligned}
\dot{p} = &\big(A_{\nu+l_\mathsf{q}} - \underline{\Upsilon}_{\nu+l_\mathsf{q}}^{-1}(\tau)\overline{\alpha}C_{\nu+l_\mathsf{q}}\big)p\\
&- \underline{\Upsilon}_{\nu+l_\mathsf{q}}^{-1}(\tau)\overline{\gamma}\left(u + \frac{1}{g_\mathsf{n}}\psi_\mathsf{n}^\top z_\mathsf{n}^\dagger\right) + \underline{\Upsilon}_{\nu+l_\mathsf{q}}^{-1}(\tau)\overline{\beta}\frac{1}{g_\mathsf{n}}y,
\end{aligned} \tag{2.2.17b}$$

$$w = C_{\nu+l_\mathsf{q}}p + \frac{\mathsf{c}_{l_\mathsf{q}}}{\tau^\nu}\frac{1}{g_\mathsf{n}}y \tag{2.2.17c}$$

where $z_\mathsf{n}^\dagger \in \mathbb{R}^{n_\mathsf{n}-\nu}$ and $q \in \mathbb{R}^{\nu+l_\mathsf{q}}$ are the states, $u \in \mathbb{R}$ and $y \in \mathbb{R}$ are the inputs,

and $w \in \mathbb{R}$ is the output. For a positive integer $i \geq 1$,

$$\underline{\Upsilon}_i(\tau) := \mathrm{diag}(\tau, \ldots, \tau^i) \in \mathbb{R}^{i \times i}, \tag{2.2.18}$$

and the vectors $\overline{\alpha} \in \mathbb{R}^{\nu+l_{\mathsf{q}}}$, $\overline{\beta} \in \mathbb{R}^{\nu+l_{\mathsf{q}}}$, and $\overline{\gamma} \in \mathbb{R}^{\nu+l_{\mathsf{q}}}$ are defined as

$$\overline{\alpha} := \begin{bmatrix} \mathsf{a}_{\nu+l_{\mathsf{q}}-1} \\ \mathsf{a}_{\nu+l_{\mathsf{q}}-2} \\ \vdots \\ \mathsf{a}_0 \end{bmatrix}, \quad \overline{\beta} := \begin{bmatrix} \mathsf{b}_{\nu+l_{\mathsf{q}}-1} \\ \mathsf{b}_{\nu+l_{\mathsf{q}}-2} \\ \vdots \\ \mathsf{b}_0 \end{bmatrix}, \quad \overline{\gamma} := \begin{bmatrix} 0_{\nu-1} \\ \mathsf{c}_{\nu+l_{\mathsf{q}}-1} \\ \vdots \\ \mathsf{c}_0 \end{bmatrix}. \tag{2.2.19}$$

We emphasize that the total order of the state-space realization (2.2.17) is now $n + l_{\mathsf{q}}$, which is less than that obtained from the conventional way in [SJ07].

Remark 2.2.3. The work in this subsection in fact generalizes the previous result of [BS14], in the sense that the Q-filter (2.2.10) here is allowed to have a higher order numerator (i.e., $l_{\mathsf{q}} \neq 0$). This additional freedom will play a crucial role in achieving both robust stability of the closed-loop system and the constraint (2.2.7) for embedding the internal model of $[r_{\mathsf{m}}(t); d_{\mathsf{m}}(t)]$ at once. ♢

2.2.3 Design of Disturbance Observer with Internal Model

Based on the results of the previous subsection, we now construct the controller (2.1.8) of interest as the combination of the reduced-order DOB (2.2.17), the baseline controller

$$\dot{c} = Ec + F(r - y), \qquad u_{\mathrm{BL}} = Jc + K(r - y) \tag{2.2.20}$$

having the same structure as the nominal controller (2.1.4), and the composite control law

$$u = u_{\mathrm{BL}} - \overline{s}_{\mathsf{w}}(w), \tag{2.2.21}$$

while the saturation function $\overline{s}_{\mathsf{w}} : \mathbb{R} \to \mathbb{R}$ and the parameters a_i, c_i, and τ of the DOB will be determined throughout this subsection.

Firstly, we set the dimension l_{q} of the numerator of $\mathrm{Q}(s;\tau)$ in (2.2.10) as $2n_{\mathsf{m}}$. Then choose the coefficients a_i, $i = 0, \ldots, 2n_{\mathsf{m}} - 1$, of the denominator of $\mathrm{Q}(s;\tau)$ such that the transfer function

$$\frac{s^{\nu+2n_{\mathsf{m}}} + \mathsf{a}_{\nu+2n_{\mathsf{m}}-1}s^{\nu+2n_{\mathsf{m}}-1} + \cdots + \mathsf{a}_{2n_{\mathsf{m}}+1}s^{2n_{\mathsf{m}}+1} + \dfrac{\overline{g}}{g_{\mathsf{n}}}\mathsf{a}_{2n_{\mathsf{m}}}s^{2n_{\mathsf{m}}} + \cdots + \dfrac{\overline{g}}{g_{\mathsf{n}}}\mathsf{a}_0}{s^{\nu+2n_{\mathsf{m}}} + \mathsf{a}_{\nu+2n_{\mathsf{m}}-1}s^{\nu+2n_{\mathsf{m}}-1} + \cdots + \mathsf{a}_{2n_{\mathsf{m}}+1}s^{2n_{\mathsf{m}}+1} + \dfrac{\underline{g}}{g_{\mathsf{n}}}\mathsf{a}_{2n_{\mathsf{m}}}s^{2n_{\mathsf{m}}} + \cdots + \dfrac{\underline{g}}{g_{\mathsf{n}}}\mathsf{a}_0} \tag{2.2.22}$$

is strictly positive real (SPR) [Kha96, Chapter 6] where $\underline{g}$ and $\overline{g}$ are the bounds of the high-frequency gain g of the plant (2.1.1) (in Assumption 2.1.1). As pointed out in the following theorem, finding the coefficients a_i is always possible even for a general form of (2.2.22).

Theorem 2.2.1. For given $\overline{g} \geq \underline{g} > 0$ and $g_{\mathsf{n}} > 0$ and positive integers k and j, there exist a_i, $i = 0, \ldots, k + j - 1$, such that the transfer function

$$\mathrm{Z}_{k,j}(s) := \frac{s^{k+j} + \mathsf{a}_{k+j-1}s^{k+j-1} + \mathsf{a}_{j+1}s^{j+1} + \dfrac{\overline{g}}{g_{\mathsf{n}}}\mathsf{a}_j s^j + \cdots + \dfrac{\overline{g}}{g_{\mathsf{n}}}\mathsf{a}_0}{s^{k+j} + \mathsf{a}_{k+j-1}s^{k+j-1} + \mathsf{a}_{j+1}s^{j+1} + \dfrac{\underline{g}}{g_{\mathsf{n}}}\mathsf{a}_j s^j + \cdots + \dfrac{\underline{g}}{g_{\mathsf{n}}}\mathsf{a}_0} \tag{2.2.23}$$

is SPR. ◊

Notice that the transfer function (2.2.22) in our case is nothing but $\mathrm{Z}_{k,j}(s)$ in (2.2.23) with $k = \nu$ and $j = 2n_{\mathsf{m}}$.

Two ways of deriving such a_i are presented in Appendix A.1. First, as a concrete proof of the theorem, a recursive design guideline is provided in Appendix A.1.1. While the recursive method may be complicated and even bring a conservative value in some cases, we also introduce a bilinear matrix inequality (BMI)-based design method in Appendix A.1.2 by recasting the problem in Theorem 2.2.1 as an optimization problem.

Next, for the selection of c_i, define a bundle of Vandermonde matrices

$$W_i(\theta;\tau) := \begin{bmatrix} 1 & (-\tau^2\theta_1)^1 & \cdots & (-\tau^2\theta_1)^i \\ \vdots & \vdots & & \vdots \\ 1 & (-\tau^2\theta_{n_{\mathsf{m}}})^1 & \cdots & (-\tau^2\theta_{n_{\mathsf{m}}})^i \end{bmatrix} \in \mathbb{R}^{n_{\mathsf{m}}\times(i+1)} \tag{2.2.24}$$

where $\theta = [\theta_1; \cdots; \theta_{n_\mathsf{m}}] := [\sigma_1^2; \cdots; \sigma_{n_\mathsf{m}}^2]$. It is noticed that $W_{n_\mathsf{m}-1}(\theta;\tau)$ is a square matrix whose determinant is given by

$$\det\big(W_{n_\mathsf{m}-1}(\theta;\tau)\big) = -\tau^2 \prod_{i\neq j}(\theta_i - \theta_j), \tag{2.2.25}$$

and thus it is invertible for any $\tau > 0$ and distinct frequencies σ_i of the sinusoids (2.1.7). With τ to be determined later in Theorem 2.2.3, the coefficients c_i of the Q-filter (2.2.10) are selected as

$$\begin{bmatrix} \mathsf{c}_1 \\ \mathsf{c}_3 \\ \vdots \\ \mathsf{c}_{2n_\mathsf{m}-1} \end{bmatrix} = W_{n_\mathsf{m}-1}^{-1}(\theta;\tau) W_{n_\mathsf{m}-1+\frac{1}{2}(\nu+n^\star)}(\theta;\tau)\underline{\alpha}_{\text{odd}}, \tag{2.2.26a}$$

$$\begin{bmatrix} \mathsf{c}_2 \\ \mathsf{c}_4 \\ \vdots \\ \mathsf{c}_{2n_\mathsf{m}} \end{bmatrix} = W_{n_\mathsf{m}-1}^{-1}(\theta;\tau) W_{n_\mathsf{m}-1+\frac{1}{2}(\nu-n^\star)}(\theta;\tau)\underline{\alpha}_{\text{even}}, \tag{2.2.26b}$$

and $\mathsf{c}_0 = \mathsf{a}_0$ where

- if ν is even, then $n^\star := 0$ and

$$\underline{\alpha}_{\text{odd}} := \begin{bmatrix} \mathsf{a}_1 \\ \mathsf{a}_3 \\ \vdots \\ \mathsf{a}_{\nu+2n_\mathsf{m}-1} \end{bmatrix} \in \mathbb{R}^{(\nu+2n_\mathsf{m})/2}, \quad \underline{\alpha}_{\text{even}} := \begin{bmatrix} \mathsf{a}_2 \\ \mathsf{a}_4 \\ \vdots \\ \mathsf{a}_{\nu+2n_\mathsf{m}-2} \\ 1 \end{bmatrix} \in \mathbb{R}^{(\nu+2n_\mathsf{m})/2};$$

- if ν is odd, then $n^\star := 1$ and

$$\underline{\alpha}_{\text{odd}} := \begin{bmatrix} \mathsf{a}_1 \\ \mathsf{a}_3 \\ \vdots \\ \mathsf{a}_{\nu+2n_{\mathsf{m}}-2} \\ 1 \end{bmatrix} \in \mathbb{R}^{(\nu+2n_{\mathsf{m}}+1)/2}, \quad \underline{\alpha}_{\text{even}} := \begin{bmatrix} \mathsf{a}_2 \\ \mathsf{a}_4 \\ \vdots \\ \mathsf{a}_{\nu+2n_{\mathsf{m}}-1} \end{bmatrix} \in \mathbb{R}^{(\nu+2n_{\mathsf{m}}-1)/2}.$$

Since each coefficient c_i in (2.2.26) is a function of τ and σ, we often use $\mathsf{c}_i(\theta;\tau)$ and $\overline{\gamma}(\theta;\tau)$ instead of c_i and $\overline{\gamma}$, respectively.

It is important to note that the fundamental reason for the selection of c_i is to put the internal model of $[r_{\mathsf{m}}(t); d_{\mathsf{m}}(t)]$ into the DOB structure in the sense of (2.2.7) (even regardless of the design parameters a_i and $\tau > 0$), as in the following lemma-.

Lemma 2.2.2. For any given a_i, $\tau > 0$, and $\sigma_i > 0$, the coefficients $\mathsf{c}_i(\theta;\tau)$ selected as in (2.2.26) satisfy the equality (2.2.7). Moreover, they have the form of $\mathsf{c}_i(\theta;\tau) = \mathsf{a}_i + \tau^2 \tilde{\mathsf{c}}_i(\theta;\tau)$, $i = 0, \dots, 2n_{\mathsf{m}}$, where each $\tilde{\mathsf{c}}_i(\theta;\tau)$ is a polynomial of τ. ◊

Proof. For the first item, it is enough to show that

$$\Big[\mathrm{D}_{\mathsf{q}}(s;\tau) - \mathrm{N}_{\mathsf{q}}(s;\tau)\Big]_{s=\pm j\sigma_i} = 0$$

for all $i = 1, \dots, n_{\mathsf{m}}$ (while $\mathrm{D}_{\mathsf{q}}(0;\tau) - \mathrm{N}_{\mathsf{q}}(0;\tau) = 0$ because $\mathsf{a}_0 = \mathsf{c}_0$). On the other hand, the second item is trivial, because

$$\begin{aligned} &W_{n_{\mathsf{m}}-1}^{-1} W_{n_{\mathsf{m}}-1+\frac{1}{2}(\nu-n^\star)} \\ &= \Big[I_{n_{\mathsf{m}}} \quad \operatorname{diag}\big((-\tau^2\theta_1)^{n_{\mathsf{m}}}, \dots, (-\tau^2\theta_{n_{\mathsf{m}}})^{n_{\mathsf{m}}}\big) \times W_{\frac{1}{2}(\nu-n^\star)} \Big]. \end{aligned}$$

For the detailed proof, the readers are referred to [JPBS16]. □

On the other hand, even though $\mathsf{c}_i(\theta;\tau)$ themselves may seem ill-defined when $\tau = 0$ (by its definition), the second item of the proposition shows $\lim_{\tau\downarrow 0} \mathsf{c}_i(\theta;\tau) = \mathsf{a}_i$ which enables us to take $\mathsf{c}_i(\theta;0) = \mathsf{a}_i$ for the analysis to come.

Notice that once a_i, c_i, and τ are given, the remaining coefficients $\mathsf{b}_i = \mathsf{b}_i(\theta;\tau)$ are automatically selected as in (2.2.15).

As the last step, the saturation function $\bar{s}_{\mathsf{w}}$ for the output w of the DOB in (2.2.21) is designed below. For this purpose, we take into account the nominal closed-loop system (2.1.3) and (2.1.4) together with an "auxiliary" internal dynamics

$$\dot{z}_{\rm aux} = Sz_{\rm aux} + Gy_{\mathsf{n}} = Sz_{\rm aux} + GC_\nu x_{\mathsf{n}}, \tag{2.2.27}$$

which mimics the actual z-dynamics (2.1.1a) with the input replaced by the nominal output y_{n}, and with the same initial condition $z_{\rm aux}(0) = z(0) \in \mathcal{Z}^0$. For this extended nominal closed-loop system, let the scalar signal

$$\begin{aligned} d_{\rm total,n} := \frac{1}{g}\Big(&\psi^\top z_{\rm aux} + \phi^\top x_{\mathsf{n}} + g\big(Jc_{\mathsf{n}} + K(r - C_\nu x_{\mathsf{n}}) + d\big) \\ &- \psi_{\mathsf{n}}^\top z_{\mathsf{n}} - \phi_{\mathsf{n}}^\top x_{\mathsf{n}} - g_{\mathsf{n}}\big(Jc_{\mathsf{n}} + K(r - C_\nu x_{\mathsf{n}})\big)\Big) \end{aligned} \tag{2.2.28}$$

be an additional output. (It will be clarified shortly that $d_{\rm total,n}$ in (2.2.28) indicates a nominal counterpart of the total disturbance in the time domain, which will be captured by the proposed DOB.) Then the extended system with respect to the input $[r(t); d(t)]$ and the output $[y_{\mathsf{n}}(t); d_{\rm total,n}(t)]$ is bounded-input bounded-output (BIBO) stable, because S is Hurwitz (by Assumption 2.1.2), and the nominal closed-loop system (2.1.3) and (2.1.4) is internally stable (by Assumption 2.1.3). It follows that the set of the partial output $d_{\rm total,n}(t)$

$$\begin{aligned} \mathcal{D}_{\rm total,n} := \Big\{ & d_{\rm total,n}(t) \text{ generated by (2.1.3), (2.1.4), and (2.2.27)} \\ & : z_{\rm aux}(0) \in \mathcal{Z}^0,\ [z_{\mathsf{n}}(0); x_{\mathsf{n}}(0); c_{\mathsf{n}}(0)] \times \mathcal{Z}_{\mathsf{n}}^0 \times \mathcal{X}^0 \times \mathcal{C}_{\mathsf{n}}^0, \\ & \|[r(t); \dot{r}(t)]\| \le \overline{r},\ \|[d(t); \dot{d}(t)]\| \le \overline{d},\ t \ge 0 \Big\} \subset \mathbb{R} \end{aligned} \tag{2.2.29}$$

is a bounded set. Finally, with a strictly larger compact set $\overline{\mathcal{D}}_{\rm total,n} \supset \mathcal{D}_{\rm total,n}$, we design $\bar{s}_{\mathsf{w}}$ in (2.2.21) as a $\mathfrak{C}^1$ and bounded function such that

$$\bar{s}_{\mathsf{w}}(w) = w, \quad \forall w \in \overline{\mathcal{D}}_{\rm total,n} \quad \text{and} \quad 0 \le \frac{\mathrm{d}}{\mathrm{d}w}\bar{s}_{\mathsf{w}} \le 1, \quad \forall w \in \mathbb{R}. \tag{2.2.30}$$

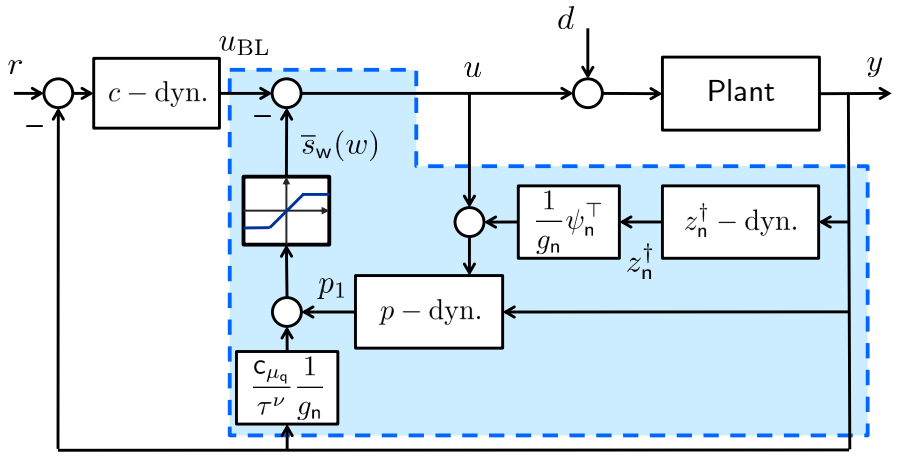

Figure 2.3: Closed-loop system with proposed DOB-based controller (2.2.17), (2.2.20), and (2.2.21)

In summary, with the design parameters determined above and sufficiently small $\tau > 0$, the proposed controller in this chapter consists of the (reduced-order) DOB (2.2.17) with the internal model, the baseline controller (2.2.20), and the composite control law (2.2.21), as is seen in Figure 2.3. We close this section by introducing our main result on the asymptotic NPR in Definition 2.1.1, whose detailed proof is given in the next section.

Theorem 2.2.3. Suppose that Assumptions 2.1.1–2.1.4 hold. Then for given $\epsilon > 0$, there is $\overline{\tau} > 0$ such that the proposed DOB-based controller (2.2.17), (2.2.20), and (2.2.21) recovers nominal performance in an asymptotic sense with ϵ-bound for all $\tau \in (0, \overline{\tau})$. In particular, an initial condition $[z_{\mathsf{n}}^{\dagger}(0); q(0); c(0)]$ of the controller corresponding to the nominal output trajectory $y_{\mathsf{n}}(t)$ with $[z_{\mathsf{n}}(0); c_{\mathsf{n}}(0)] \in \mathcal{Z}_{\mathsf{n}}^{0} \times \mathcal{C}_{\mathsf{n}}^{0}$ is given by $[z_{\mathsf{n}}^{\dagger}(0); p(0); c(0)] = [z_{\mathsf{n}}(0); 0_{\nu}; c_{\mathsf{n}}(0)]$. ◊

2.3 Performance Analysis

The proof of Theorem 2.2.3 will be proceeded as follows. In Subsection 2.3.1, we first transform the entire DOB-controlled system (2.1.1), (2.2.17), (2.2.20), and (2.2.21) into a singular perturbation form [KKO99, Kha96], especially taking into account the generating model of the modeled external input $[r_{\mathsf{m}}(t); d_{\mathsf{m}}(t)]$.

After that, to figure out transient and steady-state behaviors of the transformed system, Subsection 2.3.2 presents Lyapunov analysis in the sense of the singular perturbation theory, from which the proof of the theorem is concluded.

For convenience, hereinafter we often drop the terms (θ) and $(\theta;\tau)$ in the variable and the subscript i in the matrix $\underline{\Upsilon}_i$ if trivial.

2.3.1 Coordinate Transformation to Singular Perturbation Form

We first employ stacked state variables

$$\chi := \begin{bmatrix} z_{\mathsf{n}}^{\dagger} \\ x \\ c \end{bmatrix} \in \mathbb{R}^{n+n_{\mathsf{c}}} \quad \text{and} \quad \chi_{\mathsf{n}} := \begin{bmatrix} z_{\mathsf{n}} \\ x_{\mathsf{n}} \\ c_{\mathsf{n}} \end{bmatrix} \in \mathbb{R}^{n+n_{\mathsf{c}}} \tag{2.3.1}$$

of the actual closed-loop system (2.1.1), (2.2.17), (2.2.20), and (2.2.21), and the nominal closed-loop system (2.1.3) and (2.1.4), respectively. The initial condition $\chi_{\mathsf{n}}(0)$ is set to $\chi(0)$ (as in the statement of Definition 2.1.1).

To compute the time derivatives of the new variables, we express the x-dynamics (2.1.1b) using the nominal components in (2.1.3b) as follows:

$$\dot{x} = A_\nu x + B_\nu \left(\psi_{\mathsf{n}}^\top z_{\mathsf{n}}^{\dagger} + \phi_{\mathsf{n}}^\top x + g_{\mathsf{n}} u_{\mathrm{BL}} \right) - B_\nu g \big(\overline{s}_{\mathsf{w}}(w) - d_{\mathrm{total}} \big) \tag{2.3.2}$$

where $d_{\mathrm{total}} \in \mathbb{R}$ is defined by

$$\begin{aligned} d_{\mathrm{total}} := \frac{1}{g} \Big(& \psi^\top z + \phi^\top x + g \left(\big(Jc + K(r - C_\nu x) \big) + gd \right) \\ & - \psi_{\mathsf{n}}^\top z_{\mathsf{n}}^{\dagger} - \phi_{\mathsf{n}}^\top x - g_{\mathsf{n}} \big(Jc + K(r - C_\nu x) \big) \Big). \end{aligned} \tag{2.3.3}$$

Then with A_{n} given in Assumption 2.1.3 and the new definitions

$$\mathsf{B}_{\mathsf{n}} := \begin{bmatrix} 0 \\ g_{\mathsf{n}} B_\nu K \\ F \end{bmatrix}, \quad \mathsf{C}_{\mathsf{n}} := \begin{bmatrix} 0^\top & C_\nu & 0^\top \end{bmatrix}, \quad \mathsf{E}_\chi := \begin{bmatrix} 0 \\ -B_\nu g \\ 0 \end{bmatrix}, \tag{2.3.4}$$

it is easy to obtain that

$$y = \mathsf{C}_\mathsf{n}\chi, \qquad \dot{\chi} = \mathsf{A}_\mathsf{n}\chi + \mathsf{B}_\mathsf{n} r + \mathsf{E}_\chi\big(\overline{s}_\mathsf{w}(w) - d_{\text{total}}\big), \tag{2.3.5}$$

and

$$y_\mathsf{n} = \mathsf{C}_\mathsf{n}\chi_\mathsf{n}, \qquad \dot{\chi}_\mathsf{n} = \mathsf{A}_\mathsf{n}\chi_\mathsf{n} + \mathsf{B}_\mathsf{n} r. \tag{2.3.6}$$

It is important to note that if the output of the DOB $w(t)$ satisfies

$$w(t) \equiv d_{\text{total}}(t) \in \overline{\mathcal{D}}_{\text{total},\mathsf{n}}, \tag{2.3.7}$$

then the actual χ-dynamics (2.3.5) is the same as the nominal one (2.3.6) exactly and so, the NPR of our interest is completely achieved (that is, $y(t) \equiv y_\mathsf{n}(t)$). From this viewpoint, we call d_{total} in (2.3.3) as the "total disturbance" [SPJ+16, Han09].

For further analysis, let us define a nonsingular matrix

$$\Phi_\mathsf{n} := \begin{bmatrix} 1 & 0 & \cdots & 0 & 0 \\ -\phi_{\mathsf{n},\nu} & 1 & & 0 & 0 \\ \vdots & & \ddots & & \vdots \\ -\phi_{\mathsf{n},3} & -\phi_{\mathsf{n},4} & \cdots & 1 & 0 \\ -\phi_{\mathsf{n},2} & -\phi_{\mathsf{n},3} & \cdots & -\phi_{\mathsf{n},\nu} & 1 \end{bmatrix} \in \mathbb{R}^{\nu\times\nu}. \tag{2.3.8}$$

In addition, with the new symbols

$$\overline{\phi}_\mathsf{n} := \begin{bmatrix} \phi_{\mathsf{n},\nu} \\ \vdots \\ \phi_{\mathsf{n},1} \end{bmatrix} \in \mathbb{R}^{\nu}, \tag{2.3.9a}$$

$$\Gamma(\theta;\tau) := \begin{bmatrix} A_{\nu+l_\mathsf{q}}^{\nu-1}\underline{\Upsilon}^{-1}\overline{\gamma} & \cdots & \underline{\Upsilon}^{-1}\overline{\gamma} \end{bmatrix} \in \mathbb{R}^{(\nu+l_\mathsf{q})\times\nu}, \tag{2.3.9b}$$

the vector $\overline{\beta} = \overline{\beta}(\theta;\tau)$ in (2.2.19) can be expressed in a simpler form

$$\begin{aligned} \overline{\beta} &= \underline{\Upsilon}\Big(-\frac{\mathsf{c}_{l_\mathsf{q}}}{\tau^\nu}\underline{\Upsilon}^{-1}\overline{\alpha} + A_{\nu+l_\mathsf{q}}^{\nu}\underline{\Upsilon}^{-1}\overline{\gamma} - \phi_{\mathsf{n},\nu}A_{\nu+l_\mathsf{q}}^{\nu-1}\underline{\Upsilon}^{-1}\overline{\gamma} - \cdots - \phi_{\mathsf{n},1}\underline{\Upsilon}^{-1}\overline{\gamma}\Big) \\ &= -\frac{\mathsf{c}_{l_\mathsf{q}}}{\tau^\nu}\overline{\alpha} + \underline{\Upsilon}A_{\nu+l_\mathsf{q}}^{\nu}\underline{\Upsilon}^{-1}\overline{\gamma} - \underline{\Upsilon}_{\nu+l_\mathsf{q}}\Gamma\overline{\phi}_\mathsf{n}. \end{aligned} \tag{2.3.10}$$

We then obtain the following lemma, by which the p-dynamics (2.2.17b) can be viewed as a "fast" dynamics from the perspective of the singular perturbation theory.

Lemma 2.3.1. In the coordinate change

$$\eta := \frac{1}{\tau}\underline{\Upsilon}_{\nu+l_{\mathsf{q}}}(\tau)\left(p + \Gamma(\theta;\tau)\Phi_{\mathsf{n}}\frac{1}{g_{\mathsf{n}}}x\right), \tag{2.3.11}$$

where Φ_{n} and $\Gamma(\theta;\tau)$ are given in (2.3.8) and (2.3.9a), respectively, the p-dynamics (2.2.17b) is transformed into

$$\begin{aligned}\tau\dot{\eta} = {} & \left(A_{\nu+l_{\mathsf{q}}} - \overline{\alpha}C_{\nu+l_{\mathsf{q}}}\right)\eta \\ & + \left(1 - \frac{g}{g_{\mathsf{n}}}\right)\overline{\gamma}(\theta;\tau)\overline{s}_{\mathsf{w}}\left(C_{\nu+l_{\mathsf{q}}}\eta\right) + \frac{g}{g_{\mathsf{n}}}\overline{\gamma}(\theta;\tau)d_{\text{total}}.\end{aligned} \tag{2.3.12}$$

$\Diamond$

Proof. Using the p-dynamics (2.2.17b), the control input (2.2.21), and the x-dynamics (2.3.2), one can differentiate η in (2.3.11) as

$$\begin{aligned}\dot{\eta} = {} & \frac{1}{\tau}\underline{\Upsilon}\dot{p} + \frac{1}{\tau}\underline{\Upsilon}\Gamma\Phi_{\mathsf{n}}\frac{1}{g_{\mathsf{n}}}\dot{x} \\ = {} & \frac{1}{\tau}\underline{\Upsilon}\Bigg[\left(A_{\nu+l_{\mathsf{q}}} - \underline{\Upsilon}^{-1}\overline{\alpha}C_{\nu+l_{\mathsf{q}}}\right)p \\ & \qquad - \underline{\Upsilon}^{-1}\overline{\gamma}\left(u_{\text{BL}} - \overline{s}_{\mathsf{w}}(w) + \frac{1}{g_{\mathsf{n}}}\psi_{\mathsf{n}}^{\top}z_{\mathsf{n}}^{\dagger}\right) + \underline{\Upsilon}^{-1}\overline{\beta}\frac{1}{g_{\mathsf{n}}}C_{\nu}x\Bigg] \\ & + \frac{1}{\tau}\underline{\Upsilon}\Gamma\Phi_{\mathsf{n}}\frac{1}{g_{\mathsf{n}}}\Bigg[\left(A_{\nu} + B_{\nu}\phi_{\mathsf{n}}^{\top}\right)x \\ & \qquad + g_{\mathsf{n}}B_{\nu}\left(u_{\text{BL}} + \frac{1}{g_{\mathsf{n}}}\psi_{\mathsf{n}}^{\top}z_{\mathsf{n}}^{\dagger}\right) - gB_{\nu}\left(\overline{s}_{\mathsf{w}}(w) - d_{\text{total}}\right)\Bigg] \\ = {} & \frac{1}{\tau}\underline{\Upsilon}\left(A_{\nu+l_{\mathsf{q}}} - \underline{\Upsilon}^{-1}\overline{\alpha}C_{\nu+l_{\mathsf{q}}}\right)p + \frac{1}{\tau}\left(\overline{\gamma} - \underline{\Upsilon}\Gamma\Phi_{\mathsf{n}}B_{\nu}\frac{g}{g_{\mathsf{n}}}\right)\overline{s}_{\mathsf{w}}(w) \\ & + \frac{1}{\tau}\left(-\overline{\gamma} + \underline{\Upsilon}\Gamma\Phi_{\mathsf{n}}B_{\nu}\right)\left(u_{\text{BL}} + \frac{1}{g_{\mathsf{n}}}\psi_{\mathsf{n}}^{\top}z_{\mathsf{n}}^{\dagger}\right) \\ & + \frac{1}{\tau}\underline{\Upsilon}\left\{\underline{\Upsilon}^{-1}\overline{\beta}C_{\nu} + \Gamma\Phi_{\mathsf{n}}(A_{\nu} + B_{\nu}\phi_{\mathsf{n}}^{\top})\right\}\frac{1}{g_{\mathsf{n}}}x + \frac{1}{\tau}\underline{\Upsilon}\Gamma\Phi_{\mathsf{n}}B_{\nu}\frac{g}{g_{\mathsf{n}}}d_{\text{total}}. \\ = {} & \frac{1}{\tau}\underline{\Upsilon}\left(A_{\nu+l_{\mathsf{q}}} - \underline{\Upsilon}^{-1}\overline{\alpha}C_{\nu+l_{\mathsf{q}}}\right)p + \frac{1}{\tau}\left(1 - \frac{g}{g_{\mathsf{n}}}\right)\overline{\gamma}\overline{s}_{\mathsf{w}}(w)\end{aligned} \tag{2.3.13, 2.3.14}$$

$$+\frac{1}{\tau}\underline{\Upsilon}\left\{\underline{\Upsilon}^{-1}\overline{\beta}C_\nu+\Gamma\Phi_{\mathsf{n}}(A_\nu+B_\nu\phi_{\mathsf{n}}^\top)\right\}\frac{1}{g_{\mathsf{n}}}x+\frac{1}{\tau}\overline{\gamma}\frac{g}{g_{\mathsf{n}}}d_{\text{total}}$$

where the last equality comes from

$$\underline{\Upsilon}\Gamma(\Phi_{\mathsf{n}}B_\nu)=\underline{\Upsilon}\Gamma B_\nu=\overline{\gamma}. \tag{2.3.15}$$

From now on, we claim that the matrix in the bracket of the last law satisfies

$$\underline{\Upsilon}^{-1}\overline{\beta}C_\nu+\Gamma\Phi_{\mathsf{n}}(A_\nu+B_\nu\phi_{\mathsf{n}}^\top)=(A_{\nu+l_{\mathsf{q}}}-\underline{\Upsilon}^{-1}\overline{\alpha}C_{\nu+l_{\mathsf{q}}})\Gamma\Phi_{\mathsf{n}}. \tag{2.3.16}$$

Indeed, by the expression of $\overline{\beta}$ in (2.3.10), one has

$$\begin{aligned}
&\underline{\Upsilon}^{-1}\overline{\beta}C_\nu+\Gamma\Phi_{\mathsf{n}}(A_\nu+B_\nu\phi_{\mathsf{n}}^\top) \\
&=\left(-\frac{\mathsf{C}_{l_{\mathsf{q}}}}{\tau^\nu}\underline{\Upsilon}^{-1}\overline{\alpha}+A^\nu_{\nu+l_{\mathsf{q}}}\underline{\Upsilon}^{-1}\overline{\gamma}-\Gamma\overline{\phi}_{\mathsf{n}}\right)C_\nu+\Gamma\Phi_{\mathsf{n}}(A_\nu+B_\nu\phi_{\mathsf{n}}^\top) \\
&=-\frac{\mathsf{C}_{l_{\mathsf{q}}}}{\tau^\nu}\underline{\Upsilon}^{-1}\overline{\alpha}C_\nu+A^\nu_{\nu+l_{\mathsf{q}}}\underline{\Upsilon}^{-1}\overline{\gamma}C_\nu+\Gamma\left(-\overline{\phi}_{\mathsf{n}}C_\nu+\Phi_{\mathsf{n}}(A_\nu+B_\nu\phi_{\mathsf{n}}^\top)\right).
\end{aligned} \tag{2.3.17}$$

To proceed, we derive

$$\begin{aligned}
&-\overline{\phi}_{\mathsf{n}}C_\nu+\Phi_{\mathsf{n}}(A_\nu+B_\nu\phi_{\mathsf{n}}^\top) \\
&=\begin{bmatrix}-\phi_{\mathsf{n},\nu}&0&\cdots&0&0\\-\phi_{\mathsf{n},\nu-1}&0&\cdots&0&0\\\vdots&\vdots&&\vdots&\vdots\\-\phi_{\mathsf{n},2}&0&\cdots&0&0\\-\phi_{\mathsf{n},1}&0&\cdots&0&0\end{bmatrix}+\begin{bmatrix}0&1&&0&0\\0&-\phi_{\mathsf{n},\nu}&\ddots&0&0\\\vdots&\vdots&&\ddots&\\0&-\phi_{\mathsf{n},3}&&-\phi_{\mathsf{n},\nu}&1\\\phi_{\mathsf{n},1}&0&\cdots&0&0\end{bmatrix} \\
&=\begin{bmatrix}-\phi_{\mathsf{n},\nu}&1&&0&0\\\vdots&\vdots&\ddots&\vdots&\vdots\\-\phi_{\mathsf{n},3}&-\phi_{\mathsf{n},4}&&1&0\\-\phi_{\mathsf{n},2}&-\phi_{\mathsf{n},3}&\cdots&-\phi_{\mathsf{n},\nu}&1\\0&0&\cdots&0&0\end{bmatrix}=A_\nu\Phi_{\mathsf{n}}.
\end{aligned} \tag{2.3.18}$$

From (2.3.18) and $C_\nu = C_\nu \Phi_{\mathsf{n}}$, the last two terms in (2.3.17) are computed by

$$\begin{aligned}
&A^\nu_{\nu+l_{\mathsf{q}}} \underline{\Upsilon}^{-1} \overline{\gamma} C_\nu + \Gamma \left(-\overline{\phi}_{\mathsf{n}} C_\nu + \Phi_{\mathsf{n}} (A_\nu + B_\nu \phi_{\mathsf{n}}^\top) \right) \\
&= A^\nu_{\nu+l_{\mathsf{q}}} \underline{\Upsilon}^{-1} \overline{\gamma} C_\nu + \left[A^{\nu-1}_{\nu+l_{\mathsf{q}}} \underline{\Upsilon}^{-1} \overline{\gamma} \quad \cdots \quad \underline{\Upsilon}^{-1} \overline{\gamma} \right] A_\nu \Phi_{\mathsf{n}} \\
&= A^\nu_{\nu+l_{\mathsf{q}}} \underline{\Upsilon}^{-1} \overline{\gamma} C_\nu \Phi_{\mathsf{n}} + \left[0_{\nu+l_{\mathsf{q}}} \quad A^{\nu-1}_{\nu+l_{\mathsf{q}}} \underline{\Upsilon}^{-1} \overline{\gamma} \quad \cdots \quad A_{\nu+l_{\mathsf{q}}} \underline{\Upsilon}^{-1} \overline{\gamma} \right] \Phi_{\mathsf{n}} \\
&= A_{\nu+l_{\mathsf{q}}} \Gamma \Phi_{\mathsf{n}}. \qquad (2.3.19)
\end{aligned}$$

By applying (2.3.19) and

$$(C_{\nu+l_{\mathsf{q}}} \Gamma) \Phi_{\mathsf{n}} = \frac{\mathsf{c}_{l_{\mathsf{q}}}}{\tau^\nu} C_\nu \Phi_{\mathsf{n}} = \frac{\mathsf{c}_{l_{\mathsf{q}}}}{\tau^\nu} C_\nu \qquad (2.3.20)$$

to (2.3.17), the claim is proved.

With the matrix equalities (2.3.16) and

$$p = \tau \underline{\Upsilon}^{-1} \eta - \Gamma \Phi_{\mathsf{n}} \frac{1}{g_{\mathsf{n}}} x, \quad w = \eta_1 = C_{\nu+l_{\mathsf{q}}} \eta, \qquad (2.3.21)$$

it is easy to see that the time derivative of η in (2.3.14) becomes

$$\begin{aligned}
\dot{\eta} = \frac{1}{\tau} \underline{\Upsilon} \big(A_{\nu+l_{\mathsf{q}}} - \underline{\Upsilon}^{-1} \overline{\alpha} C_{\nu+l_{\mathsf{q}}} \big) \Big(p + \Gamma \Phi_{\mathsf{n}} \frac{1}{g_{\mathsf{n}}} x \Big) \\
+ \frac{1}{\tau} \left(1 - \frac{g}{g_{\mathsf{n}}} \right) \overline{\gamma s}_{\mathsf{w}}(w) + \frac{1}{\tau} \overline{\gamma} \frac{g}{g_{\mathsf{n}}} d_{\text{total}} \\
= \frac{1}{\tau} \underline{\Upsilon} \big(A_{\nu+l_{\mathsf{q}}} - \underline{\Upsilon}^{-1} \overline{\alpha} C_{\nu+l_{\mathsf{q}}} \big) \tau \underline{\Upsilon}^{-1} \eta + \frac{1}{\tau} \left(1 - \frac{g}{g_{\mathsf{n}}} \right) \overline{\gamma s}_{\mathsf{w}}(C_{\nu+l_{\mathsf{q}}} \eta) + \frac{1}{\tau} \overline{\gamma} \frac{g}{g_{\mathsf{n}}} d_{\text{total}}. \qquad (2.3.22)
\end{aligned}$$

Finally, substituting

$$\underline{\Upsilon} A_{\nu+l_{\mathsf{q}}} \underline{\Upsilon}^{-1} = \frac{1}{\tau} A_{\nu+l_{\mathsf{q}}}, \quad C_{\nu+l_{\mathsf{q}}} \underline{\Upsilon}^{-1} = \frac{1}{\tau} C_{\nu+l_{\mathsf{q}}} \qquad (2.3.23)$$

to (2.3.22) concludes the proof of the lemma. □

We have observed that in the coordinate (2.3.11) for the state p, the actual closed-loop system (2.1.1), (2.2.17), (2.2.20), and (2.2.21) is represented as a standard singular perturbation form with respect to the perturbation parameter τ,

consisting of (2.1.1a), (2.3.5) and (2.3.12). Following the convention of the singular perturbation theory [Kha96, KKO99], in what follows we call η as "fast" variable, while the remaining variables z, χ, $d_{\rm total}$, r, and d as "slow" variables.

In order to analyze the nature of the fast variable η, we shall study the "boundary layer" of the singularly perturbed system (2.1.1a), (2.3.5) and (2.3.12). For this purpose, assume for now that all the slow variables are frozen as their initial values (that is,

$$z = z(0) \in \mathcal{Z}^0, \quad \chi = \chi_{\mathsf{n}}(0) \in \mathcal{Z}^0_{\mathsf{n}} \times \mathcal{X}^0 \times \mathcal{C}^0_{\mathsf{n}}, \tag{2.3.24}$$

$z = z(0) \in \mathcal{Z}^0$, $\chi = \chi_{\mathsf{n}}(0) \in \mathcal{Z}^0_{\mathsf{n}} \times \mathcal{X}^0 \times \mathcal{C}^0_{\mathsf{n}}$ and $d_{\rm total} = d_{\rm total,n}(0) \in \overline{\mathcal{D}}_{\rm total,n}$), and compute a solution $\eta^\star = [\eta^\star_1; \cdots; \eta^\star_{\nu+l_{\mathsf{q}}}]$ of the *degenerating equation*

$$\begin{aligned} 0 = &\left(A_{\nu+l_{\mathsf{q}}} - \overline{\alpha} C_{\nu+l_{\mathsf{q}}}\right)\eta^\star + \left(1 - \frac{g}{g_{\mathsf{n}}}\right)\overline{\gamma}(\theta;0)\overline{s}_{\mathsf{w}}\left(C_{\nu+l_{\mathsf{q}}}\eta^\star\right) \\ &+ \frac{g}{g_{\mathsf{n}}}\overline{\gamma}(\theta;0) d_{\rm total}, \end{aligned} \tag{2.3.25}$$

which is derived by putting $\tau = 0$ into the fast dynamics (2.3.12). In particular, the last row of (2.3.25) is given by

$$\begin{aligned} 0 &= -\mathsf{a}_0\eta^\star_1 + \left(1 - \frac{g}{g_{\mathsf{n}}}\right)\mathsf{c}_0(\theta;0)\overline{s}_{\mathsf{w}}\left(C_{\nu+l_{\mathsf{q}}}\eta^\star\right) + \frac{g}{g_{\mathsf{n}}}\mathsf{c}_0(\theta;0) d_{\rm total} \\ &= \mathsf{a}_0\left(-\eta^\star_1 + \left(1 - \frac{g}{g_{\mathsf{n}}}\right)\overline{s}_{\mathsf{w}}\left(\eta^\star_1\right) + \frac{g}{g_{\mathsf{n}}} d_{\rm total}\right) \end{aligned} \tag{2.3.26}$$

where $\mathsf{a}_0 = \mathsf{c}_0(\theta;0)$ is used. We note that the right-hand side of the last row is a monotonically decreasing function of $\eta^\star_1$, because for any $\mathsf{a}_0 > 0$ and $0 < \underline{g} \le g \le \overline{g}$,

$$\begin{aligned} &\frac{\partial}{\partial \eta^\star_1}\mathsf{a}_0\left(-\eta^\star_1 + \left(1 - \frac{g}{g_{\mathsf{n}}}\right)\overline{s}_{\mathsf{w}}\left(\eta^\star_1\right) + \frac{g}{g_{\mathsf{n}}} d_{\rm total}\right) \\ &\qquad = \mathsf{a}_0\left(-1 + \left(1 - \frac{g}{g_{\mathsf{n}}}\right)\frac{\partial \overline{s}_{\mathsf{w}}}{\partial \eta^\star_1}\right) \le -\mathsf{a}_0\frac{\underline{g}}{g_{\mathsf{n}}} < 0, \quad \forall \eta^\star_1 \in \mathbb{R} \end{aligned} \tag{2.3.27}$$

by the construction of $\overline{s}_{\mathsf{w}}$. (See (2.2.30).) This yields that the solution $\eta^\star_1$ of (2.3.26) (and thus $\eta^\star$ of the overall equation (2.3.25)) is "uniquely" determined.

Moreover, using the fact that the frozen variable $d_{\rm total}$ satisfies $\overline{s}_{\mathsf{w}}\big(d_{\rm total}\big) = d_{\rm total} \in \overline{\mathcal{D}}_{\rm total,n}$, one can easily find out the explicit form of $\eta^\star$ as

$$\eta^\star = \begin{bmatrix} 1 \\ \mathsf{a}_{\nu+\mu-1} \\ \vdots \\ \mathsf{a}_{\mu+1} \\ 0_\mu \end{bmatrix} d_{\rm total} =: \overline{\alpha}^\star d_{\rm total}. \tag{2.3.28}$$

In accordance with the singular perturbation theory [Kha96, KKO99], $\eta^\star$ in (2.3.28) is called the "quasi-steady-state" of the fast variable η.

We remark that if the fast variable $\eta(t)$ lies on the boundary layer $\eta = \eta^\star$ from the beginning, then

$$w(t) = \eta_1(t) \equiv \eta_1^\star(t) = d_{\rm total}(t)$$

and therefore, the nominal performance is exactly recovered (as aforementioned below (2.3.7).) Thus the singular perturbation theory [Kha96, KKO99] may say that, as long as the stability of the slow and fast subsystems is guaranteed and τ is chosen sufficiently small, the output $y(t)$ of the χ-dynamics (2.3.5) converges to and remains close to the nominal output $y_{\mathsf{n}}(t)$ of the χ_{n}-dynamics (2.3.6). However, this interpretation is not yet sufficient for the "asymptotic" NPR. One of the obstacles we encounter is that the standard singular perturbation theory [Kha96, KKO99] leads to approximate consequences in general, which makes it vague whether or not $y(t)$ "asymptotically" converges to $y_{\mathsf{n}}(t)$ when $[r_{\mathsf{u}}(t); d_{\mathsf{u}}(t)] \equiv 0$.

As a remedy to this issue, from now on we extend the quasi-steady-state $\eta^\star$ in (2.3.28) in the sense that the effect of the modeled inputs $r_{\mathsf{m}}(t)$ and $d_{\mathsf{m}}(t)$ comes out explicitly. For this, we first revisit the auxiliary output $d_{\rm total,n}(t)$ of the extended nominal closed-loop system (2.2.27) and (2.3.6). In accordance with the linear system theory, the steady-state response of $d_{\rm total,n}(t)$, denoted by $d^\star_{\rm total,n}(t)$,

can be decomposed as

$$d^\star_{\text{total},\mathsf{n}}(t) = d^\star_{\text{total},\mathsf{nu}}(t) + d^\star_{\text{total},\mathsf{nm}}(t) \tag{2.3.29}$$

where the partial steady-state response $d^\star_{\text{total},\mathsf{nu}}(t)$ and $d^\star_{\text{total},\mathsf{nm}}(t)$ correspond to the unmodeled input $[r_\mathsf{u}(t); d_\mathsf{u}(t)]$ and the modeled one $[r_\mathsf{m}(t); d_\mathsf{m}(t)]$, respectively. In particular, the latter must have the sinusoidal form

$$d^\star_{\text{total},\mathsf{nm}}(t) = M^\star_{\text{total},\mathsf{nm},0} + \sum_{i=1}^{n_\mathsf{m}} M^\star_{\text{total},\mathsf{nm},i} \sin(\sigma_i t + \varphi^\star_{\text{total},\mathsf{nm},i}) \tag{2.3.30}$$

for some constants $M^\star_{\text{total},\mathsf{nm},i}$ and $\varphi^\star_{\text{total},\mathsf{nm},,i} \in [0, \pi)$. Now let $\upsilon^\star_\mathsf{m}(t, \theta; \tau)$ be the sufficiently smooth signal

$$\upsilon^\star_\mathsf{m} = \begin{bmatrix} \upsilon^\star_{\mathsf{m},1} \\ \vdots \\ \upsilon^\star_{\mathsf{m},\nu+l_\mathsf{q}} \end{bmatrix} := \big(\overline{\gamma}(\theta;\tau) - \overline{\gamma}(\theta;0)\big) d^\star_{\text{total},\mathsf{nm}} - \tau\overline{\alpha}^\star \dot{d}^\star_{\text{total},\mathsf{nm}}. \tag{2.3.31}$$

At last, an extension of the quasi-steady-state $\eta^\star$ is given by

$$\begin{aligned} \eta^\star_{\text{ext}} &:= \eta^\star - \begin{bmatrix} 0 \\ \upsilon^\star_{\mathsf{m},1} \\ \tau {\upsilon^\star_{\mathsf{m},1}}^{(1)} + \upsilon^\star_{\mathsf{m},2} \\ \vdots \\ \sum_{j=1}^{\nu+l_\mathsf{q}-1} \tau^{\nu+l_\mathsf{q}-1-j} {\upsilon^\star_{\mathsf{m},j}}^{(\nu+l_\mathsf{q}-1-j)} \end{bmatrix} \\ &= \overline{\alpha}^\star d_{\text{total}} - \begin{bmatrix} 0 \\ \upsilon^\star_{\mathsf{m},1}(t) \\ \tau {\upsilon^\star_{\mathsf{m},1}}^{(1)} + \upsilon^\star_{\mathsf{m},2} \\ \vdots \\ \sum_{j=1}^{\nu+l_\mathsf{q}-1} \tau^{\nu+l_\mathsf{q}-1-j} {\upsilon^\star_{\mathsf{m},j}}^{(\nu+l_\mathsf{q}-1-j)} \end{bmatrix}. \end{aligned} \tag{2.3.32}$$

The extended quasi-steady-state $\eta^\star_{\text{ext}}$ in (2.3.32) is slightly shifted from the traditional one $\eta^\star(t)$ in (2.3.28), by an amount proportional to τ and $[r_\mathsf{m}(t); d_\mathsf{m}(t)]$; that is, if $\tau = 0$ or there is no modeled input (i.e., $[r_\mathsf{m}(t); d_\mathsf{m}(t)] \equiv 0$), then the

additional term in (2.3.32) disappears and thus $\eta^\star_{\text{ext}} = \eta^\star$.

With the notion of the extended quasi-steady-state, we are now ready to present an error dynamics to be used for the convergence analysis.

Lemma 2.3.2. In the coordinate changes

$$\tilde{z} := z - z_{\text{aux}}, \quad \tilde{\chi} := \begin{bmatrix} z_{\mathsf{n}}^\dagger \\ x \\ c \end{bmatrix} - \begin{bmatrix} z_{\mathsf{n}} \\ x_{\mathsf{n}} \\ c_{\mathsf{n}} \end{bmatrix}, \quad \tilde{\eta}_{\text{ext}} := \eta - \eta^\star_{\text{ext}}, \tag{2.3.33}$$

in which η and $\eta^\star_{\text{ext}}$ are defined in (2.3.11) and (2.3.32), the closed-loop system (2.1.1), (2.2.17), (2.2.20), and (2.2.21) is transformed into

$$\dot{\tilde{z}} = S\tilde{z} + G\mathsf{C}_{\mathsf{n}}\tilde{\chi}, \tag{2.3.34a}$$

$$\dot{\tilde{\chi}} = \mathsf{A}_{\mathsf{n}}\tilde{\chi} + \mathsf{E}_\chi \Omega\big(C_{\nu+l_{\mathsf{q}}}\tilde{\eta}_{\text{ext}}, d_{\text{total}}\big), \tag{2.3.34b}$$

$$\tilde{y} := \mathsf{C}_{\mathsf{n}}\tilde{\chi}, \qquad d_{\text{total}} = d_{\text{total},\mathsf{n}}(t) + \mathsf{C}_{\text{total},1}\tilde{z} + \mathsf{C}_{\text{total},2}\tilde{\chi} \tag{2.3.34c}$$

and

$$\begin{aligned} \tau\dot{\tilde{\eta}}_{\text{ext}} = {} & (A_{\nu+l_{\mathsf{q}}} - \overline{\alpha}C_{\nu+l_{\mathsf{q}}})\tilde{\eta}_{\text{ext}} + \left(1 - \frac{g}{g_{\mathsf{n}}}\right)\overline{\gamma}(\theta;0)\Omega\big(C_{\nu+l_{\mathsf{q}}}\tilde{\eta}_{\text{ext}}, d_{\text{total}}\big) \\ & + \delta(t, \tilde{\eta}_{\text{ext},1}, d_{\text{total}}; \tau) \end{aligned} \tag{2.3.35}$$

where A_{n}, C_{n}, and E_χ are given in (2.1.5) and (2.3.4),

$$\mathsf{C}_{\text{total},1} := \frac{1}{g}\psi^\top, \tag{2.3.36a}$$

$$\mathsf{C}_{\text{total},2} := \frac{1}{g}\begin{bmatrix} -\psi_{\mathsf{n}}^\top & (\phi^\top - \phi_{\mathsf{n}}^\top) - (g - g_{\mathsf{n}})KC_\nu & (g - g_{\mathsf{n}})J \end{bmatrix}, \tag{2.3.36b}$$

and

$$\begin{aligned} \Omega(\tilde{\eta}_{\text{ext},1}, d_{\text{total}}) &:= \overline{s}_{\mathsf{w}}(w) - d_{\text{total}} \\ &= \overline{s}_{\mathsf{w}}\big(C_{\nu+l_{\mathsf{q}}}\tilde{\eta}_{\text{ext},1} + d_{\text{total}}\big) - d_{\text{total}}, \end{aligned} \tag{2.3.37a}$$

$$\delta(t, \tilde{\eta}_{\text{ext},1}, d_{\text{total}}; \tau) := \left(1 - \frac{g}{g_{\mathsf{n}}}\right)\big(\overline{\gamma}(\theta;\tau) - \overline{\gamma}(\theta;0)\big)\Omega(\tilde{\eta}_{\text{ext},1}, d_{\text{total}})$$

$$+ \big(\overline{\gamma}(\theta;\tau) - \overline{\gamma}(\theta;0)\big)(d_{\text{total}} - d^{\star}_{\text{total},\mathsf{nm}}(t))$$
$$- \tau\overline{\alpha}^{\star}(\dot{d}_{\text{total}} - \dot{d}^{\star}_{\text{total},\mathsf{nm}}(t)). \tag{2.3.37b}$$

$\Diamond$

Proof. The slow error dynamics (2.3.34) is easily obtained by subtracting the $(z_{\text{aux}}, \chi_{\mathsf{n}})$-dynamics (2.2.27) and (2.3.6) from the (z,χ)-dynamics (2.1.1a) and (2.3.6) and by noting that

$$w = C_{\nu+l_{\mathsf{q}}}\eta = C_{\nu+l_{\mathsf{q}}}\tilde{\eta}_{\text{ext}} + C_{\nu+l_{\mathsf{q}}}\eta^{\star}_{\text{ext}} = C_{\nu+l_{\mathsf{q}}}\tilde{\eta}_{\text{ext}} + d_{\text{total}}.$$

In order to derive the fast error dynamics (2.3.35), we first consider an intermediate error variable $\tilde{\eta} := \eta - \eta^{\star}$ with the original quasi-steady-state $\eta^{\star}$, which satisfies

$$\tilde{\eta}_{\text{ext},1} = \tilde{\eta}_1, \tag{2.3.38a}$$
$$\tilde{\eta}_{\text{ext},i+1} = \tilde{\eta}_{i+1} + \tau\sum_{j=1}^{i-1}\tau^{i-1-j}\upsilon^{\star}_{\mathsf{m},j}{}^{(i-j)} + \upsilon^{\star}_{\mathsf{m},i}, \tag{2.3.38b}$$
$$\forall i = 1,\dots,\nu+l_{\mathsf{q}}-1,$$

by definition. It follows from the η-dynamics (2.3.12) and (2.3.38a) that

$$\begin{aligned}
\tau\dot{\tilde{\eta}} &= \tau\dot{\eta} - \tau\dot{\eta}^{\star} \qquad (2.3.39)\\
&= \big(A_{\nu+l_{\mathsf{q}}} - \overline{\alpha}C_{\nu+l_{\mathsf{q}}}\big)\,\tilde{\eta} + \left(1 - \frac{g}{g_{\mathsf{n}}}\right)\overline{\gamma}(\theta;0)\Omega(C_{\nu+l_{\mathsf{q}}}\tilde{\eta}, d_{\text{total}})\\
&\quad + \left(1 - \frac{g}{g_{\mathsf{n}}}\right)\big(\overline{\gamma}(\theta;\tau) - \overline{\gamma}(\theta;0)\big)\Omega(C_{\nu+l_{\mathsf{q}}}\tilde{\eta}, d_{\text{total}})\\
&\quad + \big(\overline{\gamma}(\theta;\tau) - \overline{\gamma}(\theta;0)\big)d_{\text{total}} - \tau\overline{\alpha}^{\star}\dot{d}_{\text{total}}\\
&= \big(A_{\nu+l_{\mathsf{q}}} - \overline{\alpha}C_{\nu+l_{\mathsf{q}}}\big)\,\tilde{\eta} + \left(1 - \frac{g}{g_{\mathsf{n}}}\right)\overline{\gamma}(\theta;0)\Omega(C_{\nu+l_{\mathsf{q}}}\tilde{\eta}, d_{\text{total}})\\
&\quad + \upsilon^{\star}_{\mathsf{m}}(t,\theta;\tau) + \delta(t, C_{\nu+l_{\mathsf{q}}}\tilde{\eta}, d_{\text{total}};\tau).
\end{aligned}$$

Now, by differentiating $\tilde{\eta}_{\text{ext}}$ in (2.3.32) and by applying (2.3.39) and (2.3.38b) to

the result, we have the $\tilde{\eta}_{\rm ext}$-dynamics as follows:

$$\tau\dot{\tilde{\eta}}_{\rm ext} = (A_{\nu+l_{\mathsf{q}}} - \overline{\alpha}C_{\nu+l_{\mathsf{q}}})\tilde{\eta}_{\rm ext} + \left(1 - \frac{g}{g_{\mathsf{n}}}\right)\overline{\gamma}(\theta;0)\Omega\big(C_{\nu+l_{\mathsf{q}}}\tilde{\eta}_{\rm ext}, d_{\rm total}\big) + \delta(t, C_{\nu+l_{\mathsf{q}}}\tilde{\eta}_{\rm ext}, d_{\rm total};\tau) + B_{\nu+l_{\mathsf{q}}}\sum_{j=1}^{\nu+l_{\mathsf{q}}}\tau^{\nu+l_{\mathsf{q}}-j}\upsilon_{\mathsf{m},j}^{\star\,(\nu+l_{\mathsf{q}}-j)}. \tag{2.3.40}$$

The proof of the lemma is then completed by showing that the summation in (2.3.40) is actually zero. Indeed, each component of $\upsilon_{\mathsf{m}}^{\star}(t)$ in (2.3.31) is represented by (for convenience, $\mathsf{a}_{\nu+l_{\mathsf{q}}} := 1$)

$$\upsilon_{\mathsf{m},j}^{\star}(t,\theta;\tau) = \begin{cases} -\tau\mathsf{a}_{\nu+l_{\mathsf{q}}+1-j}\dot{d}_{\rm total,nm}^{\star}(t), & j = 1,\dots,\nu-1, \\ (\mathsf{c}_{l_{\mathsf{q}}}(\theta;\tau) - \mathsf{a}_{l_{\mathsf{q}}})d_{\rm total,nm}^{\star}(t) - \tau\mathsf{a}_{l_{\mathsf{q}}+1}\dot{d}_{\rm total,nm}^{\star}(t), & j = \nu, \\ (\mathsf{c}_{\nu+l_{\mathsf{q}}-j}(\theta;\tau) - \mathsf{a}_{\nu+l_{\mathsf{q}}-j})d_{\rm total,nm}^{\star}(t), & j = \nu+1,\dots,\nu+l_{\mathsf{q}}. \end{cases}$$

Hence, with the differential operator $\mathfrak{s} := \mathrm{d}/\mathrm{d}t$, one has

$$\begin{aligned} &\sum_{j=1}^{\nu+l_{\mathsf{q}}}(\tau\mathfrak{s})^{\nu+l_{\mathsf{q}}-j}\upsilon_{\mathsf{m},j}^{\star}(t,\theta;\tau) \\ &= \sum_{j=1}^{\nu-1}(\tau\mathfrak{s})^{\nu+l_{\mathsf{q}}-j}\left(-\mathsf{a}_{\nu+l_{\mathsf{q}}+1-j}(\tau\mathfrak{s})\right)d_{\rm total,nm}^{\star}(t) \\ &\quad + (\tau\mathfrak{s})^{l_{\mathsf{q}}}\left((\mathsf{c}_{l_{\mathsf{q}}}(\theta;\tau) - \mathsf{a}_{l_{\mathsf{q}}}) - \mathsf{a}_{l_{\mathsf{q}}+1}(\tau\mathfrak{s})\right)d_{\rm total,nm}^{\star}(t) \\ &\quad + \sum_{j=\nu+1}^{\nu+l_{\mathsf{q}}}(\tau\mathfrak{s})^{\nu+l_{\mathsf{q}}-j}\big(\mathsf{c}_{\nu+l_{\mathsf{q}}-j}(\theta;\tau) - \mathsf{a}_{\nu+l_{\mathsf{q}}-j}\big)d_{\rm total,nm}^{\star}(t) \\ &= \Big[-\mathsf{a}_{\nu+l_{\mathsf{q}}}(\tau\mathfrak{s})^{\nu+l_{\mathsf{q}}} - \mathsf{a}_{\nu+l_{\mathsf{q}}-1}(\tau\mathfrak{s})^{\nu+l_{\mathsf{q}}-1} - \cdots - \mathsf{a}_0 \\ &\qquad\qquad + \mathsf{c}_{l_{\mathsf{q}}}(\theta;\tau)(\tau\mathfrak{s})^{l_{\mathsf{q}}} + \cdots + \mathsf{c}_0(\theta;\tau)\Big]d_{\rm total,nm}^{\star}(t) \\ &= -\big[\mathrm{D}_{\mathsf{q}}(\mathfrak{s};\tau) - \mathrm{N}_{\mathsf{q}}(\mathfrak{s};\tau)\big]d_{\rm total,nm}^{\star}(t) \end{aligned}$$

where $\mathrm{N}_{\mathsf{q}}(s;\tau)$ and $\mathrm{D}_{\mathsf{q}}(s;\tau)$ are the numerator and denominator of $\mathrm{Q}(s;\tau)$ in (2.2.10). Since the coefficients $\mathsf{c}_i(\theta;\tau)$ are chosen such that (2.2.7) holds for any given a_i and $\tau > 0$ (as in Proposition 2.2.2), the sinusoid $d_{\rm total,nm}^{\star}(t)$ in (2.3.30)

(whose frequencies are σ_i) satisfies

$$\sum_{j=1}^{\nu+l_{\mathsf{q}}}(\tau\mathfrak{s})^{\nu+l_{\mathsf{q}}-j}\upsilon^{\star}_{\mathsf{m},j}(t,\theta;\tau) = -\big[\mathrm{D}_{\mathsf{q}}(\mathfrak{s};\tau)-\mathrm{N}_{\mathsf{q}}(\mathfrak{s};\tau)\big]d^{\star}_{\mathrm{total},\mathsf{nm}}(t)$$
$$= -\mathfrak{s}\prod_{i=1}^{n_{\mathsf{m}}}(\mathfrak{s}^2+\sigma_i^2)\mathrm{R}_{\mathsf{q}}(\mathfrak{s};\tau)d^{\star}_{\mathrm{total},\mathsf{nm}}(t) = 0,$$

which concludes the proof of the lemma. □

We also remark some properties of the nonlinear functions Ω and δ in (2.3.37), which will be useful in the following analysis.

Lemma 2.3.3. Suppose that the inclusion

$$d_{\mathrm{total}} = d_{\mathrm{total},\mathsf{n}} + \mathsf{C}_{\mathrm{total},1}\tilde{z} + \mathsf{C}_{\mathrm{total},2}\tilde{\chi} \in \overline{\mathcal{D}}_{\mathrm{total},\mathsf{n}} \tag{2.3.41}$$

holds. Then the following statements are satisfied.

(a) $\Omega(0,d_{\mathrm{total}}) = 0$ and $\Omega(\tilde{\eta}_{\mathrm{ext},1},d_{\mathrm{total}})$ belongs to the sector $[0,1]$ with respect to the input $\tilde{\eta}_{\mathrm{ext},1}$: that is,

$$0 \le \frac{\partial}{\partial\tilde{\eta}_{\mathrm{ext},1}}\Omega\big(\tilde{\eta}_{\mathrm{ext},1},d_{\mathrm{total}}\big) \le 1 \tag{2.3.42}$$

(b) For $\tau\in(0,1)$,

$$\|\delta\big(t,\tilde{\eta}_{\mathrm{ext},1},d_{\mathrm{total}};\tau\big)\| \le \tau\mathsf{k}_{\delta,1}\|\tilde{z}\| + \tau\mathsf{k}_{\delta,2}\|\tilde{\chi}\| + \tau\mathsf{k}_{\delta,3}\|\tilde{\eta}_{\mathrm{ext}}\|$$
$$+ \tau\mathsf{k}_{\delta,4}\Big(\sup_{0\le\rho\le t}\Big\|[r_{\mathsf{u}}(\rho);\dot{r}_{\mathsf{u}}(\rho);d_{\mathsf{u}}(\rho);\dot{d}_{\mathsf{u}}(\rho)]\Big\|\Big)$$
$$+ \tau\mathsf{k}_{\delta,5}e^{-\mathsf{h}_{\delta}t}$$

where $\mathsf{k}_{\delta,j}$, $j=1,\dots,4$, and h_{δ} are positive constants independent of τ.

◊

Proof. The item (a) is trivial, because of the construction of $\overline{s}_{\mathsf{w}}$. For the item (b),

we rewrite the difference between $d_{\rm total}$ and $d^\star_{\rm total,nm}$ as

$$\begin{aligned} & d_{\rm total} - d^\star_{\rm total,nm} \\ & = (d_{\rm total} - d_{\rm total,n}) + (d_{\rm total,n} - d^\star_{\rm total,n}) + (d^\star_{\rm total,n} - d^\star_{\rm total,nm}) \\ & = \mathsf{C}_{\rm total,1}\tilde{z} + \mathsf{C}_{\rm total,2}\tilde{\chi} + (d_{\rm total,n} - d^\star_{\rm total,n}) + d^\star_{\rm total,nu}. \end{aligned} \tag{2.3.43}$$

in which the last equality results from (2.3.29). It is noted that the second term $d_{\rm total,n}(t) - d^\star_{\rm total,n}(t)$ implies the transient response of $d_{\rm total,n}(t)$ by definition, which vanishes exponentially as time goes on. On the other hand, for the partial steady-state response $d^\star_{\rm total,nu}(t)$ corresponding to $[r_{\rm u}(t); d_{\rm u}(t)]$, one can obtain an upper bound of $\|[d^\star_{\rm total,nu}(t); \dot{d}^\star_{\rm total,nu}(t)]\|$ that is proportional to $\sup_{0\le\rho\le t}\|[r_{\rm u}(\rho); \dot{r}_{\rm u}(\rho); d_{\rm u}(\rho); \dot{d}_{\rm u}(\rho)]\|$. Consequently, the item (b) is derived from the item (a), the $(\tilde{z},\tilde{\chi})$-dynamics (2.3.34), the equality (2.3.43), and the fact that $\|\overline{\gamma}(\theta;\tau) - \overline{\gamma}(\theta;0)\| \le \mathsf{k}_\gamma\tau$ for a τ-independent constant $\mathsf{k}_\gamma > 0$ and for all $\tau \in (0,1)$. □

2.3.2 Lyapunov Analysis

Based on the results of the previous subsection, the rest of this section is devoted to prove Theorem 2.2.3 with the error dynamics (2.3.34) and (2.3.35).

To this end, we now present a Lyapunov function candidate for the singularly perturbed system (2.3.34) and (2.3.40) as follows. For the slow subsystems (2.3.34a) and (2.3.34b) whose system matrices S and A_{n} are Hurwitz, define

$$V_{\rm slow}(\tilde{z},\tilde{\chi}) := \tilde{z}^\top P_{\mathsf{z}}\tilde{z} + \tilde{\chi}^\top P_\chi\tilde{\chi} \tag{2.3.44}$$

where the matrices $P_{\mathsf{z}} = P_{\mathsf{z}}^\top > 0$ and $P_\chi = P_\chi^\top > 0$ are the solutions of the Lyapunov equations

$$S^\top P_{\mathsf{z}} + P_{\mathsf{z}} S = -I, \qquad \mathsf{A}_{\mathsf{n}}^\top P_\chi + P_\chi \mathsf{A}_{\mathsf{n}} = -I. \tag{2.3.45}$$

To obtain a Lyapunov function for the fast subsystem (2.3.32), let us consider the "boundary-layer system" of the singular perturbation form (2.3.34) and (2.3.35),

which is given by

$$\frac{\mathrm{d}}{\mathrm{d}\varsigma}\tilde{\eta}_{\mathrm{ext}} = (A_{\nu+l_{\mathsf{q}}} - \overline{\alpha}C_{\nu+l_{\mathsf{q}}})\tilde{\eta}_{\mathrm{ext}} + \left(1 - \frac{g}{g_{\mathsf{n}}}\right)\overline{\gamma}(\theta;0)\Omega\big(C_{\nu+l_{\mathsf{q}}}\tilde{\eta}_{\mathrm{ext}}, d_{\mathrm{total}}\big) \quad (2.3.46)$$

where $\varsigma := t/\tau$ is a scaled time variable, and the slow variable d_{total} in (2.3.46) is assumed to be frozen as $d_{\mathrm{total}} = d_{\mathrm{total}}(0) \in \overline{\mathcal{D}}_{\mathrm{total},\mathsf{n}}$. We claim that the origin of the boundary-layer system (2.3.46) is globally exponentially stable. Indeed, with the symbols $u_\eta := -(g/g_{\mathsf{n}} - 1)\Omega$ and $y_\eta := C_{\nu+l_{\mathsf{q}}}\tilde{\eta}_{\mathrm{ext}}$, one can rewrite (2.3.46) into the form of a Lur'e-type system [Kha96]

$$\frac{\mathrm{d}}{\mathrm{d}\varsigma}\tilde{\eta}_{\mathrm{ext}} = (A_{\nu+l_{\mathsf{q}}} - \overline{\alpha}C_{\nu+l_{\mathsf{q}}})\tilde{\eta}_{\mathrm{ext}} + \overline{\gamma}(\theta;0)u_\eta, \qquad y_\eta = C_{\nu+l_{\mathsf{q}}}\tilde{\eta}_{\mathrm{ext}}, \quad (2.3.47a)$$

$$u_\eta = -\left(\frac{g}{g_{\mathsf{n}}} - 1\right)\Omega\big(y_\eta, d_{\mathrm{total}}(t)\big). \quad (2.3.47b)$$

where $t = \varsigma/\tau$. Notice that for the linear subsystem (2.3.47a) (from u_η to y_η), its transfer function is given by

$$\begin{aligned} &C_{\nu+l_{\mathsf{q}}}(sI - A_{\nu+l_{\mathsf{q}}} + \overline{\alpha}C_{\nu+l_{\mathsf{q}}})^{-1}\overline{\gamma}(\theta;0) \\ &= \frac{\mathsf{a}_{l_{\mathsf{q}}}s^{l_{\mathsf{q}}} + \cdots + \mathsf{a}_1 s + \mathsf{a}_0}{s^{\nu+l_{\mathsf{q}}} + \mathsf{a}_{\nu+l_{\mathsf{q}}-1}s^{\nu+l_{\mathsf{q}}-1} + \cdots + \mathsf{a}_1 s + \mathsf{a}_0}. \end{aligned}$$

where the equalities $\mathsf{c}_i(0) = \mathsf{a}_i(0)$, $i = 0, \ldots, n_{\mathsf{m}}$ are used. Then by the selection of a_i, it follows that

$$\frac{1 + (\overline{g}/g_{\mathsf{n}} - 1)C_{\nu+l_{\mathsf{q}}}(sI - A_{\nu+l_{\mathsf{q}}} + \overline{\alpha}C_{\nu+l_{\mathsf{q}}})^{-1}\overline{\gamma}(\theta;0)}{1 + (\underline{g}/g_{\mathsf{n}} - 1)C_{\nu+l_{\mathsf{q}}}(sI - A_{\nu+l_{\mathsf{q}}} + \overline{\alpha}C_{\nu+l_{\mathsf{q}}})^{-1}\overline{\gamma}(\theta;0)} = \mathrm{Z}_{\nu,l_{\mathsf{q}}}(s)$$

is SPR [Kha96]. In addition, the item (a) of Lemma 2.3.3 and Assumption 2.1.1 imply that as long as d_{total} is included in $\overline{\mathcal{D}}_{\mathrm{total},\mathsf{n}}$ (which is the case when the slow variables are frozen), the nonlinear function $(g/g_{\mathsf{n}} - 1)\Omega$ in (2.3.47b) belongs to the sector $[\underline{g}/g_{\mathsf{n}} - 1, \overline{g}/g_{\mathsf{n}} - 1]$ with respect to the input y_η. As a result, the circle criterion [Kha96, Theorem 7.1] concludes that the origin of the Lur'e-type system (2.3.47) (and thus that of the boundary-layer system (2.3.46)) is globally

exponentially stable; more precisely, there exists a quadratic Lyapunov function

$$V_{\text{fast}}(\tilde{\eta}_{\text{ext}}) = \tilde{\eta}_{\text{ext}}^{\top} P_{\eta} \tilde{\eta}_{\text{ext}} \tag{2.3.48}$$

with a positive definite matrix $P_\eta = P_\eta^\top > 0$ such that the time derivative of V_{fast} along with (2.3.47) is given by

$$\begin{aligned} \tau \dot{V}_{\text{fast}} &= \Big((A_{\nu+l_{\mathsf{q}}} - \overline{\alpha} C_{\nu+l_{\mathsf{q}}}) \tilde{\eta}_{\text{ext}} + \overline{\gamma}(\theta;0) u_{\eta} \Big)^{\top} P_{\eta} \tilde{\eta}_{\text{ext}} \\ &\quad + \tilde{\eta}_{\text{ext}}^{\top} P_{\eta} \Big((A_{\nu+l_{\mathsf{q}}} - \overline{\alpha} C_{\nu+l_{\mathsf{q}}}) \tilde{\eta}_{\text{ext}} + \overline{\gamma}(\theta;0) u_{\eta} \Big) \\ &\leq -\tilde{\eta}_{\text{ext}}^{\top} \tilde{\eta}_{\text{ext}}. \end{aligned} \tag{2.3.49}$$

We note in advance that (2.3.49) is still valid even if $d_{\text{total}}(t)$ in (2.3.47) is not frozen but slowly varying and satisfies (2.3.41). Finally, integrating two partial candidates V_{slow} and V_{fast} into one, a Lyapunov function candidate for the overall system (2.3.34) and (2.3.35) is presented as follows:

$$\begin{aligned} V\big(\tilde{z}, \tilde{\chi}, \tilde{\eta}_{\text{ext}}\big) &:= V_{\text{slow}}(\tilde{z}, \tilde{\chi}) + \tau V_{\text{fast}}(\tilde{\eta}_{\text{ext}}) \\ &= \tilde{z}^{\top} P_{\mathsf{z}} \tilde{z} + \tilde{\chi}^{\top} P_{\chi} \tilde{\chi} + \tau \tilde{\eta}_{\text{ext}}^{\top} P_{\eta} \tilde{\eta}_{\text{ext}} \end{aligned} \tag{2.3.50}$$

For simplicity, in what follows we will use $V(t)$ instead of $V(\tilde{z}(t), \tilde{\chi}(t), \tilde{\eta}_{\text{ext}}(t))$ (and $V_{\text{slow}}(t)$ and $V_{\text{fast}}(t)$ similarly).

Before going on further, it should be pointed out that the Lyapunov level set $V(0)$ may diverge as τ approaches zero, whereas $V_{\text{slow}}(0) = 0$ by definition. To see this, we investigate the matrix $\underline{\Upsilon}(\tau)\Gamma(\theta;\tau)$ in (2.3.11), which is computed by

$$\begin{aligned} \underline{\Upsilon}(\tau)\Gamma(\theta;\tau) &= \Big[\underline{\Upsilon}(\tau) A_{\nu+l_{\mathsf{q}}}^{\nu-1} \underline{\Upsilon}^{-1}(\tau) \overline{\gamma}(\theta;\tau) \quad \cdots \quad \underline{\Upsilon}(\tau) \underline{\Upsilon}^{-1}(\tau) \overline{\gamma}(\theta;\tau) \Big] \\ &= \left[\frac{1}{\tau^{\nu-1}} A_{\nu+l_{\mathsf{q}}}^{\nu-1} \overline{\gamma}(\theta;\tau) \quad \cdots \quad \overline{\gamma}(\theta;\tau) \right]. \end{aligned}$$

Since i-th component $\mathsf{c}_i(\theta;\tau)$ of the vector $\overline{\gamma}(\theta;\tau)$ has the form of $\mathsf{c}_i(\theta;\tau) = \mathsf{a}_i + \tau^2 \tilde{\mathsf{c}}_i(\theta;\tau)$ (by Proposition 2.2.2), each component of the matrix is a polynomial

of $1/\tau$ whose order is possibly up to $\nu - 1$. This incur that

$$\begin{aligned}\tilde{\eta}_{\text{ext}}(0,\theta;\tau) &= \frac{1}{\tau}\underline{\Upsilon}(\tau)q(0) + \frac{1}{\tau}\underline{\Upsilon}(\tau)\Gamma(\theta;\tau)\Phi_{\mathsf{n}}\frac{1}{g_{\mathsf{n}}}x(0) - \eta^{\star}_{\text{ext}}(0,\sigma;\tau) \\ &= \sum_{j=-(\nu+l_{\mathsf{q}})}^{\nu} \mathsf{v}_{\eta,j}\frac{1}{\tau^j} \end{aligned} \tag{2.3.51}$$

with constant vectors $\mathsf{v}_{\eta,j} \in \mathbb{R}^{\nu+l_{\mathsf{q}}}$, $j = -(\nu + l_{\mathsf{q}}), \ldots, \nu$, by which the claim is obtained.

As an alternative way, we divide the entire time period into two subintervals. For this purpose, take $0 < \epsilon' < \epsilon/2$ such that

$$\left\| \begin{bmatrix} \mathsf{C}_{\text{total},1} & \mathsf{C}_{\text{total},2} \end{bmatrix} \right\| \epsilon' < \text{dist}\big(\mathcal{D}_{\text{total},\mathsf{n}}, \overline{\mathcal{D}}_{\text{total},\mathsf{n}}\big) \tag{2.3.52}$$

and then select sufficiently small $T^{\star} > 0$ to be independent of τ and to satisfy

$$V_{\text{slow}}(t) \le \underline{\lambda}\big(\text{diag}\big(P_{\mathsf{z}}, P_{\chi}\big)\big)\frac{\epsilon'^2}{4}, \quad \forall 0 \le t \le T^{\star}. \tag{2.3.53}$$

This selection is always possible, because (a) the slow variables $\tilde{z}$ and $\tilde{\chi}$ are initiated at the origin, and (b) the saturation function $\overline{s}_{\mathsf{w}}(w)$ in (2.3.34) makes the velocity of $\tilde{z}$ and $\tilde{\chi}$ bounded around the origin $\tilde{\chi} = 0$ (regardless of $\tilde{\eta}_{\text{ext}}$ and τ). It is obtained from (2.3.52) and (2.3.53) that for all $0 \le t \le T^{\star}$,

$$\|\tilde{z}(t)\|^2 + \|\tilde{\chi}(t)\|^2 \le \frac{1}{\underline{\lambda}\big(\text{diag}\big(P_{\mathsf{z}}, P_{\chi}\big)\big)}\Big(\tilde{z}^{\top}(t)P_{\mathsf{z}}\tilde{z}(t) + \tilde{\chi}^{\top}(t)P_{\chi}\tilde{\chi}(t)\Big) \le \frac{\epsilon'^2}{4}$$

and therefore,

$$\|y(t) - y_{\mathsf{n}}(t)\| = \|\mathsf{C}_{\mathsf{n}}\tilde{\chi}(t)\| \le \frac{\epsilon'}{2} < \frac{\epsilon}{2} \quad \text{and} \tag{2.3.54a}$$

$$d_{\text{total}}(t) = d_{\text{total},\mathsf{n}}(t) + \mathsf{C}_{\text{total},1}\tilde{z}(t) + \mathsf{C}_{\text{total},2}\tilde{\chi}(t) \in \overline{\mathcal{D}}_{\text{total},\mathsf{n}}. \tag{2.3.54b}$$

From now on, we investigate two important natures of the closed-loop system (2.3.34) and (2.3.40) in the sense of Lyapunov, especially for the transient period $0 \le t < T^{\star}$ and the steady-state period $T^{\star} \le t < \infty$. The first one is about the convergence of the fast variable $\tilde{\eta}_{\text{ext}}$.

Lemma 2.3.4. Suppose that Assumption 2.1.1 is satisfied. Then there exists $0 < \overline{\tau}_1 < 1$ such that for $\tau \in (0, \overline{\tau}_1)$,

$$V_{\rm fast}(T^\star) \le -\frac{\mathsf{k}_{\eta,1}}{\tau^{2\nu}} e^{-(\mathsf{h}_\eta/\tau)T^\star} + \tau \mathsf{k}_{\eta,2} \tag{2.3.55}$$

where $\mathsf{k}_{\eta,1}$, $\mathsf{k}_{\eta,2}$, and h_η are τ-independent positive constants. $\lozenge$

Proof. Note that the hypothesis of Lemma 2.3.3 (and therefore (2.3.49)) naturally holds during the transient period $t \in [0, T^\star]$. Thus for all $0 \le t \le T^\star$, the time derivative of $V_{\rm fast}$ along with the fast subsystem (2.3.40) and with $\tau \in (0,1)$ is computed as

$$\begin{aligned}
\tau \dot{V}_{\rm fast} &\le -\tilde{\eta}_{\rm ext}^\top \tilde{\eta}_{\rm ext} + 2\tilde{\eta}_{\rm ext}^\top P_\eta \delta\big(t, C_{\nu+l_{\mathsf{q}}} \tilde{\eta}_{\rm ext}, d_{\rm total}; \tau\big) \\
&\le -\tilde{\eta}_{\rm ext}^\top \tilde{\eta}_{\rm ext} \\
&\quad + \tau \|\tilde{\eta}_{\rm ext}\| \|2P_\eta\| \Bigg[\mathsf{k}_{\delta,1} \|\tilde{z}\| + \mathsf{k}_{\delta,2} \|\tilde{\chi}\| + \mathsf{k}_{\delta,3} \|\tilde{\eta}_{\rm ext}\| \\
&\qquad\qquad + \mathsf{k}_{\delta,4} \Bigg(\sup_{0 \le \rho \le t} \Big\| [r_{\mathsf{u}}(\rho); \dot{r}_{\mathsf{u}}(\rho); d_{\mathsf{u}}(\rho); \dot{d}_{\mathsf{u}}(\rho)] \Big\| \Bigg) + \mathsf{k}_{\delta,5} e^{-\mathsf{h}_\delta t} \Bigg] \\
&\le \Big(-1 + \tau \mathsf{k}'_{\delta,3} \Big) \tilde{\eta}_{\rm ext}^\top \tilde{\eta}_{\rm ext} \\
&\quad + \tau \mathsf{k}'_{\delta,1} \tilde{z}^\top \tilde{z} + \tau \mathsf{k}'_{\delta,2} \tilde{\chi}^\top \tilde{\chi} + \tau \mathsf{k}'_{\delta,4} \Bigg(\sup_{0 \le \rho \le t} \Big\| [r_{\mathsf{u}}(\rho); \dot{r}_{\mathsf{u}}(\rho); d_{\mathsf{u}}(\rho); \dot{d}_{\mathsf{u}}(\rho)] \Big\| \Bigg)^2 \\
&\quad + \tau \mathsf{k}'_{\delta,5} e^{-2\mathsf{h}_\delta t}
\end{aligned}$$

where $\mathsf{k}'_{\delta,i}$, $i = 1, \ldots, 5$, are some positive constants. In particular, with τ taken as $\tau \le \overline{\tau}_1 := \min\{1, 1/(2\mathsf{k}'_{\delta,3})\}$, the last inequality turns out to be

$$\begin{aligned}
\dot{V}_{\rm fast} &\le -\frac{\mathsf{h}_\eta}{\tau} V_{\rm fast} + \frac{\mathsf{k}'_{\delta,1}}{\underline{\lambda}(P_\chi)} \tilde{z}^\top P_{\mathsf{z}} \tilde{z} + \frac{\mathsf{k}'_{\delta,2}}{\underline{\lambda}(P_\chi)} \tilde{\chi}^\top P_\chi \tilde{\chi} \\
&\qquad + \mathsf{k}'_{\delta,4} \Bigg(\sup_{0 \le \rho \le t} \Big\| [r_{\mathsf{u}}(\rho); \dot{r}_{\mathsf{u}}(\rho); d_{\mathsf{u}}(\rho); \dot{d}_{\mathsf{u}}(\rho)] \Big\| \Bigg)^2 + \mathsf{k}'_{\delta,5} e^{-2\mathsf{h}_\delta t} \\
&\le -\frac{\mathsf{h}_\eta}{\tau} V_{\rm fast} + \mathsf{k}'_{\delta,12} V_{\rm slow} \\
&\qquad + \mathsf{k}'_{\delta,4} \Bigg(\sup_{0 \le \rho \le t} \Big\| [r_{\mathsf{u}}(\rho); \dot{r}_{\mathsf{u}}(\rho); d_{\mathsf{u}}(\rho); \dot{d}_{\mathsf{u}}(\rho)] \Big\| \Bigg)^2 + \mathsf{k}'_{\delta,5} e^{-2\mathsf{h}_\delta t}
\end{aligned} \tag{2.3.56}$$

where $\mathsf{h}_\eta := 1/\big(2\overline{\lambda}(P_\eta)\big)$ and $\mathsf{k}'_{\delta,12} := \max\{\mathsf{k}'_{\delta,1}/\underline{\lambda}(P_\chi), \mathsf{k}'_{\delta,2}/\underline{\lambda}(P_\chi)\}$. Now, applying the comparison lemma [Kha96] to (2.3.56), we obtain

$$
\begin{aligned}
&V_{\text{fast}}(T^\star) \qquad\qquad (2.3.57)\\
&\le e^{-(\mathsf{h}_\eta/\tau)T^\star} V_{\text{fast}}(0) + \int_0^{T^\star} e^{-(\mathsf{h}_\eta/\tau)(T^\star-\omega)} \Bigg\{ \mathsf{k}'_{\delta,12} V_{\text{slow}}(\omega) \\
&\qquad\qquad + \mathsf{k}'_{\delta,4} \Bigg(\sup_{0\le\rho\le\omega} \Big\| [r_{\mathsf{u}}(\rho); \dot{r}_{\mathsf{u}}(\rho); d_{\mathsf{u}}(\rho); \dot{d}_{\mathsf{u}}(\rho)] \Big\| \Bigg)^2 + \mathsf{k}'_{\delta,5} e^{-2\mathsf{h}_\delta \omega} \Bigg\} \mathrm{d}\omega \\
&\le e^{-(\mathsf{h}_\eta/\tau)T^\star} V_{\text{fast}}(0) + \Bigg[e^{-(\mathsf{h}_\eta/\tau)T^\star} \Bigg(\int_0^{T^\star} e^{(\mathsf{h}_\eta/\tau)\omega} d\omega \Bigg) \\
&\qquad\qquad \times \Bigg(\mathsf{k}'_{\delta,12} \underline{\lambda}\big(\mathrm{diag}\big(P_{\mathsf{z}}, P_\chi\big)\big) \frac{\epsilon'^2}{4} + \mathsf{k}'_{\delta,4} (\overline{r}^2 + \overline{d}^2) + \mathsf{k}'_{\delta,5} \Bigg) \Bigg] \\
&\le e^{-(\mathsf{h}_\eta/\tau)T^\star} V_{\text{fast}}(0) + \tau \mathsf{k}'_\delta
\end{aligned}
$$

where $\mathsf{k}_\delta > 0$ is a constant. The lemma then follows from the fact that $V_{\text{fast}}(0) = \tilde{\eta}_{\text{ext}}^\top(0) P_\eta \tilde{\eta}_{\text{ext}}(0)$ is a polynomial of $1/\tau$ due to (2.3.51). □

Since the right-hand side of (2.3.4) gets decreased as τ becomes smaller, Lemma 2.3.4 implies that the fast variable $\eta(t)$ with small τ quickly approaches near the extended quasi-steady-state $\eta(t) = \eta^\star_{\text{ext}}(t, \theta; \tau)$ as close as desired, with little effect on the slow error variables $\tilde{z}$ and $\tilde{\chi}$ for the transient period $0 \le t < T^\star$. More specifically, one can select $0 < \overline{\tau}^\star_1 < \overline{\tau}_1$ such that

$$
\begin{aligned}
V(T^\star) &= V_{\text{slow}}(T^\star) + \tau V_{\text{fast}}(T^\star) \qquad (2.3.58)\\
&\le \underline{\lambda}\big(\mathrm{diag}\big(P_{\mathsf{z}}, P_\chi\big)\big) \frac{\epsilon'^2}{4} + \tau \left(-\frac{\mathsf{k}_{\eta,1}}{\tau^{2\nu}} e^{-(\mathsf{h}_\eta/\tau)T^\star} + \tau \mathsf{k}_{\eta,2} \right) \\
&\le \underline{\lambda}\big(\mathrm{diag}\big(P_{\mathsf{z}}, P_\chi\big)\big) \frac{\epsilon'^2}{2}
\end{aligned}
$$

for all $\tau \in (0, \overline{\tau}^\star_1)$.

Next, the following lemma describes that, as long as the total disturbance $d_{\text{total}}(t)$ remains in the compact set $\overline{\mathcal{D}}_{\text{total},\mathsf{n}}$ for the steady-state period, the overall system is stable in the ISS sense with respect to the partial inputs r_{u} and d_{u}.

Lemma 2.3.5. Suppose that Assumptions 2.1.2–2.1.3 and the inclusion (2.3.41) hold. Then there exists $0 < \overline{\tau}_2 < 1$ satisfying that for $\tau \in (0, \overline{\tau}_2)$,

$$V(t) \le e^{-\mathsf{h_v}(t-T^\star)}\big(V(T^\star) + \tau \mathsf{k}_{\mathsf{v},1}\big) + \tau \mathsf{k}_{\mathsf{v},2}\bigg(\sup_{0\le\rho\le t}\Big\|[r_{\mathsf{u}}(\rho); \dot{r}_{\mathsf{u}}(\rho); d_{\mathsf{u}}(\rho); \dot{d}_{\mathsf{u}}(\rho)]\Big\|\bigg)^2, \quad \forall t \ge T^\star \tag{2.3.59}$$

where $\mathsf{k}_{\mathsf{v},1}$, $\mathsf{k}_{\mathsf{v},2}$, and $\mathsf{h_v}$ are positive constants independent on τ. ◊

Proof. The lemma can be easily proved by differentiating the Lyapunov function V in (2.3.50) and applying the comparison lemma [Kha96] to the resulting $\dot{V}$ in a similar way of Lemma 2.3.4. □

To complete the proof of the theorem, we now claim that when τ is selected sufficiently small, the requirement (2.3.41) on d_{total} is automatically satisfied for $t \ge 0$. Indeed, with $\overline{\tau}_3 := \underline{\lambda}\big(\text{diag}\big(P_{\mathsf{z}}, P_\chi\big)\big)\epsilon'^2/2(\mathsf{k}_{\mathsf{v},1} + \mathsf{k}_{\mathsf{v},2}(\overline{r}^2 + \overline{d}^2))$, the above two inequalities (2.3.58) and (2.3.59) yield that for all $\tau \le \min\{\overline{\tau}_1^\star, \overline{\tau}_2, \overline{\tau}_3\}$,

$$\begin{aligned} V_{\text{slow}}(t) \le V(t) &\le e^{-\mathsf{h_v}(t-T^\star)}\underline{\lambda}\big(\text{diag}\big(P_{\mathsf{z}}, P_\chi\big)\big)\frac{\epsilon'^2}{2} \\ &\quad + \tau\mathsf{k}_{\mathsf{v},1} + \tau\mathsf{k}_{\mathsf{v},2}\bigg(\sup_{0\le\rho\le t}\Big\|[r_{\mathsf{u}}(\rho); \dot{r}_{\mathsf{u}}(\rho); d_{\mathsf{u}}(\rho); \dot{d}_{\mathsf{u}}(\rho)]\Big\|\bigg)^2 \\ &\le \underline{\lambda}\big(\text{diag}\big(P_{\mathsf{z}}, P_\chi\big)\big)\epsilon'^2 \end{aligned} \tag{2.3.60}$$

as long as (2.3.41) is satisfied. The claim is then easily proved by contradiction, using the statement (2.3.54) and the fact that $d_{\text{total}}(t)$ belongs to the desired set $\overline{\mathcal{D}}_{\text{total},\mathsf{n}}$ at least during the transient $t \in [0, T^\star]$. In summary, we have shown that with $\tau \le \overline{\tau} := \min\{\overline{\tau}_1^\star, \overline{\tau}_2, \overline{\tau}_3\}$, both (2.1.10) and (2.2.8) are satisfied at once, which proves Theorem 2.2.3.

To gain more insight on the proposed DOB scheme, we further note that when the external input is fully modeled (i.e., $r(t) = r_{\mathsf{m}}(t)$ and $d(t) = d_{\mathsf{m}}(t)$), the DOB's output $w(t)$ can play a role as an "asymptotic" estimate of the total disturbance $d_{\text{total}}(t)$.

Corollary 2.3.6. Suppose that Assumptions 2.1.1–2.1.4 hold and $[r_{\mathsf{u}}(t); d_{\mathsf{u}}(t)] \equiv$

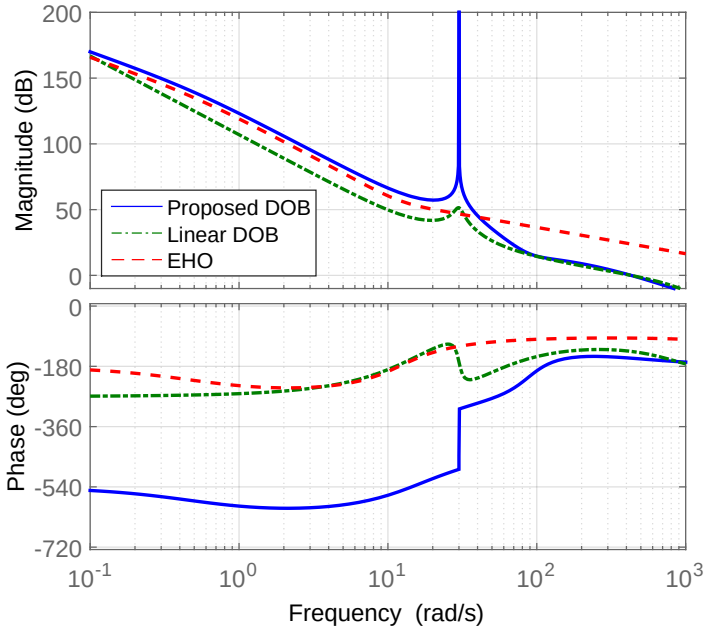

Figure 2.4: Bode plots of the open-loop transfer functions with the proposed DOB (blue solid), the linear DOB in [KC03] (green dot-dashed), and the EHO in [FK08] (red dashed) when all the saturation functions are inactive

0. Then for $\tau \in (0, \overline{\tau})$ with $\overline{\tau} > 0$ in Theorem 2.2.3,

$$\lim_{t\to\infty} \|[z_{\mathrm{aux}}(t); \chi(t)] - [z_{\mathsf{n}}(t); \chi_{\mathsf{n}}(t)]\| = 0, \quad \lim_{t\to\infty} \|w(t) - d_{\mathrm{total}}(t)\| = 0.$$

$\Diamond$

2.4 Simulation: Mechanical Positioning Systems

In this section, simulation results are presented to clarify the validity of the proposed controller (2.2.17), (2.2.20), and (2.2.21). In particular, we deal with the same problem in [KC03] in which a mechanical plant

$$\mathrm{P}(s) = \frac{1}{\mathsf{J}s^2 + \mathsf{B}s} \quad (\mathrm{m/V})$$

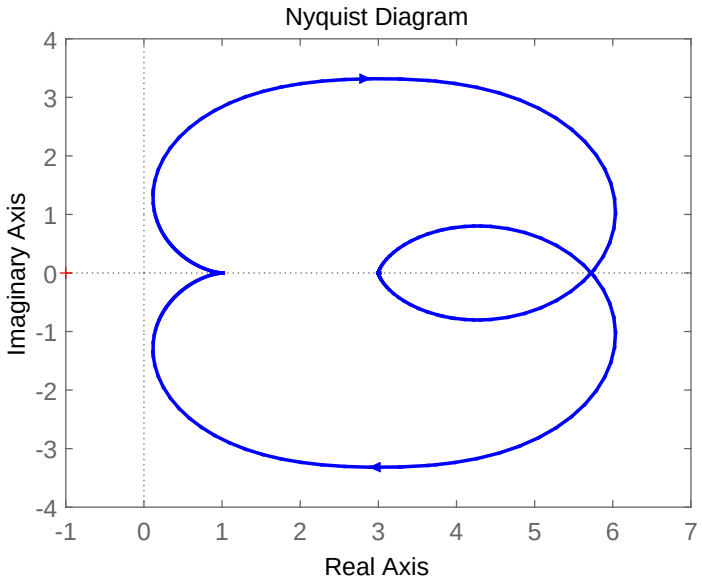

Figure 2.5: Nyquist plot of $\mathrm{Z}_{2,2}(s)$ with a_i obtained from BMI formulation

with the uncertain parameters $\mathsf{J} \in [0.2, 0.6]$ V/(m/s^2) and $\mathsf{B} \in [0, 0.15]$ V/(m/s) is taken into account. This plant is simply represented as a normal form (2.1.1) with $\phi = [0; -(\mathsf{B}/\mathsf{J})]$, $g = 1/\mathsf{J}$, and no zero dynamics (2.1.1a). The input gain g belongs to a bounded set $[\underline{g}, \overline{g}]$ with $\underline{g} = 5/3$ (m/s^2)/V and $\overline{g} = 5$ (m/s^2)/V. The state $x(t)$ is initiated at $x_1(0) \in [-0.01, 0.01]$ m and $x_2(0) = 0$ m/s. It is assumed that the disturbance $d(t)$ is bounded as $|d(t)| \leq 5$ V and has the form of $d(t) = d_{\mathsf{u}}(t) + d_{\mathsf{m}}(t)$ with a modeled part $d_{\mathsf{m}}(t) = M_{\mathsf{dm},0} + M_{\mathsf{dm},1} \sin(\sigma_1 t + \varphi_{\mathsf{dm},1})$ whose frequency σ_1 is 30 rad/s.

Let us consider a nominal system

$$\mathrm{P}_{\mathsf{n}}(s) = \frac{1}{\mathsf{J}_{\mathsf{n}} s^2 + \mathsf{B}_{\mathsf{n}} s} \quad \text{(m/V)}$$

with the nominal values $\mathsf{J}_{\mathsf{n}} = 0.6$ V/(m/s^2) and $\mathsf{B}_{\mathsf{n}} = 0$ V/(m/s), which is expressed in the state space as follows:

$$\dot{x}_{\mathsf{n}} = A_2 x_{\mathsf{n}} + B_2(\phi_{\mathsf{n}}^\top x_{\mathsf{n}} + g_{\mathsf{n}} \bar{u}), \qquad y_{\mathsf{n}} = C_2 x_{\mathsf{n}} \tag{2.4.1}$$

where $\phi_{\mathsf{n}} = [0; 0]$ and $g_{\mathsf{n}} = 1/\mathsf{J}_{\mathsf{n}} = 5/3$ (m/s^2)/V. To stabilize the nominal plant

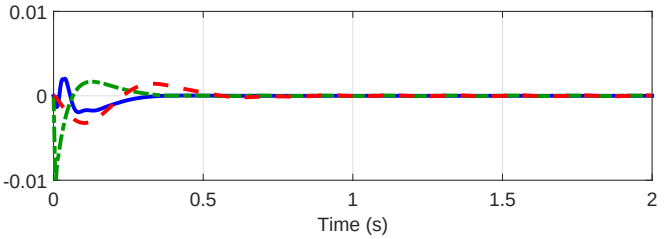

(a) Difference between $y(t)$ and $y_{\mathsf{n}}(t)$ (m)

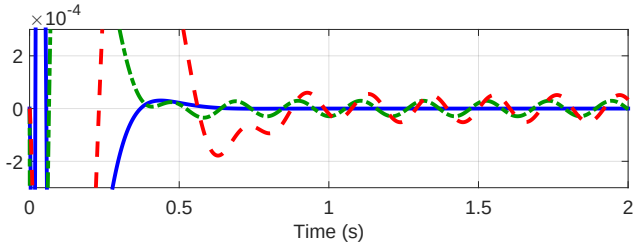

(b) Enlargement (m)

Figure 2.6: Differences between the actual output $y(t)$ and the nominal one $y_{\mathsf{n}}(t)$ when $d(t) = d_{\mathsf{m}}(t) = 2\sin(\sigma_1 t)$; the proposed DOB (blue solid), the linear DOB in [KC03] (green dot-dashed), and the EHO in [FK08] (red dashed)

(2.4.1) and to regulate its output y_{n} to the set-point $r(t) = r_{\mathsf{m}}(t) = 3 \times 10^{-2}$ m within 0.3 s for all $x_{\mathsf{n},1}(0) \in [-0.01, 0.01]$ m and $x_{\mathsf{n},2}(0) = 0$ m/s, a proportional-derivative (PD) controller is designed as

$$\bar{u} = -K_{\text{prop}}(y_{\mathsf{n}} - r) - K_{\text{deriv}}(\dot{y}_{\mathsf{n}} - \dot{r}) \tag{2.4.2}$$

where $K_{\text{deriv}} = 15$ and $K_{\text{prop}} = 150$.

From now on, we construct three different robust controllers for comparison. One is the $\mathcal{H}_\infty$-based DOB introduced in [KC03], which has the conventional structure and consists of two 6th order Q-filters[1]. The main purpose of this DOB is to suppress the disturbances that are dominant around the target frequency σ_1.

[1]The Q-filter used in its design is given by $\mathsf{Q}_{\mathcal{H}_\infty}(s) = (b_3^\star s^3 + \cdots + b_0^\star)/(a_6^\star s^6 + \cdots + a_0^\star)$ with $(b_3^\star, \ldots, b_0^\star) = (7.029 \times 10^7, 6.035 \times 10^9, 1.518 \times 10^{11}, 7.29 \times 10^{10})$ and $(a_6^\star, \ldots, a_0^\star) = (0.6, 8.257 \times 10^2, 5.571 \times 10^5, 7.297 \times 10^7, 6.533 \times 10^9, 1.518 \times 10^{11}, 7.29 \times 10^{10})$.

Another controller under consideration is the extended high-gain observer (EHO), which is known as a robust control scheme that guarantees the (approximate) NPR (i.e., the former notion in Definition 2.1.1). Following the design procedure in [FK08], we construct an EHO for the nominal closed-loop system (2.4.1) and (2.4.2) as follows:

$$\begin{aligned}\begin{bmatrix}\dot{p}_{\mathrm{eho}}\\ \dot{w}_{\mathrm{eho}}\end{bmatrix} &= \begin{bmatrix}A_2 + B_2\phi_{\mathsf{n}}^\top & B_2\\ 0 & 0\end{bmatrix}\begin{bmatrix}p_{\mathrm{eho}}\\ w_{\mathrm{eho}}\end{bmatrix}\\ &\quad + \begin{bmatrix}B_2 g_{\mathsf{n}}\\ 0\end{bmatrix} u - \underline{\Upsilon}_3^{-1}(\tau_{\mathrm{eho}})\overline{\alpha}_{\mathrm{eho}}(C_2 p_{\mathrm{eho}} - (y-r)),\\ u &= m_{\mathrm{eho}}\mathrm{sat}\left(\frac{1}{m_{\mathrm{eho}}g_{\mathsf{n}}}\left(-w_{\mathrm{eho}} - \phi_{\mathsf{n}}^\top p_{\mathrm{eho}} - \begin{bmatrix}K_{\mathrm{prop}} & K_{\mathrm{deriv}}\end{bmatrix} p_{\mathrm{eho}}\right)\right) \quad (2.4.3)\end{aligned}$$

where $p_{\mathrm{eho}} \in \mathbb{R}^2$ and $w_{\mathrm{eho}} \in \mathbb{R}$ are the states, $\mathrm{sat}(\theta) := \min(1, \max(\theta, -1))$ stands for a conventional saturation function, and $\underline{\Upsilon}_3(\tau) = \mathrm{diag}(\tau, \tau^2, \tau^3) \in \mathbb{R}^{3\times 3}$. The design parameters are selected as $\overline{\alpha}_{\mathrm{eho}} = [3; 3; 1]$ and $m_{\mathrm{eho}} = 2.8983$. In addition, we choose $\tau_{\mathrm{eho}} = 0.00015$ so that the control gain of the EHO is similar to that of the linear DOB at the target frequency σ_1. Such criterion on τ_{eho} could require relatively large control bandwidth, because the EHO is designed without taking any internal model into account.

Now, let us construct the proposed DOB-based controller to achieve the asymptotic NPR in Definition 2.1.1. To avoid the derivative of the output, we rewrite the existing nominal closed-loop system (2.4.1) and (2.4.2) as

$$\dot{x}_{\mathsf{n}} = \left(A_2 + B_2\left(\phi_{\mathsf{n}}^\top - g_{\mathsf{n}}\begin{bmatrix}K_{\mathrm{prop}} & K_{\mathrm{deriv}}\end{bmatrix}\right)\right)x_{\mathsf{n}} + B_2 g_{\mathsf{n}} u_{\mathsf{n}}, \quad u_{\mathsf{n}} = K_{\mathrm{prop}} r \quad (2.4.4)$$

with which there is no use of the output's derivative in the control input u_{n}. The system (2.4.4) now plays a role as (2.1.3) in the controller design. By repeated simulations, we compute the bounds for the nominal state $x_{\mathsf{n}}(t)$ for all initial conditions $x_{\mathsf{n}}(0) \in [-0.01, 0.01] \times \{0\}$, and find out

$$x_{\mathsf{n}}(t) \in [-0.01, 0.0307] \times [-0.0047, 0.2683], \quad \forall t \geq 0.$$

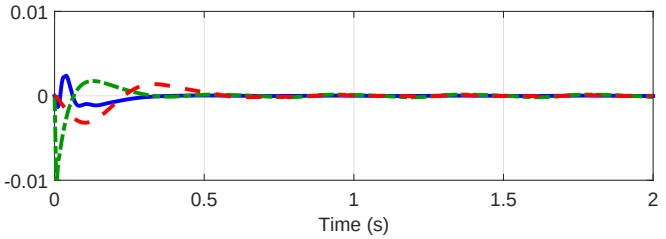

(a) Difference between $y(t)$ and $y_{\mathsf{n}}(t)$ (m)

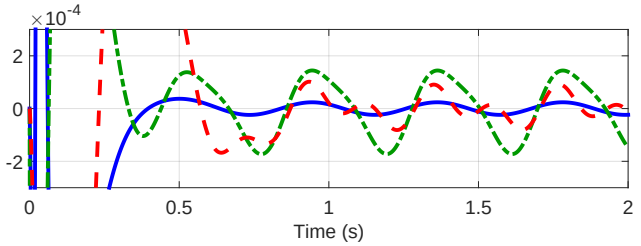

(b) Enlargement (m)

Figure 2.7: Differences between the actual output $y(t)$ and the nominal one $y_{\mathsf{n}}(t)$ when $d(t) = d_{\mathsf{m}}(t) + d_{\mathsf{u}}(t) = 2\sin(\sigma_1 t) + \sin(15t)$; the proposed DOB (blue solid), the linear DOB in [KC03] (green dot-dashed), and the EHO in [FK08] (red dashed)

This implies

$$d_{\text{total},\mathsf{n}}(t) = \frac{1}{g}(\phi^\top - \phi_{\mathsf{n}}^\top)x_{\mathsf{n}}(t) + \left(1 - \frac{g_{\mathsf{n}}}{g}\right)u_{\mathsf{n}}(t) + d(t)$$
$$\in \mathcal{D}_{\text{total},\mathsf{n}} \subset [-3.2731, 16.5730], \quad \forall t \geq 0$$

for all possible variations of B, J, and d. Using the bound of $d_{\text{total},\mathsf{n}}$, we design the saturation function $\overline{s}_{\mathsf{w}}(w)$ whose saturation level is set as $\overline{\mathcal{D}}_{\text{total},\mathsf{n}} := [-4, 17]$ (strictly larger than $\mathcal{D}_{\text{total},\mathsf{n}}$). For the construction of a_i, we solve the BMI problem (A.1.15b) via PENLAB. This results in $\overline{\alpha} = [0.8032; 0.4993; 0.0859; 0.0242]$ with which $\mathrm{Z}_{2,2}(s)$ is SPR. We choose the coefficients b_i and c_i as in (2.3.10) and (2.2.26), respectively, where the design parameter τ to be used is determined as $\tau = 0.0025$ so that two DOBs have similar control bandwidths.

For simulation, set $\mathsf{J} = 0.2$ V/(m/s^2), $\mathsf{B} = 0.1$ V/(m/s), and $x(0) = [0.01; 0]$.

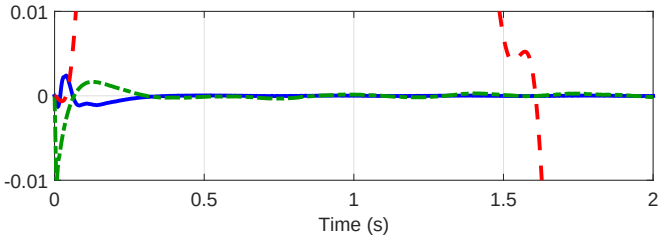

(a) Difference between $y(t)$ and $y_{\mathsf{n}}(t)$

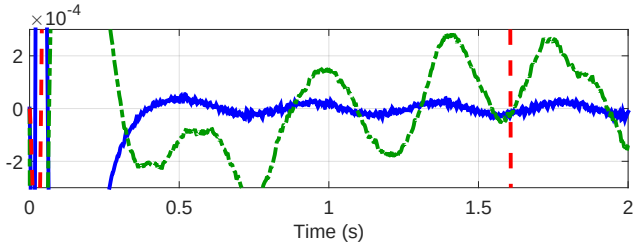

(b) Enlargement

Figure 2.8: Differences between the actual output $y(t)$ and the nominal one $y_{\mathsf{n}}(t)$ when $d(t) = d_{\mathsf{m}}(t)+d_{\mathsf{u}}(t) = 2\sin(\sigma_1 t)+\sin(15t)$ and there is a measurement noise; the proposed DOB (blue solid), the linear DOB in [KC03] (green dot-dashed), and the EHO in [FK08] (red dashed)

The simulation results for various external signals are depicted in Figures 2.6 and 2.7. It can be observed in Figure 2.6 that both the proposed DOB and the EHO guarantee acceptable transient performance, whereas the output trajectory generated by the linear DOB experiences large initial peak. Beyond the transient behavior, the proposed DOB also eliminates the effect of the modeled input $[r_{\mathsf{m}}(t); d_{\mathsf{m}}(t)]$ on the NPR completely, and therefore, the output $y(t)$ asymptotically converges to the nominal one $y_{\mathsf{n}}(t)$. Notice that this is not the case for the EHO for which no structural information on $[r_{\mathsf{m}}(t); d_{\mathsf{m}}(t)]$ is used. Moreover, all these advantages of the proposed controller are preserved even if additional unmodeled disturbance $d_{\mathsf{u}}(t) = \sin(15t)$ V enters the plant, as shown in Figure 2.7. Figure 2.8 depicts the case when there exists a measurement noise which is uniformly distributed and whose maximum magnitude is 5×10^{-5} m. Notice that the EHO loses its tracking performance, since its control bandwidth is too large

to withstand the high-frequency noise. The performance of the linear DOB is also degraded compared to the noiseless case, because of employing the PD controller directly. The effect of the noisy measurement, however, is relaxed when the proposed DOB is used.

Chapter 3

Recovery of Nominal Performance in Asymptotic Sense: Part II - An Extension with Adaptive Internal Model

We have observed in the previous chapter that by embedding the internal model into the (inverse model-based) DOB structure, the nominal tracking performance can be recovered in the asymptotic sense (of Definition 2.1.1). In this design philosophy, the exact knowledge on the generating model is of necessity. A question arising here is: can we still recover the nominal performance asymptotically, even if the generating model of the external input is not exactly known?

The main objective of this chapter is to address the problem for the (second-order) uncertain mechanical systems. For the purpose, we extend the controller design of Chapter 2 with a "frequency identifier" attached in the DOB loop. This new component plays a role for estimating the unknown frequency of the total disturbance in the steady-state period. Implemented with the frequency estimate, the parameters of the internal model in the DOB structure are updated in an "adaptive" fashion. The "adaptive internal model" embedded into the overall controller allows to estimate and compensate the total disturbance asymptotically, even without exact information on the frequency of the external input. We note in advance that as the price to pay for the extension, in this work we restrict our interest to the cases when a single sinusoidal input enters the system.

As an industrial application of the proposed controller, this paper deals with the track-following problem of optical disk drive (ODD) systems [Kim05, OMI+06, Lu09, KSJ14]. For the ODD control systems, it is of utter importance to enforce its pick-up to follow desired track on the disk with little oscillation or perturbation. In the track-following problem, a challenging issue is to suppress the effect of disk eccentricity on the pick-up. This issue can be recast as a regulation problem in the presence of a sinusoidal disturbance (as well as model uncertainty), whose frequency varies track by track in a constant linear velocity (CLV) or zoned CLV operating mode. To achieve high-precision tracking performance against these uncertainties, we propose a robust track-following control scheme by combining the proposed add-on controller with a pre-installed lead-lag compensator. Simulation and experimental results show that with the proposed control scheme, the track error signal of the ODD is regulated to zero with suitable transient response.

3.1 Problem Revisited: Mechanical System with Unknown Frequency of External Input

To begin, we focus our attention to the SISO linear mechanical system

$$\mathsf{M}\ddot{y} + \mathsf{C}\dot{y} + \mathsf{K}y = u + d \tag{3.1.1}$$

where the generalized position (or angle) $y \in \mathbb{R}$ is the output, $u \in \mathbb{R}$ is the input, $d \in \mathbb{R}$ is the disturbance that is of $\mathfrak{C}^1$. Suppose that the parameters M, C, and K are uncertain, as in the following assumption.

Assumption 3.1.1. The mass $\mathsf{M} > 0$, the damping coefficient $\mathsf{C} \geq 0$, and the spring coefficient $\mathsf{K} \geq 0$ are uncertain but bounded with known bounds; i.e., $\mathsf{M} \in [\underline{\mathsf{M}}, \overline{\mathsf{M}}]$, $\mathsf{C} \in [\underline{\mathsf{C}}, \overline{\mathsf{C}}]$, and $\mathsf{K} \in [\underline{\mathsf{K}}, \overline{\mathsf{K}}]$. $\Diamond$

With the state $x := [y, \dot{y}] \in \mathbb{R}^2$, the mechanical system (3.1.1) is represented in the state space as

$$\dot{x} = A_2 x + B_2\big(\phi^\top x + g(u+d)\big), \qquad y = C_2 x \tag{3.1.2}$$

where $x \in \mathbb{R}^2$ is the state, A_i, B_i, and C_i are given in (2.1.2), $g := 1/\mathsf{M} > 0$, and $\phi = [\phi_1; \phi_2] := [-\mathsf{K}/\mathsf{M}; -\mathsf{C}/\mathsf{M}]$. Note that the plant of interest (3.1.2) is thus the very plant (2.1.1) in the Byrnes-Isidori normal form with no zero dynamics and $\nu = n_{\mathsf{p}} = 2$, and satisfies Assumption 2.1.1 under Assumption 3.1.1. Suppose that the initial conditions $x(0)$ of the plant belong in a compact set $\mathcal{X}^0 \subset \mathbb{R}^2$.

In addition, the following mechanical system with no uncertain quantity will play the role as a nominal model of (3.1.2):

$$\mathsf{M}_{\mathsf{n}}\ddot{y}_{\mathsf{n}} + \mathsf{C}_{\mathsf{n}}\dot{y}_{\mathsf{n}} + \mathsf{K}_{\mathsf{n}}y_{\mathsf{n}} = u_{\mathsf{n}} \tag{3.1.3}$$

or equivalently,

$$\dot{x}_{\mathsf{n}} = A_2 x_{\mathsf{n}} + B_2\big(\phi_{\mathsf{n}}^\top x_{\mathsf{n}} + g_{\mathsf{n}} u_{\mathsf{n}}\big), \qquad y_{\mathsf{n}} = C_2 x_{\mathsf{n}} \tag{3.1.4}$$

where $x_{\mathsf{n}} := [y_{\mathsf{n}}; \dot{y}_{\mathsf{n}}] \in \mathbb{R}^2$, $u_{\mathsf{n}} \in \mathbb{R}$ and $y_{\mathsf{n}} \in \mathbb{R}$ are the state, input, and output of the nominal system, respectively, $g_{\mathsf{n}} := 1/\mathsf{M}_{\mathsf{n}} > 0$, and $\phi_{\mathsf{n}} = [\phi_{\mathsf{n},1}; \phi_{\mathsf{n},2}] := [-\mathsf{K}_{\mathsf{n}}/\mathsf{M}_{\mathsf{n}}; -\mathsf{C}_{\mathsf{n}}/\mathsf{M}_{\mathsf{n}}]$. It is assumed that the nominal plant (3.1.4) is governed by an output feedback controller

$$\dot{c}_{\mathsf{n}} = E c_{\mathsf{n}} + F\,(r - y_{\mathsf{n}})\,, \qquad u_{\mathsf{n}} = J c_{\mathsf{n}} + K\,(r - y_{\mathsf{n}})\,. \tag{3.1.5}$$

Here $c_{\mathsf{n}} \in \mathbb{R}^{n_{\mathsf{c}}}$ is the controller state, and $r \in \mathbb{R}$ is the reference signal for y_{n}. The dimension n_{c} of the controller is allowed to be zero, with which (3.1.5) represents a static controller. Similar to the previous chapter, we assume that $x_{\mathsf{n}}(0) \in \mathcal{X}^0$ and $c_{\mathsf{n}}(0) \in \mathcal{C}_{\mathsf{n}}^0$ with a bounded set $\mathcal{C}_{\mathsf{n}}^0$.

Assumption 3.1.2. The nominal closed-loop system (3.1.4) and (3.1.5) is internally stable; that is, the matrix

$$\mathsf{A}_{\mathsf{n}} := \begin{bmatrix} A_\nu + B_\nu \phi_{\mathsf{n}}^\top - g_{\mathsf{n}} B_\nu K C_\nu & g_{\mathsf{n}} B_\nu J \\ -F C_\nu & E \end{bmatrix} \tag{3.1.6}$$

is Hurwitz. ◊

The following assumption indicates that the external inputs $r(t)$ and $d(t)$ are modeled as sinusoidal signals with an "uncertain" frequency.

Assumption 3.1.3. The reference $r(t)$ and the disturbance $d(t)$ have the form of the sinusoids

$$r(t) = r_{\mathsf{m}}(t) = M_{\mathsf{rm},0}, \tag{3.1.7a}$$

$$d(t) = d_{\mathsf{m}}(t) = M_{\mathsf{dm},0} + M_{\mathsf{dm},1} \sin(\sigma t + \varphi_{\mathsf{dm},1}) \tag{3.1.7b}$$

where $M_{\mathsf{rm},0}$, $M_{\mathsf{dm},0}$, $M_{\mathsf{dm},1} > 0$, $\varphi_{\mathsf{dm},1}$, and $\sigma > 0$ are possibly uncertain but bounded with known bounds. In particular, $0 < \underline{\sigma} \le \sigma \le \overline{\sigma}$, $|d(t)| \le \overline{d}$, and $|r(t)| \le \overline{r}$ for some constants $\overline{d} \ge 0$, $\overline{r} \ge 0$, $\underline{\sigma} > 0$, and $\overline{\sigma} > 0$. Moreover, $[r(t); d(t)]$ is not identically zero. ◊

Now, with the notion of NPR in asymptotic sense in Definition 2.1.1, the problem considered in this chapter can be stated as follows.

Problem of Chapter 3. Given the plant (3.1.2), the nominal closed-loop system (3.1.4) and (3.1.5), and a threshold $\epsilon > 0$, to construct an output feedback controller (2.1.8) that recovers nominal performance in an asymptotic sense within ϵ-bound in the sense of Definition 2.1.1 under Assumptions 3.1.1–3.1.3. ◊

3.2 Disturbance Observer-based Controller Design with Adaptive Internal Model

A solution to the problem is presented throughout this section. The underlying idea for the controller design here is basically consistent with that in the previous chapter. However, the components of the DOB should be redesigned carefully, because the generating model of the external (modeled) inputs now cannot be utilized directly.

As an additional key component, we employ the following frequency identifier to adjust the frequency of the sinusoidal signal in an "adaptive" fashion:

$$\dot{\hat{\theta}} = \kappa \Xi^\top C_3^\top (u - C_3 \hat{\mathcal{W}}), \tag{3.2.1a}$$

$$\dot{\hat{\mathcal{W}}} = A_3 \hat{\mathcal{W}} + \Psi_u \hat{\theta} + L(u - C_3 \hat{\mathcal{W}}) + \Xi \dot{\hat{\theta}}, \tag{3.2.1b}$$

$$\dot{\Xi} = (A_3 - L C_3)\Xi + \Psi_u \tag{3.2.1c}$$

where $\hat{\theta} \in \mathbb{R}$, $\hat{\mathcal{W}} \in \mathbb{R}^3$, and $\Xi \in \mathbb{R}^3$ are the states, $u \in \mathbb{R}$ is the input of the frequency identifier (which is the same as the control input in (3.1.2)), $L \in \mathbb{R}^{3\times 1}$ is chosen such that $A_3 - LC_3$ is Hurwitz, $\Psi_u := [0; -u; 0] \in \mathbb{R}^3$, and $\kappa > 0$ is a small design parameter to be chosen later. We note in advance that $\hat{\theta}$ will serve as an estimate of the unknown value $\theta = \sigma^2$. In this regard, we select the initial condition $\hat{\theta}(0)$ in the bounded set $[\underline{\sigma}^2; \overline{\sigma}^2] \subset \mathbb{R}$, while $\hat{\mathcal{W}}(0)$ and $\Xi(0)$ are simply set as $\hat{\mathcal{W}}(0) = 0$ and $\Xi(0) = 0$.

Remark 3.2.1. The structure of the frequency identifier (3.2.1) is inspired by the "adaptive observer" presented in [BZ03, KSJ14]. It has been well-studied that if the input $u(t)$ of (3.2.1) is "exactly" generated by an exogenous model

$$\dot{\mathcal{W}}_{\mathsf{u}} = \left(A_3 - \begin{bmatrix} 0 \\ \sigma^2 \\ 0 \end{bmatrix} C_3 \right) \mathcal{W}_{\mathsf{u}}, \qquad u = C_3 \mathcal{W}_{\mathsf{u}}.$$

(or equivalently, $u(t)$ is a biased sinusoidal function whose frequency is σ), then the estimate $\hat{\theta}$ in (3.2.1) will converge to the true value $\theta := \sigma^2$ as time goes on. However, this is not true as long as $u(t)$ is the control input generated by a feedback controller. Alternatively, we will estimate the "steady-state response" of $u(t)$ (rather than $u(t)$ itself), which could be sinusoidal by the properties of linear systems. For this "slow" estimation in the steady-state period, the $\hat{\theta}$-dynamics (3.2.1a) is realized with a low gain κ as above. ♢

From now on, we construct a DOB-based controller with the estimate $\hat{\theta}$ of the true value θ, mainly by following the design method in Chapter 2 (but with some modification). Firstly, we define

$$\overline{\alpha} := \begin{bmatrix} \mathsf{a}_3 \\ \mathsf{a}_2 \\ \mathsf{a}_1 \\ \mathsf{a}_0 \end{bmatrix}, \quad \overline{\beta}(\hat{\theta}; \tau) := \begin{bmatrix} \mathsf{b}_3(\hat{\theta}; \tau) \\ \mathsf{b}_2(\hat{\theta}; \tau) \\ \mathsf{b}_1(\hat{\theta}; \tau) \\ \mathsf{b}_0(\hat{\theta}; \tau) \end{bmatrix}, \quad \overline{\gamma}(\hat{\theta}; \tau) := \begin{bmatrix} 0 \\ \mathsf{c}_2(\hat{\theta}; \tau) \\ \mathsf{c}_1(\hat{\theta}; \tau) \\ \mathsf{c}_0(\hat{\theta}; \tau) \end{bmatrix}$$

whose components are determined below (while the parameter τ will be chosen shortly). Using the design procedure in Appendix A.1, we select a_i, $i = 0, \ldots, 3$,

such that the transfer function

$$\mathrm{Z}_{2,2}(s) = \frac{s^4 + \mathsf{a}_3 s^3 + (\overline{g}/g_{\mathsf{n}})\mathsf{a}_2 s^2 + (\overline{g}/g_{\mathsf{n}})\mathsf{a}_1 s + (\overline{g}/g_{\mathsf{n}})\mathsf{a}_0}{s^4 + \mathsf{a}_3 s^3 + (\underline{g}/g_{\mathsf{n}})\mathsf{a}_2 s^2 + (\underline{g}/g_{\mathsf{n}})\mathsf{a}_1 s + (\underline{g}/g_{\mathsf{n}})\mathsf{a}_0} \tag{3.2.2}$$

is SPR. With such a_i, take $\mathsf{c}_i(\hat{\theta};\tau)$, $i = 0, \ldots, 2$, as follows:

$$\mathsf{c}_0(\hat{\theta};\tau) := \mathsf{a}_0, \tag{3.2.3a}$$

$$\mathsf{c}_1(\hat{\theta};\tau) := W_0(\hat{\theta};\tau)^{-1} W_1(\hat{\theta};\tau) \begin{bmatrix} \mathsf{a}_1 \\ \mathsf{a}_3 \end{bmatrix} = \mathsf{a}_1 - \tau^2 \mathsf{a}_3 \hat{\theta}, \tag{3.2.3b}$$

$$\mathsf{c}_2(\hat{\theta};\tau) := W_0(\hat{\theta};\tau)^{-1} W_1(\hat{\theta};\tau) \begin{bmatrix} \mathsf{a}_2 \\ 1 \end{bmatrix} = \mathsf{a}_2 - \tau^2 \hat{\theta} \tag{3.2.3c}$$

where W_i are the Vandermonde matrices with $n_{\mathsf{m}} = 1$, defined in (2.2.24). Similarly, we also choose $\mathsf{b}_i(\hat{\theta};\tau)$, $i = 0, \ldots, 3$, in the same way of (2.2.15) as

$$\mathsf{b}_3(\hat{\theta};\tau) := -\frac{\mathsf{c}_2(\hat{\theta};\tau)}{\tau^2}\mathsf{a}_3 + \frac{\mathsf{c}_1(\hat{\theta};\tau)}{\tau^2} - \frac{\mathsf{c}_2(\hat{\theta};\tau)}{\tau}\phi_{\mathsf{n},2}, \tag{3.2.4a}$$

$$\mathsf{b}_2(\hat{\theta};\tau) := -\frac{\mathsf{c}_2(\hat{\theta};\tau)}{\tau^2}\mathsf{a}_2 + \frac{\mathsf{c}_0(\hat{\theta};\tau)}{\tau^2} - \frac{\mathsf{c}_1(\hat{\theta};\tau)}{\tau}\phi_{\mathsf{n},2} - \mathsf{c}_2(\hat{\theta};\tau)\phi_{\mathsf{n},1}, \tag{3.2.4b}$$

$$\mathsf{b}_1(\hat{\theta};\tau) := -\frac{\mathsf{c}_2(\hat{\theta};\tau)}{\tau^2}\mathsf{a}_1 - \frac{\mathsf{c}_0(\hat{\theta};\tau)}{\tau}\phi_{\mathsf{n},2} - \mathsf{c}_1(\hat{\theta};\tau)\phi_{\mathsf{n},1}, \tag{3.2.4c}$$

$$\mathsf{b}_0(\hat{\theta};\tau) := -\frac{\mathsf{c}_2(\hat{\theta};\tau)}{\tau^2}\mathsf{a}_0 - \mathsf{c}_0(\hat{\theta};\tau)\phi_{\mathsf{n},1}. \tag{3.2.4d}$$

Next, to obtain a saturation function $\overline{s}_{\mathsf{w}}$ for the DOB output, we consider a nominal counterpart of the total disturbance

$$d_{\mathrm{total},\mathsf{n}} := \frac{1}{g}\Big((\phi^\top - \phi_{\mathsf{n}}^\top) x_{\mathsf{n}} + (g - g_{\mathsf{n}})\big(Jc_{\mathsf{n}} + K(r - y_{\mathsf{n}})\big) + gd \Big) \tag{3.2.5}$$

(which is the same as (2.2.28)). Since it follows from Assumption 3.1.2 that the nominal closed-loop system (3.1.4) and (3.1.5) is internally stable and the initial condition $[x_{\mathsf{n}}(0); c_{\mathsf{n}}(0)]$ is located in a bounded region $\mathcal{X}^0 \times \mathcal{C}_{\mathsf{n}}^0$, it is clear that the set

$$\mathcal{D}_{\mathrm{total},\mathsf{n}} := \Big\{ d_{\mathrm{total},\mathsf{n}}(t) \text{ in (3.2.5)} : \tag{3.2.6}$$

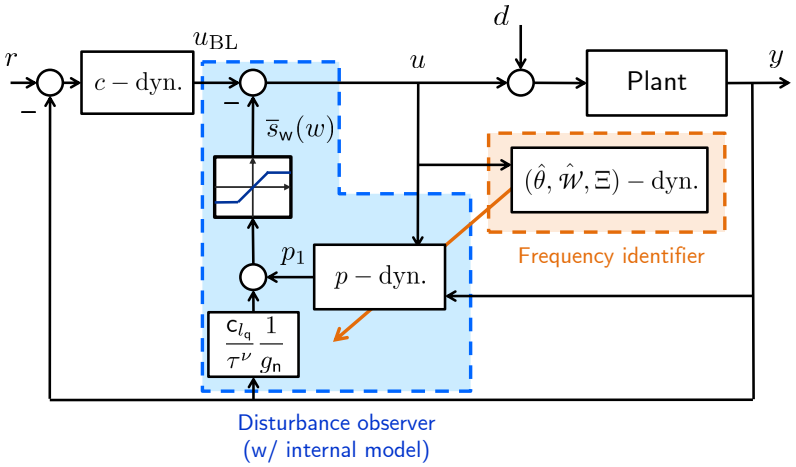

Figure 3.1: Overall configuration of closed-loop system with proposed controller (3.2.1), (3.2.7), (3.2.8), and (3.2.9)

$$\left.\begin{aligned} &[x_{\mathsf{n}}(t); c_{\mathsf{n}}(t)] \text{ generated by (3.1.4) and (3.1.5)}, \\ &[x_{\mathsf{n}}(0); c_{\mathsf{n}}(0)] \in \mathcal{X}^0 \times \mathcal{C}_{\mathsf{n}}^0, \\ &\|[r(t); \dot{r}(t)]\| \le \overline{r},\ \|[d(t); \dot{d}(t)]\| \le \overline{d},\ t \ge 0 \end{aligned}\right\} \subset \mathbb{R}$$

of all possible $d_{\text{total},\mathsf{n}}(t)$ is bounded. Let $\overline{\mathcal{D}}_{\text{total},\mathsf{n}}$ be a compact set strictly larger than $\mathcal{D}_{\text{total},\mathsf{n}}$ (that is, $\overline{\mathcal{D}}_{\text{total},\mathsf{n}} \supset \mathcal{D}_{\text{total},\mathsf{n}}$). Then, we construct a saturation function $\bar{s}_{\mathsf{w}} : \mathbb{R} \to \mathbb{R}$ that is bounded, of $\mathfrak{C}^1$, and satisfies (2.2.30) for the compact set $\overline{\mathcal{D}}_{\text{total},\mathsf{n}}$ in (3.2.6).

Finally, we propose the overall controller as the frequency identifier (3.2.1), the baseline controller

$$\dot{c} = Ec + F(r - y), \qquad u_{\mathrm{BL}} = Jc + K(r - y), \tag{3.2.7}$$

the (reduced-order) DOB implemented with $\hat{\theta}$

$$\dot{p} = \big(A_4 - \underline{\Upsilon}_4^{-1}(\tau)\overline{\alpha}C_4\big)p - \underline{\Upsilon}^{-1}(\tau)\overline{\gamma}(\hat{\theta};\tau)u + \underline{\Upsilon}^{-1}(\tau)\overline{\beta}(\hat{\theta};\tau)\frac{1}{g_{\mathsf{n}}}y, \tag{3.2.8a}$$

$$w = C_4 p + \frac{\mathsf{c}_2(\hat{\theta};\tau)}{\tau^2}\frac{1}{g_{\mathsf{n}}}y \tag{3.2.8b}$$

(where the square matrix $\underline{\Upsilon}_4(\tau)$ is given in (2.2.18)), and the composite control

law

$$u = u_{\mathrm{BL}} - \overline{s}_{\mathsf{w}}(w). \tag{3.2.9}$$

Here $c \in \mathbb{R}^{n_{\mathsf{c}}}$ and $p \in \mathbb{R}^4$ are the states of the baseline controller and the DOB, respectively. The initial condition $c(0)$ is set as in the compact set $\mathcal{C}_{\mathsf{n}}^0$, while $p(0)$ can be any bounded value. Without loss of generality, let $p(0) = 0$.

The overview of the entire controlled system is given in Figure 3.1.

3.3 Performance Analysis

We present our main result first, while its detailed proof will be given throughout the following two subsections.

Theorem 3.3.1. Suppose that Assumptions 3.1.1–3.1.3 are satisfied. Then for given $\epsilon > 0$, there exist $\overline{\kappa} > 0$ and $\overline{\tau} = \overline{\tau}(\kappa) > 0$ such that the output feedback controller (3.2.1), (3.2.7), (3.2.8), and (3.2.9) with $\kappa \in (0, \overline{\kappa})$ and $\tau \in (0, \overline{\tau}(\kappa))$ recovers the nominal performance in an asymptotic sense with ϵ-bound. $\Diamond$

3.3.1 Representation to Multiple-time Scaled Singular Perturbation Form

The first step to prove the theorem is to represent the closed-loop system (3.1.2), (3.2.1), (3.2.7), (3.2.8), and (3.2.9) into a singular perturbation form. As an intermediate task, the following lemma is presented.

Lemma 3.3.2. In the coordinate change

$$\eta = \frac{1}{\tau}\underline{\Upsilon}(\tau)\left(p + \Gamma(\hat{\theta};\tau)\Phi_{\mathsf{n}}\frac{1}{g_{\mathsf{n}}}x\right)$$

where

$$\Gamma(\hat{\theta};\tau) := \begin{bmatrix} \mathsf{c}_2(\hat{\theta};\tau)/\tau^2 & 0 \\ \mathsf{c}_1(\hat{\theta};\tau)/\tau^3 & \mathsf{c}_2(\hat{\theta};\tau)/\tau^2 \\ \mathsf{c}_0/\tau^4 & \mathsf{c}_1(\hat{\theta};\tau)/\tau^3 \\ 0 & \mathsf{c}_0/\tau^4 \end{bmatrix}, \qquad \Phi_{\mathsf{n}} := \begin{bmatrix} 1 & 0 \\ -\phi_{\mathsf{n},2} & 1 \end{bmatrix},$$

the p-dynamics (3.2.8a) is converted into

$$\tau\dot{\eta} = (A_4 - \overline{\alpha}C_4)\,\eta + \left(1 - \frac{g}{g_{\mathsf{n}}}\right)\overline{\gamma}(\hat{\theta};\tau)\bar{s}\,(C_4\eta) + \frac{g}{g_{\mathsf{n}}}\overline{\gamma}(\hat{\theta};\tau)d_{\text{total}} + \underline{\Upsilon}(\tau)\dot{\Gamma}(\hat{\theta};\tau)\Phi_{\mathsf{n}}\frac{1}{g_{\mathsf{n}}}x \tag{3.3.1}$$

where

$$\begin{aligned} d_{\text{total}} &:= \frac{1}{g}\Big((\phi^\top - \phi_{\mathsf{n}}^\top)x + (g - g_{\mathsf{n}})u_{\text{BL}} + gd\Big) \\ &= \frac{1}{g}\Big((\phi^\top - \phi_{\mathsf{n}}^\top)x + (g - g_{\mathsf{n}})\big(Jc + K(r - C_2x)\big) + gd\Big). \end{aligned} \tag{3.3.2}$$

$\lozenge$

Proof. The proof of the lemma is similar to that of Lemma 2.3.1 in the previous chapter, and therefore we skip the details here. □

Next, for ease of analysis, we will shift the equilibrium of the transformed system in Lemma 3.3.2 to the origin. Let us define stacked variables

$$\chi := \begin{bmatrix} x \\ c \end{bmatrix} \in \mathbb{R}^{2+n_{\mathsf{c}}}, \qquad \chi_{\mathsf{n}} := \begin{bmatrix} x_{\mathsf{n}} \\ c_{\mathsf{n}} \end{bmatrix} \in \mathbb{R}^{2+n_{\mathsf{c}}} \tag{3.3.3}$$

and denote the steady-state response of χ_{n} as $\chi_{\mathsf{n}}^\star$. It is easily obtained from the linear system theory that the steady-state responses of d_{total} and u_{n} have the form of

$$d_{\text{total},\mathsf{n}}^\star := \mathsf{C}_{\text{total}}\chi_{\mathsf{n}}^\star + \mathsf{D}_{\text{total}}\begin{bmatrix} r \\ d \end{bmatrix}, \qquad u_{\mathsf{n}}^\star := \mathsf{C}_{\mathsf{un}}\chi_{\mathsf{n}}^\star + \mathsf{D}_{\mathsf{un}}\begin{bmatrix} r \\ d \end{bmatrix}, \tag{3.3.4}$$

respectively, where

$$\begin{aligned} \mathsf{C}_{\text{total}} &:= \frac{1}{g}\begin{bmatrix}(\phi^\top - \phi_{\mathsf{n}}^\top) - (g - g_{\mathsf{n}})KC_\nu & (g - g_{\mathsf{n}})J\end{bmatrix}, & \mathsf{C}_{\mathsf{un}} &:= \begin{bmatrix}-KC_2 & J\end{bmatrix} \\ \mathsf{D}_{\text{total}} &:= \frac{1}{g}\begin{bmatrix}(g - g_{\mathsf{n}})K & g\end{bmatrix}, & \mathsf{D}_{\mathsf{un}} &:= \begin{bmatrix}K & 0\end{bmatrix} \end{aligned}$$

and both are sinusoids with the frequency σ. Their linear combination

$$u^\star := u_{\mathsf{n}}^\star - d_{\mathrm{total},\mathsf{n}}^\star, \tag{3.3.5}$$

thus can be expressed as the output of an (auxiliary) exogenous system

$$\dot{\mathcal{W}} = \left(A_3 - \begin{bmatrix} 0 \\ \sigma^2 \\ 0 \end{bmatrix} C_3 \right) \mathcal{W} = A_3 \mathcal{W} + \Psi_{u^\star} \theta, \qquad u^\star = C_3 \mathcal{W} \tag{3.3.6}$$

written in the observable canonical form. In addition, using the notion of the extended quasi-steady-state variable $\eta^\star$ in the previous chapter, let us define

$$\eta_{\mathrm{ext}}^\star := \overline{\alpha}^\star d_{\mathrm{total}} - \begin{bmatrix} 0 \\ \upsilon_{\mathsf{m},1}^\star \\ (\tau\mathfrak{s})\upsilon_{\mathsf{m},1}^\star + \upsilon_{\mathsf{m},2}^\star \\ (\tau\mathfrak{s})^2\upsilon_{\mathsf{m},1} + (\tau\mathfrak{s})\upsilon_{\mathsf{m},2} + \upsilon_{\mathsf{m},3} \\ (\tau\mathfrak{s})^3\upsilon_{\mathsf{m},1} + (\tau\mathfrak{s})^2\upsilon_{\mathsf{m},2} + (\tau\mathfrak{s})\upsilon_{\mathsf{m},3} + \upsilon_{\mathsf{m},4} \end{bmatrix}$$

in which $\mathfrak{s} := \mathrm{d}/\mathrm{d}t$, $\overline{\alpha}^\star := [1; \mathsf{a}_3; 0; 0]$, and

$$\upsilon_{\mathsf{m}}^\star(t, \theta; \tau) := \big(\overline{\gamma}(\theta; \tau) - \overline{\gamma}(\theta; 0)\big) d_{\mathrm{total},\mathsf{n}}^\star(t) - \tau \overline{\alpha}^\star \dot{d}_{\mathrm{total},\mathsf{n}}^\star(t).$$

We then obtain the following result, in which the overall system is expressed as a "multiple-time scaled" singular perturbation form, with small design parameters κ and τ.

Lemma 3.3.3. In the coordinate

$$\tilde{\theta} := \hat{\theta} - \theta, \qquad \tilde{\chi} := \chi - \chi_{\mathsf{n}}, \qquad \tilde{\chi}_{\mathsf{n}} := \chi_{\mathsf{n}} - \chi_{\mathsf{n}}^\star, \tag{3.3.7a}$$

$$\tilde{\mathcal{W}} := \hat{\mathcal{W}} - \mathcal{W} - \Xi\tilde{\theta}, \qquad \tilde{\eta}_{\mathrm{ext}} := \eta - \eta_{\mathrm{ext}}^\star, \tag{3.3.7b}$$

the closed-loop system (3.1.2), (3.2.1), (3.2.7), (3.2.8), and (3.2.9), and the nominal closed-loop system (3.1.4) and (3.1.5) are transformed into

- slow subsystem

$$\frac{1}{\kappa}\dot{\tilde{\theta}} = -\Xi^\top C_3^\top C_3 \Xi\tilde{\theta} + \Xi^\top \Big(\mathsf{M}_{\theta,1}\tilde{\chi} + \mathsf{M}_{\theta,2}\tilde{\chi}_{\mathsf{n}} + \mathsf{M}_{\theta,3}\tilde{\mathcal{W}} + \mathsf{E}_\theta\Omega\Big) \tag{3.3.8}$$

- intermediate subsystem

$$\dot{\tilde{\chi}} = \mathsf{A}_{\mathsf{n}}\tilde{\chi} + \mathsf{E}_\chi\Omega, \qquad \dot{\tilde{\chi}}_{\mathsf{n}} = \mathsf{A}_{\mathsf{n}}\tilde{\chi}_{\mathsf{n}}, \tag{3.3.9a}$$

$$\dot{\tilde{\mathcal{W}}} = (A_3 - LC_3)\tilde{\mathcal{W}} + \mathsf{M}_{\mathcal{W},1}\tilde{\chi} + \mathsf{M}_{\mathcal{W},2}\tilde{\chi}_{\mathsf{n}} + \mathsf{E}_{\mathcal{W}}\Omega, \tag{3.3.9b}$$

- fast subsystem

$$\tau\dot{\tilde{\eta}}_{\text{ext}} = (A_4 - \overline{\alpha}C_4)\,\tilde{\eta}_{\text{ext}} + \left(1 - \frac{g}{g_{\mathsf{n}}}\right)\overline{\gamma}(\theta;0)\Omega + \delta \tag{3.3.10}$$

where $\mathsf{M}_{\theta,i}$, $i = 1,2,3$, $\mathsf{M}_{\mathcal{W},j}$, $j = 1,2$, E_θ, and $\mathsf{E}_{\mathcal{W}}$ are some constant matrices (with appropriate dimensions) independent of τ and κ, Ξ is the solution of (3.2.1c),

$$\Omega\big(t,\tilde{\chi},\tilde{\eta}_{\text{ext},1}\big) := \bar{s}_{\mathsf{w}}\Big(\tilde{\eta}_{\text{ext},1} + \mathsf{C}_{\text{total}}\tilde{\chi} + d_{\text{total},\mathsf{n}}(t)\Big) - \Big(\mathsf{C}_{\text{total}}\tilde{\chi} + d_{\text{total},\mathsf{n}}(t)\Big), \tag{3.3.11}$$

and δ is a continuous function of the time $t \geq 0$, the state variables $[\tilde{\theta};\tilde{\chi};\tilde{\chi}_{\mathsf{n}};\tilde{\mathcal{W}};\tilde{\eta}_{\text{ext}}]$, and the parameter $\tau \geq 0$ satisfying that

$$\delta\big(t,0;\tau\big) = 0 \quad \text{and} \quad \delta\big(t,\tilde{\theta},\tilde{\chi},\tilde{\chi}_{\mathsf{n}},\tilde{\mathcal{W}},\tilde{\eta}_{\text{ext}};0\big) = 0 \tag{3.3.12}$$

for all $t \geq 0$. ◊

Proof. In the proof, we will derive the slow, intermediate, and fast dynamics in the lemma sequentially. First, let us differentiate $\tilde{\theta}$ in (3.3.9) along with the $\hat{\theta}$-dynamics (3.2.1a) as follows:

$$\begin{aligned}
\dot{\tilde{\theta}} = \dot{\hat{\theta}} - \dot{\theta} &= -\kappa\Xi^\top C_3^\top C_3\hat{\mathcal{W}} + \kappa\Xi^\top C_3^\top u - \dot{\theta} \\
&= -\kappa\Xi^\top C_3^\top C_3\big(\Xi\tilde{\theta} + \tilde{\mathcal{W}} + \mathcal{W}\big) + \kappa\Xi^\top C_3^\top u \\
&= -\kappa\Xi^\top C_3^\top C_3\Xi\tilde{\theta} + \kappa\Xi^\top\Big(-C_3^\top C_3\tilde{\mathcal{W}} + C_3^\top(u - u^\star)\Big)
\end{aligned} \tag{3.3.13}$$

in which $u^\star = C_3\mathcal{W}$ in (3.3.6) is used. It is further noted that

$$d_{\text{total}} = \mathsf{C}_{\text{total}}\chi + \mathsf{D}_{\text{total}}\begin{bmatrix} r \\ d \end{bmatrix} = \mathsf{C}_{\text{total}}\tilde{\chi} + d_{\text{total},\mathsf{n}} = \mathsf{C}_{\text{total}}\tilde{\chi} + \mathsf{C}_{\text{total}}\tilde{\chi}_{\mathsf{n}} + d^\star_{\text{total},\mathsf{n}},$$

$$u_{\text{BL}} = \mathsf{C}_{\mathsf{un}}\chi + \mathsf{D}_{\mathsf{un}}\begin{bmatrix} r \\ d \end{bmatrix} = \mathsf{C}_{\mathsf{un}}\tilde{\chi} + u_{\mathsf{n}} = \mathsf{C}_{\mathsf{un}}\tilde{\chi} + \mathsf{C}_{\mathsf{un}}\tilde{\chi}_{\mathsf{n}} + u^\star_{\mathsf{n}}.$$

On the other hand, one has

$$\begin{aligned} \bar{s}_{\mathsf{w}}(w) &= \bar{s}_{\mathsf{w}}\left(C_4 p + \frac{\mathsf{c}_2}{\tau^2}\frac{1}{g_{\mathsf{n}}}C_2 x\right) \\ &= \bar{s}_{\mathsf{w}}(C_4\eta) = \bar{s}_{\mathsf{w}}\big(C_4\tilde{\eta}_{\text{ext}} + d_{\text{total}}\big) = \bar{s}_{\mathsf{w}}\big(C_4\tilde{\eta} + \mathsf{C}_{\text{total}}\tilde{\chi} + d_{\text{total},\mathsf{n}}(t)\big). \end{aligned} \tag{3.3.14}$$

By the definition of Ω, the term $u - u^\star$ in (3.3.13) is computed by

$$\begin{aligned} u - u^\star &= u_{\text{BL}} - \bar{s}_{\mathsf{w}}(w) - \big(u^\star_{\mathsf{n}} - d^\star_{\text{total},\mathsf{n}}\big) \\ &= \big(u_{\text{BL}} - u^\star_{\mathsf{n}}\big) - \big(d_{\text{total}} - d^\star_{\text{total},\mathsf{n}}\big) - \big(\bar{s}_{\mathsf{w}}(w) - d_{\text{total}}\big) \\ &= \big(\mathsf{C}_{\mathsf{un}} - \mathsf{C}_{\text{total}}\big)\tilde{\chi} + \big(\mathsf{C}_{\mathsf{un}} - \mathsf{C}_{\text{total}}\big)\tilde{\chi}_{\mathsf{n}} - \Omega\big(\tilde{\eta}_{\text{ext},1}, d_{\text{total}}\big). \end{aligned} \tag{3.3.15}$$

Putting (3.3.15) into (3.3.13), one can obtain the $\tilde{\theta}$-dynamics as (3.3.8), with the matrices $\mathsf{M}_{\theta,3} := -C_3^\top C_3$, $\mathsf{M}_{\theta,1} = \mathsf{M}_{\theta,2} := C_3^\top(\mathsf{C}_{\mathsf{un}} - \mathsf{C}_{\text{total}})$, and $\mathsf{E}_\theta := -C_3^\top$.

It is easy to compute the $\tilde{\chi}$- and $\tilde{\chi}_{\mathsf{n}}$-dynamics in (3.3.9). To carry out the $\tilde{\mathcal{W}}$-dynamics, we first derive the time derivative of $\hat{\mathcal{W}} - \mathcal{W}$ as

$$\begin{aligned} \dot{\hat{\mathcal{W}}} - \dot{\mathcal{W}} &= \Big(A_3\hat{\mathcal{W}} + \Psi_u\hat{\theta} + L(u - C_3\hat{\mathcal{W}}) + \Xi\dot{\hat{\theta}}\Big) - \Big(A_3\mathcal{W} + \Psi_{u^\star}\theta\Big) \\ &= A_3(\hat{\mathcal{W}} - \mathcal{W}) + L(u^\star - C_3\hat{\mathcal{W}}) + \Xi\dot{\hat{\theta}} + \Psi_u(\hat{\theta} - \theta) \\ &\quad + L(u - u^\star) - (\Psi_u - \Psi_{u^\star})\theta \\ &= (A_3 - LC_3)(\hat{\mathcal{W}} - \mathcal{W}) + \Xi\dot{\tilde{\theta}} + \Psi_u\tilde{\theta} + (L - \Psi_\theta)(u - u^\star). \end{aligned}$$

(In the computation, we use the equalities $(\Psi_u - \Psi_{u^\star})\theta = \Psi_{(u-u^\star)}\theta = \Psi_\theta(u - u^\star)$.) Using the result, one has

$$\dot{\tilde{\mathcal{W}}} = \dot{\hat{\mathcal{W}}} - \dot{\mathcal{W}} - \dot{\Xi}\tilde{\theta} - \Xi\dot{\tilde{\theta}} \tag{3.3.16}$$

$$
\begin{aligned}
&= (A_3 - LC_3)(\hat{\mathcal{W}} - \mathcal{W}) + \Xi\dot{\tilde{\theta}} + \Psi_u\tilde{\theta} + (L - \Psi_\theta)(u - u^\star) - \Xi\dot{\tilde{\theta}} - \dot{\Xi}\tilde{\theta} \\
&= (A_3 - LC_3)(\hat{\mathcal{W}} - \mathcal{W}) + \Psi_u\tilde{\theta} + (L - \Psi_\theta)(u - u^\star) - ((A_3 - LC_3)\Xi + \Psi_u)\,\tilde{\theta} \\
&= (A_3 - LC_3)(\hat{\mathcal{W}} - \mathcal{W} - \Xi\tilde{\theta}) + (L - \Psi_\theta)(u - u^\star) \\
&= (A_3 - LC_3)\tilde{\mathcal{W}} + (L - \Psi_\theta)(u - u^\star) \qquad (3.3.17)
\end{aligned}
$$

Applying (3.3.15) to (3.3.17), we finally have the $\tilde{\mathcal{W}}$-dynamics as

$$
\begin{aligned}
\dot{\tilde{\mathcal{W}}} &= (A_3 - LC_3)\tilde{\mathcal{W}} + (L - \Psi_\theta)\Big((\mathsf{C}_{\mathsf{un}} - \mathsf{C}_{\text{total}})\tilde{\chi} + (\mathsf{C}_{\mathsf{un}} - \mathsf{C}_{\text{total}})\,\tilde{\chi}_{\mathsf{n}} - \Omega\Big) \\
&= (A_3 - LC_3)\tilde{\chi} + \mathsf{M}_{\mathcal{W},1}\tilde{\chi} + \mathsf{M}_{\mathcal{W},2}\tilde{\chi}_{\mathsf{n}} + \mathsf{E}_{\mathcal{W}}\Omega
\end{aligned}
$$

where $\mathsf{M}_{\mathcal{W},1} = \mathsf{M}_{\mathcal{W},2} := (L - \Psi_\theta)(\mathsf{C}_{\mathsf{un}} - \mathsf{C}_{\text{total}})$ and $\mathsf{E}_{\mathcal{W}} := -(L - \Psi_\theta)$.

Next, we differentiate $\tau\tilde{\eta}_{\text{ext}}$ along with the η-dynamics (3.3.1) in Lemma 2.3.1 as follows:

$$
\begin{aligned}
\tau\dot{\tilde{\eta}}_{\text{ext}} &= \tau\dot{\eta} - \tau\dot{\eta}^\star_{\text{ext}} \\
&= (A_4 - \overline{\alpha}C_4)\eta + \left(1 - \frac{g}{g_{\mathsf{n}}}\right)\overline{\gamma}(\hat{\theta};\tau)\bar{s}(C_4\eta) + \frac{g}{g_{\mathsf{n}}}\overline{\gamma}(\hat{\theta};\tau)d_{\text{total}} \\
&\quad + \underline{\Upsilon}(\tau)\frac{\partial\Gamma}{\partial\hat{\theta}}\dot{\hat{\theta}}\Phi_{\mathsf{n}}\frac{1}{g_{\mathsf{n}}}x - \tau\dot{\eta}^\star_{\text{ext}} \\
&= (A_4 - \overline{\alpha}C_4)(\tilde{\eta} + \eta^\star_{\text{ext}}) + \left(1 - \frac{g}{g_{\mathsf{n}}}\right)\overline{\gamma}(\hat{\theta};\tau)\bar{s}(C_4\eta) + \frac{g}{g_{\mathsf{n}}}\overline{\gamma}(\hat{\theta};\tau)C_4\eta^\star_{\text{ext}} \\
&\quad + \underline{\Upsilon}(\tau)\frac{\partial\Gamma}{\partial\hat{\theta}}\dot{\hat{\theta}}\Phi_{\mathsf{n}}\frac{1}{g_{\mathsf{n}}}x - \tau\dot{\eta}^\star_{\text{ext}} \\
&= (A_4 - \overline{\alpha}C_4)\tilde{\eta}_{\text{ext}} + \left(1 - \frac{g}{g_{\mathsf{n}}}\right)\overline{\gamma}(\theta;0)\Big(\bar{s}(C_4\tilde{\eta} + C_4\eta^\star_{\text{ext}}) - C_4\eta^\star_{\text{ext}}\Big) + \delta \\
&= (A_4 - \overline{\alpha}C_4)\tilde{\eta}_{\text{ext}} + \left(1 - \frac{g}{g_{\mathsf{n}}}\right)\overline{\gamma}(\theta;0)\Omega + \delta \qquad (3.3.18)
\end{aligned}
$$

where δ is defined by

$$
\begin{aligned}
\delta := {} & (A_4 - \overline{\alpha}C_4)\eta^\star_{\text{ext}} + \left(1 - \frac{g}{g_{\mathsf{n}}}\right)\Big(\overline{\gamma}(\hat{\theta};\tau) - \overline{\gamma}(\theta;0)\Big)\bar{s}(C_4\eta) + \overline{\gamma}(\theta;0)C_4\eta^\star_{\text{ext}} \\
& + \frac{g}{g_{\mathsf{n}}}\Big(\overline{\gamma}(\hat{\theta};\tau) - \overline{\gamma}(\theta;0)\Big)C_4\eta^\star_{\text{ext}} + \underline{\Upsilon}(\tau)\frac{\partial\Gamma}{\partial\hat{\theta}}\dot{\hat{\theta}}\Phi_{\mathsf{n}}\frac{1}{g_{\mathsf{n}}}x - \tau\dot{\eta}^\star_{\text{ext}}. \qquad (3.3.19)
\end{aligned}
$$

It is shown in Appendix A.2 that δ in (3.3.19) satisfies the desired properties,

which completes the proof of the lemma. □

3.3.2 Convergence Analysis

Since the transformed system (3.3.8), (3.3.9), and (3.3.10) in Lemma 3.3.3 is not a standard singular perturbation form, the analysis in the previous chapter is not suitable anymore. Instead, we here will separate the system into two groups for the stability analysis; the slow and intermediate subsystems (3.3.8) and (3.3.9) as a "slower" part, while the fast subsystem (3.3.10) as a "faster" part. Under this grouping, the "slower" part of the three-time scaled system can be viewed as a standard (two-time scaled) singular perturbation form with respect to the perturbation parameter κ, to which the standard singular perturbation theory is now applicable. Once κ is determined first, then one can conclude the stability of the overall system by employing the singular perturbation theory once again, in terms of another perturbation parameter τ.

One additional issue that has to be dealt with is the "initial peaking" of the fast variable $\tilde{\eta}_{\rm ext}$, as discussed in the previous chapter. We readily observe that the initial value

$$\tilde{\eta}_{\rm ext}(0) = \frac{1}{\tau}\underline{\Upsilon}(\tau)p(0) + \frac{1}{\tau}\underline{\Upsilon}(\tau)\Gamma(\hat{\theta}(0);\tau)\Phi_{\mathsf{n}}\frac{1}{g_{\mathsf{n}}}x(0) - \eta^{\star}_{\rm ext}(0,\theta;\tau), \qquad (3.3.20)$$

has the form of a polynomial of $1/\tau$ due to the structure of $\underline{\Upsilon}(\tau)\Gamma(\hat{\theta};\tau)$. Thus the set of the initial condition $\tilde{\eta}_{\rm ext}(0)$, denoted by $\mathcal{E}_0(\tau)$ (possibly dependent of τ, of course), gets larger as τ goes to zero. To tackle the second issue, let us divide the entire time period into two parts; the transient period $0 \le t < T^{\star}$ and the steady-state period $t \ge T^{\star}$ (as in the previous chapter) where $T^{\star}$ will be selected below. It is first noted that $\chi(t)$ and $\chi_{\mathsf{n}}(t)$ are assumed to be initiated at the same point in the statement of Definition 2.1.1, by which the initial condition of the slow and intermediate variables $[\tilde{\theta}(t); \tilde{\chi}(t); \tilde{\chi}_{\mathsf{n}}(t); \tilde{\mathcal{W}}(t)]$ belongs to a compact set

$$\mathcal{I}^0 \subset \Big\{ \big[\tilde{\theta}(0); \tilde{\chi}(0); \tilde{\chi}_{\mathsf{n}}(0); \tilde{\mathcal{W}}(0)\big] : \ \|\tilde{\chi}(0)\| = 0 \Big\}.$$

Let $P_\chi = P_\chi^\top > 0$ be the solution of the Lyapunov equation $\mathsf{A}_{\mathsf{n}}^\top P_\chi + P_\chi \mathsf{A}_{\mathsf{n}} = -I$,

and also let $0 < \epsilon' < \epsilon/2$ be a constant satisfying that

$$\|\mathsf{C}_{\text{total}}\|\,\epsilon' < \operatorname{dist}\big(\mathcal{D}_{\text{total},\mathsf{n}}, \overline{\mathcal{D}}_{\text{total},\mathsf{n}}.\big) \tag{3.3.21}$$

We take a larger compact set $\overline{\mathcal{I}}^0$ satisfying $\overline{\mathcal{I}}^0 \supset \mathcal{I}^0$ with the distance larger than $(\underline{\lambda}(P_\chi)/\overline{\lambda}(P_\chi))\epsilon'$. Then with the help of the saturation function $\bar{s}_{\mathsf{w}}$ again, one can select a small time instant $T^\star > 0$ (independent of τ) such that

$$\big[\tilde{\theta}(t); \tilde{\chi}(t); \tilde{\chi}_{\mathsf{n}}(t); \tilde{\mathcal{W}}(t)\big] \in \overline{\mathcal{I}}^0, \quad \forall 0 \le t \le T^\star. \tag{3.3.22}$$

In parallel with Lemma 2.3.4 in the previous chapter, the following lemma indicates that the fast variable $\tilde{\eta}_{\text{ext}}(t)$ converges around its "quasi-steady-state" $\tilde{\eta}_{\text{ext}} = 0$ with small τ for the transient period.

Lemma 3.3.4. Suppose that Assumption 3.1.1 is satisfied. Then there exists $0 < \overline{\tau}_1 < 1$ such that for $\tau \in (0, \overline{\tau}_1)$,

$$\|\tilde{\eta}_{\text{ext}}(T^\star)\| \le -\frac{\mathsf{k}_{\eta,1}}{\tau^2} e^{-(\mathsf{h}_\eta/\tau)T^\star} + \tau \mathsf{k}_{\eta,2} \tag{3.3.23}$$

where $\mathsf{k}_{\eta,1}$, $\mathsf{k}_{\eta,2}$, and h_η are τ-independent positive constants. ♢

Proof. The lemma is readily derived in the same way of Lemma 2.3.4. □

Keeping the observations on the transient behavior in mind, the remainder of this subsection is organized to analyze the overall system for the remaining time period $t \ge T^\star$. To this end, by applying $\tau = 0$ to the $\tilde{\eta}_{\text{ext}}$-dynamics (3.3.10) and by rewriting the result in the scaled time $\varsigma := (t - T^\star)/\tau$ with the slower variable $\tilde{\chi}$ being fixed, we obtain the "boundary-layer system (of the overall system)" as follows:

$$\frac{\mathrm{d}}{\mathrm{d}\varsigma}\tilde{\eta}_{\text{ext}} = (A_4 - \overline{\alpha}C_4)\tilde{\eta}_{\text{ext}} + \left(1 - \frac{g}{g_{\mathsf{n}}}\right)\overline{\gamma}(\theta;0)\Omega\big(0, \tilde{\chi}, \tilde{\eta}_{\text{ext},1}\big) \tag{3.3.24}$$

the initial condition of (3.3.24) is assumed to belong in $\underline{\mathcal{E}}^0$. By repeating the proof of Lemma 3.3.4 along with (3.3.24), one obtains the following corollary.

Corollary 3.3.5. The origin of the boundary-layer system (3.3.24) is exponentially stable with the region of attraction containing $\underline{\mathcal{E}}^0$. $\Diamond$

To discuss on the stability of the remaining part, we compute the "reduced system (of the overall system)" (which is the "slower" part (3.3.8) and (3.3.9) of the overall system on the boundary layer $\tilde{\eta}_{\text{ext}} = 0$) as follows (to avoid confusion on the terminology, we use $\circ$ in the superscript to indicate that the variable is for the reduced system):

$$\begin{aligned}\frac{1}{\kappa}\dot{\tilde{\theta}}^\circ &= -\Xi^{\circ\top} C_3^\top C_3 \Xi^\circ \tilde{\theta}^\circ \\ &\quad + \Xi^{\circ\top}\left(\mathsf{M}_{\theta,3}\tilde{\mathcal{W}}^\circ + \mathsf{M}_{\theta,1}\tilde{\chi}^\circ + \mathsf{M}_{\theta,2}\tilde{\chi}_{\mathsf{n}}^\circ + \mathsf{E}_\theta \Omega^\circ\right), \end{aligned} \tag{3.3.25a}$$

and

$$\dot{\tilde{\chi}}^\circ = \mathsf{A}_{\mathsf{n}}\tilde{\chi}^\circ + \mathsf{E}_\chi \Omega^\circ, \tag{3.3.25b}$$

$$\dot{\tilde{\chi}}_{\mathsf{n}}^\circ = \mathsf{A}_{\mathsf{n}}\tilde{\chi}_{\mathsf{n}}^\circ, \tag{3.3.25c}$$

$$\dot{\tilde{\mathcal{W}}}^\circ = \big(A_3 - LC_3\big)\tilde{\mathcal{W}}^\circ + \mathsf{M}_{\mathcal{W},1}\tilde{\chi}^\circ + \mathsf{M}_{\mathcal{W},2}\tilde{\chi}_{\mathsf{n}}^\circ + \mathsf{E}_{\mathcal{W}}\Omega^\circ \tag{3.3.25d}$$

where $\Omega^\circ(t,\tilde{\chi}^\circ) := \bar{s}_{\mathsf{w}}\big(\mathsf{C}_{\text{total}}\tilde{\chi}^\circ + d_{\text{total},\mathsf{n}}\big) - \big(\mathsf{C}_{\text{total}}\tilde{\chi}^\circ + d_{\text{total},\mathsf{n}}\big)$ and

$$\begin{aligned}\dot{\Xi}^\circ &= (A_3 - LC_3)\Xi^\circ \\ &\quad + \begin{bmatrix} 0 \\ -1 \\ 0 \end{bmatrix}\left(u^\star + (\mathsf{C}_{\mathsf{un}} - \mathsf{C}_{\text{total}})\tilde{\chi}^\circ + (\mathsf{C}_{\mathsf{un}} - \mathsf{C}_{\text{total}})\,\tilde{\chi}_{\mathsf{n}}^\circ - \Omega^\circ\right). \end{aligned} \tag{3.3.25e}$$

Then we are now ready to derive the stability of the reduced system.

Lemma 3.3.6. Suppose that Assumptions are satisfied. Then there exists $\overline{\kappa} > 0$ such that for $\kappa \in (0, \overline{\kappa})$,

(a) the partial state trajectory $\tilde{\chi}^\circ(t)$ of the reduced system (3.3.25) initiated in $\overline{\mathcal{I}}^0$ satisfies

$$\|\tilde{\chi}^\circ(t)\| < \frac{\epsilon}{2}, \quad \forall t \geq T^\star; \tag{3.3.26}$$

(b) the origin of the reduced system (3.3.25) is exponentially stable with the region of attraction containing $\overline{\mathcal{I}}^0$.

$\Diamond$

Proof. To prove the item (a), we take a look at the $\tilde{\chi}^\circ$-dynamics

$$\begin{aligned}\dot{\tilde{\chi}}^\circ &= \mathsf{A}_\mathsf{n}\tilde{\chi}^\circ + \mathsf{E}_\chi\Omega^\circ \\ &= \mathsf{A}_\mathsf{n}\tilde{\chi}^\circ + \mathsf{E}_\chi\Big(\bar{s}_\mathsf{w}\big(\mathsf{C}_{\text{total}}\tilde{\chi}^\circ + d_{\text{total},\mathsf{n}}(t)\big) - \big(\mathsf{C}_{\text{total}}\tilde{\chi}^\circ + d_{\text{total},\mathsf{n}}(t)\big)\Big)\end{aligned} \tag{3.3.27}$$

where the initial condition $\tilde{\chi}(T^\star)$ satisfies $\|\tilde{\chi}(T^\star)\| < \epsilon'$. For the analysis, let us employ a Lyapunov function candidate $V_\chi(\tilde{\chi}^\circ) := (\tilde{\chi}^\circ)^\top P_\chi(\tilde{\chi}^\circ)$ where P_χ is the solution of the Lyapunov equation $\mathsf{A}_\mathsf{n}^\top P_\chi + P_\chi\mathsf{A}_\mathsf{n} = -I$. We now claim that the set

$$\overline{\mathcal{V}} := \left\{\tilde{\chi}^\circ :\ V_\chi(\tilde{\chi}^\circ) < \underline{\lambda}(P_\chi)\frac{\epsilon'^2}{4}\right\}$$

is positive invariant. The claim is proved by contradiction. Suppose that there exists a finite time $T' \geq T^\star$ such that $V_\chi\big(\tilde{\chi}^\circ(T')\big) > \underline{\lambda}(P_\chi)(\epsilon'^2/4)$. Then by the continuity of the solution, one can always find $T^\star \leq T'' < T'$ such that the solution $\tilde{\chi}(t)$ encounters the boundary of $\overline{\mathcal{V}}$; that is, $V_\chi(\tilde{\chi}^\circ(T'')) = \underline{\lambda}(P_\chi)(\epsilon'^2/4)$. On the other hand, it is clear that as long as $\tilde{\chi}^\circ(t)$ is located in $\overline{\mathcal{V}}$, $\|\tilde{\chi}^\circ(t)\| < \epsilon'/2$ and thus $\mathsf{C}_{\text{total}}\tilde{\chi}^\circ(t) + d_{\text{total},\mathsf{n}}(t) \in \overline{\mathcal{D}}_{\text{total},\mathsf{n}}$. This leads to

$$\Omega^\circ(t,\chi^\circ(t)) = \bar{s}_\mathsf{w}\Big(\mathsf{C}_{\text{total}}\tilde{\chi}^\circ(t) + d_{\text{total},\mathsf{n}}(t)\Big) - \Big(\mathsf{C}_{\text{total}}\tilde{\chi}^\circ(t) + d_{\text{total},\mathsf{n}}(t)\Big) = 0 \tag{3.3.28}$$

for $T^\star \leq t \leq T''$. Thus for that time period, we have

$$\dot{V}_\chi(\tilde{\chi}^\circ(t)) = \big(\mathsf{A}_\mathsf{n}\tilde{\chi}^\circ(t)\big)^\top P_\chi\big(\tilde{\chi}^\circ(t)\big) + \big(\tilde{\chi}^\circ(t)\big)^\top P_\chi\big(\mathsf{A}_\mathsf{n}\tilde{\chi}^\circ(t)\big) < 0,$$

which yields that $V_\chi(\tilde{\chi}^\circ(T'')) < V_\chi(\tilde{\chi}^\circ(T^\star)) \leq \underline{\lambda}(P_\chi)(\epsilon'^2/4)$. This contradicts $V_\chi(\tilde{\chi}^\circ(T'')) = \underline{\lambda}(P_\chi)(\epsilon'^2/4)$, which completes the proof of the claim, and thus that of Item (a) since $\tilde{\chi}^\circ(T^\star) \in \overline{\mathcal{V}}$.

For the proof of the second item, we notice that the equalities (3.3.28) are satisfied for all $t \geq T^\star$ (by the discussions so far). Thus the reduced system

(3.3.25a)–(3.3.25d) (of the overall system) can be rewritten by the standard singular perturbation form (with a new scaled time $\varsigma := \kappa t$)

- slow subsystem (of the "reduced system" of the overall system)

$$\frac{\mathrm{d}}{\mathrm{d}\varsigma}\tilde{\theta}^{\circ} = -\Xi^{\circ\top} C_3^{\top} C_3 \Xi^{\circ} \tilde{\theta}^{\circ} + \Xi^{\circ\top} \left(\mathsf{M}_{\theta,1} \tilde{\chi}^{\circ} + \mathsf{M}_{\theta,2} \tilde{\chi}_{\mathsf{n}}^{\circ} + \mathsf{M}_{\theta,3} \tilde{\mathcal{W}}^{\circ} \right), \quad (3.3.29)$$

- fast subsystem (of the "reduced system" of the overall system)

$$\kappa \frac{\mathrm{d}}{\mathrm{d}\varsigma} \tilde{\chi}^{\circ} = \mathsf{A}_{\mathsf{n}} \tilde{\chi}^{\circ}, \quad (3.3.30a)$$

$$\kappa \frac{\mathrm{d}}{\mathrm{d}\varsigma} \tilde{\chi}_{\mathsf{n}}^{\circ} = \mathsf{A}_{\mathsf{n}} \tilde{\chi}_{\mathsf{n}}^{\circ}, \quad (3.3.30b)$$

$$\kappa \frac{\mathrm{d}}{\mathrm{d}\varsigma} \tilde{\mathcal{W}}^{\circ} = \left(A_3 - L C_3 \right) \tilde{\mathcal{W}}^{\circ} + \mathsf{M}_{\mathcal{W},1} \tilde{\chi}^{\circ} + \mathsf{M}_{\mathcal{W},2} \tilde{\chi}_{\mathsf{n}}^{\circ}. \quad (3.3.30c)$$

It is obvious that the origin of the fast subsystem (3.3.30) is globally exponentially stable. In accordance with the singular perturbation theory [Kha96, Theorem 11.4], it is enough for Item (b) to show that the origin of the following reduced dynamics is exponentially stable, which is computed by putting the quasi-steady-state (of the "reduced system" of the overall system) $[\tilde{\theta}^{\circ}; \tilde{\chi}^{\circ}; \tilde{\chi}_{\mathsf{n}}^{\circ}; \tilde{\mathcal{W}}^{\circ}] = 0$ into (3.3.29):

$$\frac{1}{\kappa} \dot{\tilde{\theta}}^{\circ} = -\Xi^{\circ\top} C_3^{\top} C_3 \Xi^{\circ} \tilde{\theta}^{\circ} \quad (3.3.31)$$

where $\Xi^{\circ}(t)$ is the solution of

$$\kappa \frac{\mathrm{d}}{\mathrm{d}\varsigma} \Xi^{\circ} = (A_3 - L C_3) \Xi^{\circ} + \begin{bmatrix} 0 \\ -1 \\ 0 \end{bmatrix} u^{\star}(t)$$

and $t = \varsigma/\kappa$. Note that the Ξ°-dynamics is input-to-state stable (ISS) and its input $u^{\star}(t) = u_{\mathsf{n}}^{\star}(t) - d_{\mathrm{total},\mathsf{n}}^{\star}(t)$ is a bounded sinusoidal signal of the frequency $\sigma > 0$. This yields that $C_3 \Xi^{\circ}(t)$ is "persistently exciting" [IS96, Thm. 5.2.1]; that

is, there exist positive constants $\underline{\mathsf{h}}_\Xi$, $\overline{\mathsf{h}}_\Xi$, and Δ_Ξ such that

$$0 < \underline{\mathsf{h}}_\Xi \leq \int_t^{t+\Delta_\Xi} \Xi^{\circ\top}(\rho) C_3^\top C_3 \Xi^\circ(\rho) \mathrm{d}\rho \leq \overline{\mathsf{h}}_\Xi,$$

which implies that the origin of the $\tilde{\theta}^\circ$-dynamics (3.3.31) is exponentially stable. In summary, by the singular perturbation theory [Kha96, Thm. 11.4], there exists $\overline{\kappa} > 0$ such that the origin of (3.3.25) is exponentially stable for all $\kappa \in (0, \overline{\kappa})$. □

We have observed so far in Corollary 3.3.5 and Lemma 3.3.6 that the origin of both the boundary-layer system (3.3.24) and the reduced system (3.3.25) (with fixed $\kappa \in (0, \overline{\kappa})$) are exponentially stable. Thus the following lemma follows from the singular perturbation theory [Kha96, Thm. 11.4] with respect to the perturbation parameter τ.

Lemma 3.3.7. For given $\epsilon > 0$ and $\kappa \in (0, \overline{\kappa})$ with $\overline{\kappa}$ in Lemma 3.3.6, there exists $0 < \overline{\tau} = \overline{\tau}(\kappa) < \overline{\tau}_1$ such that for $\tau \in (0, \overline{\tau}(\kappa))$, the singularly perturbed system (3.3.8), (3.3.9), and (3.3.10), initiated at $[\tilde{\theta}(T^\star); \tilde{\chi}(T^\star); \tilde{\chi}(T^\star); \tilde{\mathcal{W}}(T^\star)] \in \overline{\mathcal{I}}^0$ and $\tilde{\eta}_{\mathrm{ext}}(T^\star) \in \underline{\mathcal{E}}^0$, satisfies the following statements.

(a) the origin of the system is exponentially stable with the region of attraction containing $\overline{\mathcal{I}}^0 \times \underline{\mathcal{E}}^0$;

(b) the partial state trajectory $\tilde{\chi}(t)$ satisfies

$$\|\tilde{\chi}(t) - \tilde{\chi}^\circ(t)\| < \frac{\epsilon}{2}, \quad \forall t \geq T^\star \tag{3.3.32}$$

where $\tilde{\chi}^\circ(t)$ is the solution of (3.3.31) initiated at $\tilde{\chi}^\circ(T^\star) = \tilde{\chi}(T^\star)$.

◊

The first item of Lemma 3.3.7 naturally implies that $\mathsf{C}_\mathsf{n}\tilde{\chi}(t) = y(t) - y_\mathsf{n}(t)$ exponentially converges to zero as time goes on (or equivalently, (2.1.10) in Definition 2.1.1 holds with $[r_\mathsf{u}(t); d_\mathsf{u}(t)] \equiv 0$). On the other hand, combining (3.3.32) with Item (a) of Lemma 3.3.6, one has

$$\|\tilde{\chi}(t)\| \leq \|\tilde{\chi}(t) - \tilde{\chi}^\circ(t)\| + \|\tilde{\chi}^\circ(t)\| < \frac{\epsilon}{2} + \frac{\epsilon}{2} = \epsilon, \quad \forall t \geq T^\star.$$

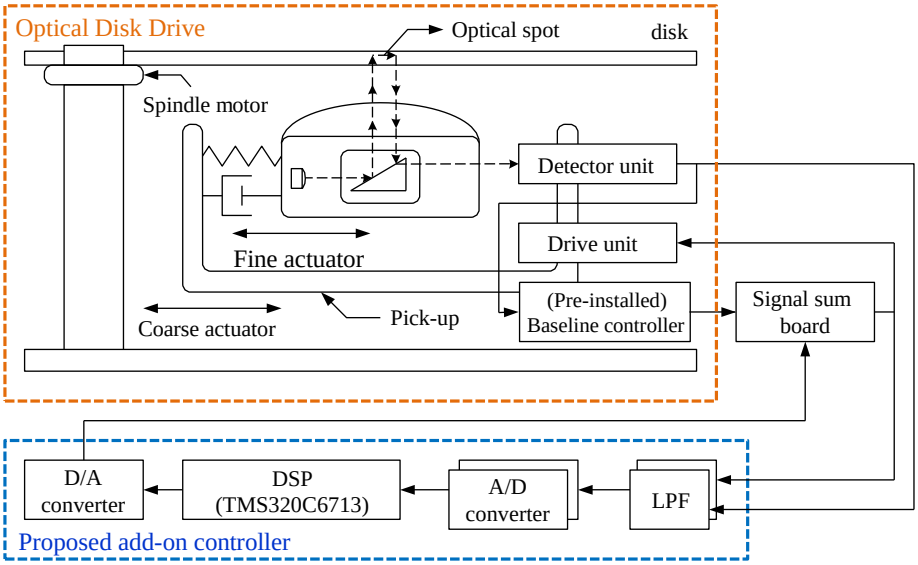

Figure 3.2: Diagram of ODD systems for experiment

Note that $\|\tilde{\chi}(t)\|$ is smaller than $\epsilon/2$ for the transient period $0 \leq t \leq T^\star$. These facts conclude the proof of the theorem.

3.4 Industrial Application: Optical Disk Drive

In this section, we apply the proposed controller to an optical disk drive (ODD) system. As shown in [Kim05], track following problem for ODD such as CD-ROM or DVD-ROM is to control the position of pick-up (more precisely, optical spot) so that it follows the desired track of disk media which is usually deviated from the concentric circles due to the disk eccentricity. The position of the pick-up is controlled by two cooperative actuators; a fine actuator and a coarse actuator, which are briefly depicted in Figure 3.2. While the coarse actuator moves slowly across the entire disk radius, the fine actuator has faster response for a small displacement. For instance, the optical spot of CD-ROM must follow the track within 0.1 μm while the displacement error caused by the disk eccentricity amounts to more than 280 μm in the worst case. The fine actuator should take care of relatively large disturbances, because the disturbance, whose frequency is synchronized with the disk rotation, is too fast to be caught up by

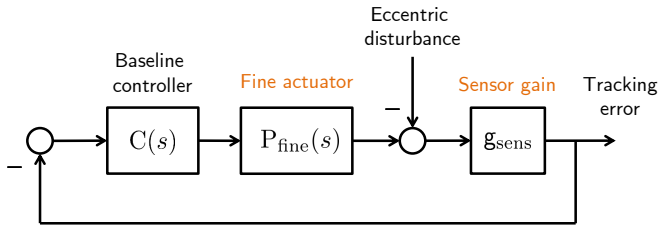

(a) Track-following servo system of the ODD systems

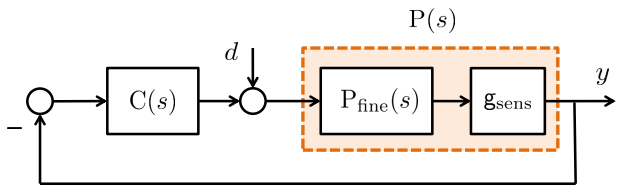

(b) Equivalent block diagram of (a)

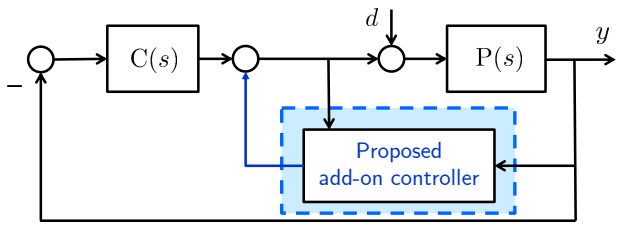

(c) Servo system with the proposed add-on controller

Figure 3.3: Configuration of ODD control system

the coarse actuator. For this reason, the fine actuator plays a central role for track following. In what follows, we consider the fine actuator only.

The closed-loop system of the track-following servo system for the ODD systems is illustrated in Figure 3.3-(a). Here $\mathrm{P}_{\mathrm{fine}}(s)$ is a fine actuator, $\mathrm{C}(s)$ is a (pre-installed) baseline controller, and $\mathrm{g}_{\mathrm{sens}}$ is a sensor gain that converts the position displacement into voltage. Since the fine actuator $\mathrm{P}_{\mathrm{fine}}(s)$ is a linear time-invariant system, we can consider that it is equivalent to the block diagram (b) of Figure 3.3. In particular, the fine actuator is modeled by a mass-spring-damper system (i.e., a second order system having full relative degree) and then

its transfer function with the sensor gain $\mathrm{P}(s) := \mathrm{P}_{\text{fine}}(s) \times \mathsf{g}_{\text{sens}}$ can be described as follows:

$$\mathrm{P}(s) = \frac{\mathsf{N}_0}{s^2 + \mathsf{D}_1 s + \mathsf{D}_0} \times \mathsf{g}_{\text{sens}} \quad (\text{V/V}). \tag{3.4.1}$$

where D_1, D_0, and N_0 are real numbers. Comparing (3.4.1) with (3.1.1), we have

$$\mathsf{M} = \frac{1}{\mathsf{N}_0 \times \mathsf{g}_{\text{sens}}}, \qquad \mathsf{C} = \frac{\mathsf{D}_1}{\mathsf{N}_0 \times \mathsf{g}_{\text{sens}}}, \qquad \mathsf{K} = \frac{\mathsf{D}_0}{\mathsf{N}_0 \times \mathsf{g}_{\text{sens}}}.$$

In Figure 3.3, the disturbance caused by the disk eccentricity can be regarded as a sinusoidal signal with unknown magnitude and phase, which can be represented by

$$d(t) = M_{\mathsf{dm},1} \sin\left(\sigma t + \varphi_{\mathsf{dm},1}\right)$$

where $M_{\mathsf{dm},1}$ and $\varphi_{\mathsf{dm},1}$ are some constants, and σ is the frequency that depends on the rotation speed of the disk. Also, the reference $r(t)$ in Assumption 3 is set as zero in the usual ODD control systems.

3.4.1 Simulation Results

Now, we carry out a computer simulation in order to illustrate the effectiveness of the proposed controller. From [KSJ14], we first consider the nominal parameters of M, C, and K as follows:

$$\mathsf{M}_{\mathsf{n}} = \frac{1}{818.22 \times \mathsf{g}_{\text{sens}}}, \quad \mathsf{C}_{\mathsf{n}} = \frac{64.73}{818.22 \times \mathsf{g}_{\text{sens}}}, \quad \mathsf{K}_{\mathsf{n}} = \frac{166800}{818.22 \times \mathsf{g}_{\text{sens}}} \tag{3.4.2}$$

where the sensor gain g_{sens} is 1.25×10^6 V/m. As the baseline controller (3.1.5) that stabilizes $\mathrm{P}_{\mathsf{n}}(s)$ with the parameters (3.4.2), we assume that the following lead-lag compensator has already been designed:

$$\mathrm{C}(s) = \frac{0.4178s^2 + 1316s + 188000}{s^2 + 41860s + 3134000}.$$

In order to show the robustness of the proposed controller, it is also assumed that the parameters of the actual plant (3.4.1) are perturbed by ± 50 % compared to

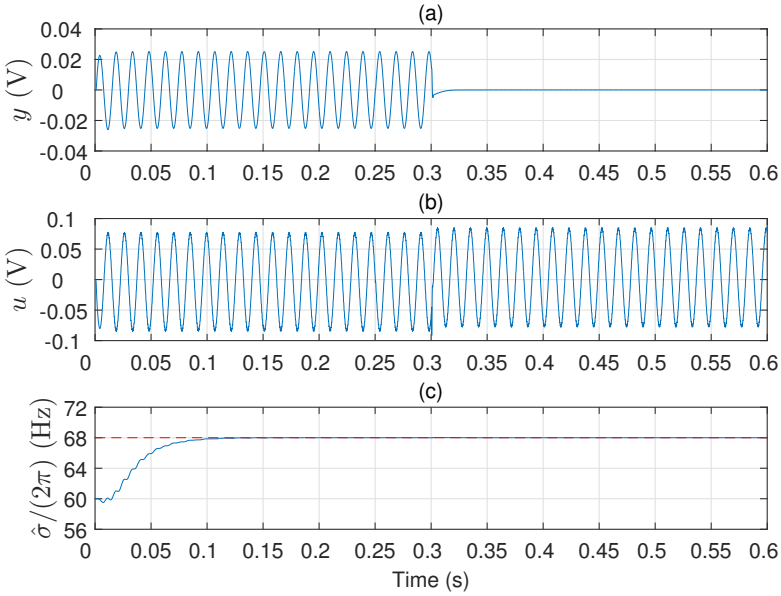

Figure 3.4: Simulation results for the proposed add-on controller (3.2.1) and (3.2.8). (a) Plant output y. (b) Control input u. (c) Frequency estimate $\hat{\sigma}/(2\pi)$ (solid) and true value $\sigma/(2\pi)$ (dashed).

its nominal values (3.4.2); for the simulation, D_1 and D_0 are set as $3/2$ times their nominal values, while N_0 as $1/2$ times its counterpart.

For simulation purposes, we assume that the disk rotation frequency σ is fixed as $2\pi \times 68$ rad/s, while its estimate $\hat{\sigma}$ (defined by the square root of $|\hat{\theta}|$) is initiated at $2\pi \times 60$ rad/s. Based on the nominal values (3.4.2), the design parameters of the proposed controller are chosen as $\tau = 0.005$, $\overline{\alpha} = [4; 6; 4; 1]$, $\kappa = 5.0 \times 10^{17}$, and $L = [1.144 \times 10^{-4}; 1.655 \times 10^{-1}; 1.644] \times 10^{6}$. It is also supposed that the output w of the proposed add-on controller is injected into the control loop at 0.3 s (that is, $u(t) = u_{\mathrm{BL}}(t)$ for $0 \le t < 0.3$ and $u(t) = u_{\mathrm{BL}}(t) - \overline{s}_{\mathsf{w}}(w(t))$ for $0.3 \le t \le 0.6$).[1] The simulation results using MATLAB/Simulink are shown in Figure 3.4. It is clear that the frequency estimate $\hat{\sigma}$ approaches the true value σ after 0.15 s and the plant output y (tracking error) converges to zero after 0.35 s. This implies that the DOB-based controller eliminates the sinusoidal disturbance

[1] This is only for comparison between tracking performances with and without the add-on controller and is not necessary for the proper operation of the add-on controller (as theoretically proved in Theorem 3.3.1 and seen in Figure 3.7).

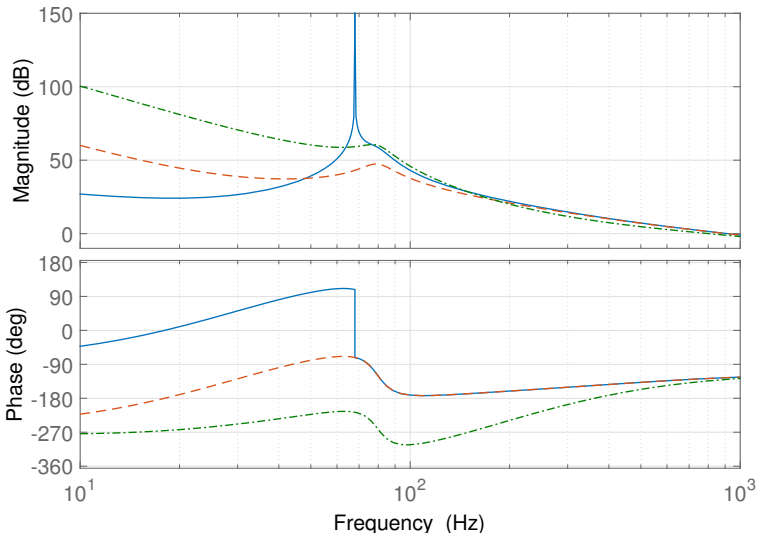

Figure 3.5: Open-loop transfer functions of the ODD controlled systems with the proposed add-on controller (blue solid), the conventional DOB with $\tau = 0.005$ (orange dashed), and the conventional DOB with $\tau = 0.001$ (green dash-dotted).

perfectly in the steady-state.

We note that the same conclusion cannot be made by the conventional DOB. For comparison, let us construct a conventional DOB instead of the proposed controller in Figure 3.3-(c). From the philosophy of the "high-order DOB" (or "type-k DOB") [CYC+03, PJSB12, YKIH97], a linear DOB is designed with the inverse model $\mathrm{P}_\mathsf{n}^{-1}(s)$ of the nominal plant $\mathrm{P}_\mathsf{n}(s) = 1/(\mathsf{M}_\mathsf{n}s^2 + \mathsf{C}_\mathsf{n}s + \mathsf{K}_\mathsf{n})$ and the 4th-order Q-filter

$$\mathrm{Q}_{\text{type}-2}(s;\tau') = \frac{6(\tau's)^2 + 4(\tau's) + 1}{(\tau's)^4 + 4(\tau's)^3 + 6(\tau's)^2 + 4(\tau's) + 1}$$

where $\tau' > 0$ determines the cutoff frequency of $\mathrm{Q}_{\text{type}-2}(s;\tau')$ (i.e., the smaller τ' is, the larger the cutoff frequency is). Here, τ' is selected within the range $0.001 \leq \tau' \leq 0.005$ so that the control bandwidth is similar to that of the proposed controller with $\tau = 0.005$. (See Figure 3.5 for the corresponding open-loop transfer functions.)

Now, we repeat the same simulation in Figure 3.4 with the (conventional)

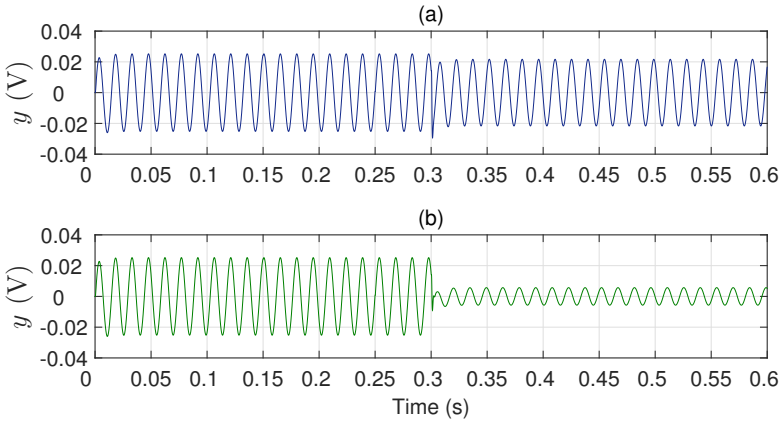

Figure 3.6: Simulation results for the conventional DOBs. (a) $\tau = 0.002$. (b) $\tau = 0.001$.

Parameter	Value	Unit
Sample rate	88.2	kHz
Resolution	16	Bits
Input range	± 2.5	V

Table 3.1: Specifications of A/D and D/A converter.

type-2 DOB above. The result can be seen in Figure 3.6. In the figure, the type-2 DOB seems to suppress the disturbance effectively as long as the bandwidth of $\mathrm{Q}_{\mathrm{type-2}}(s;\tau')$ is sufficiently large; however, the effect of the disturbance cannot be completely eliminated in all cases. The same conclusion on the performance of the DOBs can be reached from the sensitivity function analysis with Figure 3.5.

Remark 3.4.1. As well-known in the literature, in Figure 3.5, it is not possible to derive the exact open-loop transfer function when the nonlinear controller (3.2.8) is used. Nonetheless, one can compute its approximation by assuming that (a) the estimate $\hat{\theta}$ in (3.2.8) is fixed as its target value θ and (b) the saturation function $\bar{s}_{\mathsf{w}}$ in (3.2.8) is inactive; so, the p-dynamics (3.2.8) turns out to be linear. It should be noted that these assumptions are naturally satisfied in the steady-state period, as shown in Theorem 3.3.1. $\Diamond$

Although our theoretical result was derived in terms of constant frequency

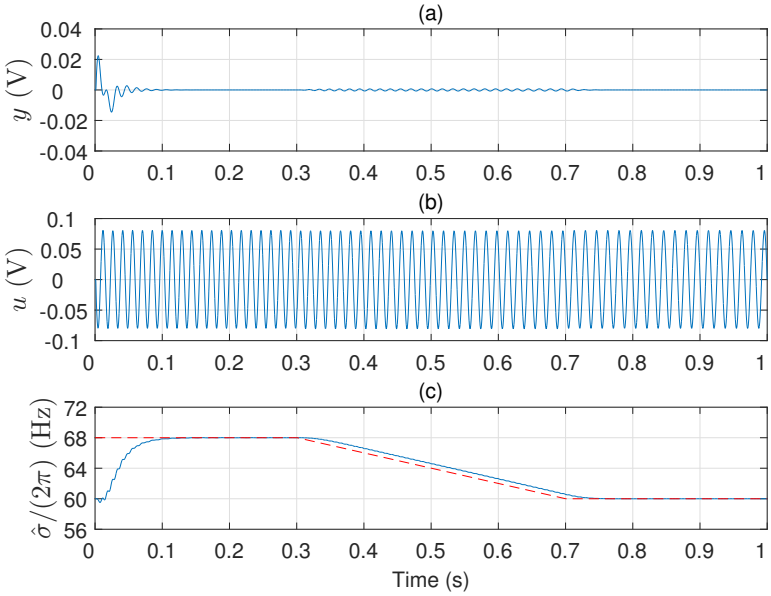

Figure 3.7: Simulation results for the proposed add-on controller (3.2.1) and (3.2.8) with slowly varying frequency. (a) Plant output y. (b) Control input u. (c) Frequency estimate $\hat{\sigma}/(2\pi)$ (solid) and true value $\sigma/(2\pi)$ (dashed).

σ, we perform additional simulation for the case when the frequency σ is slowly varying. Figure 3.7 depicts the simulation result where the proposed DOB-based controller begins to operate at $t = 0$ s (i.e., $u(t) = u_{\mathrm{BL}}(t) - \bar{s}_{\mathsf{w}}(w(t))$ for $t \geq 0$) and the actual frequency $\sigma(t)$ moves from $2\pi \times 68$ rad/s to $2\pi \times 60$ rad/s during $0.3 \leq t \leq 0.7$. It is shown that the estimate $\hat{\sigma}$ catches up the time-varying σ, and consequently the output y is rarely perturbed due to the proposed DOB-based controller.

3.4.2 Experimental Results

The inner-loop part of the proposed DOB-based controller is implemented using DSP (TMS320C6713 manufactured by Texas Instruments Incorporated) with analog to digital (A/D) and digital to analog (D/A) converter, which is depicted in Figure 3.2. The features of A/D and D/A converter are given in Table 3.1. In Figure 3.2, the low pass filter (LPF) is placed in front of A/D converter

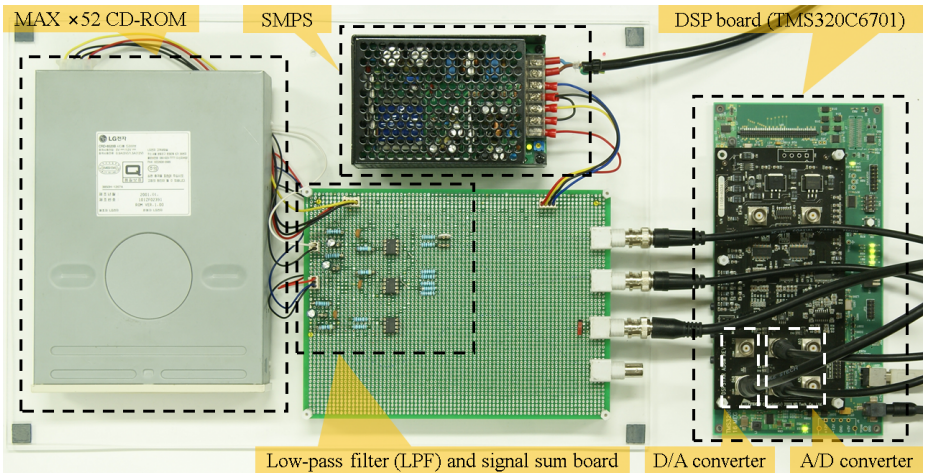

Figure 3.8: Experiment setup.

Parameter	Value	Unit
Operation voltage	±15	V
Slew rate	3000	V/μs
Unit gain bandwidth	100	MHz
Common mode rejection ratio (CMRR)	110	dB

Table 3.2: Specifications of operational amplifier.

because the measured tracking error signal contains high-frequency noise. The filter is passive RC (resistor capacitor) type, and its cut-off frequency is about 338.6 Hz. A picture of the actual experiment setup is shown in Figure 3.8. We perform an experiment where the proposed add-on controller is applied as in the computer simulation of Figure 3.4. The experiment results in Figure 3.9 show the convergence of $\hat{\sigma}$ toward the actual frequency $2\pi \times 68$ rad/s and the regulation of the plant output y, as expected in the simulation part. (The reason why the tracking error y is not cancelled out perfectly might result from the added LPF (to reduce the measurement noise at high frequency), the residual measurement noise, and the quantization error of the A/D converter.)

Remark 3.4.2. As a matter of fact, several operational amplifiers (Op Amp, LM6172 manufactured by Texas Instruments Incorporated) are used in voltage

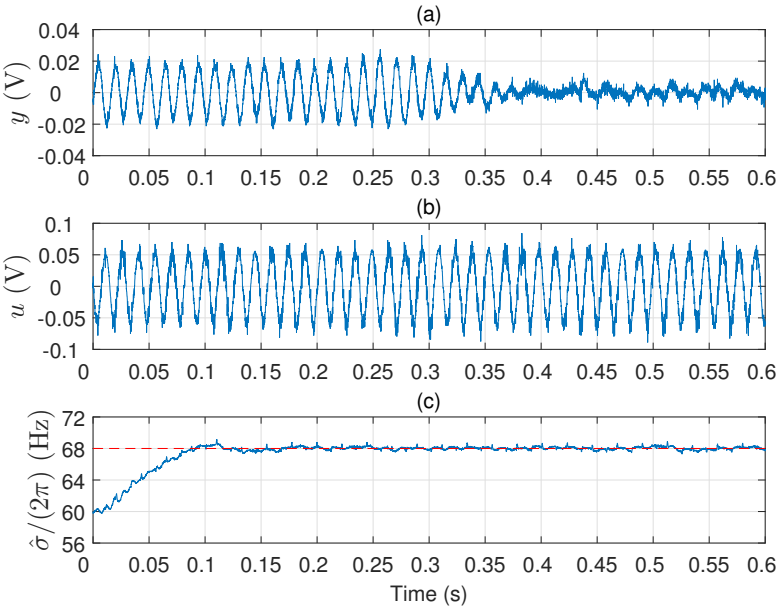

Figure 3.9: Experimental results for the proposed add-on controller (3.2.1) and (3.2.8). (a) Plant output y. (b) Control input u. (c) Frequency estimate $\hat{\sigma}/(2\pi)$ (solid) and true value $\sigma/(2\pi)$ (dashed).

follower (called *unity gain buffer*) in front of LPF and the signal sum board. Also, the LPF is implemented as a passive RC type, as aforementioned. These components may introduce signal delay and distortion in the measurement signals and the control input. For this reason, unlike the simulation results at 0.3 s, the output y in the experiment results gradually decreases over about 0.05 s. The features of the Op Amp are given in Table 3.2. ♢

Chapter 4

Guaranteeing Almost Fault-free Performance from Transient to Steady-state: Disturbance Observer-based Fault Tolerant Control

In response to the growing need for assessing high-level objectives, modern control systems usually have complicated structures. For instance, in the framework of CPS, a variant of CT and DT components are integrated and collaborate with each other, for the purpose of overcoming the limitations of traditional control systems [Lee08]. Unfortunately, the increased complexity often puts these systems into a dangerous situation resulting from faults and failures on the system components or some malicious cyber-attacks injected through data networks. These undesirable events not only degrade the overall performance of the system but also destabilize the closed-loop system, which may threaten the safety of mankind as reported by several catastrophic accidents [BFN+14, Gor09].

It is in this context that a tremendous research effort has been devoted to develop fault tolerant control (FTC) schemes in the last two decades (see the survey papers [ZJ08, YJ15] and the references therein). Two major approaches for the FTC designs have emerged in literature: passive and active FTC approaches. The first strategy is to employ a fixed controller during system operation without any detection and isolation of faults, while the other one is to reconfigure the controller structure via estimated information on the faults. Over the active FTC, the passive FTC has advantages that the design is simpler and faster response

may be ensured, at the cost of requiring knowledge on the faults in the design stage. On the other hand, the active FTC schemes are able to handle even unanticipated faults outside an expected boundary by adjusting sudden changes of the system characteristics automatically, yet at the same time additional delays may take place because of the use of fault detection/isolation algorithms. (See [ZJ08, YJ15] and the references therein.)

While numerous researches in both directions have been performed in literature, the problem of guaranteeing a "transient" tracking performance at the moment of actuator faults still has not been fully dealt with yet. The management of the transient behavior may be of particular importance to critical control systems such as power grids [LLC+17] and aircrafts, whose transient malfunctions possibly result in considerable loss of efficiency and discomfort of mankind. To the best of the authors' knowledge, only a few studies have addressed the problem [CM15, BSP14]. In [CM15], an active FTC scheme was proposed by combining an adaptive sliding mode control with a backstepping control. While this approach preserves a satisfactory post-fault transient response as much as desired, it inherently leads to high computational complexity and requires the exact information on the high-frequency gain matrix of the plant, which restricts the class of model uncertainty dealt with. On the other hand, the authors of [BSP14] introduced an adaptive-type FTC for the transient response control of spacecraft. Main drawbacks of this scheme are that full state information is explicitly used in the controller design and the transient response cannot be shaped arbitrarily.

In this chapter, we present an output feedback FTC scheme that recovers an (almost) "fault-free" nominal tracking performance during the "entire" time period, for a class of multi-input single-output (MISO) linear systems under actuator faults, parametric uncertainty, and external disturbances. Our central idea is to directly estimate a "lumped" signal representing all the effect of actuator faults, model uncertainty, and external disturbance at once and compensate it on-line, rather than try to detect the fault itself as in the traditional active FTC approaches (which possibly introduce an additional delay). To implement the idea, in this work a passive FTC is constructed by following the DOB approach. It should be noted that when it comes to our problem, the inverse model-based

DOB designs in the literature are not applicable directly. This is because (a) most of the works dealt only with square systems, and (b) the DOB in [BS08, BS09] requires the minimum phaseness of the plant, which may be lost when an actuator fault happens. For this reason, a fixed control allocation (CA) law comes into the picture in our FTC design [JF13]. In particular, provided that the MISO plant is of minimum phase in an input-wise sense, we propose a design guideline for the CA law, with which the plant (with a virtual "scalar" input) remains of minimum phase robustly against any patterns of actuator faults and parametric uncertainties. With the aid of the CA law, we propose a new inverse model-based DOB design for the augmented SISO system in order to quickly compensate all admissible abrupt changes of system caused by the actuator faults. It will be proved via the singular perturbation theory [Hop66, KKO99] that the proposed DOB-based FTC, consisting of the DOB and the CA law, resolves the problem of interest.

A few additional remarks on the proposed FTC are: (a) our result is semi-global so that any large (but bounded) parametric uncertainty and actuator faults can be handled; and (b) without utilizing structural knowledge on the disturbance, the performance recovery of the DOB-based FTC is approximate; however, the approximation error can be made small arbitrarily.

4.1 Problem Formulation

We consider a MISO linear plant

$$\dot{\mathtt{x}} = \mathbf{A}\mathtt{x} + \mathbf{B}(u + d), \quad y = \mathbf{C}\mathtt{x} \tag{4.1.1}$$

where $\mathtt{x} \in \mathbb{R}^n$ is the state, $y \in \mathbb{R}$ is the output, $d = [d_1; \ldots; d_m] \in \mathbb{R}^m$ is the disturbance, $u = [u_1; \ldots; u_m] \in \mathbb{R}^m$ is the actuator input, and $\mathbf{A} \in \mathbb{R}^{n\times n}$, $\mathbf{B} =: [\mathbf{B}_1, \ldots, \mathbf{B}_m] \in \mathbb{R}^{n\times m}$, and $\mathbf{C} \in \mathbb{R}^{1\times n}$ are unknown matrices satisfying that $(\mathbf{A}, \mathbf{B})$ is controllable and $(\mathbf{C}, \mathbf{A})$ is observable. The disturbance $d(t)$ is of $\mathfrak{C}^2$, and $d(t)$ and its time derivative are bounded with known bounds. It is assumed that the initial condition $\mathtt{x}(0)$ belongs to a bounded set.

Throughout this paper, we pay our attention to a particular class of MISO

systems (4.1.1) that are of minimum phase in an "input-wise" sense, stated as follows.

Assumption 4.1.1. Each SISO subsystem $\mathbf{C}(sI - \mathbf{A})^{-1}\mathbf{B}_i$, $i = 1, \ldots, m$, of (4.1.1) satisfies the following conditions:

(a) The system has the relative degree $\nu \geq 1$ uniformly on $i = 1, \ldots, m$; more precisely, $\mathbf{C}\mathbf{A}^j\mathbf{B}_i = 0$ for all $j = 0, \ldots, \nu-2$, and $\mathbf{C}\mathbf{A}^{\nu-1}\mathbf{B}_i \neq 0$ with known sign;

(b) The numerator of its transfer function, denoted by $\mathrm{N}_i(s)$, is included in the set of Hurwitz polynomials

$$\mathcal{N}_i := \left\{ \mathrm{N}_i(s) = \mathsf{N}_{i,n-\nu}s^{n-\nu} + \mathsf{N}_{i,n-\nu-1}s^{n-\nu-1} + \cdots + \mathsf{N}_{i,0} : \mathsf{N}_{i,j} \in [\underline{\mathsf{N}}_{i,j}, \overline{\mathsf{N}}_{i,j}] \right\} \tag{4.1.2}$$

where $\underline{\mathsf{N}}_{i,j}$ and $\overline{\mathsf{N}}_{i,j}$ are known constants.

$\Diamond$

Without loss of generality, let $\mathbf{C}\mathbf{A}^{\nu-1}\mathbf{B} > 0$ for all $i = 1, \ldots, m$.

The first item of Assumption 4.1.1 admits a coordinate change

$$\begin{bmatrix} x \\ \zeta \end{bmatrix} := \begin{bmatrix} \mathbf{T}_{\mathtt{x}} \\ \mathbf{T}_{\zeta} \end{bmatrix} \mathtt{x} \tag{4.1.3}$$

for the state $\mathtt{x}$ such that $\mathbf{T}_{\mathtt{x}} := [\mathbf{C}; \mathbf{C}\mathbf{A}; \cdots; \mathbf{C}\mathbf{A}^{\nu-1}] \in \mathbb{R}^{\nu \times n}$ and $[\mathbf{T}_{\mathtt{x}}; \mathbf{T}_{\zeta}] \in \mathbb{R}^{n \times n}$ is nonsingular. In the coordinate, the plant (4.1.1) of our interest is newly represented as the form

$$\dot{x} = A_\nu x + B_\nu\big(\phi^\top x + \psi^\top z + g\,(u + d)\,\big), \qquad y = C_\nu x, \tag{4.1.4a}$$

$$\dot{\zeta} = S\zeta + Gx + H\,(u + d)\,, \tag{4.1.4b}$$

Here, for an integer $i \geq 1$, the matrices A_i, B_i, and C_i are defined as

$$A_i := \begin{bmatrix} 0_{i-1} & I_{i-1} \\ 0 & 0_{i-1}^\top \end{bmatrix} \in \mathbb{R}^{i \times i}, \quad B_i := \begin{bmatrix} 0_{i-1} \\ 1 \end{bmatrix} \in \mathbb{R}^{i \times 1}, \quad C_i := \begin{bmatrix} 1 & 0_{i-1}^\top \end{bmatrix} \in \mathbb{R}^{1 \times i},$$

while the matrices $\phi \in \mathbb{R}^{\nu}$, $\psi \in \mathbb{R}^{n-\nu}$, $g := [g_1, \ldots, g_m] \in \mathbb{R}^{1\times m}$, $S \in \mathbb{R}^{(n-\nu)\times(n-\nu)}$, $G \in \mathbb{R}^{(n-\nu)\times\nu}$, and $H =: [H_1, \ldots, H_m] \in \mathbb{R}^{(n-\nu)\times m}$ are uncertain by definition. It is easy to see that $g_i = \mathbf{C}\mathbf{A}^{\nu-1}\mathbf{B}_i > 0$, and $0 < \underline{g}_i \leq g_i \leq \overline{g}_i$ with positive constants $\underline{g}_i$ and $\overline{g}_i$. Under the assumptions, one can also see that $x(0) \in \mathcal{X}^0$ and $\zeta(0) \in \mathcal{S}^0$ for some compact sets $\mathcal{X}^0 \subset \mathbb{R}^{\nu}$ and $\mathcal{S}^0 \subset \mathbb{R}^{n-\nu}$. Keeping the equivalence of (4.1.1) and (4.1.4) in mind, in what follows we mainly regard (4.1.4) as the plant to be controlled.

We suppose that in addition to the model uncertainty and the external disturbance, at most $m-1$ actuator faults may take place during the operation. For its detailed description, let us define $T_i > 0$, $i = 1, \ldots, m$, as the time instant when the i-th actuator is under fault. To prevent the controllability of (4.1.4) from losing, it is natural to assume that there exists at least one $i \in [m]$ satisfying that $T_i = \infty$. Then

$$\mu(t) := \{i : \ t < T_i\} \in 2^{[m]} \setminus \{\emptyset\} \tag{4.1.5}$$

stands for the set of indices, of which the actuators operates normally at the moment t. On the other hand, for given $\mu \in 2^{[m]} \setminus \{\emptyset\}$ the indicator matrix $\Lambda_\mu \in \mathbb{R}^{m\times m}$ is defined as a diagonal matrix $\Lambda_\mu = \mathrm{diag}(\Lambda_{\mu,1}, \ldots, \Lambda_{\mu,m})$ where $\Lambda_{\mu,i} = 1$ if $i \in \mu$ and $\Lambda_{\mu,i} = 0$ otherwise. With these symbols, the following assumption on the actuator failure is made.

Assumption 4.1.2. The actuator input $u(t)$ of the plant (4.1.4) is the form of

$$u(t) = \Lambda_{\mu(t)} u_{\mathrm{con}}(t) + \left(I - \Lambda_{\mu(t)}\right) u^\star_{\mathrm{flt}} \tag{4.1.6}$$

where $\mu(t)$ is defined as (4.1.5), $u_{\mathrm{con}} =: [u_{\mathrm{con},1}, \cdots, u_{\mathrm{con},m}]^\top \in \mathbb{R}^m$ is the input signal generated by a controller, and $u^\star_{\mathrm{flt}} =: [u_{\mathrm{flt},1}, \ldots, u_{\mathrm{flt},m}]^\top \in \mathbb{R}^m$ is an unknown constant vector contained in an (arbitrarily large but) bounded set. Moreover, there exists a dwell time $\Delta_{\mathrm{dwell}} > 0$ such that the failure moments T_i in (4.1.5) satisfy $\min_{i,j\in[m]}(|T_i - T_j|) \geq \Delta_{\mathrm{dwell}}$. ◊

Remark 4.1.1. The class of actuator faults considered in Assumption 4.1.2 include the lock-in-place (or stuck) fault (i.e., $u^\star_{\mathrm{flt},i} = u_i(T_i)$) and the floating fault (i.e., $u^\star_{\mathrm{flt},i} = u^\star_i$ for an unknown $u^\star_i$). ◊

The main purpose of this chapter is to force the considered plant (4.1.4) to behave as a "fault-free" nominal model, in view of the output trajectory. Since the worst scenario we may encounter (in the sense of actuator failure) is that only one healthy actuator is left, it would be reasonable to consider the following SISO system as a nominal model of (4.1.4):

$$\dot{x}_{\mathsf{n}} = A_\nu x_{\mathsf{n}} + B_\nu\big(\phi_{\mathsf{n}}^\top x_{\mathsf{n}} + \psi_{\mathsf{n}}^\top \zeta_{\mathsf{n}} + g_{\mathsf{n}} v_{\mathsf{n}}\big), \qquad y_{\mathsf{n}} = C_\nu x_{\mathsf{n}}, \tag{4.1.7a}$$

$$\dot{\zeta}_{\mathsf{n}} = S_{\mathsf{n}}\zeta_{\mathsf{n}} + G_{\mathsf{n}} x_{\mathsf{n}} + H_{\mathsf{n}} v_{\mathsf{n}} \tag{4.1.7b}$$

where $x_{\mathsf{n}} \in \mathbb{R}^\nu$ and $\zeta_{\mathsf{n}} \in \mathbb{R}^{n-\nu}$ are the nominal states, $v_{\mathsf{n}} \in \mathbb{R}$ is the nominal (scalar) input, and $y_{\mathsf{n}} \in \mathbb{R}$ is the nominal output. The matrices ϕ_{n}, ψ_{n}, G_{n}, S_{n}, M_{n}, and H_{n} are nominal components, and the initial conditions $x_{\mathsf{n}}(0)$ and $\zeta_{\mathsf{n}}(0)$ are located in $\mathcal{X}^0$ above and a compact subset $\mathcal{S}_{\mathsf{n}}^0$ of $\mathbb{R}^{n-\nu}$, respectively. (For some technical reason, let $\mathcal{S}_{\mathsf{n}}^0$ be larger than a bounded set $\{(H_{\mathsf{n}}/g_{\mathsf{n}})B_\nu^\top x_{\mathsf{n}}(0) : x_{\mathsf{n}}(0) \in \mathcal{X}^0\}$.) It is supposed that without any uncertain factor, a (static or dynamic) output feedback controller

$$\dot{c}_{\mathsf{n}} = Ec_{\mathsf{n}} + F(r - y_{\mathsf{n}}), \qquad v_{\mathsf{n}} = Jc_{\mathsf{n}} + K(r - y_{\mathsf{n}}) \tag{4.1.8}$$

is constructed *a priori* for the nominal model (4.1.7), in which $c_{\mathsf{n}} \in \mathbb{R}^{n_{\mathsf{c}}}$ is the controller state initiated in a compact set $\mathcal{C}_{\mathsf{n}}^0$, $r \in \mathbb{R}$ is the reference signal for y_{n} such that $r(t)$ is $\mathfrak{C}^2$, and $r(t)$ and $\dot{r}(t)$ are bounded, and E, F, J, and K are some matrices. We assume that the controller (4.1.8) stabilizes the nominal closed-loop system (4.1.7) and (4.1.8) and ensures a satisfactory tracking performance.

Now, we are ready to state the problem under consideration.

Problem of Chapter 4: Provided that Assumptions 4.1.1 and 4.1.2 hold and a threshold $\epsilon > 0$ is given, to construct an output feedback fault tolerant controller (FTC)

$$\dot{\varrho} = f_{\mathrm{ftc}}(\varrho, y, r), \qquad u_{\mathrm{con}} = h_{\mathrm{ftc}}(\varrho, y, r) \tag{4.1.9}$$

such that (a) the state $[x(t); \zeta(t)]$ of the closed-loop system (4.1.4), (4.1.6), and

(4.1.9) is bounded during the system operation, and (b) its output $y(t)$ satisfies

$$\|y(t) - y_{\mathsf{n}}(t)\| < \epsilon, \quad \forall t \geq 0, \tag{4.1.10}$$

where $y_{\mathsf{n}}(t)$ is an output trajectory of the nominal closed-loop system (4.1.7) and (4.1.8) with $x(0) = x_{\mathsf{n}}(0) \in \mathcal{X}^0$ (or equivalently, $[y_{\mathsf{n}}(0), \ldots, y_{\mathsf{n}}^{(\nu-1)}(0)]^\top = [y(0), \ldots, y^{(\nu-1)}(0)]^\top$) and some $[\zeta_{\mathsf{n}}(0); c_{\mathsf{n}}(0)] \in \mathcal{S}_{\mathsf{n}}^0 \times \mathcal{C}_{\mathsf{n}}^0$. ■

The second item in the problem statement, which is our primary concern, means that the FTC (4.1.9) recovers a pre-defined "fault-free" tracking performance of the nominal closed-loop system (4.1.7) and (4.1.8) in approximate but arbitrarily accurate sense. More importantly, this recovery is desired to be achieved for transient (as well steady-state) periods including the failure moments, $t = T_i$.

4.2 Design of Disturbance Observer-based Fault Tolerant Controller

In this section, we propose an output feedback FTC (4.1.9) that solves the problem of this chapter, based on the DOB approach. It should be noted that the usual DOB designs in the literature are not directly applicable to our problem. This is because, the previous works mostly took into account square systems (i.e., systems having the same number of inputs and outputs) with the number of inputs known, whereas the plant (4.1.4) and (4.1.6) considered here has an uncertain number of redundant inputs (in which such uncertainty follows from possible actuator faults)

As a simple way to avoid this difficulty, we here employ an auxiliary "scalar" input $v \in \mathbb{R}$ and allocate it into the control input $u_{\mathrm{con}}(t)$ of (4.1.4) as

$$u_{\mathrm{con}}(t) = \boldsymbol{\kappa} v(t) \tag{4.2.1}$$

where $\boldsymbol{\kappa} = [\boldsymbol{\kappa}_1; \cdots; \boldsymbol{\kappa}_m] \in \mathbb{R}^{m \times 1}$ is a constant vector. The underlying rationale behind the fixed CA law (4.2.1) is that the plant (4.1.4) and (4.1.6) augmented

with (4.2.1), computed by

$$\dot{x} = A_\nu x + B_\nu\Big(\phi^\top x + \psi^\top \zeta + g\Lambda_\mu \boldsymbol{\kappa} v + g(1-\Lambda_\mu)u_{\rm flt}^\star + gd\Big), \quad y = C_\nu x, \tag{4.2.2a}$$

$$\dot{\zeta} = S\zeta + Gx + H\Lambda_\mu \boldsymbol{\kappa} v + H(1-\Lambda_\mu)u_{\rm flt}^\star + Hd, \tag{4.2.2b}$$

now can be viewed as a SISO system with respect to the auxiliary input v; more importantly, this property is invariant on the pattern of the actuator faults. Another advantage of (4.2.1) is that the design parameter $\boldsymbol{\kappa}$ explicitly appears in the new input matrix $[g\Lambda_\mu\boldsymbol{\kappa}; H\Lambda_\mu\boldsymbol{\kappa}]$ of the SISO system (4.2.2), which brings an opportunity to handle the system zeros of (4.2.2). This is of utter importance to us, since the DOB design basically follows the philosophy of high-gain technique [BS08, BS09] where the controlled plant is necessarily of minimum phase. In the next subsection, we will show that this requirement can always be obtained (even in the presence of model uncertainty and actuator faults) by selecting $\boldsymbol{\kappa}$ appropriately.

4.2.1 Static Gain of Control Allocation Law

We start by introducing a natural definition of the minimum phaseness for the system (4.2.2).

Definition 4.2.1. The system (4.2.2) with the switching signal $\mu(t)$ in (4.1.5) is said to *be of μ-invariant minimum phase* if it is of minimum phase for any constant $\mu \in 2^{[m]} \setminus \{\emptyset\}$. ◊

The following lemma then provides a simple necessary and sufficient condition for the μ-invariant minimum phaseness.

Lemma 4.2.1. All the systems (4.1.4) satisfying Assumption 4.1.1 are of μ-invariant minimum phase if and only if, for the set

$$\mathcal{K}_\mu := \Big\{\sum\nolimits_{i\in\mu} \boldsymbol{\kappa}_i \mathrm{N}_i(s) : \mathrm{N}_i(s) \in \mathcal{N}_i \text{ in (4.1.2)}\Big\}, \tag{4.2.3}$$

every polynomials in $\bigcup_{\mu\in 2^{[m]}\setminus\{\emptyset\}} \mathcal{K}_\mu$ are Hurwitz. ◊

Proof. The lemma can be easily proved by showing that for the transfer function of (4.1.4) with a constant set $\mu \in 2^{[m]} \setminus \{\emptyset\}$, its numerator is the same as $\sum_{i\in\mu} \boldsymbol{\kappa}_i \mathrm{N}_i(s)$. □

Motivated by the result of Lemma 4.2.1, the main goal of this subsection is to design the static gain $\boldsymbol{\kappa}$ in (4.2.1) that makes every elements of $\bigcup_{2^{[m]}\setminus\{\emptyset\}} \mathcal{K}_\mu$ in Lemma 4.2.1 Hurwitz. In the following, such $\boldsymbol{\kappa}$ will be selected in an iterative way. For this, let us consider the equality

$$\bigcup\nolimits_{2^{[k+1]}\setminus\{\emptyset\}} \mathcal{K}_\mu = \mathcal{K}_{\{k+1\}} \cup \Big(\bigcup\nolimits_{\mu\in 2^{[k]}\setminus\{\emptyset\}} \mathcal{K}_\mu\Big) \cup \Big(\bigcup\nolimits_{\mu\in 2^{[k]}\setminus\{\emptyset\}} \mathcal{K}_{\mu\cup\{k+1\}}\Big) \quad (4.2.4)$$

for $k = 0, \ldots, m-1$, which presents a recursive decomposition of $\bigcup_{2^{[k+1]}\setminus\{\emptyset\}} \mathcal{K}_\mu$. We here note that the set $\bigcup_{\mu\in 2^{[k]}\setminus\{\emptyset\}} \mathcal{K}_\mu$ in the recursive relation (4.2.4) is well-defined only with partial components $\boldsymbol{\kappa}_1, \ldots, \boldsymbol{\kappa}_k$ of $\boldsymbol{\kappa}$. It is also pointed out that for any polynomial $\mathrm{N}_i(s) \in \mathcal{N}_i$, its leading coefficient $\mathsf{N}_{i,n-\nu}$ is the same as the i-th component $g_i > 0$ of the high-frequency gain matrix g of (4.1.4).

We now claim that if $\boldsymbol{\kappa}_i > 0$, $i = 1, \ldots, k$ (with $k \leq m-2$), are chosen such that the polynomials in $\bigcup_{\mu\in 2^{[k]}\setminus\{\emptyset\}} \mathcal{K}_\mu$ are all Hurwitz, then there exists $\boldsymbol{\kappa}_{k+1} > 0$ with which the polynomials in $\bigcup_{\mu\in 2^{[k+1]}\setminus\{\emptyset\}} \mathcal{K}_\mu$ are also Hurwitz. Under the hypothesis and Item (b) of Assumption 4.1.1, the first two sets in the right hand-side of (4.2.4) naturally consist only of stable polynomials, regardless of the vaule of $\boldsymbol{\kappa}_{k+1}$. On the other hand, for each $\mu \in 2^{[k]} \setminus \{\emptyset\}$ an element of $\mathcal{K}_{\mu\cup\{k+1\}}$ is the form of

$$\mathrm{K}_{\mu\cup\{k+1\}}(s) := \boldsymbol{\kappa}_{k+1}\mathrm{N}_{k+1}(s) + \sum\nolimits_{i\in\mu} \boldsymbol{\kappa}_i \mathrm{N}_i(s). \quad (4.2.5)$$

Notice that because $\boldsymbol{\kappa}_i \mathrm{N}_{i,n-\nu} > 0$ for all $i = 1, \ldots, k$ and the latter polynomial $\sum_{i\in\mu} \boldsymbol{\kappa}_i \mathrm{N}_i(s)$ in (4.2.5) is Hurwitz by definition, all the coefficients of $\mathrm{K}_{\mu\cup\{k+1\}}(s)$ above must be positive. It is then obtained from the Kharitonov's theorem [BCK95] that for given $\mu \in 2^{[k]} \setminus \{\emptyset\}$ and $\boldsymbol{\kappa}_{k+1} > 0$, all the uncertain polynomials $\mathrm{K}_{\mu\cup\{k+1\}}(s)$ in $\mathcal{K}_{\mu\cup\{k+1\}}$ are Hurwitz if and only if the following four ex-

treme polynomials are Hurwitz:

$$\mathrm{K}^{\star}_{\mu\cup\{k+1\},\mathsf{j}}(s) := \boldsymbol{\kappa}_{k+1}\mathrm{N}^{\star}_{k+1,\mathsf{j}}(s) + \sum\nolimits_{i\in\mu} \boldsymbol{\kappa}_i \mathrm{N}^{\star}_{i,\mathsf{j}}(s), \qquad \forall\, \mathsf{j} = \mathsf{a},\mathsf{b},\mathsf{c},\mathsf{d} \tag{4.2.6}$$

where for $i = 1, \ldots, m$,

$$\begin{aligned}
&\mathrm{N}^{\star}_{i,\mathsf{a}}(s) && (4.2.7a)\\
&\quad := \overline{\mathsf{N}}_{i,n-\nu}s^{n-\nu} + \overline{\mathsf{N}}_{i,n-\nu-1}s^{n-\nu-1} + \underline{\mathsf{N}}_{i,n-\nu-2}s^{n-\nu-2} + \underline{\mathsf{N}}_{i,n-\nu-3}s^{n-\nu-3} + \cdots,\\
&\mathrm{N}^{\star}_{i,\mathsf{b}}(s) && (4.2.7b)\\
&\quad := \overline{\mathsf{N}}_{i,n-\nu}s^{n-\nu} + \underline{\mathsf{N}}_{i,n-\nu-1}s^{n-\nu-1} + \underline{\mathsf{N}}_{i,n-\nu-2}s^{n-\nu-2} + \overline{\mathsf{N}}_{i,n-\nu-3}s^{n-\nu-3} + \cdots,\\
&\mathrm{N}^{\star}_{i,\mathsf{c}}(s) && (4.2.7c)\\
&\quad := \underline{\mathsf{N}}_{i,n-\nu}s^{n-\nu} + \underline{\mathsf{N}}_{i,n-\nu-1}s^{n-\nu-1} + \overline{\mathsf{N}}_{i,n-\nu-2}s^{n-\nu-2} + \overline{\mathsf{N}}_{i,n-\nu-3}s^{n-\nu-3} + \cdots,\\
&\mathrm{N}^{\star}_{i,\mathsf{d}}(s) && (4.2.7d)\\
&\quad := \overline{\mathsf{N}}_{i,n-\nu}s^{n-\nu} + \underline{\mathsf{N}}_{i,n-\nu-1}s^{n-\nu-1} + \underline{\mathsf{N}}_{i,n-\nu-2}s^{n-\nu-2} + \overline{\mathsf{N}}_{i,n-\nu-3}s^{n-\nu-3} + \cdots.
\end{aligned}$$

We emphasize that $\mathrm{N}^{\star}_{i,\mathsf{j}}(s)$ in (4.2.7) are the very extreme polynomials of $\mathrm{N}_i(s)$ of the set $\mathcal{N}_i$ in (4.1.2), all of which are thus Hurwitz by the Kharitonov's theorem and Item (b) of Assumption 4.1.2. It then follows from the root locus technique that for each $\mathsf{j} \in \{\mathsf{a},\ldots,\mathsf{d}\}$, there exists sufficiently large $\underline{\boldsymbol{\kappa}}_{\mu\cup\{k+1\},\mathsf{j}} > 0$ such that $\mathrm{K}^{\star}_{\mu\cup\{k+1\},\mathsf{j}}(s)$ in (4.2.6) is Hurwitz for all $\boldsymbol{\kappa}_{k+1} > \underline{\boldsymbol{\kappa}}_{\mu\cup\{k+1\},\mathsf{j}} > 0$. At last, take $\boldsymbol{\kappa}_{k+1}$ sufficiently large to satisfy

$$\boldsymbol{\kappa}_{k+1} > \max_{\mu\in 2^{[k+1]}\setminus\{\emptyset\}} \left\{ \max_{\mathsf{j}=\{\mathsf{a},\mathsf{b},\mathsf{c},\mathsf{d}\}} \left\{ \underline{\boldsymbol{\kappa}}_{\mu\cup\{k+1\},\mathsf{j}} \right\} \right\} \tag{4.2.8}$$

so that all the uncertain polynomials of $\bigcup_{\mu\in 2^{[k+1]}\setminus\{\emptyset\}} \mathcal{K}_{\mu\cup\{k+1\}}$ (and thus those of $\bigcup_{\mu\in 2^{[k+1]}\setminus\{\emptyset\}} \mathcal{K}_{\mu}$ in the left hand-side of (4.2.4)) are Hurwitz.

By repeating this routine up to $m-1$ steps, we propose a design guideline for the static gain $\boldsymbol{\kappa}$.

Procedure 4.2.2. (Static gain $\boldsymbol{\kappa}$ of control allocation law)

STEP 0 Take $\boldsymbol{\kappa}_1 > 0$ arbitrarily so that all the polynomials of $\bigcup_{2^{[1]}\setminus\{\emptyset\}} \mathcal{K}_{\mu}$ ($= \mathcal{K}_{\{1\}}$) are Hurwitz.

STEP k ($k = 1, \ldots, m-1$) For each $\mu \in 2^{[k+1]} \setminus \{\emptyset\}$ and each $\mathsf{j} \in \{\mathsf{a}, \ldots, \mathsf{d}\}$, select $\underline{\boldsymbol{\kappa}}_{\mu\cup\{k+1\},\mathsf{j}} > 0$ such that with $\boldsymbol{\kappa}_i$ derived by the previous steps, the extreme polynomials $\mathrm{K}^{\star}_{\mu\cup\{k+1\},\mathsf{j}}(s)$ in (4.2.6) are Hurwitz for all $\boldsymbol{\kappa}_{k+1} > \underline{\boldsymbol{\kappa}}_{\mu\cup\{k+1\},\mathsf{j}} > 0$. Choose $\boldsymbol{\kappa}_{k+1}$ to satisfy (4.2.8).

STEP m With $\boldsymbol{\kappa}_i$ selected in the above steps, take $\boldsymbol{\kappa} = [\boldsymbol{\kappa}_1; \cdots; \boldsymbol{\kappa}_m]$.

$\Diamond$

Theorem 4.2.3. Under Assumption 4.1.1, the SISO system (4.2.2) with $\boldsymbol{\kappa}$ computed by Procedure 4.2.2 is of μ-invariant minimum-phase. $\Diamond$

Proof. The proof is trivial and thus it is omitted. $\square$

4.2.2 Representation to Byrnes-Isidori Normal Form

As a prerequisite for the DOB design, in this subsection we represent the augmented system (4.2.2) and the nominal model (4.1.7) into a Byrnes-Isidori normal form [Kha96, Chapter 11].

For the former dynamics, we first introduce a variable

$$z_\mu := \zeta - \frac{1}{g\Lambda_\mu\boldsymbol{\kappa}} H\Lambda_\mu\boldsymbol{\kappa}B_\nu^\top x = \zeta - \frac{1}{g\Lambda_\mu\boldsymbol{\kappa}} H\Lambda_\mu\boldsymbol{\kappa}x_\nu \in \mathbb{R}^{n-\nu}. \tag{4.2.9}$$

It is noted that with $\boldsymbol{\kappa}_i > 0$,

$$0 < \min_{i\in\{1,\ldots,m\}} \{\underline{g}_i\boldsymbol{\kappa}_i\} \le g\Lambda_\mu\boldsymbol{\kappa} = \sum\nolimits_{i\in\mu} g_i\boldsymbol{\kappa}_i \le \sum\nolimits_{i=1}^{m} \overline{g}_i\boldsymbol{\kappa}_i \tag{4.2.10}$$

directly hold for all constant sets $\mu \in 2^{[m]} \setminus \{\emptyset\}$. This implies that (4.2.9) is well-defined for any $\mu(t)$ in (4.1.5). The following lemma then says that for a time period within which no fault occurs, the composite variable (x, z_μ) can serve as a new coordinate that represents (4.2.2) into a Byrnes-Isidori normal form.

Lemma 4.2.4. Let $\underline{T}$ and $\overline{T}$ be positive constants such that $\mu(t)$ in (4.1.5) is fixed for $\underline{T} \le t < \overline{T}$. Then during that period, the SISO system (4.2.2) is represented in the coordinate change (x, z_μ) with (4.2.9) as

$$\dot{x} = A_\nu x + B_\nu\big(\boldsymbol{\phi}_\mu^\top x + \boldsymbol{\psi}_\mu^\top z_\mu + \mathbf{g}_\mu v + d_{\mathbf{x},\mu}\big), \qquad y = C_\nu x, \tag{4.2.11a}$$

$$\dot{z}_\mu = \mathbf{S}_\mu z_\mu + \mathbf{G}_\mu x + d_{\mathsf{z},\mu} \tag{4.2.11b}$$

where

$$\boldsymbol{\phi}_\mu^\top := \phi^\top + \frac{H\Lambda_\mu \boldsymbol{\kappa}}{g\Lambda_\mu\boldsymbol{\kappa}}\psi^\top B_\nu^\top, \qquad \boldsymbol{\psi}_\mu^\top := \psi^\top, \qquad \mathbf{g}_\mu := g\Lambda_\mu\boldsymbol{\kappa},$$
$$\mathbf{S}_\mu := S - \frac{H\Lambda_\mu\boldsymbol{\kappa}}{g\Lambda_\mu\boldsymbol{\kappa}}\psi^\top, \qquad \mathbf{G}_\mu := G - \frac{H\Lambda_\mu\boldsymbol{\kappa}}{g\Lambda_\mu\boldsymbol{\kappa}}\phi^\top + \left(S - \frac{H\Lambda_\mu\boldsymbol{\kappa}}{g\Lambda_\mu\boldsymbol{\kappa}}\psi^\top\right)\frac{H\Lambda_\mu\boldsymbol{\kappa}}{g\Lambda_\mu\boldsymbol{\kappa}}B_\nu^\top,$$
$$\mathbf{H}_\mu := H\Lambda_\mu\boldsymbol{\kappa}$$

and

$$d_{\mathsf{x},\mu} := G(1-\Lambda_\mu)u_{\mathrm{flt}}^\star + Gd,$$
$$d_{\mathsf{z},\mu} := \left(H(1-\Lambda_\mu) - \frac{H\Lambda_\mu\boldsymbol{\kappa}}{g\Lambda_\mu\boldsymbol{\kappa}}g(1-\Lambda_\mu)\right)u_{\mathrm{flt}}^\star + \left(H - \frac{H\Lambda_\mu\boldsymbol{\kappa}}{g\Lambda_\mu\boldsymbol{\kappa}}g\right)d.$$

$\Diamond$

Proof. The lemma is easily proved by differentiating $z_{\mu(t)}(t) = z_\mu(t)$ along with the (x,ζ)-dynamics (4.2.2), and we skip the details. □

Note that all the matrices and the external signals in the (x, z_μ)-dynamics are uncertain but bounded with known bounds, as those in the original dynamics (4.2.2) do. From this fact, one can find out some bounds for the uncertain parameters, uniformly on $\mu \in 2^{[k]} \setminus \{\emptyset\}$; in particular, let $\mathcal{D}_{\mathsf{x}} \subset \mathbb{R}$ and $\mathcal{D}_{\mathsf{z}} \subset \mathbb{R}$ be compact sets such that $d_{\mathsf{x},\mu(t)}(t) \in \mathcal{D}_{\mathsf{x}}$, and $d_{\mathsf{z},\mu(t)}(t) \in \mathcal{D}_{\mathsf{z}}$ for all $t \geq 0$ and all admissible $\mu(t)$ in (4.1.5). On the other hand, we also observe that the set of the initial conditions $z_{\mu(0)}(0) = z_{\{1,\dots,m\}}(0)$ is bounded by

$$\left\{ z_{\mu(0)}(0) = \zeta(0) - \frac{H\boldsymbol{\kappa}}{g\boldsymbol{\kappa}}B_\nu^\top x(0) : \ \zeta(0) \in \mathcal{S}^0, \ x(0) \in \mathcal{X}^0 \right\} \subset \mathcal{Z}^0$$

for a μ-independent compact subset $\mathcal{Z}^0$ of $\mathbb{R}^{n-\nu}$.

A similar result can be derived for the nominal model (4.1.7). Indeed, in considering a coordinate $[x_{\mathsf{n}}; z_{\mathsf{n}}]$ where

$$z_{\mathsf{n}} := \zeta_{\mathsf{n}} - \frac{1}{g_{\mathsf{n}}}H_{\mathsf{n}}B_\nu^\top x_{\mathsf{n}} = \zeta_{\mathsf{n}} - \frac{1}{g_{\mathsf{n}}}H_{\mathsf{n}}x_{\mathsf{n},\nu}, \tag{4.2.12}$$

one can readily express the nominal model (4.1.7) as the form

$$\dot{x}_{\mathsf{n}} = A_\nu x_{\mathsf{n}} + B_\nu \left(\boldsymbol{\phi}_{\mathsf{n}}^\top x_{\mathsf{n}} + \boldsymbol{\psi}_{\mathsf{n}}^\top z_{\mathsf{n}} + \mathbf{g}_{\mathsf{n}} v_{\mathsf{n}} \right), \qquad y_{\mathsf{n}} = C_\nu x_{\mathsf{n}}, \tag{4.2.13a}$$

$$\dot{z}_{\mathsf{n}} = \mathbf{S}_{\mathsf{n}} z_{\mathsf{n}} + \mathbf{G}_{\mathsf{n}} x_{\mathsf{n}} \tag{4.2.13b}$$

where

$$\boldsymbol{\phi}_{\mathsf{n}}^\top := \phi_{\mathsf{n}}^\top + \frac{1}{g_{\mathsf{n}}} H_{\mathsf{n}} \psi_{\mathsf{n}}^\top B_\nu^\top, \qquad \boldsymbol{\psi}_{\mathsf{n}}^\top := \psi_{\mathsf{n}}^\top, \qquad \mathbf{g}_{\mathsf{n}} = g_{\mathsf{n}},$$
$$\mathbf{S}_{\mathsf{n}} := S_{\mathsf{n}} - \frac{H_{\mathsf{n}}}{g_{\mathsf{n}}} \psi_{\mathsf{n}}^\top, \qquad \mathbf{G}_{\mathsf{n}} := G_{\mathsf{n}} - \frac{H_{\mathsf{n}}}{g_{\mathsf{n}}} \phi_{\mathsf{n}}^\top + \left(S - \frac{H_{\mathsf{n}}}{g_{\mathsf{n}}} \psi_{\mathsf{n}}^\top \right) \frac{H_{\mathsf{n}}}{g_{\mathsf{n}}} B_\nu^\top.$$

Similar to $\mathcal{Z}^0$, we denote the set of possible initial conditions $z_{\mathsf{n}}(0)$ for all $\zeta_{\mathsf{n}}(0) \in \mathcal{S}_{\mathsf{n}}^0$ and $x_{\mathsf{n}}(0) \in \mathcal{X}^0$ as $\mathcal{Z}_{\mathsf{n}}^0$.

We note in advance that the bounds for the plant (4.2.11) and the nominal model (4.2.13) will be utilized for the DOB design in the following subsection.

4.2.3 Disturbance Observer-based Controller

In this subsection, we complete the design of the FTC (4.1.9) by constructing a DOB-based controller for the augmented SISO system (4.2.2). As in other relevant works, the DOB-based controller to be proposed here consists of two parts; baseline controller and DOB. Among them, the former part is designed by duplicating the existing structure (4.1.8) with y_{n} replaced by y as

$$\dot{c} = Ec + F(r - y), \qquad v_{\mathrm{BL}} = Jc + K(r - y) \tag{4.2.14}$$

where $c \in \mathbb{R}^{n_{\mathsf{c}}}$ is the state of (4.2.14) initiated in $\mathcal{C}_{\mathsf{n}}^0$. Hence, the remainder of this subsection is devoted to construct the DOB.

As the first task for the DOB design, we choose a_i, $i = 0, \ldots, \nu - 1$, such that the transfer function

$$\frac{s^\nu + \mathsf{a}_{\nu-1} s^{\nu-1} + \cdots + \mathsf{a}_1 s + (\overline{\mathbf{g}}/\mathbf{g}_{\mathsf{n}})\mathsf{a}_0}{s^\nu + \mathsf{a}_{\nu-1} s^{\nu-1} + \cdots + \mathsf{a}_1 s + (\underline{\mathbf{g}}/\mathbf{g}_{\mathsf{n}})\mathsf{a}_0} \tag{4.2.15}$$

is SPR [Kha96, Chapter 6] where

$$\underline{\mathbf{g}} := \min\left\{\mathbf{g}_{\mathsf{n}}, \min_{i\in\{1,\ldots,m\}}\{\underline{g}_i\boldsymbol{\kappa}_i\}\right\} > 0 \quad \text{and} \quad \overline{\mathbf{g}} := \max\left\{\mathbf{g}_{\mathsf{n}}, \sum_{i=1}^{m}\overline{g}_i\boldsymbol{\kappa}_i\right\} \tag{4.2.16}$$

via the proposed design guidelines in Appendix A.1.

Next, based on the normal form expressions (4.2.11) and (4.2.13), we compute some compact sets in which the nominal state $[x_{\mathsf{n}}(t); z_{\mathsf{n}}(t); c_{\mathsf{n}}(t)]$ and the partial actual state $z_{\mu(t)}(t)$ are expected to remain during system operation. For the former variable, it is noted in advance that the nominal closed-loop system (4.1.8) and (4.2.13) will play a role as a (stable and time-invariant) reference model for the switched system (4.1.9) and (4.2.11), which experiences at most $m-1$ switches in the dynamics. To take into account the effect of switching dynamics, bounded sets for the nominal states $x(t)$, $z_{\mathsf{n}}(t)$, and $c_{\mathsf{n}}(t)$ are derived in a recursive way as follows (for initialization, let $\mathcal{X}^0_{\langle 0\rangle} := \mathcal{X}^0$, $\mathcal{Z}^0_{\mathsf{n},\langle 0\rangle} := \mathcal{Z}^0_{\mathsf{n}}$, and $\mathcal{C}^0_{\langle 0\rangle} := \mathcal{C}^0_{\mathsf{n}}$):

Procedure 4.2.5. (Bounds of nominal states x_{n}, z_{n}, and c_{n})

STEP j $(j = 0, \ldots, m-1)$ Select bounded sets $\mathcal{X}_{\langle j\rangle} \subset \mathbb{R}^{\nu}$, $\mathcal{Z}_{\mathsf{n},\langle j\rangle} \subset \mathbb{R}^{n-\nu}$, and $\mathcal{C}_{\mathsf{n},\langle j\rangle} \subset \mathbb{R}^{n_{\mathsf{c}}}$ such that the solution $[x_{\mathsf{n}}(t); z_{\mathsf{n}}(t); c_{\mathsf{n}}(t)]$ of (4.1.8) and (4.2.13) initiated in $\mathcal{X}^0_{\langle j\rangle} \times \mathcal{Z}^0_{\mathsf{n},\langle j\rangle} \times \mathcal{C}^0_{\mathsf{n},\langle j\rangle}$ belongs to $\mathcal{X}_{\langle j\rangle} \times \mathcal{Z}_{\mathsf{n},\langle j\rangle} \times \mathcal{C}_{\mathsf{n},\langle j\rangle}$ for all admissible reference signal r. Then take large compact sets $\overline{\mathcal{X}}_{\langle j\rangle}$, $\overline{\mathcal{Z}}_{\mathsf{n},\langle j\rangle}$, and $\overline{\mathcal{C}}_{\mathsf{n},\langle j\rangle}$ to satisfy

$$\mathcal{X}_{\langle j\rangle} \times \mathcal{Z}_{\mathsf{n},\langle j\rangle} \times \mathcal{C}_{\mathsf{n},\langle j\rangle} \overset{\epsilon/m}{\sqsubset} \overline{\mathcal{X}}_{\langle j\rangle} \times \overline{\mathcal{Z}}_{\mathsf{n},\langle j\rangle} \times \overline{\mathcal{C}}_{\mathsf{n},\langle j\rangle}. \tag{4.2.17}$$

Set $\mathcal{X}^0_{\langle j+1\rangle} := \overline{\mathcal{X}}_{\langle j\rangle}$, $\mathcal{Z}^0_{\mathsf{n},\langle j+1\rangle} := \overline{\mathcal{Z}}_{\mathsf{n},\langle j\rangle}$, and $\mathcal{C}^0_{\mathsf{n},\langle j+1\rangle} := \overline{\mathcal{C}}_{\mathsf{n},\langle j\rangle}$.

STEP m Take $\mathcal{X} := \mathcal{X}_{\langle m-1\rangle}$, $\overline{\mathcal{X}} := \overline{\mathcal{X}}_{\langle m-1\rangle}$, $\mathcal{Z}_{\mathsf{n}} := \mathcal{Z}_{\mathsf{n},\langle m-1\rangle}$, $\overline{\mathcal{Z}} := \overline{\mathcal{Z}}_{\mathsf{n},\langle m-1\rangle}$, $\mathcal{C}_{\mathsf{n}} := \mathcal{C}_{\mathsf{n},\langle m-1\rangle}$, and $\overline{\mathcal{C}}_{\mathsf{n}} := \overline{\mathcal{C}}_{\mathsf{n},\langle m-1\rangle}$.

$\Diamond$

We note in advance that all the trajectories $[x_{\mathsf{n}}(t); z_{\mathsf{n}}(t); c_{\mathsf{n}}(t)]$ of the nominal closed-loop system in the analysis to come will belong to the bounded region $\mathcal{X} \times \mathcal{Z}_{\mathsf{n}} \times \mathcal{C}_{\mathsf{n}}$. On the other hand, the slightly larger set $\overline{\mathcal{X}} \times \overline{\mathcal{Z}}_{\mathsf{n}} \times \overline{\mathcal{C}}_{\mathsf{n}}$ will be used

as a bound for the actual counterpart $[x(t); z_{\mathsf{n}}^{\dagger}(t); c(t)]$ (in the presence of up to $m-1$ actuator faults) of the nominal state, in which $z_{\mathsf{n}}^{\dagger}$ will be presented shortly in (4.2.21c).

From now on, we derive a bound for the partial state z_μ of the actual plant (4.2.11). The way of computing its bound is basically similar to that for the nominal state above, whereas the main difference comes from the fact that z_μ may jump at every failure moments. To take a look at the jumping behavior, we remark that the vector field of the (x, ζ)-dynamics (4.1.4) is piecewise continuous on t, by which the solution $[x(t); \zeta(t)]$ is continuous on t [Kha96, Chapter 3]. From the continuity of $\zeta(t)$, it follows that at each switching time $t = T \in \{T_1, \ldots, T_m\}$, $z_{\mu(t)}(t)$ jumps from $\lim_{t \nearrow T} z_{\mu(t)}(t)$ to

$$\begin{aligned} z_{\mu(T)}(T) &= \zeta(T) - \frac{H\Lambda_{\mu(T)\boldsymbol{\kappa}}}{g\Lambda_{\mu(T)\boldsymbol{\kappa}}} B_\nu^\top x(T) \\ &= \lim_{t \nearrow T} z_{\mu(t)}(t) + \lim_{t \nearrow T} \frac{H\Lambda_{\mu(t)\boldsymbol{\kappa}}}{g\Lambda_{\mu(t)\boldsymbol{\kappa}}} B_\nu^\top x(t) - \frac{H\Lambda_{\mu(T)\boldsymbol{\kappa}}}{g\Lambda_{\mu(T)\boldsymbol{\kappa}}} B_\nu^\top x(T). \end{aligned}$$

On the other hand, by the property of the Byrnes-Isidori normal form, the system (4.2.2) is of μ-invariant minimum phase if and only if the matrix $\mathbf{S}_\mu$ in (4.2.11) is Hurwitz for all $\mu \in 2^{[m]} \setminus \{\emptyset\}$. Therefore with $\boldsymbol{\kappa}$ obtained by the proposed guideline and the external inputs x and $d_{\mathbf{x},\mu}$ being bounded, the solution $z_\mu(t)$ of (4.2.11b) must belong to a bounded region during the time period between the sequential failure moments. Summing up these findings, we compute a bound of z_μ as follows (let $\mathcal{Z}^0_{\langle 0 \rangle} = \mathcal{Z}^0$ for initialization):

Procedure 4.2.6. (Bound of actual state z_μ)

STEP j $(j = 0, \ldots, m-1)$: Take a compact set $\mathcal{Z}_{\langle j \rangle} \subset \mathbb{R}^{n-\nu}$ such that

$$\begin{aligned} \mathcal{Z}_{\langle j \rangle} \supset \Big\{ & z_\mu(t) \text{ of (4.2.11b) initiated in } \mathcal{Z}^0_{\langle j \rangle} : \\ & x \in \overline{\mathcal{X}},\ d_{\mathsf{z},\mu} \in \mathcal{D}_{\mathsf{z}},\ \mu \in 2^{[m]} \setminus \{\emptyset\} \Big\}. \end{aligned} \tag{4.2.18}$$

Choose a bounded set $\mathcal{Z}^0_{\langle j+1 \rangle} \subset \mathbb{R}^{n-\nu}$ satisfying that

$$\mathcal{Z}^0_{\langle j+1 \rangle} \supset \Big\{ z + \frac{1}{\mathbf{g}_\mu} \mathbf{H}_\mu B_\nu^\top x - \frac{1}{\mathbf{g}_\mu} \mathbf{H}_\mu B_\nu^\top x : \tag{4.2.19}$$

$$z \in \mathcal{Z}_{\langle j \rangle},\ x \in \overline{\mathcal{X}},\ \mu \in 2^{[m]} \setminus \{\emptyset\}\Big\}.$$

STEP m Take $\mathcal{Z} := \mathcal{Z}_{\langle m-1 \rangle}$.

$\Diamond$

To proceed, with the sets obtained via Procedures 4.2.5 and 4.2.6, we define a set

$$\begin{aligned}\mathcal{D}_{\text{total}} := \Big\{ d_{\text{total},\mu} := \frac{1}{\mathbf{g}_\mu}\Big(& \boldsymbol{\phi}_\mu^\top x + \boldsymbol{\psi}_\mu^\top z_\mu + \mathbf{g}_\mu\big(Jc + K(r - C_\nu x)\big) + \mathbf{g}_\mu d_{\mathtt{x},\mu} \\ & - \boldsymbol{\phi}_{\mathsf{n}}^\top x - \boldsymbol{\psi}_{\mathsf{n}}^\top z_{\mathsf{n}}^\dagger - \mathbf{g}_{\mathsf{n}}\big(Jc + K(r - C_\nu x)\big)\Big) : \quad (4.2.19) \\ z_\mu \in \mathcal{Z},\ [x; z_{\mathsf{n}}^\dagger; c] \in \overline{\mathcal{X}} \times \overline{\mathcal{Z}}_{\mathsf{n}} \times \overline{\mathcal{C}}_{\mathsf{n}},\ d_{\mathtt{x},\mu} \in \mathcal{D}_{\mathtt{x}},\ \mu \in 2^{[m]} \setminus \{\emptyset\}\Big\}.\end{aligned}$$

and take a larger compact set $\overline{\mathcal{D}}_{\text{total}} \supset \mathcal{D}_{\text{total}}$. Using the compact sets $\overline{\mathcal{W}}$ and $\overline{\mathcal{X}}$, we now design two saturation functions $\bar{s}_{\mathsf{w}} : \mathbb{R} \to \mathbb{R}$ and $\bar{s}_{\mathtt{x}} : \mathbb{R}^\nu \to \mathbb{R}^\nu$ that are of $\mathfrak{C}^1$, bounded, and satisfy

$$\bar{s}_{\mathsf{w}}(w) = w, \quad \forall w \in \overline{\mathcal{D}}_{\text{total}}, \quad \text{and} \quad 0 \le \frac{\mathrm{d}}{\mathrm{d}w}\bar{s}_{\mathsf{w}} \le 1, \quad \forall w \in \mathbb{R}, \tag{4.2.20a}$$

$$\bar{s}_{\mathtt{x}}(q) = q, \quad \forall q \in \overline{\mathcal{X}}, \quad \text{and} \quad 0 \le \frac{\mathrm{d}}{\mathrm{d}q}\bar{s}_{\mathtt{x}} \le 1, \quad \forall q \in \mathbb{R}^\nu. \tag{4.2.20b}$$

Integrating the components above into one, we propose a DOB as follows:

$$\dot{p} = \big(A_\nu - \underline{\Upsilon}_\nu^{-1}(\tau)\overline{\alpha}C_\nu\big)\, p + \frac{\mathsf{a}_0}{\tau^\nu}B_\nu v, \tag{4.2.21a}$$

$$\dot{q} = \Big(A_\nu - B_\nu \underline{\alpha}^\top \overline{\Upsilon}_\nu(\tau)^{-1}\Big)\, q + \frac{\mathsf{a}_0}{\tau^\nu}B_\nu y, \tag{4.2.21b}$$

$$\dot{z}_{\mathsf{n}}^\dagger = \mathbf{S}_{\mathsf{n}} z_{\mathsf{n}}^\dagger + \mathbf{G}_{\mathsf{n}}\bar{s}_{\mathtt{x}}\big(q\big), \tag{4.2.21c}$$

$$\begin{aligned} w &= -C_\nu p + \frac{1}{\mathbf{g}_{\mathsf{n}}}\Big(\dot{q}_\nu - \boldsymbol{\phi}_{\mathsf{n}}^\top q - \boldsymbol{\psi}_{\mathsf{n}}^\top z_{\mathsf{n}}^\dagger\Big) \qquad (4.2.21d) \\ &= -C_\nu p + \frac{1}{\mathbf{g}_{\mathsf{n}}}\Big(-\underline{\alpha}^\top \overline{\Upsilon}_\nu(\tau)^{-1} q + \frac{a_0}{\tau^\nu} y - \boldsymbol{\phi}_{\mathsf{n}}^\top q - \boldsymbol{\psi}_{\mathsf{n}}^\top z_{\mathsf{n}}^\dagger\Big) \end{aligned}$$

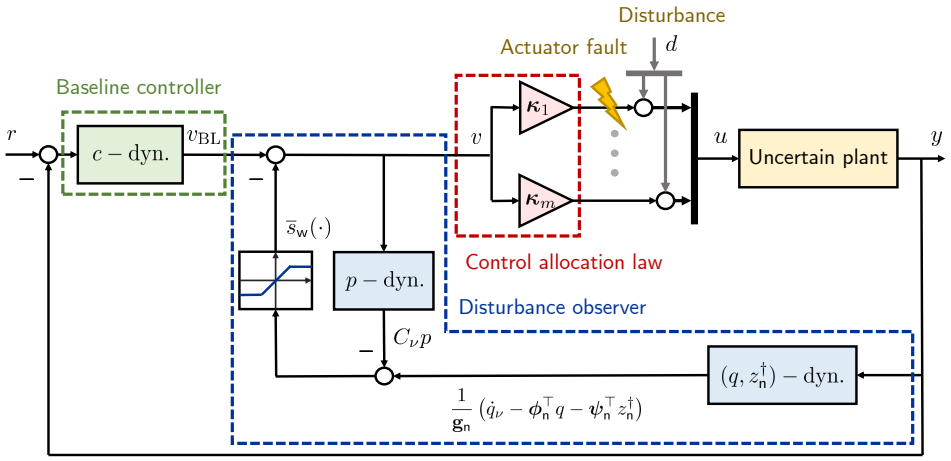

Figure 4.1: Overall configuration of proposed DOB-based FTC consisting of input allocation law (4.2.1), baseline controller (4.2.14), and DOB (4.2.21)

where $\tau > 0$ is a small design parameter that will be taken in Theorem 4.3.1,

$$\underline{\alpha} := \begin{bmatrix} \mathsf{a}_0 \\ \vdots \\ \mathsf{a}_{\nu-1} \end{bmatrix} \in \mathbb{R}^\nu, \quad \overline{\alpha} := \begin{bmatrix} \mathsf{a}_{\nu-1} \\ \vdots \\ \mathsf{a}_0 \end{bmatrix} \in \mathbb{R}^\nu,$$

$\underline{\Upsilon}_\nu(\tau) := \mathrm{diag}(\tau, \tau^2, \ldots, \tau^\nu) \in \mathbb{R}^{\nu\times\nu}$, and $\overline{\Upsilon}_\nu(\tau) := \mathrm{diag}(\tau^\nu, \tau^{\nu-1}, \ldots, \tau) \in \mathbb{R}^{\nu\times\nu}$. The initial conditions $p(0)$ and $q(0)$ are taken arbitrarily to be contained in a compact set $\mathcal{F}_{\mathsf{pq}}^0 \subset \mathbb{R}^{2\nu}$. On the other hand, for $z_{\mathsf{n}}^\dagger(0)$ we take a slightly smaller set $\underline{\mathcal{Z}}_{\mathsf{n}}^0 \subset \mathcal{Z}_{\mathsf{n}}^0$ than $\mathcal{Z}_{\mathsf{n}}^0$ such that a nonempty and bounded set satisfies

$$z_{\mathsf{n}}^\dagger(0) - \frac{1}{g_{\mathsf{n}}} H_{\mathsf{n}} B_\nu^\top x_{\mathsf{n}}(0) \in \mathcal{S}_{\mathsf{n}}^0 \tag{4.2.22}$$

for all $z_{\mathsf{n}}^\dagger(0) \in \underline{\mathcal{Z}}_{\mathsf{n}}^0$ and $x_{\mathsf{n}}(0) \in \mathcal{X}^0$. (Such nonempty $\underline{\mathcal{Z}}_{\mathsf{n}}^0$ always exists by the definition of $\mathcal{S}_{\mathsf{n}}^0$.) With the set, choose $z_{\mathsf{n}}^\dagger(0) \in \underline{\mathcal{Z}}_{\mathsf{n}}^0$.

Remark 4.2.1. It can be readily seen that with $\bar{s}_{\mathsf{w}}$ and $\bar{s}_{\mathbf{x}}$ being inactive, the proposed DOB (4.2.21) becomes simplified into the conventional structure presented in literature, whose Q-filter has the form of a low-pass filter $\mathrm{Q}(s;\tau) = \mathsf{a}_0/((\tau s)^\nu + \mathsf{a}_{\nu-1}(\tau s)^{\nu-1} + \cdots + \mathsf{a}_1(\tau s) + \mathsf{a}_0)$. ◊

Summarizing the discussions so far, we construct the FTC (4.1.9) as the combination of the fixed CA law (4.2.1), the baseline controller (4.2.14), the DOB (4.2.21), and the composite control law

$$v = v_{\mathrm{BL}} - \overline{s}_{\mathsf{w}}(w). \tag{4.2.23}$$

The configuration of the overall system controlled by the proposed FTC is given in Figure 4.1.

4.3 Performance Analysis

This subsection is organized to show that the proposed DOB-based FTC (4.2.1), (4.2.14), (4.2.21), and (4.2.23) with small τ solves the problem of interest, especially in the sense of the following theorem.

Theorem 4.3.1. Suppose that Assumptions 4.1.1 and 4.1.2 hold. Then for given $\epsilon > 0$, there exists $\overline{\tau} > 0$ such that for all $\tau \in (0, \overline{\tau})$, the solution of the closed-loop system (4.1.4), (4.1.6), (4.2.1), (4.2.14), and (4.2.21), initiated at $[x(0); \zeta(0); z_{\mathsf{n}}^{\dagger}(0); c(0); p(0); q(0)] \in \mathcal{X}^0 \times \mathcal{S}^0 \times \underline{\mathcal{Z}}_{\mathsf{n}}^0 \times \mathcal{C}^0 \times \mathcal{F}_{\mathsf{pq}}^0$, satisfies the following statements:

(a) $[x(t); \zeta(t)] \in \overline{\mathcal{X}} \times \overline{\mathcal{S}}_{\mathsf{n}}$ for all $t \geq 0$;

(b)
$$\left\| [x(t); z_{\mathsf{n}}^{\dagger}(t); c(t)] - [x_{\mathsf{n}}^{\star}(t); z_{\mathsf{n}}^{\star}(t); c_{\mathsf{n}}^{\star}(t)] \right\| < \epsilon, \quad \forall t \geq 0 \tag{4.3.1}$$

where $[x_{\mathsf{n}}^{\star}(t); z_{\mathsf{n}}^{\star}(t); c_{\mathsf{n}}^{\star}(t)]$ is the trajectory $[x_{\mathsf{n}}(t); z_{\mathsf{n}}(t); c_{\mathsf{n}}(t)]$ of the nominal closed-loop system (4.1.7) and (4.1.8), initiated at $[x_{\mathsf{n}}(0); z_{\mathsf{n}}(0); c_{\mathsf{n}}(0)] = [x(0); z_{\mathsf{n}}^{\dagger}(0); c(0)] \in \mathcal{X}^0 \times \mathcal{Z}_{\mathsf{n}}^0 \times \mathcal{C}_{\mathsf{n}}^0$.

$\Diamond$

We point out that in the coordinate $[x; \zeta_{\mathsf{n}}^{\dagger}; c]$ with $\zeta_{\mathsf{n}}^{\dagger} := z_{\mathsf{n}}^{\dagger} + (H_{\mathsf{n}}/g_{\mathsf{n}}) B_{\nu}^{\top} x_{\mathsf{n}}(0)$, the inequality (4.3.1) in Theorem 4.3.1 is rewritten by

$$\left\| [x(t); \zeta_{\mathsf{n}}^{\dagger}(t); c(t)] - [x_{\mathsf{n}}^{\star}(t); \zeta_{\mathsf{n}}^{\star}(t); c_{\mathsf{n}}^{\star}(t)] \right\| < \epsilon$$

where $\zeta_{\mathsf{n}}^\star(t) := z_{\mathsf{n}}^\star(t) + (H_{\mathsf{n}}/g_{\mathsf{n}})B_\nu^\top x_{\mathsf{n}}^\star(t)$ initiated at

$$\zeta_{\mathsf{n}}^\star(0) = z_{\mathsf{n}}^\star(0) + \frac{1}{g_{\mathsf{n}}} H_{\mathsf{n}} B_\nu^\top x_{\mathsf{n}}^\star(0) = z_{\mathsf{n}}^\dagger(0) + \frac{1}{g_{\mathsf{n}}} H_{\mathsf{n}} B_\nu^\top x(0) \in \mathcal{S}_{\mathsf{n}}^0.$$

The theorem will be proved in the following steps. First, with a coordinate transformation for p and q, we represent the overall system (together with the Byrnes-Isidori normal form (4.2.11) and (4.2.13)) into the standard singular perturbation form (Lemma 4.3.2). In particular, it will be seen that on the boundary layer in view of the singular perturbation theory, the $(x, z_{\mathsf{n}}^\dagger, c)$-dynamics, a part of the slow subsystem, behaves as the nominal closed-loop system (i.e., the $(x_{\mathsf{n}}, z_{\mathsf{n}}, c_{\mathsf{n}})$-dynamics (4.2.11) and (4.1.8)) for any patterns of actuator failure. Since the discontinuity on z_μ makes the singular perturbation theory inapplicable for the entire time period, we alternatively apply the Tickonov's theorem [Hop66] to "each" subinterval of time between two sequential moments of failure (Lemma 4.3.3). By doing so, we will see that the actual state $[x(t); z_{\mathsf{n}}^\dagger(t); c(t)]$ could remain close to a nominal trajectory $[x_{\mathsf{n}}(t); z_{\mathsf{n}}(t); c_{\mathsf{n}}(t)]$ at least for a while, even though the latter is not necessarily the same as $[x_{\mathsf{n}}^\star(t); z_{\mathsf{n}}^\star(t); c_{\mathsf{n}}^\star(t)]$. Nonetheless, the difference between these nominal trajectories is negligible due to stability of the nominal closed-loop system, which concludes Theorem 4.3.1.

We begin the proof by representing the overall system into a singular perturbation form [Kha96, KKO99].

Lemma 4.3.2. Let $\underline{T} > 0$ and $\overline{T} > 0$ be such that $\mu(t)$ in (4.1.5) is constant for $\underline{T} \le t < \overline{T}$. Then with the coordinate changes (4.2.9) and

$$\xi := \overline{\Upsilon}_\nu(\tau)^{-1}\big(\Pi(\tau)q - x\big), \tag{4.3.2a}$$

$$\eta := \frac{1}{\tau}\underline{\Upsilon}_\nu(\tau)p + \frac{\mathsf{a}_0}{\mathbf{g}_{\mathsf{n}}}\overline{\Upsilon}_\nu(\tau)^{-1}\big(\Pi(\tau)q - x\big) = \frac{1}{\tau}\underline{\Upsilon}_\nu(\tau)p + \frac{\mathsf{a}_0}{\mathbf{g}_{\mathsf{n}}}\xi \tag{4.3.2b}$$

where

$$\Pi(\tau) := \frac{1}{\mathsf{a}_0}\begin{bmatrix} \mathsf{a}_0 & \mathsf{a}_1\tau & \cdots & \mathsf{a}_{\nu-1}\tau^{\nu-1} \\ 0 & \mathsf{a}_0 & \ddots & \vdots \\ \vdots & & \ddots & \mathsf{a}_1\tau \\ 0 & \cdots & & \mathsf{a}_0 \end{bmatrix} \in \mathbb{R}^{\nu\times\nu}, \tag{4.3.3}$$

the closed-loop system (4.1.4), (4.1.6), (4.2.1), (4.2.14), (4.2.21), and (4.2.23) is transformed into a standard singular perturbation form for $\underline{T} \le t < \overline{T}$, with respect to the perturbation parameter τ:

- slow subsystems: the augmented plant (4.2.11) and

$$\dot{z}_{\mathsf{n}}^{\dagger} = \mathbf{S}_{\mathsf{n}} z_{\mathsf{n}}^{\dagger} + \mathbf{G}_{\mathsf{n}} \bar{s}_{\mathtt{x}} \big(\Pi(\tau)^{-1} (x + \overline{\Upsilon}_{\nu}(\tau)\xi) \big) \tag{4.3.4a}$$

- fast subsystems:

$$\tau \dot{\xi} = (A_{\nu} - \overline{\alpha} C_{\nu})\xi - B_{\nu} \left(\boldsymbol{\phi}_{\mu} x + \boldsymbol{\psi}_{\mu}^{\top} z_{\mu} + \mathbf{g}_{\mu} v + d_{\mathtt{x},\mu} \right), \tag{4.3.5a}$$

$$\begin{aligned} \tau \dot{\eta} = {} & (A_{\nu} - \overline{\alpha} C_{\nu})\eta \\ & + \mathsf{a}_0 B_{\nu} \left(\left(1 - \frac{\mathbf{g}_{\mu}}{\mathbf{g}_{\mathsf{n}}} \right) v - \frac{1}{\mathbf{g}_{\mathsf{n}}} \left(\boldsymbol{\phi}_{\mu}^{\top} x + \boldsymbol{\psi}_{\mu}^{\top} z_{\mu} + d_{\mathtt{x},\mu} \right) \right) \end{aligned} \tag{4.3.5b}$$

where

$$\begin{aligned} v = {} & Jc + K(r - C_{\nu} x) \\ & - \bar{s}_{\mathsf{w}} \left(-C_{\nu}\eta - \frac{1}{\mathbf{g}_{\mathsf{n}}} \left(\boldsymbol{\phi}_{\mathsf{n}}^{\top} \Pi(\tau)^{-1} (x + \overline{\Upsilon}_{\nu}(\tau)\xi) + \boldsymbol{\psi}_{\mathsf{n}}^{\top} z_{\mathsf{n}}^{\dagger} \right) \right). \end{aligned} \tag{4.3.6}$$

$\Diamond$

Proof. It is easy to derive the slow subsystems (4.3.4) from Lemma 4.3.5 and $q = \Pi(\tau)^{-1}(x + \overline{\Upsilon}_{\nu}(\tau)\xi)$, while the remaining part of the proof is devoted to compute the fast subsystems (4.3.5). By definition, we have

$$\dot{q}_{\nu} = -\frac{\mathsf{a}_0}{\tau^{\nu}} q_1 - \frac{\mathsf{a}_1}{\tau^{\nu-1}} q_2 - \cdots - \frac{\mathsf{a}_{\nu-1}}{\tau} q_{\nu} + \frac{\mathsf{a}_0}{\tau^{\nu}} x_1 = -\mathsf{a}_0 \xi_1 \tag{4.3.7}$$

and thus,

$$p_1 - \frac{1}{\mathbf{g}_{\mathsf{n}}} \dot{q}_{\nu} = C_{\nu}(1/\tau) \underline{\Upsilon}_{\nu}(\tau) p + \frac{\mathsf{a}_0}{\mathbf{g}_{\mathsf{n}}} C_{\nu} \xi = C_{\nu} \eta.$$

Then the time derivative of ξ_i is computed by: for $i = 1, \ldots, \nu - 1$,

$$\dot{\xi}_i = \frac{1}{\tau^{\nu+1-i}} \Big(\frac{1}{\mathsf{a}_0} \left(\mathsf{a}_0 \dot{q}_i + \tau \mathsf{a}_1 \dot{q}_{i+1} + \cdots + \tau^{\nu-i-1} \mathsf{a}_{\nu-i-1} \dot{q}_{\nu-1} + \tau^{\nu-i} \mathsf{a}_{\nu-i} \dot{q}_{\nu} \right) - \dot{x}_i \Big)$$

$$
\begin{aligned}
&= \frac{1}{\tau}\left(\frac{1}{\tau^{\nu-i}} \left(\frac{1}{\mathsf{a}_0}(\mathsf{a}_0 q_{i+1} + \tau \mathsf{a}_1 q_{(i+1)+1} + \cdots + \tau^{\nu-(i+1)} \mathsf{a}_{\nu-(i+1)} q_\nu) - x_{i+1} \right) \right) \\
&\quad + \frac{1}{\tau}\frac{\mathsf{a}_{\nu-i}}{\mathsf{a}_0}\dot{q}_\nu \\
&= \frac{1}{\tau}\xi_{i+1} - \frac{\mathsf{a}_{\nu-i}}{\tau}\xi_1
\end{aligned} \tag{4.3.8}
$$

while for $i = \nu$,

$$
\dot{\xi}_\nu = \frac{1}{\tau}(\dot{q}_\nu - \dot{x}_\nu) = -\frac{1}{\tau}\mathsf{a}_0\xi_1 - \frac{1}{\tau}\left(\boldsymbol{\phi}_\mu^\top x + \boldsymbol{\psi}_\mu^\top z_\mu + \mathbf{g}_\mu v + d_{x,\mu} \right). \tag{4.3.9}
$$

This gives (4.3.5a) and (4.3.6). On the other hand, to obtain the η-dynamics (4.3.5b) we define an intermediate variable $\hat{\eta} := (1/\tau)\underline{\Upsilon}_\nu(\tau)p$, with which $\eta := \hat{\eta} + (\mathsf{a}_0/\mathbf{g}_\mathsf{n})\xi$. Using the p-dynamics (4.2.21a), one has

$$
\begin{aligned}
\tau\dot{\hat{\eta}} = \underline{\Upsilon}_\nu(\tau)\dot{p} &= \underline{\Upsilon}_\nu(\tau)\left(\left(A_\nu - \underline{\Upsilon}_\nu^{-1}(\tau)\overline{\alpha}C_\nu \right) \tau \underline{\Upsilon}_\nu(\tau)^{-1}\hat{\eta} + \frac{\mathsf{a}_0}{\tau^\nu}B_\nu v \right) \\
&= (A_\nu - \overline{\alpha}C_\nu)\hat{\eta} + \mathsf{a}_0 B_\nu v.
\end{aligned} \tag{4.3.10}
$$

Now, differentiating $\eta = \hat{\eta} + (\mathsf{a}_0/\mathbf{g}_\mathsf{n})\xi$ with the $\hat{\eta}$-dynamics (4.3.10) and the ξ-dynamics (4.3.5a) leads to

$$
\begin{aligned}
\tau\dot{\eta} = &\left((A_\nu - \overline{\alpha}C_\nu)\hat{\eta} + \mathsf{a}_0 B_\nu v \right) \\
&+ \frac{\mathsf{a}_0}{\mathbf{g}_\mathsf{n}}\left((A_\nu - \overline{\alpha}C_\nu)\xi - B_\nu \left(\boldsymbol{\phi}_\mu^\top x + \boldsymbol{\psi}_\mu^\top z_\mu + \mathbf{g}_\mu v + d_{x,\mu} \right) \right).
\end{aligned}
$$

This directly implies (4.3.5b) and concludes the proof. □

To figure out the quasi-steady-state behavior of the singularly perturbed system (4.3.4)–(4.3.5), it is for now assumed that the slow variables μ, x, $z_\mathsf{n}^\dagger$, c, z_μ, $d_{\mathbf{x},\mu}$, and $d_{\mathbf{z},\mu}$ are frozen as

$$
\mu \in 2^{[m]} \setminus \{\emptyset\},\ [x; z_\mathsf{n}^\dagger; c] \in \overline{\mathcal{X}} \times \overline{\mathcal{Z}}_\mathsf{n} \times \overline{\mathcal{C}}_\mathsf{n},\ z_\mu \in \mathcal{Z},\ d_{\mathbf{x},\mu} \in \mathcal{D}_\mathbf{x},\ d_{\mathbf{z},\mu} \in \mathcal{D}_\mathbf{z}. \tag{4.3.11}
$$

Under the hypothesis, we now compute a (possibly μ-dependent) solution $\xi_\mu^\star =: [\xi_{\mu,1}^\star; \cdots; \xi_{\mu,\nu}^\star]$ and $\eta_\mu^\star =: [\eta_{\mu,1}^\star; \cdots; \eta_{\mu,\nu}^\star]$ of the following degenerating equation (which is obtained by putting $\tau = 0$ and $[\xi; \eta] = [\xi_\mu^\star; \eta_\mu^\star]$ into the fast dynamics

(4.3.5)):

$$0 = -\mathsf{a}_{\nu-i}\xi^\star_{\mu,1} + \xi^\star_{\mu,i+1}, \quad \forall i = 1,\dots,\nu-1, \tag{4.3.12a}$$

$$\begin{aligned} 0 = -\mathsf{a}_0\xi^\star_{\mu,1} - \Big[&\boldsymbol{\phi}_\mu^\top x + \boldsymbol{\psi}_\mu^\top z_\mu + \mathbf{g}_\mu\big(Jc + K(r - C_\nu x)\big) + \mathbf{g}_\mu d_{\mathsf{x},\mu} \\ &- \mathbf{g}_\mu \overline{s}_{\mathsf{w}}\left(-\eta^\star_{\mu,1} - \frac{1}{\mathbf{g}_{\mathsf{n}}}(\boldsymbol{\phi}_{\mathsf{n}}^\top x + \boldsymbol{\psi}_{\mathsf{n}}^\top z^\dagger_{\mathsf{n}})\right)\Big] \end{aligned}$$

and

$$0 = -\mathsf{a}_{\nu-i}\eta^\star_{\mu,1} + \eta^\star_{\mu,i+1}, \quad \forall i = 1,\dots,\nu-1, \tag{4.3.12b}$$

$$\begin{aligned} 0 = -\mathsf{a}_0\eta^\star_{\mu,1} + \mathsf{a}_0\Bigg[&\left(1 - \frac{\mathbf{g}_\mu}{\mathbf{g}_{\mathsf{n}}}\right)\big(Jc + K(r - C_\nu x)\big) \\ &- \left(1 - \frac{\mathbf{g}_\mu}{\mathbf{g}_{\mathsf{n}}}\right)\overline{s}_{\mathsf{w}}\left(-\eta^\star_{\mu,1} - \frac{1}{\mathbf{g}_{\mathsf{n}}}(\boldsymbol{\phi}_{\mathsf{n}}^\top x + \boldsymbol{\psi}_{\mathsf{n}}^\top z^\dagger_{\mathsf{n}})\right) - \frac{1}{\mathbf{g}_{\mathsf{n}}}(\boldsymbol{\phi}_\mu^\top x + \boldsymbol{\psi}_\mu^\top z_\mu + d_{\mathsf{x},\mu})\Bigg] \end{aligned}$$

(where $\Pi(0) = I$ and $\overline{\Upsilon}_\nu(0) = 0$ are used). It can be seen that the degenerating equation (4.3.12) admits a solution

$$\xi^\star_{\mu,1} = -\frac{1}{\mathsf{a}_0}\left(\boldsymbol{\phi}_{\mathsf{n}}^\top x + \boldsymbol{\psi}_{\mathsf{n}}^\top z^\dagger_{\mathsf{n}} + \mathbf{g}_{\mathsf{n}}\big(Jc + K(r - C_\nu x)\big)\right), \tag{4.3.13a}$$

$$\begin{aligned} \eta^\star_{\mu,1} = &\left(\frac{\mathbf{g}_{\mathsf{n}}}{\mathbf{g}_\mu} - 1\right)\left(Jc + K(r - C_\nu x) + \frac{1}{\mathbf{g}_{\mathsf{n}}}(\boldsymbol{\phi}_{\mathsf{n}}^\top x + \boldsymbol{\psi}_{\mathsf{n}}^\top z^\dagger_{\mathsf{n}})\right) \\ &- \frac{1}{\mathbf{g}_\mu}(\boldsymbol{\phi}_\mu^\top x + \boldsymbol{\psi}_\mu^\top z_\mu + \mathbf{g}_\mu d_{\mathsf{x},\mu}), \end{aligned} \tag{4.3.13b}$$

$$\xi^\star_{\mu,i} = 0 \ \text{ and } \ \eta^\star_{\mu,i} = 0, \quad \forall i = 2,\dots,\nu. \tag{4.3.13c}$$

It should be emphasized that (4.3.13) is in fact the "unique" solution of (4.3.12), because the right hand-side of the last row of (4.3.12b) is a strictly decreasing function of $\eta^\star_{\mu,1}$ by the property of $\overline{s}_{\mathsf{w}}$. In the computation of the solution, one may verify that with the slow variables frozen (as in (4.3.11)), the input of $\overline{s}_{\mathsf{w}}$

$$-\eta^\star_{\mu,1} - \frac{1}{\mathbf{g}_{\mathsf{n}}}(\boldsymbol{\phi}_{\mathsf{n}}^\top x + \boldsymbol{\psi}_{\mathsf{n}}^\top z^\dagger_{\mathsf{n}}) = d_{\text{total},\mu} \tag{4.3.14}$$

belongs to $\mathcal{D}_{\text{total}}$ in (4.2.19) so that the saturation function is inactive.

It readily follows that on the boundary layer $[\xi;\eta] = [\xi^\star_\mu;\eta^\star_\mu]$ and with $\tau = 0$, the singularly perturbed system (4.3.4)–(4.3.5) becomes reduced into the z_μ-

dynamics (4.2.11b) and

$$\dot{x} = A_\nu x + B_\nu\big(\boldsymbol{\phi}_{\mathsf{n}}^\top x + \boldsymbol{\psi}_{\mathsf{n}}^\top z_{\mathsf{n}}^\dagger + \mathbf{g}_{\mathsf{n}}(Jc + K(r - C_\nu x))\big), \tag{4.3.15a}$$

$$\dot{z}_{\mathsf{n}}^\dagger = \mathbf{S}_{\mathsf{n}} z_{\mathsf{n}}^\dagger + \mathbf{G}_{\mathsf{n}} x, \tag{4.3.15b}$$

$$\dot{c} = Ec + F(r - C_\nu x). \tag{4.3.15c}$$

It should be emphasize that (4.3.15a)–(4.3.15c) is decoupled from the remaining z_μ-dynamics, having exactly the same dynamics as the (μ-independent) stable nominal closed-loop system (4.1.8) and (4.2.13). Thus in the singular perturbation theoretic point of view, one may expect that the two trajectories $[x(t); z_{\mathsf{n}}^\dagger(t); c(t)]$ and $[x_{\mathsf{n}}(t); z_{\mathsf{n}}(t); c_{\mathsf{n}}(t)]$ might be close to each other with small perturbation parameter τ. This is indeed the case for the subintervals of time between two sequential moments of failure, as in the following lemma.

Lemma 4.3.3. Suppose that Assumptions 4.1.1 and 4.1.2 hold. Let $P = P^\top > 0$ be the solution of the Lyapunov equation $P\mathsf{A}_{\mathsf{n}} + \mathsf{A}_{\mathsf{n}}^\top P = -I$ where A_{n} is the system matrix of the nominal closed-loop system (4.1.8) and (4.2.13). Then for given constant set $\mu' \in 2^{[m]} \setminus \{\emptyset\}$ and $\epsilon > 0$, there exists $\overline{\tau}_{\mu'} > 0$ such that if

- $\mu(t) = \mu'$ for a time period $\underline{T} \le t < \overline{T}$ satisfying $\overline{T} - \underline{T} > \Delta_{\text{dwell}}$;
- $[x(\underline{T}); z_{\mathsf{n}}^\dagger(\underline{T}); c(\underline{T})] \in \mathcal{X}_{\langle j\rangle}^0 \times \mathcal{Z}_{\mathsf{n},\langle j\rangle}^0 \times \mathcal{C}_{\mathsf{n},\langle j\rangle}^0$, and $z_{\mu'}(\underline{T}) \in \mathcal{Z}_{\langle j\rangle}^0$ for some $j \in \{0, \ldots, m-1\}$;
- $[p(\underline{T}); q(\underline{T})] \in \mathcal{F}_{\mathsf{pq}}$ where $\mathcal{F}_{\mathsf{pq}} \subset \mathbb{R}^{2\nu}$ is a bounded set independent of τ,

then the state trajectory of the closed-loop system (4.1.4), (4.1.6), (4.2.1), (4.2.14), (4.2.21), and (4.2.23) satisfies the following statements for all $\tau \in (0, \overline{\tau}_{\mu'})$:

(a) for all $\underline{T} \le t < \overline{T}$, the partial state $[x(t); z_{\mathsf{n}}^\dagger(t); c(t)]$ belongs to $\overline{\mathcal{X}}_{\langle j\rangle} \times \overline{\mathcal{Z}}_{\mathsf{n},\langle j\rangle} \times \overline{\mathcal{C}}_{\mathsf{n},\langle j\rangle}$ and satisfies

$$\big\|[x(t); z_{\mathsf{n}}^\dagger(t); c(t)] - [x_{\mathsf{n}}(t); z_{\mathsf{n}}(t); c_{\mathsf{n}}(t)]\big\| < \frac{\epsilon}{m}\sqrt{\frac{\underline{\lambda}(P)}{\overline{\lambda}(P)}} \tag{4.3.16}$$

where $[x_{\mathsf{n}}(t); z_{\mathsf{n}}(t); c_{\mathsf{n}}(t)]$ is the solution of the nominal closed-loop system (4.1.8) and (4.2.13) initiated at $[x_{\mathsf{n}}(\underline{T}); z_{\mathsf{n}}(\underline{T}); c_{\mathsf{n}}(\underline{T})] = [x(\underline{T}); z_{\mathsf{n}}^\dagger(\underline{T}); c(\underline{T})]$;

(b) $z_{\mu'}(t)$ remains in $\mathcal{Z}_{\langle j \rangle}$ for all $\underline{T} \leq t < \overline{T}$;

(c) there exists a τ-independent bounded set $\overline{\mathcal{F}}_{\mathsf{pq}}$ such that $[p(\overline{T}); q(\overline{T})] \in \overline{\mathcal{F}}_{\mathsf{pq}}$.

$\Diamond$

Proof. We here briefly sketch the proof (especially for Item (a)), while the detailed proof is similar to that of the theorems in the previous chapters. Roughly speaking, the lemma will be proved by applying the Tichonov's theorem [Hop66] to the singularly perturbed form (4.3.4)–(4.3.5). It is clear that the reduced subsystem (4.3.15) is stable, because the internal dynamics (4.2.11) of the actual plant is stable by the selection of $\boldsymbol{\kappa}$. We now investigate the stability of the fast subsystem (4.3.5), which is a requirement of the Tichonov's theorem [Hop66]. To this end, we define the error variables

$$\tilde{\xi}_{\mu'} := \xi - \xi^{\star}_{\mu'} \quad \text{and} \quad \tilde{\eta}_{\mu'} := \eta - \eta^{\star}_{\mu'} \tag{4.3.17}$$

(where $\xi^{\star}_{\mu'}$ and $\eta^{\star}_{\mu'}$ are given in (4.3.13)). By differentiating (4.3.17) with respect to a scaled time $\varsigma := t/\tau$ and put $\tau = 0$ to the resulting equations (so that the slow variables are frozen in the time scale ς), one obtains the "boundary-layer system" as follows:

$$\frac{\mathrm{d}}{\mathrm{d}\varsigma}\tilde{\xi}_{\mu'} = (A_\nu - \overline{\alpha} C_\nu)\tilde{\xi}_{\mu'} + B_\nu \mathbf{g}_{\mu'} \Big(\overline{s}_{\mathsf{w}} \left(y_\eta + d_{\mathrm{total},\mu'} \right) - d_{\mathrm{total},\mu'} \Big), \tag{4.3.18a}$$

$$\begin{aligned} \frac{\mathrm{d}}{\mathrm{d}\varsigma}\tilde{\eta}_{\mu'} &= (A_\nu - \overline{\alpha} C_\nu)\tilde{\eta}_{\mu'} - \mathsf{a}_0 B_\nu u_\eta, \\ y_\eta &:= -C_\nu \tilde{\eta}_{\mu'}, \quad u_\eta = -\left(\frac{\mathbf{g}_{\mu'}}{\mathbf{g}_{\mathsf{n}}} - 1 \right) \left(\overline{s}_{\mathsf{w}}(y_\eta + d_{\mathrm{total},\mu'}) - d_{\mathrm{total},\mu'} \right) \end{aligned} \tag{4.3.18b}$$

where $d_{\mathrm{total},\mu'}$ is defined in (4.3.14) and the origin is an equilibrium point of (4.3.18). We now claim that the origin of the boundary-layer system (4.3.18) is globally exponentially stable. Indeed, the transfer function of the linear subsystem (from u_η to y_η) in (4.3.18b) is given by $\mathrm{L}(s) := \mathsf{a}_0/(s^\nu + \mathsf{a}_{\nu-1} s^{\nu-1} + \cdots + \mathsf{a}_0)$, while the nonlinearity $\left(\mathbf{g}_{\mu'}/\mathbf{g}_{\mathsf{n}} - 1 \right) \left(\overline{s}_{\mathsf{w}}(y_\eta + d_{\mathrm{total},\mu'}) - d_{\mathrm{total},\mu'} \right)$ in u_η belongs to the sector $[\underline{\mathbf{g}}/\mathbf{g}_{\mathsf{n}} - 1, \overline{\mathbf{g}}/\mathbf{g}_{\mathsf{n}} - 1]$. Therefore, from the the circle criterion [Kha96,

Theorem 7.1] and the fact that

$$\frac{1+(\overline{\mathsf{g}}/\mathsf{g}_\mathsf{n}-1)\mathrm{L}(s)}{1+(\underline{\mathsf{g}}/\mathsf{g}_\mathsf{n}-1)\mathrm{L}(s)}=\frac{s^\nu+\mathsf{a}_{\nu-1}s^{\nu-1}+\cdots+\mathsf{a}_1 s+(\overline{\mathsf{g}}/\mathsf{g}_\mathsf{n})\mathsf{a}_0}{s^\nu+\mathsf{a}_{\nu-1}s^{\nu-1}+\cdots+\mathsf{a}_1 s+(\underline{\mathsf{g}}/\mathsf{g}_\mathsf{n})\mathsf{a}_0} \tag{4.3.19}$$

is SPR, it is derived that the origin of the $\tilde{\eta}_{\mu'}$-dynamics (4.3.18b) is globally exponentially stable. On the other hand, with the coefficients a_i of the strictly positive real transfer function (4.3.19) and with $\underline{\mathsf{g}}/\mathsf{g}_\mathsf{n} \leq 1 \leq \overline{\mathsf{g}}/\mathsf{g}_\mathsf{n}$, we have that the characteristic polynomial $s^\nu+\mathsf{a}_{\nu-1}s^{\nu-1}+\cdots+\mathsf{a}_1 s+\mathsf{a}_0$ of the matrix $A_\nu-\overline{\alpha}C_\nu$ is Hurwitz. This concludes the claim.

For the remainder of the proof, it is noted that the initial value $[\xi(\underline{T});\eta(\underline{T})]$ of the fast variables may diverge as τ goes to zero. Nonetheless, one can deal with this peaking phenomenon in a similar way in the previous chapters; that is, by dividing the entire time period $\underline{T} \leq t \leq \overline{T}$ into the transient period $\underline{T} \leq t < \underline{T}+\Delta'$ and the steady-state period $\underline{T}+\Delta' \leq t \leq \overline{T}$, with a small constant $0<\Delta'<\Delta_{\mathrm{dwell}}/2$. We omit the details. □

To proceed, take $\overline{\tau}$ in the statement of Theorem 4.3.1 as

$$0<\overline{\tau}<\min_{\mu'\in 2^{[m]}\setminus\{\emptyset\}}\{\overline{\tau}_{\mu'}\}.$$

In addition, denote the number of the actuator faults that occurs during system operation as $m_{\mathrm{flt}} \leq m-1$. Then the moments T_i of actuator faults, $i=1,\ldots,m$, can be rearranged in chronological order by $T_{\langle j\rangle} \in \{T_1,\ldots,T_m\}$, $j=1,\ldots,m$, to satisfy $T_{\langle 0\rangle} := 0 < T_{\langle 1\rangle} < T_{\langle 2\rangle} < \cdots < T_{\langle m_{\mathrm{flt}}\rangle} < T_{\langle m_{\mathrm{flt}}+1\rangle} = \cdots = T_{\langle m-1\rangle} = T_{\langle m\rangle} = \infty$.

As the last step of the proof, we show that with $\tau<\overline{\tau}$, the distance between $[x(t);z_\mathsf{n}^\dagger(t);c(t)]$ and $[x_\mathsf{n}^\star(t);z_\mathsf{n}^\star(t);c_\mathsf{n}^\star(t)]$ is smaller than ϵ for each period $T_{\langle j\rangle} \leq t < T_{\langle j+1\rangle}$. For this, by repeating Lemma 4.3.3 iteratively up to $j=m_{\mathrm{flt}}$, we obtain that for $T_{\langle j\rangle} \leq t < T_{\langle j+1\rangle}$

$$\left\|[x(t);z_\mathsf{n}^\dagger(t);c(t)]-[x_{\mathsf{n},\langle j\rangle}(t);z_{\mathsf{n},\langle j\rangle}(t);c_{\mathsf{n},\langle j\rangle}(t)]\right\| < \frac{\epsilon}{m}\sqrt{\frac{\underline{\lambda}(P)}{\overline{\lambda}(P)}} \leq \frac{\epsilon}{m} \tag{4.3.20}$$

where $[x_{\mathsf{n},\langle j\rangle}(t);z_{\mathsf{n},\langle j\rangle}(t);c_{\mathsf{n},\langle j\rangle}(t)]$ stands for the trajectory $[x_\mathsf{n}(t);z_\mathsf{n}(t);c_\mathsf{n}(t)]$ of

the nominal closed-loop system (4.1.8) and (4.2.13) with the initial condition $[x_{\mathsf{n},\langle j\rangle}(T_{\langle j\rangle}); z_{\mathsf{n},\langle j\rangle}(T_{\langle j\rangle}); c_{\mathsf{n},\langle j\rangle}(T_{\langle j\rangle})] = [x(T_{\langle j\rangle}); z_{\mathsf{n}}^{\dagger}(T_{\langle j\rangle}); c(T_{\langle j\rangle})]$ (so that the solution is well-defined for the truncated time period $T_{\langle j\rangle} \le t < \infty$). With a bundle of the nominal trajectories, we define the error variables

$$\begin{bmatrix} \tilde{x}_{\mathsf{n},\langle j\rangle} \\ \tilde{z}_{\mathsf{n},\langle j\rangle} \\ \tilde{c}_{\mathsf{n},\langle j\rangle} \end{bmatrix} := \begin{bmatrix} x_{\mathsf{n},\langle j\rangle} \\ z_{\mathsf{n},\langle j\rangle} \\ c_{\mathsf{n},\langle j\rangle} \end{bmatrix} - \begin{bmatrix} x_{\mathsf{n},\langle j-1\rangle} \\ z_{\mathsf{n},\langle j-1\rangle} \\ c_{\mathsf{n},\langle j-1\rangle} \end{bmatrix} \tag{4.3.21}$$

for $j = 1, \ldots, m_{\mathrm{flt}}$, whose time derivative is computed by

$$\frac{\mathrm{d}}{\mathrm{d}t} \begin{bmatrix} \tilde{x}_{\mathsf{n},\langle j\rangle} \\ \tilde{z}_{\mathsf{n},\langle j\rangle} \\ \tilde{c}_{\mathsf{n},\langle j\rangle} \end{bmatrix} = \mathsf{A}_{\mathsf{n}} \begin{bmatrix} \tilde{x}_{\mathsf{n},\langle j\rangle} \\ \tilde{z}_{\mathsf{n},\langle j\rangle} \\ \tilde{c}_{\mathsf{n},\langle j\rangle} \end{bmatrix}, \quad \forall T_{\langle j\rangle} \le t < T_{\langle j+1\rangle}. \tag{4.3.22}$$

Since $[x_{\mathsf{n},\langle j\rangle}(T_{\langle j\rangle}); z_{\mathsf{n},\langle j\rangle}(T_{\langle j\rangle}); c_{\mathsf{n},\langle j\rangle}(T_{\langle j\rangle})] = [x(T_{\langle j\rangle}); z_{\mathsf{n}}^{\dagger}(T_{\langle j\rangle}); c(T_{\langle j\rangle})]$ by definition, one has

$$\begin{aligned} \left\| \begin{bmatrix} \tilde{x}_{\mathsf{n},\langle j\rangle}(T_{\langle j\rangle}) \\ \tilde{z}_{\mathsf{n},\langle j\rangle}(T_{\langle j\rangle}) \\ \tilde{c}_{\mathsf{n},\langle j\rangle}(T_{\langle j\rangle}) \end{bmatrix} \right\| &= \left\| \begin{bmatrix} x_{\mathsf{n},\langle j\rangle}(T_{\langle j\rangle}) \\ z_{\mathsf{n},\langle j\rangle}(T_{\langle j\rangle}) \\ c_{\mathsf{n},\langle j\rangle}(T_{\langle j\rangle}) \end{bmatrix} - \begin{bmatrix} x_{\mathsf{n},\langle j-1\rangle}(T_{\langle j\rangle}) \\ z_{\mathsf{n},\langle j-1\rangle}(T_{\langle j\rangle}) \\ c_{\mathsf{n},\langle j-1\rangle}(T_{\langle j\rangle}) \end{bmatrix} \right\| \\ &= \left\| \begin{bmatrix} x(T_{\langle j\rangle}) \\ z_{\mathsf{n}}^{\dagger}(T_{\langle j\rangle}) \\ c(T_{\langle j\rangle}) \end{bmatrix} - \begin{bmatrix} x_{\mathsf{n},\langle j-1\rangle}(T_{\langle j\rangle}) \\ z_{\mathsf{n},\langle j-1\rangle}(T_{\langle j\rangle}) \\ c_{\mathsf{n},\langle j-1\rangle}(T_{\langle j\rangle}) \end{bmatrix} \right\| < \frac{\epsilon}{m} \sqrt{\frac{\underline{\lambda}(P)}{\overline{\lambda}(P)}} \end{aligned}$$

where the last inequality follows from (4.3.16) in the previous step $j-1$. Now, we differentiate the Lyapunov function candidate

$$V_{\mathsf{n},\langle j\rangle} := \begin{bmatrix} \tilde{x}_{\mathsf{n},\langle j\rangle} \\ \tilde{z}_{\mathsf{n},\langle j\rangle} \\ \tilde{c}_{\mathsf{n},\langle j\rangle} \end{bmatrix}^{\top} P \begin{bmatrix} \tilde{x}_{\mathsf{n},\langle j\rangle} \\ \tilde{z}_{\mathsf{n},\langle j\rangle} \\ \tilde{c}_{\mathsf{n},\langle j\rangle} \end{bmatrix}$$

along with the j-th error dynamics (4.3.22), by which it is obtained that $\dot{V}_{\mathsf{n},\langle j\rangle} = -\left\|[\tilde{x}_{\mathsf{n},\langle j\rangle}; \tilde{z}_{\mathsf{n},\langle j\rangle}; \tilde{c}_{\mathsf{n},\langle j\rangle}]\right\|^2 \le -(1/\overline{\lambda}(P)) V_{\mathsf{n},\langle j\rangle}$. Thus, the comparison lemma [Kha96,

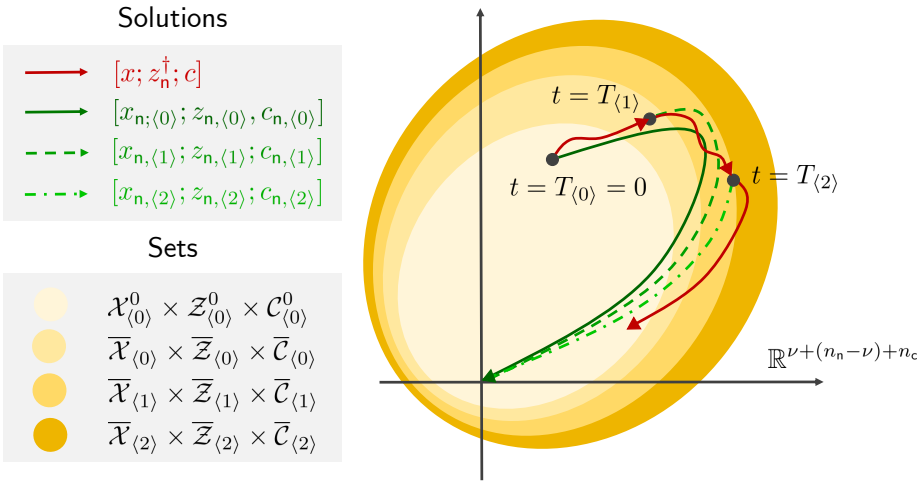

Figure 4.2: Visualization of proof of (4.3.1) when $m_{\mathsf{flt}} = 2$

Lemma 3.4] implies that

$$\left\| \begin{bmatrix} \tilde{x}_{\mathsf{n},\langle j\rangle}(t) \\ \tilde{z}_{\mathsf{n},\langle j\rangle}(t) \\ \tilde{c}_{\mathsf{n},\langle j\rangle}(t) \end{bmatrix} \right\| \leq \sqrt{\frac{\overline{\lambda}(P)}{\underline{\lambda}(P)}} e^{-t/(2\overline{\lambda}(P))} \left\| \begin{bmatrix} \tilde{x}_{\mathsf{n},\langle j\rangle}(T_{\langle j\rangle}) \\ \tilde{z}_{\mathsf{n},\langle j\rangle}(T_{\langle j\rangle}) \\ \tilde{c}_{\mathsf{n},\langle j\rangle}(T_{\langle j\rangle}) \end{bmatrix} \right\| < \frac{\epsilon}{m}$$

for all $T_{\langle j\rangle} \leq t < T_{\langle j+1\rangle}$ and $j = 1, \ldots, m_{\mathsf{flt}}$. Finally, it results from Young's inequality, $[x_{\mathsf{n},\langle 0\rangle}(t); z_{\mathsf{n},\langle 0\rangle}(t); c_{\mathsf{n},\langle 0\rangle}(t)] = [x^{\star}_{\mathsf{n}}(t); z^{\star}_{\mathsf{n}}(t); c^{\star}_{\mathsf{n}}(t)]$, and (4.3.20) that

$$\begin{aligned} \left\| \begin{bmatrix} x(t) \\ z^{\dagger}_{\mathsf{n}}(t) \\ c(t) \end{bmatrix} - \begin{bmatrix} x^{\star}_{\mathsf{n}}(t) \\ z^{\star}_{\mathsf{n}}(t) \\ c^{\star}_{\mathsf{n}}(t) \end{bmatrix} \right\| &\leq \left\| \begin{bmatrix} x(t) \\ z^{\dagger}_{\mathsf{n}}(t) \\ c(t) \end{bmatrix} - \begin{bmatrix} x_{\mathsf{n},\langle j\rangle}(t) \\ z_{\mathsf{n},\langle j\rangle}(t) \\ c_{\mathsf{n},\langle j\rangle}(t) \end{bmatrix} \right\| + \sum\nolimits_{k=1}^{j} \left\| \begin{bmatrix} \tilde{x}_{\mathsf{n},\langle k\rangle}(t) \\ \tilde{z}_{\mathsf{n},\langle k\rangle}(t) \\ \tilde{c}_{\mathsf{n},\langle k\rangle}(t) \end{bmatrix} \right\| \\ &< \frac{\epsilon}{m} + j \times \frac{\epsilon}{m} < \epsilon \end{aligned}$$

for all $T_{\langle j\rangle} \leq t < T_{\langle j+1\rangle}$, $j = 0, \ldots, m_{\mathsf{flt}} \leq m - 1$. This completes the proof of the theorem. An illustrative example for (5.1.1) is depicted in Figure 4.2.

4.4 Simulation: Fault Tolerant Control of Boeing 747

As an example, we take into account the 4-th order linearized lateral model of the Boeing 747 presented in [GY11, TCJ02]. In particular, with the unknown parameters $\mathsf{w}_{\mathsf{x},i} \in [0.7, 1.3]$ and $\mathsf{w}_{\mathsf{u},i} \in [0.97, 1.03]$ that represents parametric uncertainty on the dimensional derivative of rolling moment, the system considered here is represented as (4.1.4) where $y = x \in \mathbb{R}$ is the yaw rate (rad/s), ζ_1 is the side-slip angle (rad), ζ_2 is the roll rate (rad/s), ζ_3 is the roll angle (rad), $u = (u_1, u_2, u_3) \in \mathbb{R}^3$ is the the control input (rad) that expresses the three rudder servos, and the matrices are defined as $\phi = -0.115\mathsf{w}_{\mathsf{x},1}$, $\psi = \begin{bmatrix} 0.598\mathsf{w}_{\mathsf{x},2}, -0.0318\mathsf{w}_{\mathsf{x},3}, 0 \end{bmatrix}$, $g = \begin{bmatrix} 0.4715\mathsf{w}_{\mathsf{u},1}, 0.5\mathsf{w}_{\mathsf{u},2}, 0.3\mathsf{w}_{\mathsf{u},3} \end{bmatrix}$, and S, M, and H are known matrices with suitable dimensions. (Without loss of generality, we here multiply -1 into the original input matrix in [TCJ02] so that $g_i > 0$ holds.) We assume that $x(0) \in [-0.04, 0.04]$, $\zeta(0) \in [-0.004, 0.004] \times [-0.02, 0.02] \times [-0.015, 0.015]$, $\Delta_{\mathrm{dwell}} \geq 10$ s, $\|d_i(t)\| \leq 0.005$, $\|\dot{d}_i(t)\| \leq 0.025$, and $\|u^\star_{\mathrm{flt},i}\| \leq 0.1$. The problem under consideration is to ensure the output $y(t)$ to track the reference signal $r(t) = 0.02\sin(0.2t)$ rad/s in the presence of both model uncertainty and actuator failures.

To address the problem, the proposed DOB-based FTC is constructed as follows. First, we take a nominal model (4.1.7) as the system with $S_{\mathsf{n}} = S$, $M_{\mathsf{n}} = M$, $N_{\mathsf{n}} = N_3$, $G_{\mathsf{n}} = G_3$, $\phi_{\mathsf{n}} = \phi$, and $\psi_{\mathsf{n}} = \psi$ where the uncertain parameters are set as $\mathsf{w}_{\mathsf{x}} = \mathsf{w}_{\mathsf{u}} = 0$. To achieve a satisfactory nominal tracking performance, the nominal controller (4.1.8) is designed as a proportional-integral (PI) controller with $E = 0$, $F = 1$, $J = K_{\mathrm{int}} := 17$, $K = K_{\mathrm{prop}} := 3.4$, and $c_{\mathsf{n}}(0) = 0$. Next, by the proposed design algorithm in Subsection 4.2.1, we set the gain $\boldsymbol{\kappa}$ of the input allocation law (4.2.1) as $\boldsymbol{\kappa} = [1/3; 1/3; 1/3]$. After that, the DOB-based controller (4.2.14) and (4.2.21) is built up with $\mathsf{a}_0 = 1$, $\tau = 0.04$, $c(0) = 0$, $p(0) = q(0) = 0$, $z^\dagger_{\mathsf{n}}(0) = [0, 0, 0]^\top$ and the saturation functions $\overline{s}_{\mathsf{w}}$ and $\overline{s}_{\mathsf{x}}$ obtained by $\overline{\mathcal{D}}_{\mathrm{total}} := [-0.51, 0.51]$ and $\overline{\mathcal{X}} = [-0.041, 0.041]$.

For comparison, we perform the simulations with two types of controllers; one is the proposed DOB-based FTC, while the other is the PI controller with the input allocation law (4.2.1) (i.e., the FTC without the DOB part). In the

following simulations, a stochastic measurement noise under uniform distribution enters the system whose maximum magnitude is 10^{-4} rad/s, while the input disturbances are set as $d_1(t) = 0.0035\sin(1.05t)$, $d_2(t) = 0.004\sin(2.1t)$, and $d_3(t) = 0.025\sin(4.5t)$. For the simulation, the uncertain parameters $\mathsf{w}_{\mathsf{x},i}$ and $\mathsf{w}_{\mathsf{u},i}$ are taken as 0.7 and 0.97, respectively.

Figure 4.3 depicts the simulation result when two lock-in-place actuator faults take place as: $u^{\star}_{\mathrm{flt},3} = u_3(T_3)$ for $T_3 = 50$ s and $u^{\star}_{\mathrm{flt},2} = u_2(T_2)$ for $T_2 = 100$ s. It is shown that unlike the PI control-based FTC, our proposed FTC almost recovers the fault-free tracking performance for entire time period, while all the state variables remain bounded. A similar result can be found in Figure 4.4, in which the actuator faults have the floating form of $u^{\star}_{\mathrm{flt},2} = 0.06$ for $T_2 = 50$ s and $u^{\star}_{\mathrm{flt},3} = 0.06$ for $T_3 = 100$ s, and additional output disturbance $d_{\mathsf{y}}(t) = 0.002\sin(4t)$ rad/s affects the system.

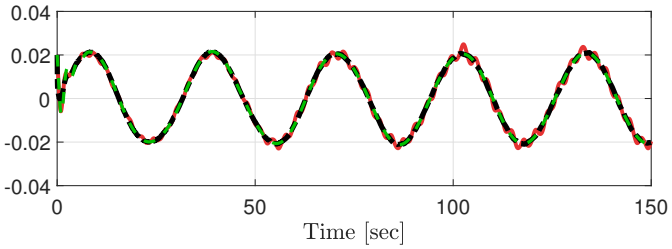

(a) Output (rad/s): actual output $y(t)$ with (black dash-dotted) and without DOB (red solid), and nominal output $y_{\mathrm{n}}(t)$ (green dashed)

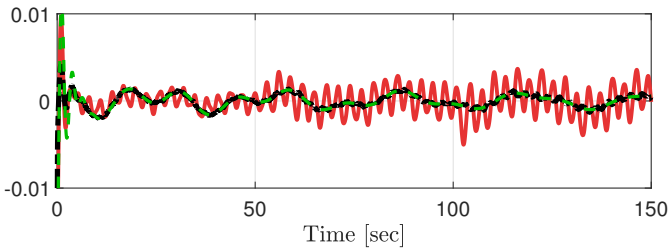

(b) Tracking error (rad/s): actual error $r(t) - y(t)$ with (black dash-dotted) and without DOB (red solid), and nominal error $r(t) - y_{\mathrm{n}}(t)$ (green dashed)

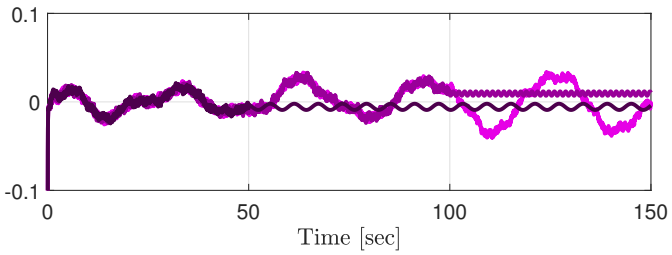

(c) Control input (rad): $u_1(t)$ (darkest), $u_3(t)$ (intermediate), $u_2(t)$ (brightest)

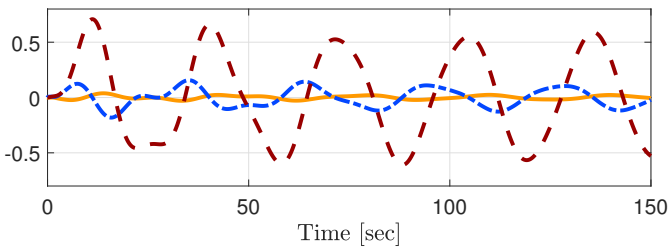

(d) Partial state ζ: $\zeta_1(t)$ rad/s (yellow solid), $\zeta_2(t)$ rad (blue dash-dotted), $\zeta_3(t)$ rad/s (brown dashed)

Figure 4.3: Simulation results when two lock-in-place faults take place

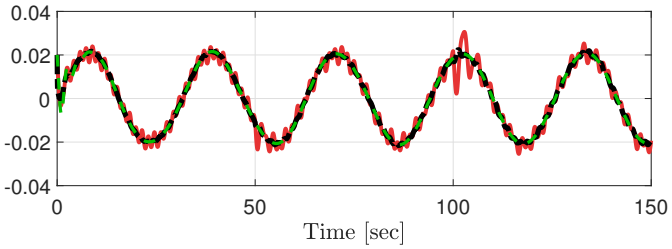

(a) Output (rad/s): actual output $y(t)$ with (black dash-dotted) and without DOB (red solid), and nominal output $y_n(t)$ (green dashed)

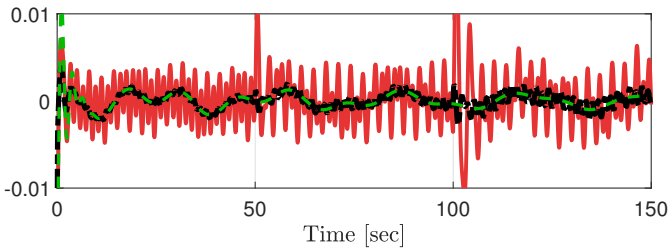

(b) Tracking error (rad/s): actual error $r(t) - y(t)$ with (black dash-dotted) and without DOB (red solid), and nominal error $r(t) - y_n(t)$ (green dashed)

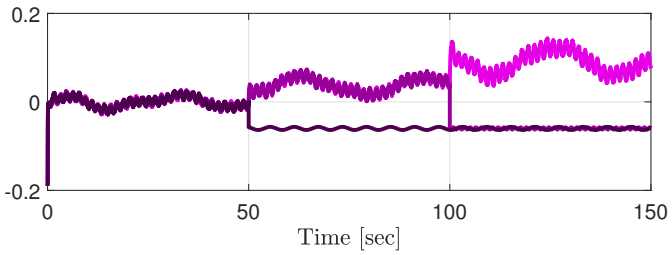

(c) Control input (rad): $u_1(t)$ (darkest), $u_2(t)$ (intermediate), $u_3(t)$ (brightest)

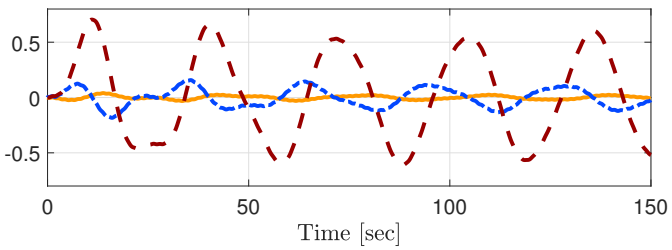

(d) Partial state ζ: $\zeta_1(t)$ rad/s (yellow solid), $\zeta_2(t)$ rad (blue dash-dotted), $\zeta_3(t)$ rad/s (brown dashed)

Figure 4.4: Simulation results when two floating faults sequentially occur

Chapter 5

Stability, Performance, and Designs of Discrete-time Disturbance Observers for Sampled-data Systems: A Fast Sampling Approach

Although the physical plants, for which the DOB scheme is applied, are mostly CT systems, the DOB-based controller is typically implemented in a digital device with a "sampler" and a "holder" (usually zero-order holder (ZOH)). The implementation issue has encouraged a series of substantial researches on the design of a DT-DOB, which are categorized mainly in two directions. The first one is just to transform a pre-designed CT-DOB into its discrete-time counterpart via various discretization methods [KC03, YCC03, TLT00]. The second one is, on the other hand, to construct a DT-DOB directly for a discretized plant model like in [WTS00, KK99], where the discretization takes into account inherent properties of sampled-data systems. Despite the increased attention paid to the DT-DOB so far, however, it seems that there is still some gap to the full understanding about robust stability under plant uncertainties (as well as effective compensation of external disturbances). Indeed, most of the existing results on robust stability employed the small-gain theorem, so that only a sufficient condition for stability is obtained. This makes it difficult to handle large uncertainties, and there lacks a design procedure for Q-filters.

More recently, a new approach was proposed in [LJS12], which is based on the CT result of [SJ09] that does not rely on the small-gain theorem. In the work

of [LJS12], the real CT plant is approximately discretized for the analysis, under the presumption that fast sampling will make the approximation error negligible in practice. However, as we shall see in this chapter, it is not true in general (especially for systems having relative degree greater than two) and the sampled-data controlled system may become unstable when the sampling proceeds fast.

In this chapter, motivated by those works [LJS12, SJ09], we present an "almost necessary and sufficient" condition for robust stability of DT-DOB-controlled systems under fast sampling. (Here it is "almost" since some degenerate cases still remain inconclusive.) Since the analysis is based on the exact discretization of the plant (and the DOB will be designed directly in the DT domain), our result is not an approximation anymore. Development of the stability condition begins by recalling the fact that fast sampling process may generate unstable "sampling zeros" [HYA93, ÅHS84, YG14], in particular for the systems having relative degree greater than two. In this work, we will reveal a strong connection between these extra zeros and the stability of the DT-DOB controlled system, which cannot be observed from the CT-DOB analysis or from any approximations.

More importantly, the result of this work presents a "generalized" framework for robust stability analysis, in the sense that it is available (a) "in whichever way" the DT-DOB is designed, and (b) no matter how the CT plant has "arbitrarily large" model uncertainty. For the former, we generalize the DT-DOB structure by using a generic form of the discretization methods. This generalization allows us to deal with "a large class of" the DT-DOB designs, and also to emphasize the importance of the discretized nominal model in the guaranteeing stability of the overall system. For example, it will be seen that if the nominal model in the DOB structure is "exactly" discretized (in the sense of zero-order holding operation), the proposed stability condition incurs that the closed-loop system cannot be stable with high relative degree of the CT plants, regardless of the Q-filter and model uncertainties.

Based on the stability result, this work also provides new systematic design procedures for the DT-DOB. A primary goal is to meet the robust stability condition always under "arbitrarily large" (but bounded) plant uncertainties and under unstable sampling zeros. One of the main ingredients to establish the proposed

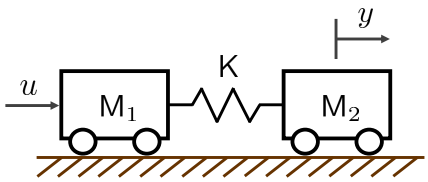

Figure 5.1: Two-mass-spring system

robust stability condition is to "approximately" discretize the nominal plant model (while the real plant model is exactly discretized for analysis) not to block the effect of the sampling zeros on the DOB loop. Then the sampling zeros appear in the proposed stability condition together with the coefficients of the Q-filter, and they possibly do not cause much trouble as long as the Q-filter is suitably designed. Moreover, inspired by the CT-DOB designs in Chapter 2, we propose an advanced design guideline to embed the disturbance model into the DT-DOB structure.

5.1 Motivating Example: Stability Issue of Disturbance Observers in Sampled-data Frameworks

As an illustrative example that motivates the work of this chapter, we take a look at the benchmark problem [WB92] with the CT two-mass-spring system depicted in Figure 5.1. The plant under consideration is modeled by a 4th-order system as

$$\mathrm{P}(s) = \frac{\mathsf{K}}{\mathsf{M}_1\mathsf{M}_2 s^4 + \mathsf{K}(\mathsf{M}_1 + \mathsf{M}_2)s^2} \tag{5.1.1}$$

where M_1 and M_2 are masses of the carts, and K is the spring coefficient. It is assumed that the parameters have bounded uncertainty as $\mathsf{M}_i \in [0.5, 2]$, and $\mathsf{K} \in [0.8, 1.2]$.

The particular interest here is to investigate how the sampling process affects the stability of the DOB controlled systems. To see this, we will build up two types of the DOB-based controllers for comparison. The first one is a typical

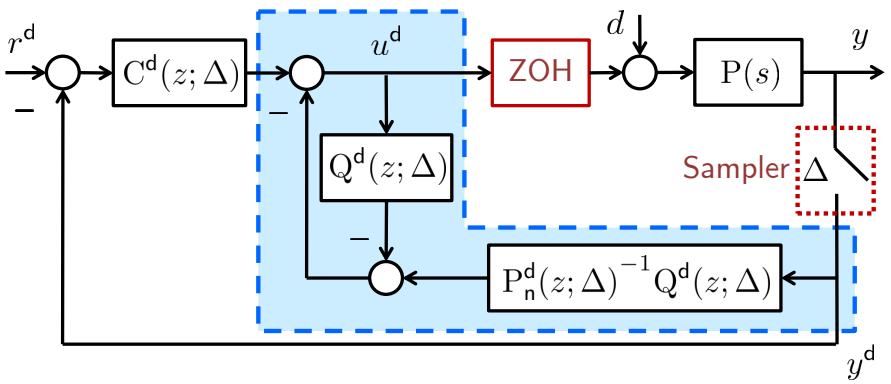

Figure 5.2: Overall controlled system with DT-DOB (blue dotted block): $\mathrm{Q}^{\mathsf{d}}(z;\Delta)$, $\mathrm{P}_{\mathsf{n}}^{\mathsf{d}}(z;\Delta)$, and $\mathrm{C}^{\mathsf{d}}(z;\Delta)$ stand for DT Q-filter (5.3.4), DT nominal model (5.3.2a), and DT controller (5.3.2b), respectively.

CT-DOB-based controller (implemented in the CT domain) in Figure 1.2, whose components are given as follows: the CT nominal model

$$\mathrm{P}_{\mathsf{n}}(s) = \frac{\mathsf{K}_{\mathsf{n}}}{\mathsf{M}_{\mathsf{n},1}\mathsf{M}_{\mathsf{n},2}s^4 + \mathsf{K}_{\mathsf{n}}(\mathsf{M}_{\mathsf{n},1} + \mathsf{M}_{\mathsf{n},2})s^2} \tag{5.1.2}$$

with the nominal parameters $\mathsf{K}_{\mathsf{n}} = 1$ and $\mathsf{M}_1 = \mathsf{M}_2 = 1$; the CT baseline controller

$$\mathrm{C}(s) = \frac{-6.8308175s^2 + 1.8486865s + 0.28043397}{s^2 + 4.2752492s + 6.0786141}$$

(presented in [BHLO06]) which stabilizes the CT nominal closed-loop system; and the CT Q-filter

$$\mathrm{Q}(s;\tau) = \frac{1}{(\tau s)^4 + 4(\tau s)^3 + 6(\tau s)^2 + 4(\tau s) + 1} \tag{5.1.3}$$

whose coefficients are selected simply as binomial ones, while $\tau = 0.015$. On the other hand, the second one is a DT-DOB-based controller that is implemented in the "sampled-data" framework as in Figure 5.2, with

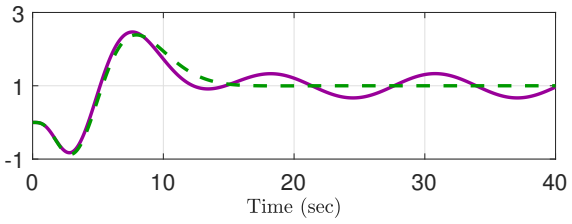

(a) Output y

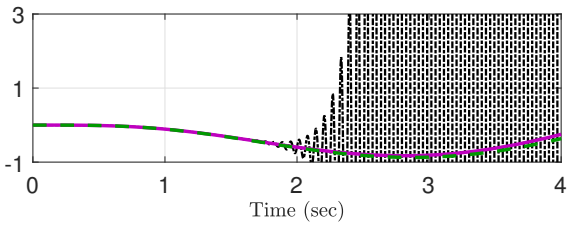

(b) Enlargement

Figure 5.3: Simulation results with CT-DOB controlled system (purple solid), DT-DOB controlled system (black dotted), and CT nominal closed-loop system (green dashed)

- sampler (where $\Delta > 0$ stands for the sampling period):

$$y^{\mathsf{d}}[k] = y(k\Delta); \tag{5.1.4}$$

- zero-order holder (ZOH):

$$u(t) = u^{\mathsf{d}}[k], \quad \forall k\Delta \leq t < (k+1)\Delta; \tag{5.1.5}$$

and the sampled reference $r^{\mathsf{d}}[k] := r(k\Delta)$. In this example, the DT nominal model $\mathrm{P}_{\mathsf{n}}^{\mathsf{d}}(z;\Delta)$ and the DT baseline controller $\mathrm{C}^{\mathsf{d}}(z;\Delta)$ are obtained by discretizing the CT counterparts via the forward difference method; i.e.,

$$\mathrm{P}_{\mathsf{n},\mathrm{fw}}^{\mathsf{d}}(z;\Delta) = \mathrm{P}_{\mathsf{n}}\left(\frac{z-1}{\Delta}\right), \quad \mathrm{C}_{\mathsf{n},\mathrm{fw}}^{\mathsf{d}}(z;\Delta) = \mathrm{C}_{\mathsf{n}}\left(\frac{z-1}{\Delta}\right). \tag{5.1.6}$$

In addition, we here employ the following "all-pass" filter (which is a prototypical

low-pass filter in a sense) as the DT Q-filter $\mathrm{Q}^{\mathsf{d}}(z;\Delta)$;

$$\mathrm{Q}^{\mathsf{d}}(z;\Delta) = \mathrm{Q}^{\mathsf{d}}_{\mathrm{all}}(z;\Delta) = \frac{1}{z^4}. \tag{5.1.7}$$

We note that $\mathrm{Q}^{\mathsf{d}}_{\mathrm{all}}(z;\Delta)$ above also can be regarded as a discretization result of (5.1.3) by the forward difference method.

For the simulation, we set $\mathrm{P}(s) = \mathrm{P}_{\mathsf{n}}(s)$ (i.e., there is no model uncertainty), the input disturbance $d(t) = \sin(0.5t)$, the reference $r(t) = 1$, and $\Delta = 0.015$s. The simulation results are depicted in Figure 5.3. The result is somewhat surprising, since it tells that the stability of the DT-DOB controlled system is not directly concluded by that of the relevant CT-DOB controlled system and even violated only by the sampling process (e.g., without any model uncertainty). The observation highlights the importance of further analysis on the DT-DOB controlled systems in the sampled-data framework, which is the main concern of this chapter.

5.2 Basics on Sampled-data Systems

As a prerequisite for the discussions to come, we briefly remind the natures of the sampled-data systems first. Consider a CT plant written in the state space

$$\dot{\mathtt{x}} = \mathbf{A}\mathtt{x} + \mathbf{B}(u+d), \qquad y = \mathbf{C}\mathtt{x} \tag{5.2.1}$$

where $\mathtt{x} \in \mathbb{R}^n$ is the state, $u \in \mathbb{R}$ is the control input, $y \in \mathbb{R}$ is the output, $d \in \mathbb{R}$ is the disturbance, and $\mathbf{A} \in \mathbb{R}^{n\times n}$, $\mathbf{B} \in \mathbb{R}^{n\times 1}$, and $\mathbf{C} \in \mathbb{R}^{1\times n}$ are constant matrices. With the Laplace transforms $\mathrm{u}(s) = \mathcal{L}(u(t))$, $\mathrm{y}(s) = \mathcal{L}(y(t))$, and $\mathrm{d}(s) = \mathcal{L}(d(t))$ of the CT signals, another expression of (5.2.1) is given by

$$\mathrm{y}(s) = \mathrm{P}(s)(\mathrm{u}(s) + \mathrm{d}(s)) \tag{5.2.2}$$

where $\mathrm{P}(s) = \mathbf{C}(sI - \mathbf{A})^{-1}\mathbf{B}$. For ease of explanation, we particularly rewrite $\mathrm{P}(s)$ as, without loss of generality,

$$\mathrm{P}(s) = \frac{g\prod_{i=1}^{n-\nu}(s-\mathsf{z}_i)}{\prod_{i=1}^{n}(s-\mathsf{p}_i)} =: \frac{\mathrm{N}(s)}{\mathrm{D}(s)} \tag{5.2.3}$$

where ν is the relative degree of $\mathrm{P}(s)$, and z_i, p_i, and $g > 0$ are the zeros, poles, and the high-frequency gain of $\mathrm{P}(s)$, respectively. Without loss of generality, the polynomials $\mathrm{N}(s)$ and $\mathrm{D}(s)$ are assumed to be coprime.

In this setting, the sampled-data system consisting of the CT plant (5.2.1), the sampler (5.1.4), and the ZOH (5.1.5) can be represented in time domain as follows (throughout this chapter, we will use the superscript d to indicate that a parameter or a variable is associated with the DT domain):

$$\mathtt{x}^{\mathsf{d}}[k+1] = \mathbf{A}^{\mathsf{d}}\mathtt{x}^{\mathsf{d}}[k] + \mathbf{B}^{\mathsf{d}}u^{\mathsf{d}}[k] + \overline{d}^{\mathsf{d}}[k], \qquad y^{\mathsf{d}}[k] = \mathbf{C}^{\mathsf{d}}\mathtt{x}^{\mathsf{d}}[k] \tag{5.2.4}$$

where $\mathtt{x}^{\mathsf{d}}[k] := \mathtt{x}(k\Delta)$, $u^{\mathsf{d}}[k] := u(k\Delta)$, $y^{\mathsf{d}}[k] = y(k\Delta)$ (as in (5.1.4)), and

$$\overline{d}^{\mathsf{d}}[k] := \int_{k\Delta}^{(k+1)\Delta} e^{\mathbf{A}((k+1)\Delta-\rho)}\mathbf{B}d(\rho)\mathrm{d}\rho \in \mathbb{R}^n, \tag{5.2.5}$$

and the matrices $\mathbf{A}^{\mathsf{d}}$, $\mathbf{B}^{\mathsf{d}}$, and $\mathbf{C}^{\mathsf{d}}$ are given by

$$\mathbf{A}^{\mathsf{d}}(\Delta) := e^{\mathbf{A}\Delta}, \quad \mathbf{B}^{\mathsf{d}}(\Delta) := \int_0^{\Delta} e^{\mathbf{A}\rho}\mathbf{B}\mathrm{d}\rho, \quad \mathbf{C}^{\mathsf{d}} := \mathbf{C}. \tag{5.2.6}$$

Similar to (5.2.2), with the definitions $\mathrm{u}^{\mathsf{d}}(z) := \mathcal{Z}\{u^{\mathsf{d}}[k]\}$, $\mathrm{y}^{\mathsf{d}}(z) := \mathcal{Z}\{y^{\mathsf{d}}[k]\}$, and $\overline{\mathrm{d}}^{\mathsf{d}}(z) := \mathcal{Z}\{\overline{d}^{\mathsf{d}}[k]\}$, one can represent the sampled-data system (5.2.4) in the frequency domain

$$\mathrm{y}^{\mathsf{d}}(z) = \mathrm{P}^{\mathsf{d}}(z;\Delta)\mathrm{u}^{\mathsf{d}}(z) + \overline{\mathrm{W}}^{\mathsf{d}}(z;\Delta)\overline{\mathrm{d}}^{\mathsf{d}}(z) \tag{5.2.7}$$

where

$$\begin{aligned}\mathrm{P}^{\mathsf{d}}(z;\Delta) &:= \mathbf{C}^{\mathsf{d}}\big(zI - \mathbf{A}^{\mathsf{d}}(\Delta)\big)^{-1}\mathbf{B}^{\mathsf{d}}(\Delta) \qquad (5.2.8a)\\ &= \mathcal{Z}\left(\frac{1-e^{-\Delta s}}{s}\mathrm{P}(s)\right) =: \frac{\mathrm{N}^{\mathsf{d}}(z;\Delta)}{\mathrm{D}^{\mathsf{d}}(z;\Delta)},\end{aligned}$$

$$\begin{aligned}\overline{\mathrm{W}}^{\mathsf{d}}(z;\Delta) &:= \mathbf{C}^{\mathsf{d}}\big(zI - \mathbf{A}^{\mathsf{d}}(\Delta)\big)^{-1} \\ &=: \frac{1}{\mathrm{D}^{\mathsf{d}}(z;\Delta)}\begin{bmatrix}\mathrm{N}^{\mathsf{d}}_{\overline{\mathsf{w}},1}(z;\Delta) & \cdots & \mathrm{N}^{\mathsf{d}}_{\overline{\mathsf{w}},n}(z;\Delta)\end{bmatrix}\end{aligned} \tag{5.2.8b}$$

with some polynomials $\mathrm{N}^{\mathsf{d}}(z;\Delta)$, $\mathrm{N}^{\mathsf{d}}_{\overline{\mathsf{w}},i}(z;\Delta)$, and $\mathrm{D}^{\mathsf{d}}(z;\Delta)$ of z.

From now on, we focus on the DT transfer function $\mathrm{P}^{\mathsf{d}}(z;\Delta)$ in (5.2.8a) from $\mathrm{u}^{\mathsf{d}}(z)$ to $\mathrm{y}^{\mathsf{d}}(z)$. Since $\mathrm{P}^{\mathsf{d}}(z;\Delta)$ "exactly" represents the input-to-output relation of the sampled-data system with the ZOH, it is often called *ZOH equivalent model* of $\mathrm{P}(s)$. As a well-known consequence of the sampling process, the following lemma highlights that the sampled-data model $\mathrm{P}^{\mathsf{d}}(z;\Delta)$ has $\nu - 1$ "extra" DT zeros for almost every $\Delta > 0$, compared with its CT counterpart $\mathrm{P}(s)$.

Lemma 5.2.1. [ÅHS84, YG14] For given CT plant $\mathrm{P}(s)$ in (5.2.3), there exists a measure-zero set $\mathcal{T}_{\mathrm{P}} \subset \mathbb{R}_{>0}$ such that the ZOH equivalent model $\mathrm{P}^{\mathsf{d}}(z;\Delta)$ in (5.2.8a) has relative degree 1 for all $\Delta \in \mathbb{R}_{>0} \setminus \mathcal{T}_{\mathrm{P}}$: more precisely, for all $\Delta \in \mathbb{R}_{>0} \setminus \mathcal{T}_{\mathrm{P}}$, $\mathrm{P}^{\mathsf{d}}(z;\Delta)$ is of the form

$$\mathrm{P}(z;\Delta) = \frac{\mathrm{N}^{\mathsf{d}}(z;\Delta)}{\mathrm{D}^{\mathsf{d}}(z;\Delta)} = \frac{g\mathrm{M}^{\mathsf{d}}(z;\Delta)\displaystyle\prod_{i=1}^{n-\nu}\frac{z - \mathsf{z}^{\mathsf{d}}_i(\Delta)}{\Delta}}{\displaystyle\prod_{i=1}^{n}\frac{z - \mathsf{p}^{\mathsf{d}}_i(\Delta)}{\Delta}} \tag{5.2.9}$$

where $\mathsf{z}^{\mathsf{d}}_i : \mathbb{R}_{>0} \setminus \mathcal{T}_{\mathrm{P}} \to \mathbb{C}$ and $\mathsf{p}^{\mathsf{d}}_i : \mathbb{R}_{>0} \setminus \mathcal{T}_{\mathrm{P}} \to \mathbb{C}$ are functions of Δ, and $\mathrm{M}^{\mathsf{d}}(z;\Delta)$ is a polynomial of z with order $\nu - 1$. Moreover, as $\Delta \to 0^+$,

- $\mathsf{p}^{\mathsf{d}}_i(\Delta) \to 1$ for $i = 1, \cdots, n$,
- $\mathsf{z}^{\mathsf{d}}_i(\Delta) \to 1$ for $i = 1, \cdots, n - \nu$,
- $\mathrm{M}^{\mathsf{d}}(z;\Delta) \to \mathrm{E}_{\nu-1}(z)/\nu! =: \mathrm{M}^{\star}(z)$

where

$$\mathrm{E}_{\nu-1}(z) := \mathsf{E}_{\nu-1,\nu-1}z^{\nu-1} + \mathsf{E}_{\nu-1,\nu-2}z^{\nu-2} + \cdots + \mathsf{E}_{\nu-1,0} \tag{5.2.10}$$

is the Euler-Frobenius polynomial of order $\nu - 1$, with the coefficients $\mathsf{E}_{\nu-1,j} := \sum_{l=1}^{\nu-j}(-1)^{\nu-j-l}l^{\nu}\binom{\nu+1}{\nu-j-l}$ for $j = 0, \ldots, \nu - 1$. ◊

We further note that $\mathsf{z}_i^{\mathsf{d}}(\Delta)$ can be approximated by $e^{\mathsf{z}_i\Delta}$ (with a suitable rearrangement of z_i) with sufficiently small Δ. In this regard, we call $\mathsf{z}_i^{\mathsf{d}}(\Delta)$ as the *intrinsic zeros*, while the remaining ones (i.e., the roots of $\mathrm{M}^{\mathsf{d}}(z;\Delta)=0$) as the *sampling zeros*. The above lemma points out that unlike the intrinsic zeros, the limiting behavior of the sampling zeros is solely determined by the Euler-Frobenius polynomial $\mathrm{E}_{\nu-1}(z)$. Some important properties of the polynomial are summarized below.

Proposition 5.2.2. ([YG14]) The Euler-Frobenius polynomial $\mathrm{E}_{\nu-1}(z)$ in (5.2.10) satisfies the following statements:

(a) $\mathsf{E}_{\nu-1,0}=\mathsf{E}_{\nu-1,\nu-1}=1$ and $\mathsf{E}_{\nu-1,i}=\mathsf{E}_{\nu-1,\nu-i}$ for all $i=0,\ldots,\nu-1$;

(b) $\mathrm{E}_{\nu-1}(1)=\nu!$;

(c) For $\nu\geq 3$, there exists at least one root of $\mathrm{E}_{\nu-1}(z)=0$ outside the unit circle;

(d) All the roots of $\mathrm{E}_{\nu-1}(z)=0$ are single and negative real.

$\Diamond$

A remarkable lesson from Lemma 5.2.1 and Proposition 5.2.2 is that with high relative degree ν of $\mathrm{P}(s)$ (that is, $\nu\geq 3$), the sampled-data model $\mathrm{P}^{\mathsf{d}}(z;\Delta)$ is "inherently" of non-minimum phase (in the DT domain) under fast sampling. We will show shortly that this nature incurs a significant difference between the stability results of the CT- and DT-DOB schemes in the end.

5.3 Generic Representation of Discrete-time Disturbance Observer

We now turn our attention to the DT-DOB-based controller in Figure 5.2. On top of the basic configuration in Figure 5.2, several ways to construct the DT-DOB-based controller have been introduced in the literature, along with specific design methods for $\mathrm{Q}^{\mathsf{d}}(z;\Delta)$, $\mathrm{P}_{\mathsf{n}}^{\mathsf{d}}(z;\Delta)$, and $\mathrm{C}^{\mathsf{d}}(z;\Delta)$. Rather than specifying the

structure, in this chapter we are interested in taking various types of DT-DOB-based controllers into account in the stability analysis. For this purpose, we here present a "generic" representation of the DT-DOB-based control scheme.

Let us begin with the DT nominal model $\mathrm{P}_{\mathsf{n}}^{\mathsf{d}}(z;\Delta)$ and the DT outer-loop controller $\mathrm{C}^{\mathsf{d}}(z;\Delta)$. A common way to obtain them is to discretize a CT nominal model

$$\mathrm{P}_{\mathsf{n}}(s) = \frac{g_{\mathsf{n}} \prod_{i=1}^{n_{\mathsf{n}}-\nu}(s-\mathsf{z}_{\mathsf{n},i})}{\prod_{i=1}^{n_{\mathsf{n}}}(s-\mathsf{p}_{\mathsf{n},i})} =: \frac{\mathrm{N}_{\mathsf{n}}(s)}{\mathrm{D}_{\mathsf{n}}(s)} \tag{5.3.1a}$$

of $\mathrm{P}(s)$ and a CT baseline controller

$$\mathrm{C}(s) = \frac{g_{\mathsf{c}} \prod_{i=1}^{n_{\mathsf{c}}-\nu_{\mathsf{c}}}(s-\mathsf{z}_{\mathsf{c},i})}{\prod_{i=1}^{n_{\mathsf{c}}}(s-\mathsf{p}_{\mathsf{c},i})} =: \frac{\mathrm{N}_{\mathsf{c}}(s)}{\mathrm{D}_{\mathsf{c}}(s)}, \tag{5.3.1b}$$

respectively, where $g_{\mathsf{n}} > 0$ and $g_{\mathsf{c}} \neq 0$ are the high-frequency gains, $\mathsf{z}_{\mathsf{n},i}$ and $\mathsf{z}_{\mathsf{c},i}$ are the CT zeros, $\mathsf{p}_{\mathsf{n},i}$ and $\mathsf{p}_{\mathsf{c},i}$ are the CT poles. It is assumed that $\mathrm{C}(s)$ is designed to stabilize the CT nominal model $\mathrm{P}_{\mathsf{n}}(s)$. Here, it should be noted that even for fixed CT transfer functions $\mathrm{P}_{\mathsf{n}}(s)$ and $\mathrm{C}(s)$, their discretized transfer functions $\mathrm{P}_{\mathsf{n}}^{\mathsf{d}}(z;\Delta)$ and $\mathrm{C}^{\mathsf{d}}(z;\Delta)$ may "not" be unique, because many discretization methods are enabled in general. Keeping this in mind, the following assumption is made to represent the discretization results $\mathrm{P}_{\mathsf{n}}^{\mathsf{d}}(z;\Delta)$ and $\mathrm{C}^{\mathsf{d}}(z;\Delta)$ in explicit forms "uniformly" in the discretization methods.

Assumption 5.3.1. The DT transfer functions $\mathrm{P}_{\mathsf{n}}^{\mathsf{d}}(z;\Delta)$ and $\mathrm{C}^{\mathsf{d}}(z;\Delta)$ in Figure 5.2 have the form

$$\mathrm{P}_{\mathsf{n}}^{\mathsf{d}}(z;\Delta) = \frac{\mathrm{N}_{\mathsf{n}}^{\mathsf{d}}(z;\Delta)}{\mathrm{D}_{\mathsf{n}}^{\mathsf{d}}(z;\Delta)} := \frac{g_{\mathsf{n}}^{\mathsf{d}}(\Delta)\mathrm{M}_{\mathsf{n}}^{\mathsf{d}}(z;\Delta) \displaystyle\prod_{i=1}^{n_{\mathsf{n}}-\nu} \frac{z-\mathsf{z}_{\mathsf{n},i}^{\mathsf{d}}(\Delta)}{\Delta}}{\displaystyle\prod_{i=1}^{n_{\mathsf{n}}} \frac{z-\mathsf{p}_{\mathsf{n},i}^{\mathsf{d}}(\Delta)}{\Delta}}, \tag{5.3.2a}$$

$$\mathrm{C}^{\mathsf{d}}(z;\Delta) = \frac{\mathrm{N}_{\mathsf{c}}^{\mathsf{d}}(z;\Delta)}{\mathrm{D}_{\mathsf{c}}^{\mathsf{d}}(z;\Delta)} =: \frac{g_{\mathsf{c}}^{\mathsf{d}}(\Delta)\mathrm{M}_{\mathsf{c}}^{\mathsf{d}}(z;\Delta) \displaystyle\prod_{i=1}^{n_{\mathsf{c}}-\nu_{\mathsf{c}}} \frac{z-\mathsf{z}_{\mathsf{c},i}^{\mathsf{d}}(\Delta)}{\Delta}}{\displaystyle\prod_{i=1}^{n_{\mathsf{c}}} \frac{z-\mathsf{p}_{\mathsf{c},i}^{\mathsf{d}}(\Delta)}{\Delta}} \tag{5.3.2b}$$

for all $\Delta \in \mathbb{R}_{>0} \setminus \mathcal{T}_{\mathsf{nc}}$, in which $\mathcal{T}_{\mathsf{nc}}$ is a measure zero subset of $\mathbb{R}_{>0}$ satisfying

	FDM	BDM	BT	MPZ
$g_{\mathsf{n}}^{\mathsf{d}}$	g_{n}	$g_{\mathsf{n}}\frac{\prod_{i=1}^{n-\nu}(1-\Delta \mathsf{z}_{\mathsf{n},i})}{\prod_{i=1}^{n}(1-\Delta \mathsf{p}_{\mathsf{n},i})}$	$g_{\mathsf{n}}\frac{\prod_{i=1}^{n-\nu}\left(1-\frac{\Delta \mathsf{z}_{\mathsf{n},i}}{2}\right)}{\prod_{i=1}^{n}\left(1-\frac{\Delta \mathsf{p}_{\mathsf{n},i}}{2}\right)}$	$g_{\mathsf{n}}\frac{\prod_{i=1}^{n}\frac{e^{\Delta \mathsf{p}_{\mathsf{n},i}}-1}{\Delta \mathsf{p}_{\mathsf{n},i}}}{\prod_{i=1}^{n-\nu}\frac{e^{\Delta \mathsf{z}_{\mathsf{n},i}}-1}{\Delta \mathsf{z}_{\mathsf{n},i}}}$
$\mathrm{M}_{\mathsf{n}}^{\mathsf{d}}$	1	z^{ν}	$\frac{(z+1)^{\nu}}{2^{\nu}}$	$\frac{(z+1)^{\nu}}{2^{\nu}}$
$\mathsf{z}_{\mathsf{n},i}^{\mathsf{d}}$	$1+\Delta \mathsf{z}_{\mathsf{n},i}$	$\frac{1}{1-\Delta \mathsf{z}_{\mathsf{n},i}}$	$\frac{1+\frac{\Delta \mathsf{z}_{\mathsf{n},i}}{2}}{1-\frac{\Delta \mathsf{z}_{\mathsf{n},i}}{2}}$	$e^{\Delta \mathsf{z}_{\mathsf{n},i}}$
$\mathsf{p}_{\mathsf{n},i}^{\mathsf{d}}$	$1+\Delta \mathsf{p}_{\mathsf{n},i}$	$\frac{1}{1-\Delta \mathsf{p}_{\mathsf{n},i}}$	$\frac{1+\frac{\Delta \mathsf{p}_{\mathsf{n},i}}{2}}{1-\frac{\Delta \mathsf{p}_{\mathsf{n},i}}{2}}$	$e^{\Delta \mathsf{p}_{\mathsf{n},i}}$

Table 5.1: Discretization (5.3.2a) of $\mathrm{P}_{\mathsf{n}}(s)$ in (5.3.1a) resulting from various methods; forward difference method (FDM), backward difference method (BDM), bilinear transformation (BT), and matched pole zero method (MPZ).

$\inf(\mathcal{T}_{\mathsf{nc}}) > 0$, and $\mathrm{M}_{\mathsf{n}}^{\mathsf{d}}(z;\Delta)$ and $\mathrm{M}_{\mathsf{c}}^{\mathsf{d}}(z;\Delta)$ are polynomials of z with order $0 \leq n_{\mathsf{mn}} \leq \nu_{\mathsf{n}}$ and $0 \leq n_{\mathsf{mc}} \leq \nu_{\mathsf{c}}$, respectively. The real numbers $g_{\mathsf{n}}^{\mathsf{d}}$ and $g_{\mathsf{c}}^{\mathsf{d}}$, and the complex numbers $\mathsf{z}_{\mathsf{n},i}^{\mathsf{d}}$, $\mathsf{z}_{\mathsf{c},i}^{\mathsf{d}}$, $\mathsf{p}_{\mathsf{n},i}^{\mathsf{d}}$, and $\mathsf{p}_{\mathsf{c},i}^{\mathsf{d}}$ are functions of Δ that are well-defined for all $\Delta \in \mathbb{R}_{>0} \setminus \mathcal{T}_{\mathsf{nc}}$. Moreover, as $\Delta \to 0^{+}$,

$$g_{\mathsf{n}}^{\mathsf{d}}(\Delta) \to g_{\mathsf{n}}, \qquad g_{\mathsf{c}}^{\mathsf{d}}(\Delta) \to g_{\mathsf{c}}, \tag{5.3.3a}$$

$$\mathrm{M}_{\mathsf{n}}^{\mathsf{d}}(z;\Delta) \to \mathrm{M}_{\mathsf{n}}^{\star}(z), \qquad \mathrm{M}_{\mathsf{c}}^{\mathsf{d}}(z;\Delta) \to \mathrm{M}_{\mathsf{c}}^{\star}(z), \tag{5.3.3b}$$

$$\frac{\mathsf{z}_{\mathsf{n},i}^{\mathsf{d}}(\Delta)-1}{\Delta} \to \mathsf{z}_{\mathsf{n},i}, \qquad \frac{\mathsf{z}_{\mathsf{c},i}^{\mathsf{d}}(\Delta)-1}{\Delta} \to \mathsf{z}_{\mathsf{c},i}, \tag{5.3.3c}$$

$$\frac{\mathsf{p}_{\mathsf{n},i}^{\mathsf{d}}(\Delta)-1}{\Delta} \to \mathsf{p}_{\mathsf{n},i}, \qquad \frac{\mathsf{p}_{\mathsf{c},i}^{\mathsf{d}}(\Delta)-1}{\Delta} \to \mathsf{p}_{\mathsf{c},i} \tag{5.3.3d}$$

where $\mathrm{M}_{\mathsf{n}}^{\star}(z)$ and $\mathrm{M}_{\mathsf{c}}^{\star}(z)$ are polynomials of order n_{mn} and n_{mc} satisfying $\mathrm{M}_{\mathsf{n}}^{\star}(1) = 1$ and $\mathrm{M}_{\mathsf{c}}^{\star}(1) = 1$, respectively. $\lozenge$

As a matter of fact, Assumption 5.3.1 is satisfied with many widely-used discretization methods. Possible candidates include (but are not limited to) the forward ($s = (z-1)/\Delta$) and backward ($s = (z-1)/(\Delta z)$) difference methods,

the bilinear transformation ($s = (2(z-1))/(\Delta(z+1))$), and the matched pole zero method [FPW98], all of which are associated with $\mathcal{T}_{\mathsf{nc}} = \emptyset$. The results of these mentioned methods are summarized in Table 5.1.

On the other hand, similar to most of the previous works, we set the DT Q-filter $\mathrm{Q}^{\mathsf{d}}(z;\Delta)$ as a stable low-pass filter. Particularly, in order to gain additional design freedom, it is allowed that the coefficients of $\mathrm{Q}^{\mathsf{d}}(z;\Delta)$ possibly depend on the sampling period Δ; in other words,

$$\mathrm{Q}^{\mathsf{d}}(z;\Delta) = \frac{\mathsf{c}^{\mathsf{d}}_{l_{\mathsf{q}}}(\Delta)(z-1)^{l_{\mathsf{q}}} + \cdots + \mathsf{c}^{\mathsf{d}}_0(\Delta)}{(z-1)^{n_{\mathsf{q}}} + \mathsf{a}^{\mathsf{d}}_{n_{\mathsf{q}}-1}(\Delta)(z-1)^{n_{\mathsf{q}}-1} + \cdots + \mathsf{a}^{\mathsf{d}}_0(\Delta)} =: \frac{\mathrm{N}^{\mathsf{d}}_{\mathsf{q}}(z;\Delta)}{\mathrm{D}^{\mathsf{d}}_{\mathsf{q}}(z;\Delta)} \quad (5.3.4)$$

where $\mathsf{c}^{\mathsf{d}}_i(\Delta) \in \mathbb{R}$ and $\mathsf{a}^{\mathsf{d}}_i(\Delta) \in \mathbb{R}$ are functions of Δ satisfying that $\mathsf{c}^{\mathsf{d}}_i(\Delta) \to \mathsf{c}^{\star}_i$ and $\mathsf{a}^{\mathsf{d}}_i(\Delta) \to \mathsf{a}^{\star}_i$ as $\Delta \to 0^+$, $\mathsf{c}^{\mathsf{d}}_0(\Delta) = \mathsf{a}^{\mathsf{d}}_0(\Delta)$ for all $\Delta \in \mathbb{R}_{>0}$, and $\mathsf{c}^{\star}_0 = \mathsf{a}^{\star}_0 \neq 0$. (The second condition is requested for the low-pass filtering property of the Q-filter.) The relative degree $n_{\mathsf{q}} - l_{\mathsf{q}}$ of $\mathrm{Q}^{\mathsf{d}}(z;\Delta)$ is chosen as $n_{\mathsf{q}} - l_{\mathsf{q}} \geq \max\{\nu - n_{\mathsf{mn}}, 1\}$ so that the block $\mathrm{P}^{\mathsf{d}}_{\mathsf{n}}(z;\Delta)^{-1}\mathrm{Q}^{\mathsf{d}}(z;\Delta)$ in Figure 5.2 is implementable and $\mathrm{Q}^{\mathsf{d}}(z;\Delta)$ itself is strictly proper.

We conclude this section by noting that the DT-DOB-based controller of our interest has the structure depicted in Figure 5.3 and consists of the inverse of the DT nominal model (5.3.2a), the DT baseline controller (5.3.2b), and the DT Q-filter (5.3.4).

Remark 5.3.1. Another widely-employed realization of the DT-DOB scheme is depicted in Figure 5.4 [CT12]. In the figure, a n_{d}-step delay function $z^{-n_{\mathsf{d}}}$ and a re-defined nominal model $\tilde{\mathrm{P}}^{\mathsf{d}}_{\mathsf{n}}(z;\Delta) := z^{n_{\mathsf{d}}}\mathrm{P}^{\mathsf{d}}_{\mathsf{n}}(z;\Delta)$ are used (so that the inverse $\tilde{\mathrm{P}}^{\mathsf{d}}_{\mathsf{n}}(z;\Delta)^{-1}$ can stand alone). Even though the two DT-DOB structures in Figures 5.2 and 5.4 seem different from each other, they are in fact equivalent in the input-to-output sense, by simply taking the Q-filter in the latter structure to satisfy $\mathrm{Q}^{\mathsf{d}}(z;\Delta) = z^{-n_{\mathsf{d}}}\tilde{\mathrm{Q}}^{\mathsf{d}}(z;\Delta)$. In this regard, throughout this paper we will focus on the DT-DOB structure in Figure 5.2. $\Diamond$

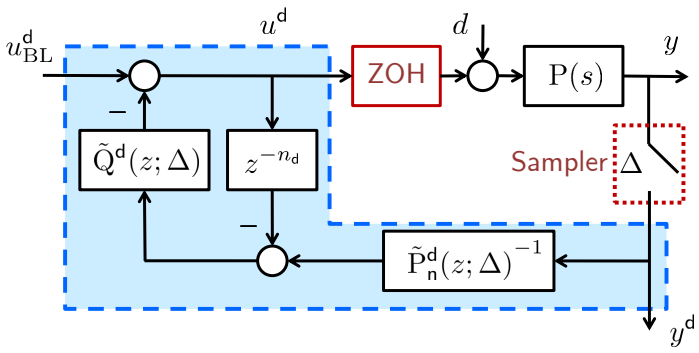

Figure 5.4: An equivalent block diagram of DT-DOB

5.4 Almost Necessary and Sufficient Condition for Robust Internal Stability under Fast Sampling

5.4.1 Main Result

As the main result of this chapter, we now derive a robust stability condition for the DT-DOB controlled system in Figure 5.2. We assume that the CT plant $\mathrm{P}(s)$ has bounded parametric uncertainty.

Assumption 5.4.1. The CT plant $\mathrm{P}(s)$ in (5.2.3) is contained in the set of uncertain systems

$$\mathcal{P} := \left\{ \mathrm{P}(s) = \frac{\mathsf{N}_{n-\nu}s^{n-\nu} + \cdots + \mathsf{N}_0}{s^n + \mathsf{D}_{n-1}s^{n-1} + \cdots \mathsf{D}_0} \ : \ \mathsf{N}_i \in [\underline{\mathsf{N}}_i, \overline{\mathsf{N}}_i],\ \mathsf{D}_i \in [\underline{\mathsf{D}}_i, \overline{\mathsf{D}}_i] \right\} \quad (5.4.1)$$

where $\underline{\mathsf{N}}_i$, $\overline{\mathsf{N}}_i$, $\underline{\mathsf{D}}_i$, and $\overline{\mathsf{D}}_i$ are known constants. $\Diamond$

We now take a look at the transfer function matrix from $[\mathrm{r}^{\mathsf{d}}(z); \overline{\mathrm{d}}^{\mathsf{d}}(z)]$ to $[\mathrm{e}^{\mathsf{d}}(z); \mathrm{u}^{\mathsf{d}}(z); \mathrm{y}^{\mathsf{d}}(z)]$, which is computed by (hereinafter, we often omit the term

$(z;\Delta)$ in DT transfer functions and polynomials when it is obvious.)

$$\frac{1}{\mathrm{Q}^{\mathsf{d}}(\mathrm{P}^{\mathsf{d}}-\mathrm{P}_{\mathsf{n}}^{\mathsf{d}})+\mathrm{P}_{\mathsf{n}}^{\mathsf{d}}(1+\mathrm{P}^{\mathsf{d}}\mathrm{C}^{\mathsf{d}})}\begin{bmatrix}\mathrm{Q}^{\mathsf{d}}(\mathrm{P}^{\mathsf{d}}-\mathrm{P}_{\mathsf{n}}^{\mathsf{d}})+\mathrm{P}_{\mathsf{n}}^{\mathsf{d}} & -\overline{\mathrm{W}}^{\mathsf{d}}\mathrm{P}_{\mathsf{n}}^{\mathsf{d}}(1-\mathrm{Q}^{\mathsf{d}})\\ \mathrm{P}_{\mathsf{n}}^{\mathsf{d}}\mathrm{C}^{\mathsf{d}} & -\overline{\mathrm{W}}^{\mathsf{d}}(\mathrm{P}_{\mathsf{n}}^{\mathsf{d}}\mathrm{C}^{\mathsf{d}}+\mathrm{Q}^{\mathsf{d}})\\ \mathrm{P}^{\mathsf{d}}\mathrm{P}_{\mathsf{n}}^{\mathsf{d}}\mathrm{C}^{\mathsf{d}} & \overline{\mathrm{W}}^{\mathsf{d}}\mathrm{P}_{\mathsf{n}}^{\mathsf{d}}(1-\mathrm{Q}^{\mathsf{d}})\end{bmatrix}. \tag{5.4.2}$$

The DT-DOB controlled system is said to be *internally stable* if all of the transfer functions in (5.4.2) are Schur stable. The closed-loop system is said to be *robustly internally stable* if the system is internally stable for all $\mathrm{P}(s)\in\mathcal{P}$ in Assumption 5.4.1. It is clear that the closed-loop system is robustly internally stable if and only if the characteristic polynomial

$$\mathbf{\Psi}^{\mathsf{d}}:=\big(\mathrm{D}^{\mathsf{d}}\mathrm{D}_{\mathsf{c}}^{\mathsf{d}}+\mathrm{N}^{\mathsf{d}}\mathrm{N}_{\mathsf{c}}^{\mathsf{d}}\big)\mathrm{N}_{\mathsf{n}}^{\mathsf{d}}\mathrm{D}_{\mathsf{q}}^{\mathsf{d}}+\mathrm{N}_{\mathsf{q}}^{\mathsf{d}}\mathrm{D}_{\mathsf{c}}^{\mathsf{d}}\big(\mathrm{N}^{\mathsf{d}}\mathrm{D}_{\mathsf{n}}^{\mathsf{d}}-\mathrm{N}_{\mathsf{n}}^{\mathsf{d}}\mathrm{D}^{\mathsf{d}}\big) \tag{5.4.3}$$

of (5.4.2) is Schur for all $\mathrm{P}(s)\in\mathcal{P}$. Note that by definition, for almost every Δ the degree $\deg\big(\mathbf{\Psi}^{\mathsf{d}}(z;\Delta)\big)$ of the characteristic polynomial is fixed as $n+n_{\mathsf{c}}+n_{\mathsf{n}}+n_{\mathsf{q}}-\nu$.

The main idea of our stability analysis is to investigate the "limiting" behavior of the characteristic polynomial $\mathbf{\Psi}^{\mathsf{d}}(z;\Delta)$ (which is dependent of the sampling period Δ) as Δ approaches zero. The following technical lemma will play a crucial role in the analysis.

Lemma 5.4.1. Let $\mathrm{X}^{\mathsf{d}}(z)$ and $\mathrm{Y}^{\mathsf{d}}(z;T)$ be polynomials of the complex variable z where $\lim_{T\to 0}\mathrm{Y}^{\mathsf{d}}(z;T)=0$. Assume that $\deg(\mathrm{X}^{\mathsf{d}}(z))=n$ and $\deg(\mathrm{Y}^{\mathsf{d}}(z;T))=l\geq 0$, and let $\mathsf{x}_i^{\star}$, $i=1,\dots,n$, be the roots of $\mathrm{X}^{\mathsf{d}}(z)=0$. Then n roots of $\mathrm{X}^{\mathsf{d}}(z)+\mathrm{Y}^{\mathsf{d}}(z;T)=0$, say $\mathsf{x}_i^{\mathsf{d}}(T)$, $i=1,\dots,n$, satisfy $\lim_{T\to 0}\mathsf{x}_i^{\mathsf{d}}(T)=\mathsf{x}_i^{\star}$ (even if $\mathrm{X}^{\mathsf{d}}(z)+\mathrm{Y}^{\mathsf{d}}(z;T)=0$ may have more than n roots for $T>0$). ♢

Proof. This lemma is a natural extension of [SJ09, Lemma 1] and can be proved by the Rouche's theorem [Fla83]. We omit the detailed derivation of the lemma. □

In the following analysis, we will utilize the explicit form (5.2.9) of $\mathrm{P}^{\mathsf{d}}(z;\Delta)$ given in Lemma 5.2.1 instead of the exact expression (5.2.8a), by relying on the sufficiently small Δ. This idea might be clear as long as $\mathrm{P}(s)$ is fixed. Yet since

a "bundle" of the uncertain CT plants in Assumption 5.4.1 should be considered concurrently, it may be still questionable whether or not one small sampling period Δ admits (5.2.9) "for all" $\mathrm{P}(s) \in \mathcal{P}$. Fortunately, this is not a hurdle in a sense, as described in the following lemma.

Lemma 5.4.2. Suppose that Assumption 5.4.1 holds. Then for the sets $\mathcal{T}_{\mathrm{P}}$ in Lemma 5.2.1 associated with $\mathrm{P}(s) \in \mathcal{P}$,

$$\Delta^{\star}_{\mathcal{P}} := \inf\Big(\bigcup\nolimits_{\mathrm{P}(s)\in\mathcal{P}} \mathcal{T}_{\mathrm{P}(s)} \Big) > 0. \tag{5.4.4}$$

$\Diamond$

Proof. By the definition of the relative degree of a DT transfer function, $\mathrm{P}^{\mathsf{d}}(z;T)$ has the relative degree larger than 1 for some $T > 0$ if and only if the DT step response $y^{\mathsf{d}}_{\mathrm{step}}[k]$ of $\mathrm{P}^{\mathsf{d}}(z;T)$ is zero at $k = 1$, or equivalently, the CT step response $y_{\mathrm{step}}(t)$ is zero at $t = T$ (where the latter equivalence comes from the fact that holding DT step input via the ZOH generates the CT step input.) Therefore, $\mathcal{T}_{\mathrm{P}(s)}$ is the same as the set of these zero-crossing instants $t = T$ of the CT step response. From the calculus of variation, the zero-crossing instant T must satisfy

$$y_{\mathrm{step}}(T) = 0 \quad \text{where} \quad y_{\mathrm{step}}(t) := \mathbf{C} \int_0^t e^{\mathbf{A}(t-\rho)} \mathbf{B} \mathrm{d}\rho. \tag{5.4.5}$$

It is obtained from [Kha96, Theorem 3.4] that the solution $y_{\mathrm{step}}(t)$ in (5.4.5) is continuous on the variation of $(\mathbf{A}, \mathbf{B}, \mathbf{C})$, and T also does. This concludes the proof. □

It is obvious that $\deg\big(\mathbf{\Psi}^{\mathsf{d}}(z;\Delta)\big) = n + n_{\mathsf{c}} + n_{\mathsf{n}} + n_{\mathsf{q}} - \nu$ is satisfied for all $\Delta \in (0, \Delta^{\star}_{\mathcal{P}})$. As an intermediate step, the following lemma shows the limiting behavior of the roots of $\mathbf{\Psi}^{\mathsf{d}}(z;\Delta) = 0$ in the conventional z-domain.

Lemma 5.4.3. Let $\overline{n} := (n - \nu) + n_{\mathsf{n}} + n_{\mathsf{c}}$ and

$$\Psi^{\mathsf{d}}_{\mathrm{fast}}(z) := \mathrm{M}^{\star}_{\mathsf{n}}(z)\big(\mathrm{D}^{\star}_{\mathsf{q}}(z) - \mathrm{N}^{\star}_{\mathsf{q}}(z)\big) + \frac{g}{g_{\mathsf{n}}} \mathrm{M}^{\star}(z) \mathrm{N}^{\star}_{\mathsf{q}}(z) \tag{5.4.6}$$

where $\mathrm{N}^{\star}_{\mathsf{q}}(z) := \lim_{\Delta\to 0^+} \mathrm{N}^{\mathsf{d}}_{\mathsf{q}}(z;\Delta)$ and $\mathrm{D}^{\star}_{\mathsf{q}}(z) := \lim_{\Delta\to 0^+} \mathrm{D}^{\mathsf{d}}_{\mathsf{q}}(z;\Delta)$. Then as $\Delta \to$

0^+, $\overline{n}$ roots of $\mathbf{\Psi}^{\mathsf{d}}(z;\Delta)=0$ approach $1+j0$, while the remaining $(\deg(\mathbf{\Psi}^{\mathsf{d}})-\overline{n})$ roots converge to those of $\Psi^{\mathsf{d}}_{\mathrm{fast}}(z)=0$. $\Diamond$

Proof. For ease of explanation, we define two polynomials

$$\Psi^{\mathsf{d}}_1 := \big(\mathrm{D}^{\mathsf{d}}\mathrm{D}^{\mathsf{d}}_{\mathsf{c}} + \mathrm{N}^{\mathsf{d}}\mathrm{N}^{\mathsf{d}}_{\mathsf{c}}\big)\mathrm{N}^{\mathsf{d}}_{\mathsf{n}} \quad \text{and} \quad \Psi^{\mathsf{d}}_2 := \big(\mathrm{N}^{\mathsf{d}}\mathrm{D}^{\mathsf{d}}_{\mathsf{n}} - \mathrm{N}^{\mathsf{d}}_{\mathsf{n}}\mathrm{D}^{\mathsf{d}}\big)\mathrm{D}^{\mathsf{d}}_{\mathsf{c}},$$

from which $\mathbf{\Psi}^{\mathsf{d}}(z;\Delta)$ in (5.4.3) is decomposed by $\mathbf{\Psi}^{\mathsf{d}}(z;\Delta)=\Psi^{\mathsf{d}}_1(z;\Delta)\mathrm{D}^{\mathsf{d}}_{\mathsf{q}}(z;\Delta)+\Psi^{\mathsf{d}}_2(z;\Delta)\mathrm{N}^{\mathsf{d}}_{\mathsf{q}}(z;\Delta)$. By multiplying $\Delta^{\overline{n}}$ to these components, one can obtain that for $\Delta\in\mathbb{R}_{>0}\setminus(\mathcal{T}_{\mathcal{P}}\cup\mathcal{T}_{\mathsf{nc}})$ (where $\mathcal{T}_{\mathcal{P}}:=\bigcup_{\mathrm{P}(s)\in\mathcal{P}}\mathcal{T}_{\mathrm{P}(s)}$ for simplicity),

$$\begin{aligned}
&\Delta^{\overline{n}}\Psi^{\mathsf{d}}_1(z;\Delta)\\
&=(\Delta^{n}\mathrm{D}^{\mathsf{d}})(\Delta^{n_{\mathsf{c}}}\mathrm{D}^{\mathsf{d}}_{\mathsf{c}})(\Delta^{n-\nu}\mathrm{N}^{\mathsf{d}}_{\mathsf{n}})+\Delta^{\nu+\nu_{\mathsf{c}}}(\Delta^{n-\nu}\mathrm{N}^{\mathsf{d}})(\Delta^{n_{\mathsf{c}}-\nu_{\mathsf{c}}}\mathrm{N}^{\mathsf{d}}_{\mathsf{c}})(\Delta^{n-\nu}\mathrm{N}^{\mathsf{d}}_{\mathsf{n}})\\
&=\prod_{i=1}^{n}\big(z-\mathsf{p}^{\mathsf{d}}_i\big)\prod_{i=1}^{n_{\mathsf{c}}}\big(z-\mathsf{p}^{\mathsf{d}}_{\mathsf{c},i}\big)g^{\mathsf{d}}_{\mathsf{n}}\mathrm{M}^{\mathsf{d}}_{\mathsf{n}}\prod_{i=1}^{n-\nu}\big(z-\mathsf{z}^{\mathsf{d}}_{\mathsf{n},i}\big)\\
&\qquad+\Delta^{\nu+\nu_{\mathsf{c}}}g\mathrm{M}^{\mathsf{d}}\prod_{i=1}^{n-\nu}(z-\mathsf{z}^{\mathsf{d}}_i)g^{\mathsf{d}}_{\mathsf{c}}\mathrm{M}^{\mathsf{d}}_{\mathsf{c}}\prod_{i=1}^{n_{\mathsf{c}}-\nu_{\mathsf{c}}}\big(z-\mathsf{z}^{\mathsf{d}}_{\mathsf{c},i}\big)g^{\mathsf{d}}_{\mathsf{n}}\mathrm{M}^{\mathsf{d}}_{\mathsf{n}}\prod_{i=1}^{n-\nu}\big(z-\mathsf{z}^{\mathsf{d}}_{\mathsf{n},i}\big),\\
&\Delta^{\overline{n}}\Psi^{\mathsf{d}}_2(z;\Delta)\\
&=(\Delta^{n-\nu}\mathrm{N}^{\mathsf{d}})(\Delta^{n}\mathrm{D}^{\mathsf{d}}_{\mathsf{n}})(\Delta^{n_{\mathsf{c}}}\mathrm{D}^{\mathsf{d}}_{\mathsf{c}})-(\Delta^{n-\nu}\mathrm{N}^{\mathsf{d}}_{\mathsf{n}})(\Delta^{n}\mathrm{D}^{\mathsf{d}})(\Delta^{n_{\mathsf{c}}}\mathrm{D}^{\mathsf{d}}_{\mathsf{c}})\\
&=g\mathrm{M}^{\mathsf{d}}(z;\Delta)\prod_{i=1}^{n-\nu}(z-\mathsf{z}^{\mathsf{d}}_i)\prod_{i=1}^{n}(z-\mathsf{p}^{\mathsf{d}}_{\mathsf{n},i})\prod_{i=1}^{n_{\mathsf{c}}}(z-\mathsf{p}^{\mathsf{d}}_{\mathsf{c},i})\\
&\qquad-g^{\mathsf{d}}_{\mathsf{n}}\mathrm{M}^{\mathsf{d}}_{\mathsf{n}}\prod_{i=1}^{n-\nu}\big(z-\mathsf{z}^{\mathsf{d}}_{\mathsf{n},i}\big)\prod_{i=1}^{n}\big(z-\mathsf{p}^{\mathsf{d}}_i\big)\prod_{i=1}^{n_{\mathsf{c}}}\big(z-\mathsf{p}^{\mathsf{d}}_{\mathsf{c},i}\big).
\end{aligned}$$

It is noted that as Δ goes to zero, all the complex numbers $\mathsf{z}^{\mathsf{d}}_i(\Delta)$, $\mathsf{p}^{\mathsf{d}}_i(\Delta)$, $\mathsf{z}^{\mathsf{d}}_{\mathsf{n},i}(\Delta)$, $\mathsf{p}^{\mathsf{d}}_{\mathsf{n},i}(\Delta)$, $\mathsf{z}^{\mathsf{d}}_{\mathsf{c},i}(\Delta)$, and $\mathsf{p}^{\mathsf{d}}_{\mathsf{c},i}(\Delta)$ converge to $1+j0$ (by Assumption 5.3.1 and Lemma 5.2.1). Thus one has

$$\begin{aligned}
\lim_{\Delta\to0^+}\Delta^{\overline{n}}\Psi^{\mathsf{d}}_1(z;\Delta)&=g_{\mathsf{n}}\mathrm{M}^{\star}_{\mathsf{n}}(z)(z-1)^{\overline{n}},\\
\lim_{\Delta\to0^+}\Delta^{\overline{n}}\Psi^{\mathsf{d}}_2(z;\Delta)&=\big(g\mathrm{M}^{\star}(z)-g_{\mathsf{n}}\mathrm{M}^{\star}_{\mathsf{n}}(z)\big)(z-1)^{\overline{n}}.
\end{aligned}$$

With these limits, we now have

$$\begin{aligned}
&\lim_{\Delta\to 0^+} \Delta^{\overline{n}}\boldsymbol{\Psi}^{\mathsf{d}}(z;\Delta)\\
&\lim_{\Delta\to 0^+} \Delta^{\overline{n}}\Psi_1^{\mathsf{d}}(z;\Delta)\mathrm{D}_{\mathsf{q}}^{\mathsf{d}}(z;\Delta) + \Delta^{\overline{n}}\Psi_2^{\mathsf{d}}(z;\Delta)\mathrm{N}_{\mathsf{q}}^{\mathsf{d}}(z;\Delta)\\
&= g_{\mathsf{n}}(z-1)^{\overline{n}}\Big(\mathrm{M}_{\mathsf{n}}^{\star}(z)(\mathrm{D}_{\mathsf{q}}^{\star}(z) - \mathrm{N}_{\mathsf{q}}^{\star}(z)) + \frac{g}{g_{\mathsf{n}}}\mathrm{M}^{\star}(z)\mathrm{N}_{\mathsf{q}}^{\star}(z)\Big)\\
&= g_{\mathsf{n}}(z-1)^{\overline{n}}\Psi_{\mathrm{fast}}^{\mathsf{d}}(z) \qquad (5.4.7)
\end{aligned}$$

where the degree of $\Psi_{\mathrm{fast}}^{\mathsf{d}}(z)$ is given by $\deg(\boldsymbol{\Psi}^{\mathsf{d}}) - \overline{n}$. Noting that the roots of $\Delta^{\overline{n}}\boldsymbol{\Psi}^{\mathsf{d}}(z;\Delta) = 0$ are the same as those of $\boldsymbol{\Psi}^{\mathsf{d}}(z;\Delta) = 0$ for any $\Delta > 0$, the proof is concluded from Lemma 5.4.1 with $\mathrm{X}^{\mathsf{d}}(z) = g_{\mathsf{n}}(z-1)^{\overline{n}}\Psi_{\mathrm{fast}}^{\mathsf{d}}(z)$ and $\mathrm{Y}^{\mathsf{d}}(z;\Delta) = \Delta^{\overline{n}}\boldsymbol{\Psi}^{\mathsf{d}}(z;\Delta) - g_{\mathsf{n}}(z-1)^{\overline{n}}\Psi_{\mathrm{fast}}^{\mathsf{d}}(z)$. □

For convenience, we denote the roots of $\boldsymbol{\Psi}^{\mathsf{d}}(z;\Delta) = 0$ as $\mathsf{x}_i^{\mathsf{d}}(\Delta)$, and rearrange them to satisfy $\lim_{\Delta\to 0^+}\mathsf{x}_i^{\mathsf{d}}(\Delta) = 1 + j0$ for all $i = 1,\ldots,\overline{n}$ without loss of generality. From the viewpoint of the DT singular perturbation theory, the first $\overline{n}$ roots are called "slow modes" of the DT-DOB controlled system, while the remaining ones as "fast modes". Notice that Lemma 5.4.3 demonstrates the limiting behavior of the fast modes only, whereas the stability of the slow modes (for the limiting case) is not clear yet. For further discussion, we present the following lemma on the slow modes.

Lemma 5.4.4. Suppose that Assumption 5.3.1 holds. Then for all $i = 1,\ldots,\overline{n}$, $\mathsf{s}_i^{\mathsf{d}}(\Delta) := (\mathsf{x}_i^{\mathsf{d}}(\Delta) - 1)/\Delta$ converges to the roots $s = \mathsf{s}_i^{\star}$ of the polynomial

$$\Psi_{\mathrm{slow}}(s) := \mathrm{N}(s)\big(\mathrm{D}_{\mathsf{n}}(s)\mathrm{D}_{\mathsf{c}}(s) + \mathrm{N}_{\mathsf{n}}(s)\mathrm{N}_{\mathsf{c}}(s)\big) = 0. \qquad (5.4.8)$$

◊

Proof. For the proof, we employ a complex variable

$$s^{\mathsf{d}} := \frac{z-1}{\Delta} \qquad (5.4.9)$$

which associates with the "incremental" operator [YG14]. With this symbol, the

characteristic polynomial $\mathbf{\Psi}^{\mathsf{d}}(z;\Delta)$ of our interest is rewritten in s^{d}-domain as

$$\mathbf{\Psi}^{\mathsf{i}}(s^{\mathsf{d}};\Delta) := \mathbf{\Psi}^{\mathsf{d}}(1+\Delta s^{\mathsf{d}};\Delta). \tag{5.4.10}$$

Then the lemma is proved by showing that as $\Delta \to 0^+$, the roots of $\mathbf{\Psi}^{\mathsf{i}}(s^{\mathsf{d}};\Delta)=0$, given by $\mathsf{s}_i^{\mathsf{d}}(\Delta)$, approach $\mathsf{s}_i^\star$ for $i=1,\dots,\overline{n}$. After some computation, one can readily obtain that

$$\mathbf{\Psi}^{\mathsf{i}} = (\mathrm{D}^{\mathsf{i}}\mathrm{D}_{\mathsf{c}}^{\mathsf{i}} + \mathrm{N}^{\mathsf{i}}\mathrm{N}_{\mathsf{c}}^{\mathsf{i}})\mathrm{N}_{\mathsf{n}}^{\mathsf{i}}\mathrm{D}_{\mathsf{q}}^{\mathsf{i}} + \mathrm{N}_{\mathsf{q}}^{\mathsf{i}}\mathrm{D}_{\mathsf{c}}^{\mathsf{i}}(\mathrm{N}^{\mathsf{i}}\mathrm{D}_{\mathsf{n}}^{\mathsf{i}} - \mathrm{N}_{\mathsf{n}}^{\mathsf{i}}\mathrm{D}^{\mathsf{i}}).$$

where each component is given by

$$\begin{aligned}
\mathrm{N}^{\mathsf{i}}(s^{\mathsf{d}};\Delta) &:= \mathrm{N}^{\mathsf{d}}(1+\Delta s^{\mathsf{d}};\Delta), \quad \mathrm{D}^{\mathsf{i}}(s^{\mathsf{d}};\Delta) := \mathrm{D}^{\mathsf{d}}(1+\Delta s^{\mathsf{d}};\Delta),\\
\mathrm{N}_{\mathsf{n}}^{\mathsf{i}}(s^{\mathsf{d}};\Delta) &:= \mathrm{N}_{\mathsf{n}}^{\mathsf{d}}(1+\Delta s^{\mathsf{d}};\Delta)\\
&= g_{\mathsf{n}}^{\mathsf{d}}(\Delta)\mathrm{M}_{\mathsf{n}}^{\mathsf{d}}(1+\Delta s^{\mathsf{d}};\Delta)\prod_{i=1}^{n-\nu}\left(s^{\mathsf{d}} - \frac{\mathsf{z}_{\mathsf{n},i}^{\mathsf{d}}(\Delta)-1}{\Delta}\right),\\
\mathrm{D}_{\mathsf{n}}^{\mathsf{i}}(s^{\mathsf{d}};\Delta) &:= \mathrm{D}_{\mathsf{n}}^{\mathsf{d}}(1+\Delta s^{\mathsf{d}};\Delta) = \prod_{i=1}^{n}\left(s^{\mathsf{d}} - \frac{\mathsf{p}_{\mathsf{n},i}^{\mathsf{d}}(\Delta)-1}{\Delta}\right),\\
\mathrm{N}_{\mathsf{c}}^{\mathsf{i}}(s^{\mathsf{d}};\Delta) &:= \mathrm{N}_{\mathsf{c}}^{\mathsf{d}}(1+\Delta s^{\mathsf{d}};\Delta)\\
&= g_{\mathsf{c}}^{\mathsf{d}}(\Delta)\mathrm{M}_{\mathsf{c}}^{\mathsf{d}}(1+\Delta s^{\mathsf{d}};\Delta)\prod_{i=1}^{n_{\mathsf{c}}-\nu_{\mathsf{c}}}\left(s^{\mathsf{d}} - \frac{\mathsf{z}_{\mathsf{c},i}^{\mathsf{d}}(\Delta)-1}{\Delta}\right),\\
\mathrm{D}_{\mathsf{c}}^{\mathsf{i}}(s^{\mathsf{d}};\Delta) &:= \mathrm{D}_{\mathsf{c}}^{\mathsf{d}}(1+\Delta s^{\mathsf{d}};\Delta) = \prod_{i=1}^{n_{\mathsf{c}}}\left(s^{\mathsf{d}} - \frac{\mathsf{p}_{\mathsf{c},i}^{\mathsf{d}}(\Delta)-1}{\Delta}\right),\\
\mathrm{N}_{\mathsf{q}}^{\mathsf{i}}(s^{\mathsf{d}};\Delta) &:= \mathrm{N}_{\mathsf{q}}^{\mathsf{d}}(1+\Delta s^{\mathsf{d}};\Delta) = \mathsf{c}_{l_{\mathsf{q}}}^{\mathsf{d}}(\Delta)(\Delta s^{\mathsf{d}})^{l_{\mathsf{q}}} + \cdots + \mathsf{c}_0^{\mathsf{d}}(\Delta),\\
\mathrm{D}_{\mathsf{q}}^{\mathsf{i}}(s^{\mathsf{d}};\Delta) &:= \mathrm{D}_{\mathsf{q}}^{\mathsf{d}}(1+\Delta s^{\mathsf{d}};\Delta) = (\Delta s^{\mathsf{d}})^{n_{\mathsf{q}}} + \mathsf{a}_{n_{\mathsf{q}}-1}^{\mathsf{d}}(\Delta)(\Delta s^{\mathsf{d}})^{n_{\mathsf{q}}-1} + \cdots + \mathsf{a}_0^{\mathsf{d}}(\Delta).
\end{aligned}$$

Under Assumption 5.3.1, it follows that as $\Delta \to 0^+$,

$$\begin{aligned}
\mathrm{N}_{\mathsf{n}}^{\mathsf{i}}(s^{\mathsf{d}};\Delta) &\to \mathrm{N}_{\mathsf{n}}(s^{\mathsf{d}}), \qquad \mathrm{D}_{\mathsf{n}}^{\mathsf{i}}(s^{\mathsf{d}};\Delta) \to \mathrm{D}_{\mathsf{n}}(s^{\mathsf{d}}),\\
\mathrm{N}_{\mathsf{c}}^{\mathsf{i}}(s^{\mathsf{d}};\Delta) &\to \mathrm{N}_{\mathsf{c}}(s^{\mathsf{d}}), \qquad \mathrm{D}_{\mathsf{c}}^{\mathsf{i}}(s^{\mathsf{d}};\Delta) \to \mathrm{D}_{\mathsf{c}}(s^{\mathsf{d}}),
\end{aligned}$$

while $\mathrm{N}_{\mathsf{q}}^{\mathsf{i}}(s^{\mathsf{d}};\Delta) \to \mathsf{c}_0^\star = \mathsf{a}_0^\star$, and $\mathrm{D}_{\mathsf{q}}^{\mathsf{i}}(s^{\mathsf{d}};\Delta) \to \mathsf{a}_0^\star$ by definition. On the other

hand, the DT sampled-data model represented in the incremental form converges to the corresponding CT plant under fast sampling [YG14, Lemma 5.11]: that is, as $\Delta \to 0^+$, $\mathrm{N}^{\mathsf{i}}(s^{\mathsf{d}};\Delta) \to \mathrm{N}(s^{\mathsf{d}})$ and $\mathrm{D}^{\mathsf{i}}(s^{\mathsf{d}};\Delta) \to \mathrm{D}(s^{\mathsf{d}})$. Putting all the limits together, we have

$$\begin{aligned}\lim_{\Delta\to 0^+} \mathbf{\Psi}^{\mathsf{i}}(s^{\mathsf{d}};\Delta) &= (\mathrm{D}\mathrm{D}_{\mathsf{c}} + \mathrm{N}\mathrm{N}_{\mathsf{c}})\mathrm{N}_{\mathsf{n}}\mathsf{a}_0^\star + \mathsf{a}_0^\star \mathrm{D}_{\mathsf{c}}(\mathrm{N}\mathrm{D}_{\mathsf{n}} - \mathrm{N}_{\mathsf{n}}\mathrm{D}) \\ &= \mathsf{a}_0^\star \mathrm{N}(\mathrm{D}\mathrm{D}_{\mathsf{c}} + \mathrm{N}\mathrm{N}_{\mathsf{c}}) = \mathsf{a}_0^\star \Psi_{\mathrm{slow}}(s^{\mathsf{d}}).\end{aligned}$$

The remainder of the proof can be derived in a similar way of Lemma 5.4.3, with the help of Lemma 5.4.1. □

Now, we are ready to present our main result on the robust stability.

Theorem 5.4.5. Suppose that Assumptions 5.3.1 and 5.4.1 hold. Then there exists $\overline{\Delta} > 0$ such that for almost every $\Delta \in (0, \overline{\Delta})$, the DT-DOB controlled system is robustly internally stable if the following conditions hold:

(a) $\mathrm{C}(s)$ internally stabilizes $\mathrm{P}_{\mathsf{n}}(s)$ (that is, $\mathrm{N}_{\mathsf{n}}(s)\mathrm{N}_{\mathsf{c}}(s) + \mathrm{D}_{\mathsf{n}}(s)\mathrm{D}_{\mathsf{c}}(s)$ is Hurwitz);

(b) $\mathrm{P}(s) \in \mathcal{P}$ is of minimum phase;

(c) The polynomial $\Psi^{\mathsf{d}}_{\mathrm{fast}}(z)$ in (5.4.6) is Schur for $\mathrm{P}(s) \in \mathcal{P}$.

Moreover, the converse is also true except marginal cases (i.e., there is $\overline{\Delta}' > 0$ such that for any $\Delta \in (0, \overline{\Delta}')$, the closed-loop system is not robustly internally stable if some roots of $\mathrm{N}_{\mathsf{n}}(s)\mathrm{N}_{\mathsf{c}}(s) + \mathrm{D}_{\mathsf{n}}(s)\mathrm{D}_{\mathsf{c}}(s) = 0$ or some zeros of $\mathrm{P}(s)$ have positive real part, or some roots of $\Psi^{\mathsf{d}}_{\mathrm{fast}}(z)$ are outside the unit circle). ◊

Proof. Without loss of generality, let $\overline{n}_{\mathsf{s}} \geq 0$ be the number of the stable roots $s = \mathsf{s}_i^\star$ of $\Psi_{\mathrm{slow}}(s) = 0$, and rearrange $\mathsf{s}_i^\star$ and the corresponding $\mathsf{s}_i^{\mathsf{d}}(\Delta)$ such that $\mathsf{s}_i^\star$, $i = 1, \ldots, \overline{n}_{\mathsf{s}}$, are in the open left-half plane (in s^{d}-domain), while $\mathsf{s}_i^\star$, $i = \overline{n}_{\mathsf{s}} + 1, \ldots, \overline{n}$, are in the open right-half plane.

From now on, we claim that there exists $\overline{\Delta}_{\mathsf{s}} > 0$ such that for $\Delta \in (0, \overline{\Delta}_{\mathsf{s}})$, $\mathsf{x}_i^{\mathsf{d}}(\Delta) = 1 + \Delta \mathsf{s}_i^{\mathsf{d}}(\Delta)$, $i = 1, \ldots, \overline{n}_{\mathsf{s}}$, are located inside the unit circle (in z-domain). Indeed, since all the $\mathsf{s}_i^\star$ are not on the imaginary axis, one can choose $\epsilon^{\mathsf{d}} > 0$ such

that for $i = 1, \ldots, \overline{n}$, each ball $\mathcal{B}(\mathsf{s}_i^\star, \epsilon^{\mathsf{d}})$ (a) includes no root of $\Psi_{\text{slow}}(s) = 0$ except $s = \mathsf{s}_i^\star$ itself and (b) does not intersect with the imaginary axis (in s-domain). In addition, by the limiting behavior of $\mathsf{s}_i^{\mathsf{d}}(\Delta) = (\mathsf{x}_i^{\mathsf{d}}(\Delta) - 1)/\Delta$ in Lemma 5.4.4, there exists $\overline{\Delta}_{\mathsf{s},1} > 0$ such that for $\Delta \in (0, \overline{\Delta}_{\mathsf{s},1})$, all the $\mathsf{s}_i^{\mathsf{d}}(\Delta)$, $i = 1, \ldots, \overline{n}_{\mathsf{s}}$, remain in $\mathcal{B}(\mathsf{s}_i^\star, \epsilon^{\mathsf{d}})$. We also select sufficiently large numbers $\mathsf{h}_{1,i}$ and $\mathsf{h}_{2,i}$, $i = 1, \ldots, \overline{n}_{\mathsf{s}}$, such that

$$\mathsf{h}_{1,i} > (|\mathrm{Re}(\mathsf{s}_i^\star)| + \epsilon^{\mathsf{d}})^2 + (|\mathrm{Im}(\mathsf{s}_i^\star)| + \epsilon^{\mathsf{d}})^2 > 0 \quad \text{and} \quad \mathsf{h}_{2,i} > -\mathrm{Re}(\mathsf{s}_i^\star) - \epsilon^{\mathsf{d}} > 0.$$

Using these terms, we finally take

$$\overline{\Delta}_{\mathsf{s}} < \min\left\{ \frac{2\mathsf{h}_{2,1}}{\mathsf{h}_{1,1}}, \cdots, \frac{2\mathsf{h}_{2,\overline{n}_{\mathsf{s}}}}{\mathsf{h}_{1,\overline{n}_{\mathsf{s}}}}, \overline{\Delta}_{\mathsf{s},1} \right\}.$$

Then for $\Delta \in (0, \overline{\Delta}_{\mathsf{s}})$ and for $i = 1, \ldots, \overline{n}_{\mathsf{s}}$, one has

$$\begin{aligned}
&\mathrm{Re}(\mathsf{s}_i^{\mathsf{d}}(\Delta)) < \mathrm{Re}(\mathsf{s}_i^\star) + \epsilon^{\mathsf{d}} < -\mathsf{h}_{2,i}, \\
&\mathrm{Re}(\mathsf{s}_i^{\mathsf{d}}(\Delta))^2 + \mathrm{Im}(\mathsf{s}_i^{\mathsf{d}}(\Delta))^2 < (|\mathrm{Re}(\mathsf{s}_i^\star)| + \epsilon^{\mathsf{d}})^2 + (|\mathrm{Im}(\mathsf{s}_i^\star)| + \epsilon^{\mathsf{d}})^2 < \mathsf{h}_{1,i}, \\
&2\mathsf{h}_{2,i} > \Delta \mathsf{h}_{1,i}.
\end{aligned}$$

and therefore, each $1 + \Delta \mathsf{s}_i^{\mathsf{d}}(\Delta)$ satisfies

$$\begin{aligned}
\|\mathsf{x}^{\mathsf{d}}(\Delta)\|^2 = \|1 + \Delta \mathsf{s}_i^{\mathsf{d}}(\Delta)\|^2 &= \big(1 + \Delta \mathrm{Re}(\mathsf{s}_i^{\mathsf{d}}(\Delta))\big)^2 + \big(\Delta \mathrm{Im}(\mathsf{s}_i^{\mathsf{d}}(\Delta))\big)^2 \\
&= 1 + 2\Delta \mathrm{Re}(\mathsf{s}_i^{\mathsf{d}}(\Delta)) + \Delta^2 \mathrm{Re}(\mathsf{s}_i^{\mathsf{d}}(\Delta))^2 + \Delta^2 \mathrm{Im}(\mathsf{s}_i^{\mathsf{d}}(\Delta))^2 \\
&< 1 - 2\Delta \mathsf{h}_{2,i} + \Delta^2 \mathsf{h}_{1,i} = 1 - \Delta(2\mathsf{h}_{2,i} - \Delta \mathsf{h}_{1,i}) < 1.
\end{aligned}$$

This indicates that all $\mathsf{x}_i^{\mathsf{d}}(\Delta)$ is inside the unit circle for all $\Delta \in (0, \overline{\Delta}_{\mathsf{s}})$, which completes the proof of the claim. On the other hand, it is obvious that for $\Delta \in (0, \overline{\Delta}_{\mathsf{s}})$ and $i = \overline{n}_{\mathsf{s}} + 1, \ldots, \overline{n}$, $\mathrm{Re}(1 + \Delta \mathsf{s}_i^{\mathsf{d}}(\Delta)) > 1 + \mathrm{Re}(\mathsf{s}_i^\star) - \epsilon^{\mathsf{d}} > 1$ so that $\mathsf{x}_i^{\mathsf{d}}(\Delta)$ are located outside the unit circle.

We have shown that the $\overline{n}_{\mathsf{s}}$ roots $z = \mathsf{x}_i^{\mathsf{d}}(\Delta) = 1 + \Delta \mathsf{s}_i^{\mathsf{d}}(\Delta)$ of $\mathbf{\Psi}^{\mathsf{d}}(z; \Delta) = 0$ remain inside (or outside, respectively) the unit circle for all $\Delta \in (0, \overline{\Delta}_{\mathsf{s}})$ as the corresponding $\mathsf{s}_i^\star$ lies on the open left half-plane (or open right-half plane, respectively). At last, combining this observation with Lemmas 5.4.1 and 5.4.3,

one can conclude the proof of the theorem. □

Remark 5.4.1. The stability condition described in Theorem 5.4.5 is less conservative than those in previous works in the following two senses. First, while many earlier studies provided sufficient conditions for stability only (based on the small gain theorem), Theorem 5.4.5 presents an almost necessary and sufficient stability condition under fast sampling. Furthermore, due to the generalized DOB structure in Section 5.3, a larger class of DT-DOB design methods can be taken into account by Theorem 5.4.5. ◊

5.4.2 Issue 1: Exact vs. Approximate Discretization of $\mathrm{P_n}(s)$

Similar to the CT-DOB cases, the discretization $\mathrm{P_n^d}(z;\Delta)$ of $\mathrm{P_n}(s)$ will be employed as a nominal model of the actual system $\mathrm{P^d}(z;\Delta)$ in the DT-DOB designs. Noting that mismatch between the actual and nominal models, $\mathrm{P^d}(z;\Delta)$ and $\mathrm{P_n^d}(z;\Delta)$, usually yields model uncertainty to be compensated by the DOB, a possible candidate for $\mathrm{P_n^d}(z;\Delta)$ might be the ZOH equivalent model of $\mathrm{P_n}(s)$; that is,

$$\mathrm{P_n^d}(z;\Delta) = \mathrm{P_{n,ZOH}^d}(z;\Delta) = \mathcal{Z}\left(\frac{1-e^{-\Delta s}}{s}\mathrm{P_n}(s)\right) \tag{5.4.11}$$

(so that $\mathrm{P}(s) = \mathrm{P_n}(s)$ implies $\mathrm{P^d}(z;\Delta) = \mathrm{P_n^d}(z;\Delta)$). However, our stability result shows that this exact discretization of $\mathrm{P_n}(s)$ may not be enabled as long as the CT plant $\mathrm{P}(s)$ has high relative degree (even if there is no uncertainty on the CT plant).

Corollary 5.4.6. Suppose that $\mathrm{P}(s)$ satisfies Assumption 5.4.1 and $\nu \geq 3$, and $\mathrm{P_n^d}(z;\Delta) = \mathrm{P_{n,ZOH}^d}(z;\Delta)$ as in (5.4.11). Then there exists $\overline{\Delta}' > 0$ such that the DT-DOB controlled system is not internally stable for any $\mathrm{P}(s) \in \mathcal{P}$ and for all $\Delta \in (0, \overline{\Delta}')$. ◊

Proof. The corollary directly follows from Theorem 5.4.5 with

$$\Psi_{\mathrm{fast}}^{\mathsf{d}}(z) = \frac{\mathrm{E}_{\nu-1}(z)}{\nu!}\left(\mathrm{D_q^\star}(z) - \mathrm{N_q^\star}(z) + \frac{g}{g_{\mathsf{n}}}\mathrm{N_q^\star}(z)\right)$$

and the fact that $\mathrm{E}_{\nu-1}(z)$ is not Schur for all $\nu \geq 3$ (by Proposition 5.2.2). □

In short, in the DT-DOB design for high-order CT plants with $\nu \geq 3$, the way of discretizing $\mathrm{P}_{\mathsf{n}}(s)$ must be "approximate" (for instance, the discretization methods in Table 5.1). We will come back to this point in Section 5.6 where design guidelines for the DT-DOB are presented.

5.4.3 Issue 2: Importance of Q-filter Design

In the theory of CT-DOB, it has been reported that as long as the CT plant $\mathrm{P}(s)$ is of minimum phase and has no model uncertainty, the CT-DOB controlled system (in Figure 1.2) is inherently stable with "any" stable Q-filter [CYC+03]. Therefore, it might make sense in some ideal cases to select the Q-filter as a typical CT low-pass filter

$$\mathrm{Q}(s;\tau) = \mathrm{Q}_{\mathrm{bin}}(s;\tau) = \frac{\mathsf{a}_{\mathrm{bin},0}}{(\tau s)^{n_{\mathsf{q}}} + \mathsf{a}_{\mathrm{bin},n_{\mathsf{q}}-1}(\tau s)^{n_{\mathsf{q}}-1} + \cdots + \mathsf{a}_{\mathrm{bin},0}}$$

where $l \geq \nu$, the coefficients $\mathsf{a}_{\mathrm{bin},i}$ are binomial (that is, $\mathsf{a}_{\mathrm{bin},i} = \binom{n_{\mathsf{q}}}{i}$, $i = 0,\ldots,n_{\mathsf{q}}$), and $\tau > 0$ is chosen "arbitrarily" to cover a frequency range of disturbances.

When it comes to the DT-DOBs used for the sampled-data systems, however, this is not the case anymore. Such a naive selection of the DT Q-filter can violate the stability of the DT-DOB controlled system, even without any plant uncertainty. To clarify this point, we set a "prototypical" stable low-pass filter

$$\mathrm{Q}^{\mathsf{d}}(z;\Delta) = \mathrm{Q}^{\mathsf{d}}_{\mathrm{bin}}(z) = \frac{1}{z^{n_{\mathsf{q}}}}, \tag{5.4.12}$$

which is an all-pass filter in DT domain, as the DT Q-filter for a while. Then with widely-used discretization methods for $\mathrm{P}_{\mathsf{n}}(s)$, we obtain the following negative results.

Proposition 5.4.7. Suppose that Assumption 5.4.1 holds and $\mathrm{Q}^{\mathsf{d}}(z;\Delta)$ has the form of (5.4.12). Then there exists $\overline{\Delta}' > 0$ such that the DT-DOB controlled system is not internally stable for all $\Delta \in (0, \overline{\Delta}')$ and for all $\mathrm{P}(s) \in \mathcal{P}$, if

(a) $\nu \geq 3$ and $\mathrm{P}_{\mathsf{n}}^{\mathsf{d}}(z;\Delta)$ is obtained by discretizing $\mathrm{P}_{\mathsf{n}}(s)$ via the forward difference method, or

(b) $\nu \geq 2$ and $\mathrm{P}_{\mathsf{n}}^{\mathsf{d}}(z;\Delta)$ is obtained by discretizing $\mathrm{P}_{\mathsf{n}}(s)$ via the bilinear transformation (or the matched pole zero method).

$\Diamond$

Proof. The proposition is proved by showing that $\Psi_{\mathrm{fast}}^{\mathsf{d}}(z)$ in Theorem 5.4.5 is not Schur for all $g/g_{\mathsf{n}} \in (0,\infty)$. We here provide the proof of the second case (i.e., Item (b)) only, while the remaining case can be derived in a similar way. Notice that the degree of $\mathrm{M}_{\mathsf{n}}(z;\Delta) = \mathrm{M}_{\mathsf{n}}^{\star}(z)$ is ν and thus $\mathrm{P}_{\mathsf{n}}^{\mathsf{d}}(z;\Delta)$ under consideration is biproper. From this, the degree n_{q} of the Q-filter can be arbitrarily set as $n_{\mathsf{q}} \geq 1$. The Q-filter and the nominal model in the considered situation result in

$$\begin{aligned}\Psi_{\mathrm{fast}}^{\mathsf{d}}(z) &= \mathrm{M}_{\mathsf{n}}^{\star}(z)(z^{n_{\mathsf{q}}}-1) + \frac{g}{g_{\mathsf{n}}}\mathrm{M}^{\star}(z) \\ &= \frac{1}{2^{\nu}}\Big[(z+1)^{\nu}(z^{n_{\mathsf{q}}}-1) + \mathsf{k}\mathsf{E}_{\nu-1,\nu-1}z^{\nu-1} + \cdots + \mathsf{k}\mathsf{E}_{\nu-1,0}\Big]\end{aligned}$$

where $\mathsf{E}_{\nu-1,i}$ are the coefficients of the Euler-Frobenius polynomial $\mathrm{E}_{\nu-1}(z)$ and $\mathsf{k} := 2^{\nu}(g/g_{\mathsf{n}})(1/\nu!) > 0$. Now, by applying the Jury's stability test [PN07] to the first two and the last two coefficients of the polynomial in the bracket with $\mathsf{E}_{\nu-1,0} = 1$, it follows that $\Psi_{\mathrm{fast}}^{\mathsf{d}}(z)$ above is Schur only if the following two inequalities hold simultaneously:

$$|\mathsf{k}-1| < 1 \text{ and} \tag{5.4.13a}$$

$$|(\mathsf{k}-1)^2 - 1| > \begin{cases} |(\nu-1)(\mathsf{k}-1) - ((1-\nu) + \mathsf{k}\mathsf{E}_{\nu-1,1})| & \text{if } n_{\mathsf{q}} = 1, \\ |\nu(\mathsf{k}-1) - (-\nu + \mathsf{k}\mathsf{E}_{\nu-1,1})| & \text{if } n_{\mathsf{q}} \geq 2. \end{cases} \tag{5.4.13b}$$

Notice that $\mathsf{E}_{\nu-1,1} = 2^{\nu} - \nu - 1$ and $|(\mathsf{k}-1)^2 - 1| = -(\mathsf{k}-1)^2 + 1$ for all k satisfying $|\mathsf{k}-1| < 1$. Therefore, the inequalities in (5.4.13) can be rewritten by

$$0 < \mathsf{k} < 2 \quad \text{and} \quad -\mathsf{k}^2 + 2\mathsf{k} > \begin{cases} 2^{\nu}\mathsf{k} & \text{if } n_{\mathsf{q}} = 1, \\ (2^{\nu}-1)\mathsf{k} & \text{if } n_{\mathsf{q}} \geq 2. \end{cases} \tag{5.4.14}$$

It is straightforward that under the constraint $0 < \mathsf{k} < 2$, the inequality (5.4.14) is violated in both two cases for all $\nu \geq 2$, which completes the proof. □

It is noted that Proposition 5.4.7 provides a theoretical analysis of the phenomenon shown in the motivating example. Obviously, as highlighted by Theorem 5.4.5, the disparity between the stability results of the CT-DOBs and DT-DOBs mainly follows from the "sampling zeros" which is an inherent characteristic of the sampled-data systems.

Remark 5.4.2. Putting the emphasis on the structure of the prototypical Q-filter, the finding in Proposition 5.4.7 also can be interpreted by a "rule-of-thumb" that a high-gain and high-bandwidth control scheme may fail when it is applied to a nonminimum-phase system. Indeed, as in the CT-DOB cases, the DT-DOB structure in Figure also includes a hidden component $1/(1-\mathrm{Q}^{\mathsf{d}}(e^{j\omega\Delta};\Delta))$ implicitly, which has an infinite gain at the low-frequency range. Unfortunately, at least one zero of $\mathrm{P}^{\mathsf{d}}(z;\Delta)$ with $\nu \geq 3$ must lie outside the unit circle with fast sampling (by Proposition 5.2.2). Thus according to the rule-of-thumb, with the all-pass filter $\mathrm{Q}^{\mathsf{d}}_{\mathrm{bin}}(z) = 1/z^{\nu}$ which ensures $\mathrm{Q}^{\mathsf{d}}_{\mathrm{bin}}(e^{j\omega\Delta}) \approx 1$ in a wide frequency range, the high-gain property of the DOB will be problematic for the nonminimum-phase system. ◊

5.4.4 Issue 3: Indirect vs. Direct Designs of Discrete-time Disturbance Observers

The finding in the previous subsection enlightens that a naive discretization of a CT-DOB may destabilize the closed-loop system in the sampled-data setting. A relevant question is: is the indirect design of the DT-DOB (by discretizing a well-designed CT-DOB) "fundamentally" insufficient to guarantee the overall stability for the sampled-data system? To answer the question, we discretize a CT Q-filter

$$\mathrm{Q}(s;\tau) = \frac{\mathsf{c}_{l_{\mathsf{q}}}(\tau s)^{l_{\mathsf{q}}} + \cdots + \mathsf{c}_0}{(\tau s)^{n_{\mathsf{q}}} + \mathsf{a}_{n_{\mathsf{q}}-1}(\tau s)^{n_{\mathsf{q}}-1} + \cdots + \mathsf{a}_0} \tag{5.4.15}$$

by using the forward difference method as follows:

$$\mathrm{Q}^{\mathsf{d}}(z;\Delta) = \mathrm{Q}^{\mathsf{d}}_{\mathrm{ind}}(z;\Delta) = \frac{\mathsf{c}_{l_{\mathsf{q}}}\big(\mathsf{r}(z-1)\big)^{l_{\mathsf{q}}} + \cdots + \mathsf{c}_0}{\big(\mathsf{r}(z-1)\big)^{n_{\mathsf{q}}} + \mathsf{a}_{n_{\mathsf{q}}-1}\big(\mathsf{r}(z-1)\big)^{n_{\mathsf{q}}-1} + \cdots + \mathsf{a}_0} \tag{5.4.16}$$

where $\mathsf{r} := \tau/\Delta$ denotes the ratio between τ and Δ. Then the following proposition points out that the stability condition of the associated DT-DOB (with (5.4.16)) can be "simplified" into that of the CT-DOB (with the original Q-filter (5.4.15)) in [SJ09], as long as the sampling process runs much faster than the CT-DOB.

Proposition 5.4.8. Suppose that Assumption hold and the coefficients a_i and c_i of the CT Q-filter (5.4.15) are selected such that

$$\Psi_{\mathrm{fast,CT}}(s) = \mathrm{D}_{\mathsf{q}}(s;1) - \mathrm{N}_{\mathsf{q}}(s;1) + \frac{g}{g_{\mathsf{n}}}\mathrm{N}_{\mathsf{q}}(s;1) \tag{5.4.17}$$

is Hurwitz. Then there exists $\underline{\mathsf{r}} > 0$ such that for all $\mathsf{r} > \underline{\mathsf{r}}$, the polynomial $\Psi^{\mathsf{d}}_{\mathrm{fast}}(z)$ in (5.4.6) corresponding to the DT Q-filter (5.4.16) is Schur. ♢

Proof. The proposition is derived by applying Lemma 5.4.1 to $\Psi^{\mathsf{d}}_{\mathrm{fast}}(z)$ with T in the lemma set as $1/\mathsf{r}$. □

Proposition 5.4.8 inspires us to design the DT-DOB in an "alternative (or indirect)" way; i.e., discretizing a CT-DOB without handling the stability constraints in Theorem 6.2.2 directly. Nonetheless, direct design methods possibly have several advantages over such an indirect method, such as a relaxation of the bandwidth constraint of the Q-filter. We will discuss more on this topic in the simulation part.

5.5 Performance Analysis of Discrete-time Disturbance Observers in Frequency Domain

In this section, we briefly look at the performance of the DT-DOB-based controller in the frequency domain. In parallel with the analysis for the CT-

DOBs, a particular interest here is to observe that the DT-DOB "recovers the nominal performance" under fast sampling.

To see this, we remind the definition of the "scaled" DT Fourier transform of a DT signal.

Definition 5.5.1. [FG12] For a sequence $\mathtt{x}^{\mathtt{d}}[k]$ and the sampling period $\Delta > 0$, the scaled DT Fourier transform of $\mathtt{x}^{\mathtt{d}}[k]$ is given by

$$\mathcal{F}_\Delta(\mathtt{x}^{\mathtt{d}}[k]) := \Delta \sum_{k=-\infty}^{\infty} \mathtt{x}^{\mathtt{d}}[k] e^{-j\omega\Delta k}. \tag{5.5.1}$$

$\Diamond$

With the scaled DT Fourier transform $\mathrm{u}_\Delta^{\mathtt{d}}(e^{j\omega\Delta}) := \mathcal{F}_\Delta(u^{\mathtt{d}}[k])$ of $u^{\mathtt{d}}[k]$, the Fourier transform $\mathrm{y}(j\omega)$ of the CT plant's output $y(t)$ can be represented by [YG14, FG12]

$$\mathrm{y}(j\omega) = \frac{1}{\Delta}\mathrm{P}(j\omega)\mathrm{H}_0(j\omega;\Delta)\mathrm{u}_\Delta^{\mathtt{d}}(e^{j\omega\Delta}) + \mathrm{P}(j\omega)\mathrm{d}(j\omega) \tag{5.5.2}$$

where $\mathrm{P}(s) = \mathbf{C}(sI - \mathbf{A})^{-1}\mathbf{B}$ and $\mathrm{H}_0(s;\Delta) = (1 - e^{-\Delta s})/s$. In turn, one can write the scaled DT Fourier transform $\mathrm{y}_\Delta^{\mathtt{d}}(e^{j\omega\Delta}) := \mathcal{F}_\Delta(y^{\mathtt{d}}[k])$ of $y^{\mathtt{d}}[k]$ in the "folded" form:

$$\begin{aligned}
\mathrm{y}_\Delta^{\mathtt{d}}(e^{j\omega\Delta}) &= \sum_{k=-\infty}^{\infty} \mathrm{y}\left(j\omega + j\frac{2\pi k}{\Delta}\right) \\
&= \sum_{k=-\infty}^{\infty} \left(\frac{1}{\Delta}\mathrm{P}\Big(j\omega + j\frac{2\pi k}{\Delta}\Big)\mathrm{H}_0\Big(j\omega + j\frac{2\pi k}{\Delta};\Delta\Big)\mathrm{u}_\Delta^{\mathtt{d}}(e^{j\omega\Delta})\right. \\
&\qquad \left. + \mathrm{P}\Big(j\omega + j\frac{2\pi k}{\Delta}\Big)\mathrm{d}\Big(j\omega + j\frac{2\pi k}{\Delta}\Big)\right) \\
&= \mathrm{P}^{\mathtt{d}}(e^{j\omega\Delta};\Delta)\mathrm{u}_\Delta^{\mathtt{d}}(e^{j\omega\Delta}) + \mathrm{d}_{\mathrm{fold}}^{\mathtt{d}}(j\omega;\Delta).
\end{aligned} \tag{5.5.3}$$

where

$$\mathrm{d}_{\mathrm{fold}}^{\mathtt{d}}(j\omega;\Delta) := \sum_{k=-\infty}^{\infty} \mathrm{P}\left(j\omega + j\frac{2\pi k}{\Delta}\right)\mathrm{d}\left(j\omega + j\frac{2\pi k}{\Delta}\right) \tag{5.5.4}$$

represents the influence of the CT disturbance $d(t)$ on the DT output $y^{\mathtt{d}}[k]$ under

the "folding" (or "aliasing") effect. On the other hand, in the DT-DOB-based control structure (Figure 5.2), the (scaled) DT Fourier transform $\mathrm{u}_\Delta^{\mathsf{d}}(e^{j\omega\Delta})$ has the form of

$$\begin{aligned}\mathrm{u}_\Delta^{\mathsf{d}}(e^{j\omega\Delta}) = \Delta\mathrm{u}^{\mathsf{d}}(e^{j\omega\Delta}) &= \Delta\left(\frac{1}{\mathrm{P}_{\mathsf{n}}^{\mathsf{d}}(1-\mathrm{Q}^{\mathsf{d}})}\Big(\mathrm{P}_{\mathsf{n}}^{\mathsf{d}}\mathrm{C}^{\mathsf{d}}\mathrm{r}^{\mathsf{d}} - (\mathrm{Q}^{\mathsf{d}}+\mathrm{P}_{\mathsf{n}}^{\mathsf{d}}\mathrm{C}^{\mathsf{d}})\mathrm{y}^{\mathsf{d}}\Big)\right)\\ &= \frac{1}{\mathrm{P}_{\mathsf{n}}^{\mathsf{d}}(1-\mathrm{Q}^{\mathsf{d}})}\Big(\mathrm{P}_{\mathsf{n}}^{\mathsf{d}}\mathrm{C}^{\mathsf{d}}\mathrm{r}_\Delta^{\mathsf{d}} - (\mathrm{Q}^{\mathsf{d}}+\mathrm{P}_{\mathsf{n}}^{\mathsf{d}}\mathrm{C}^{\mathsf{d}})\mathrm{y}_\Delta^{\mathsf{d}}\Big)\end{aligned} \tag{5.5.5}$$

in which $\mathrm{r}_\Delta^{\mathsf{d}}(e^{j\omega\Delta}) := \mathcal{F}_\Delta(\mathrm{u}^{\mathsf{d}}[k])$. Substituting (5.5.3) into (5.5.5), one has

$$\mathrm{u}_\Delta^{\mathsf{d}}(e^{j\omega\Delta}) = \mathrm{T}_{\mathsf{ur}}^{\mathsf{d}}(e^{j\omega\Delta};\Delta)\mathrm{r}_\Delta^{\mathsf{d}}(e^{j\omega\Delta}) + \mathrm{T}_{\mathsf{ud},\mathrm{fold}}^{\mathsf{d}}(e^{j\omega\Delta};\Delta)\mathrm{d}_{\mathrm{fold}}^{\mathsf{d}}(j\omega;\Delta) \tag{5.5.6}$$

where

$$\mathrm{T}_{\mathsf{ur}}^{\mathsf{d}} := \frac{\mathrm{P}_{\mathsf{n}}^{\mathsf{d}}\mathrm{C}^{\mathsf{d}}}{\mathrm{Q}^{\mathsf{d}}(\mathrm{P}^{\mathsf{d}}-\mathrm{P}_{\mathsf{n}}^{\mathsf{d}}) + \mathrm{P}_{\mathsf{n}}^{\mathsf{d}}(1+\mathrm{P}^{\mathsf{d}}\mathrm{C}^{\mathsf{d}})}, \tag{5.5.7a}$$

$$\mathrm{T}_{\mathsf{ud},\mathrm{fold}}^{\mathsf{d}} := -\frac{\mathrm{Q}^{\mathsf{d}}+\mathrm{P}_{\mathsf{n}}^{\mathsf{d}}\mathrm{C}^{\mathsf{d}}}{\mathrm{Q}^{\mathsf{d}}(\mathrm{P}^{\mathsf{d}}-\mathrm{P}_{\mathsf{n}}^{\mathsf{d}}) + \mathrm{P}_{\mathsf{n}}^{\mathsf{d}}(1+\mathrm{P}^{\mathsf{d}}\mathrm{C}^{\mathsf{d}})}. \tag{5.5.7b}$$

In short, putting the result into each (5.5.2) and (5.5.3), we obtain

- the "at-sample" response

$$\mathrm{y}_\Delta^{\mathsf{d}}(e^{j\omega\Delta}) = \mathrm{T}_{\mathsf{yr}}^{\mathsf{d}}(e^{j\omega\Delta};\Delta)\mathrm{r}_\Delta^{\mathsf{d}}(e^{j\omega\Delta}) + \mathrm{T}_{\mathsf{yd}}^{\mathsf{d}}(e^{j\omega\Delta};\Delta)\mathrm{d}_{\mathrm{fold}}^{\mathsf{d}}(j\omega;\Delta) \tag{5.5.8}$$

  where

$$\mathrm{T}_{\mathsf{yr}}^{\mathsf{d}}(z;\Delta) := \mathrm{P}^{\mathsf{d}}\mathrm{T}_{\mathsf{ur}}^{\mathsf{d}} = \frac{\mathrm{P}^{\mathsf{d}}\mathrm{P}_{\mathsf{n}}^{\mathsf{d}}\mathrm{C}^{\mathsf{d}}}{\mathrm{Q}^{\mathsf{d}}(\mathrm{P}^{\mathsf{d}}-\mathrm{P}_{\mathsf{n}}^{\mathsf{d}}) + \mathrm{P}_{\mathsf{n}}^{\mathsf{d}}(1+\mathrm{P}^{\mathsf{d}}\mathrm{C}^{\mathsf{d}})}, \tag{5.5.9a}$$

$$\begin{aligned}\mathrm{T}_{\mathsf{yd},\mathrm{fold}}^{\mathsf{d}}(z;\Delta) &:= \mathrm{P}^{\mathsf{d}}\mathrm{T}_{\mathsf{ud},\mathrm{fold}}^{\mathsf{d}} + 1\\ &= \frac{\mathrm{P}_{\mathsf{n}}^{\mathsf{d}}(1-\mathrm{Q}^{\mathsf{d}})}{\mathrm{Q}^{\mathsf{d}}(\mathrm{P}^{\mathsf{d}}-\mathrm{P}_{\mathsf{n}}^{\mathsf{d}}) + \mathrm{P}_{\mathsf{n}}^{\mathsf{d}}(1+\mathrm{P}^{\mathsf{d}}\mathrm{C}^{\mathsf{d}})}.\end{aligned} \tag{5.5.9b}$$

- the 'inter-sample" response

$$\begin{aligned}\mathrm{y}^{\mathsf{d}}(j\omega) = &\frac{1}{\Delta}\mathrm{P}(j\omega)\mathrm{H}_0(j\omega;\Delta)\mathrm{T}_{\mathsf{ur}}^{\mathsf{d}}(e^{j\omega\Delta};\Delta)\mathrm{r}_\Delta^{\mathsf{d}}(e^{j\omega\Delta})\\ &+ \frac{1}{\Delta}\mathrm{P}(j\omega)\mathrm{H}_0(j\omega;\Delta)\mathrm{T}_{\mathsf{ud},\mathrm{fold}}^{\mathsf{d}}(e^{j\omega\Delta};\Delta)\mathrm{d}_{\mathrm{fold}}^{\mathsf{d}}(j\omega;\Delta) + \mathrm{P}(j\omega)\mathrm{d}(j\omega).\end{aligned} \tag{5.5.10}$$

For further analysis, we assume for now that the Fourier transforms $\mathrm{d}(j\omega)$ and $\mathrm{r}(j\omega)$ of the CT external inputs $d(t)$ and $r(t)$ are dominant in a low-frequency range $\omega \in [0, \overline{\omega}]$: that is, $\mathrm{d}(j\omega) = 0$ and $\mathrm{r}(j\omega) = 0$ for all $\omega > \overline{\omega}$. Under the hypothesis, it follows that if Δ is taken to satisfy $0 < \Delta < (2\pi)/\overline{\omega}$, then for all $0 \le \omega \le (\pi/\Delta)$ (i.e., the frequency range below the Nyquist frequency),

$$\mathrm{r}^{\mathsf{d}}_{\Delta}(e^{j\omega\Delta}) = \sum_{k=-\infty}^{\infty} \mathrm{r}\left(j\omega + j\frac{2\pi k}{\Delta}\right) = \mathrm{r}(j\omega) \tag{5.5.11a}$$

$$\mathrm{d}^{\mathsf{d}}_{\mathrm{fold}}(j\omega;\Delta) = \sum_{k=-\infty}^{\infty} \mathrm{P}\left(j\omega + j\frac{2\pi k}{\Delta}\right)\mathrm{d}\left(j\omega + j\frac{2\pi k}{\Delta}\right) = \mathrm{P}(j\omega)\mathrm{d}(j\omega). \tag{5.5.11b}$$

In addition, we also suppose that Δ is sufficiently small such that

$$\mathrm{Q}^{\mathsf{d}}(e^{j\omega\Delta};\Delta) \approx 1 \tag{5.5.12}$$

for all $\omega \in [0, \overline{\omega}]$. Then for that low-frequency range, the at-sample response of the output $y(t)$ is approximated by

$$\mathrm{y}^{\mathsf{d}}_{\Delta}(e^{j\omega\Delta}) \approx \frac{\mathrm{P}^{\mathsf{d}}_{\mathsf{n}}\mathrm{C}^{\mathsf{d}}}{1 + \mathrm{P}^{\mathsf{d}}_{\mathsf{n}}\mathrm{C}^{\mathsf{d}}}(e^{j\omega\Delta};\Delta)\mathrm{r}^{\mathsf{d}}_{\Delta}(e^{j\omega\Delta}) \tag{5.5.13}$$

This indicates that under fast sampling, the performance of the nominal closed-loop system is recovered at sampled outputs by the DT-DOB-based controller. Moreover, similar conclusion can be obtained for the "inter-sample" response. To see this, we further assume that in the frequency range $\omega \in [0, \overline{\omega}]$,

$$\mathrm{P}^{\mathsf{d}}_{\mathsf{n}}(e^{j\omega\Delta};\Delta) \approx \mathrm{P}_{\mathsf{n}}(j\omega), \quad \mathrm{C}^{\mathsf{d}}(e^{j\omega\Delta};\Delta) \approx \mathrm{C}(j\omega), \tag{5.5.14a}$$

$$\begin{aligned}\mathrm{P}^{\mathsf{d}}(e^{j\omega\Delta};\Delta) &= \sum_{k=-\infty}^{\infty} \frac{1}{\Delta}\mathrm{P}\Big(j\omega + j\frac{2\pi k}{\Delta}\Big)\mathrm{H}_0\Big(j\omega + j\frac{2\pi k}{\Delta};\Delta\Big) \\ &\approx \frac{1}{\Delta}\mathrm{P}(j\omega)\mathrm{H}_0(j\omega;\Delta) \approx \mathrm{P}(j\omega)\end{aligned} \tag{5.5.14b}$$

(where all the approximations are possibly achieved by taking a small Δ). Then

it is easy to derive from (5.5.10) and (5.5.14) that

$$\mathrm{y}(j\omega) \approx \frac{\mathrm{P_n C}}{1+\mathrm{P_n C}}(j\omega)\mathrm{r}(j\omega) \tag{5.5.15}$$

in the low-frequency range $\omega \in [0, \overline{\omega}]$.

It is also important to note that, as long as the CT disturbance $d(t)$ is fully modeled as sum of biased sinusoidal signals (as in (2.1.7b))

$$d(t) = d_{\mathsf{m}}(t) = M_{\mathsf{dm},0} + \sum_{i=1}^{n_{\mathsf{m}}} M_{\mathsf{dm},i} \sin\big(\sigma_i t + \varphi_{\mathsf{dm},i}\big), \tag{5.5.16}$$

its "perfect" (rather than approximate) rejection in the "at-sample" response would be possible in a sense. Indeed, the Fourier transform $\mathrm{d}(j\omega)$ of the sinusoidal function (5.5.16) has a non-zero value only at $\omega = 0$ or $\omega = \pm\sigma_i$, $i = 1, \ldots, n_{\mathsf{m}}$, and its folded version $\mathrm{d}^{\mathsf{d}}_{\mathrm{fold}}(j\omega;\Delta)$ in (5.5.11) also does below the Nyquist frequency (with sufficiently small $\Delta < \Delta^{\star}_{\mathcal{P}}$). Therefore, if the DT Q-filter $\mathrm{Q}^{\mathsf{d}}(z;\Delta)$ in (5.3.4) is properly designed such that

$$\mathrm{Q}^{\mathsf{d}}(e^{\pm j\sigma_i\Delta};\Delta) = 1 + j0, \quad \forall i = 1, \ldots, n_{\mathsf{m}}, \tag{5.5.17}$$

(while $\mathrm{Q}^{\mathsf{d}}(1;\Delta) = 1 + j0$ naturally holds because $\mathsf{a}_0 = \mathsf{c}_0$), then we obtain that

$$\mathrm{T}^{\mathsf{d}}_{\mathsf{yd}}(e^{j\omega\Delta};\Delta)\mathrm{d}^{\mathsf{d}}_{\mathrm{fold}}(j\omega;\Delta) = 0 \tag{5.5.18}$$

below the Nyquist frequency. In other words, the effect of the modeled disturbance on the at-sample response y^{d} in (5.5.8) is completely eliminated in the frequency domain. We point out that another expression of (5.5.17) is

$$\mathrm{D}^{\mathsf{d}}_{\mathsf{q}}(z;\Delta) - \mathrm{N}^{\mathsf{d}}_{\mathsf{q}}(z;\Delta) = (z-1)\prod_{i=1}^{n_{\mathsf{m}}}\Big(z^2 - 2\cos(\sigma_i\Delta)z + 1\Big)\mathrm{R}^{\mathsf{d}}_{\mathsf{q}}(z;\Delta) \tag{5.5.19}$$

with a polynomial $\mathrm{R}^{\mathsf{d}}_{\mathsf{q}}(z;\Delta)$ of z, which can be regarded as a "DT counterpart" of (2.2.7).

5.6 Direct Design Methods for Discrete-time Disturbance Observers

The stability analysis in Section 5.4 reveals an explicit constraint on the DT-DOB design (i.e., Item (c) of Theorem 5.4.5), and this requirement is not automatically satisfied in general. As aforementioned, this is mainly because $\Psi^{\mathsf{d}}_{\text{fast}}(z)$ to be Schur is influenced by the sampling zeros of $\mathrm{P}^{\mathsf{d}}(z;\Delta)$, the discretization method for $\mathrm{P}_{\mathsf{n}}(s)$, and the uncertain parameter g in a complicated form. Obviously, all these factors should be taken into account carefully in the DT-DOB design.

In this regard, in this section we present systematic design procedures of the DT-DOB, provided that the plant (5.2.3) is uncertain in the sense of Assumption 5.4.1. In particular, our design guidelines are of two types dependent of whether the generating model of $d(t)$ is explicitly used, both of which satisfies Item (c) of Theorem 5.4.5 under the assumption.

To derive the design procedures, the following technical lemmas are required.

Lemma 5.6.1. Let $\mathrm{h}^{\mathsf{d}}(z)$ be a Schur polynomial and let $\mathrm{g}^{\mathsf{d}}(z)$ be a polynomial whose roots have the real part smaller than 1. Then there exists $\overline{\mathsf{k}}_1 > 0$ such that

$$\mathrm{h}^{\mathsf{d}}(z)(z-1) + \mathsf{k}\mathrm{g}^{\mathsf{d}}(z)$$

is Schur for all $\mathsf{k} \in (0, \overline{\mathsf{k}}_1)$. ◊

Lemma 5.6.2. Suppose that the Nyquist plot of a transfer function

$$\mathrm{L}^{\mathsf{d}}(z) = \frac{\mathrm{p}^{\mathsf{d}}(z)}{(z-1)^k \mathrm{q}^{\mathsf{d}}(z)} \tag{5.6.1}$$

does not cut the line $\mathcal{E}(\underline{g}/g_{\mathsf{n}}, \overline{g}/g_{\mathsf{n}})$ where k is a positive integer, $\mathrm{p}^{\mathsf{d}}(z)$ is a polynomial satisfying $\mathrm{p}^{\mathsf{d}}(1) > 0$, and $\mathrm{q}^{\mathsf{d}}(z)$ is a Hurwitz polynomial. Then there exists $\overline{\mathsf{k}}_2 > 0$ such that the Nyquist plot of

$$\frac{\mathrm{p}^{\mathsf{d}}(z)}{(z-1)^k \mathrm{q}^{\mathsf{d}}(z)} + \mathsf{k}\frac{1}{(z-1)^{k+1}\mathrm{q}^{\mathsf{d}}(z)} \tag{5.6.2}$$

does not cut the line $\mathcal{E}(\underline{g}/g_{\mathsf{n}}, \overline{g}/g_{\mathsf{n}})$ for all $\mathsf{k} \in (0, \overline{\mathsf{k}}_2)$. $\Diamond$

The proofs of these lemmas are largely similar to Lemmas A.1.1 and A.1.2 in Appendix A.1, and thus we omit the details.

5.6.1 Design with Simplest Structure of Q-filter

We set the DT Q-filter $\mathrm{Q}^{\mathsf{d}}(z;\Delta)$ as the simplest form of the DT low-pass filter

$$\begin{aligned}\mathrm{Q}^{\mathsf{d}}(z;\Delta) = \mathrm{Q}^{\mathsf{d}}_{\mathrm{simp}}(z) &:= \frac{\mathsf{a}^{\star}_{\mathrm{simp},0}}{(z-1)^{n_{\mathsf{q}}} + \mathsf{a}^{\star}_{\mathrm{simp},n_{\mathsf{q}}-1}(z-1)^{n_{\mathsf{q}}-1} + \cdots + \mathsf{a}^{\star}_{\mathrm{simp},0}} \\ &=: \frac{\mathrm{N}^{\mathsf{d}}_{\mathsf{q},\mathrm{simp}}(z)}{\mathrm{D}^{\mathsf{d}}_{\mathsf{q},\mathrm{simp}}(z)} \end{aligned} \tag{5.6.3}$$

where the constants $\mathsf{a}^{\star}_{\mathrm{simp},i}$, $i = 0, \ldots, n_{\mathsf{q}} - 1$, are design parameters, and $n_{\mathsf{q}} \geq \max\{\nu - n_{\mathsf{mn}}, 1\}$ (so that $\mathrm{P}_{\mathsf{n}}^{-1}(z;\Delta)\mathrm{Q}^{\mathsf{d}}(z;\Delta)$ is implementable). On the other hand, the CT nominal model $\mathrm{P}_{\mathsf{n}}(s)$ is discretized such that the associated limiting polynomial $\mathrm{M}^{\star}_{\mathsf{n}}(z)$ in Assumption 5.3.1 is Schur (e.g., the forward and backward difference methods among the methods listed in Table 5.1).

With the DT Q-filter $\mathrm{Q}^{\mathsf{d}}(z;\Delta) = \mathrm{Q}^{\mathsf{d}}_{\mathrm{simp}}(z)$, $\Psi^{\mathsf{d}}_{\mathrm{fast}}(z)$ in (5.4.6) turns out to be

$$\begin{aligned}\Psi^{\mathsf{d}}_{\mathrm{fast,simp}}(z) := \mathrm{M}^{\star}_{\mathsf{n}}(z)\big((z-1)^{n_{\mathsf{q}}} + \mathsf{a}^{\star}_{\mathrm{simp},n_{\mathsf{q}}-1}(z-1)^{n_{\mathsf{q}}-1} + \cdots + \mathsf{a}^{\star}_{\mathrm{simp},0}\big) \\ + \frac{g}{g_{\mathsf{n}}}\mathrm{M}^{\star}(z)\mathsf{a}^{\star}_{\mathrm{simp},0}.\end{aligned}$$

We now show that for any given bound $[\underline{g}, \overline{g}]$ of g, there exist $\mathsf{a}^{\star}_{\mathrm{simp},i}$, $i = 0, \ldots, n_{\mathsf{q}} - 1$, satisfying that both $\Psi^{\mathsf{d}}_{\mathrm{fast,simp}}(z)$ and $\mathrm{D}^{\mathsf{d}}_{\mathsf{q},\mathrm{simp}}(z)$ above are Schur for all $g \in [\underline{g}, \overline{g}]$ (where the latter polynomial is needed to be Schur because of the stability of $\mathrm{Q}^{\mathsf{d}}(z;\Delta)$). Firstly, take $\mathsf{a}^{\star}_{\mathrm{simp},1}, \ldots, \mathsf{a}^{\star}_{\mathrm{simp},n_{\mathsf{q}}-1}$ to make the polynomial $(z-1)^{n_{\mathsf{q}}-1} + \mathsf{a}^{\star}_{\mathrm{simp},n_{\mathsf{q}}-1}(z-1)^{n_{\mathsf{q}}-2} + \cdots + \mathsf{a}^{\star}_{\mathrm{simp},1}$ is Schur. Then both

$$\mathrm{h}^{\mathsf{d}}_{\mathsf{a}}(z) := \mathrm{M}^{\star}_{\mathsf{n}}(z)\big((z-1)^{n_{\mathsf{q}}-1} + \mathsf{a}^{\star}_{\mathrm{simp},n_{\mathsf{q}}-1}(z-1)^{n_{\mathsf{q}}-2} + \cdots + \mathsf{a}^{\star}_{\mathrm{simp},1}\big) \tag{5.6.4a}$$

$$\mathrm{h}^{\mathsf{d}}_{\mathsf{b}}(z) := (z-1)^{n_{\mathsf{q}}-1} + \mathsf{a}^{\star}_{\mathrm{simp},n_{\mathsf{q}}-1}(z-1)^{n_{\mathsf{q}}-2} + \cdots + \mathsf{a}^{\star}_{\mathrm{simp},1} \tag{5.6.4b}$$

are Schur. On the other hand, it is obtained from Item (c) of Proposition 5.2.2 that all the roots of $\mathrm{M}^{\star}(z) =: \mathrm{g}^{\mathsf{d}}_{\mathsf{a}}(z)$ have the real part smaller than 1. Then by

Lemma 5.6.1, one can choose $\overline{\mathsf{k}}_{\rm simp} > 0$ such that

$$\mathrm{h}_{\mathsf{a}}^{\mathsf{d}}(z)(z-1) + \mathsf{k}\mathrm{g}_{\mathsf{a}}^{\mathsf{d}}(z) \quad \text{and} \quad \mathrm{h}_{\mathsf{b}}^{\mathsf{d}}(z)(z-1) + \mathsf{k} \tag{5.6.5}$$

are Schur for all $\mathsf{k} \in (0, \overline{\mathsf{k}}_{\rm simp})$. Now select $\mathsf{a}^{\star}_{{\rm simp},0} \in \big(0, \min\{1, g_{\mathsf{n}}/\overline{g}\}\overline{\mathsf{k}}_{\rm simp}\big)$, from which $\overline{\mathsf{k}}_{\rm simp} > \mathsf{a}^{\star}_{{\rm simp},0}$ and $\overline{\mathsf{k}}_{\rm simp} > (\overline{g}/g_{\mathsf{n}})\mathsf{a}^{\star}_{{\rm simp},0} \geq (g/g_{\mathsf{n}})\mathsf{a}^{\star}_{{\rm simp},0} > 0$ for all $g \in [\underline{g}, \overline{g}]$. It is concluded that $\Psi^{\mathsf{d}}_{{\rm fast,simp}}(z)$ and $\mathrm{D}^{\mathsf{d}}_{\mathsf{q},{\rm simp}}(z)$ are Schur for all $g \in [\underline{g}, \overline{g}]$.

We summarize the discussions so far as follows:

Procedure 5.6.3. (Design of DT-DOB-based controller with simplest structure of Q-filter)

STEP 0 Select a CT nominal model $\mathrm{P}_{\mathsf{n}}(s)$ and a CT baseline controller $\mathrm{C}(s)$ such that the CT nominal closed-loop system is stable and the nominal tracking performance is satisfactory. Discretize the components to satisfy Assumption 5.3.1 and to make $\mathrm{M}^{\star}_{\mathsf{n}}(z)$ Schur. Choose $\mathsf{a}^{\star}_{{\rm simp},1}, \ldots, \mathsf{a}^{\star}_{{\rm simp},n_{\mathsf{q}}-1}$ such that $\mathrm{h}_{\mathsf{a}}^{\mathsf{d}}(z)$ and $\mathrm{h}_{\mathsf{b}}^{\mathsf{d}}(z)$ in (5.6.4) are Schur.

STEP 1 Take $\overline{\mathsf{k}}_{\rm simp} > 0$ satisfying that the two polynomials in (5.6.5) (with $\mathrm{g}_{\mathsf{a}}^{\mathsf{d}}(z) = \mathrm{M}^{\star}(z)$) are Schur for all $\mathsf{k} \in (0, \overline{\mathsf{k}}_{\rm simp})$ and select $\mathsf{a}^{\star}_{{\rm simp},0} \in \big(0, \min\{1, g_{\mathsf{n}}/\overline{g}\}\overline{\mathsf{k}}_{\rm simp}\big)$.

STEP 2 Construct the DT-DOB-based controller as in Figure 5.2 with the DT nominal model $\mathrm{P}^{\mathsf{d}}_{\mathsf{n}}(z;\Delta)$ and the DT baseline controller $\mathrm{C}^{\mathsf{d}}(z;\Delta)$ obtained in Step 0, and with the Q-filter $\mathrm{Q}^{\mathsf{d}}(z;\Delta) = \mathrm{Q}^{\mathsf{d}}_{\rm simp}(z)$ in (5.6.3) whose coefficients $\mathsf{a}^{\star}_{{\rm simp},i}$ are determined by Steps 0 and 1.

$\Diamond$

Theorem 5.6.4. Suppose that Assumption 5.4.1 holds. Then the DT-DOB controller obtained by Procedure 5.6.3 satisfies Item (c) of Theorem 5.4.5. $\Diamond$

5.6.2 Design to Embed Disturbance Model

As aforementioned, we here are interested in constructing a DT-DOB that satisfies both Item (c) of Theorem 5.4.5 and the equality (5.5.19) at once. For

ease of construction, we take the DT nominal model $\mathrm{P}_{\mathsf{n}}^{\mathsf{d}}(z;\Delta)$ by discretizing $\mathrm{P}_{\mathsf{n}}(s)$ via the backward difference method; that is,

$$\mathrm{P}_{\mathsf{n}}^{\mathsf{d}}(z;\Delta) = \mathrm{P}_{\mathsf{n},\mathrm{bw}}^{\mathsf{d}}(z;\Delta) := \mathrm{P}_{\mathsf{n}}\left(\frac{z-1}{\Delta z}\right). \tag{5.6.6}$$

Since $\mathrm{P}_{\mathsf{n},\mathrm{bw}}^{\mathsf{d}}(z;\Delta)$ is biproper, it is allowed to employ the following DT Q-filter that has the relative degree as 1:

$$\begin{aligned}\mathrm{Q}^{\mathsf{d}}(z;\Delta) = \mathrm{Q}_{\mathrm{im}}^{\mathsf{d}}(z;\Delta) &:= \frac{\mathsf{c}_{\mathrm{im},n_{\mathsf{q}}-1}^{\mathsf{d}}(\Delta)(z-1)^{n_{\mathsf{q}}-1} + \cdots + \mathsf{c}_{\mathrm{im},0}^{\mathsf{d}}(\Delta)}{(z-1)^{n_{\mathsf{q}}} + \mathsf{a}_{\mathrm{im},n_{\mathsf{q}}-1}^{\mathsf{d}}(\Delta)(z-1)^{n_{\mathsf{q}}-1} + \cdots + \mathsf{a}_{\mathrm{im},0}^{\mathsf{d}}(\Delta)} \\ &=: \frac{\mathrm{N}_{\mathsf{q},\mathrm{im}}^{\mathsf{d}}(z;\Delta)}{\mathrm{D}_{\mathsf{q},\mathrm{im}}^{\mathsf{d}}(z;\Delta)}\end{aligned} \tag{5.6.7}$$

where the degree n_{q} is set as $n_{\mathsf{q}} = 2n_{\mathsf{m}} + 1$. Now, with the constants $\mathsf{a}_{\mathrm{im},i}(\Delta) = \mathsf{a}_{\mathrm{im},i}^{\star}$ to be designed shortly, we select the coefficients $\mathsf{c}_{\mathrm{im},i}(\Delta)$ of the numerator of the Q-filter as follows:

$$\mathsf{c}_{\mathrm{im},i}(\Delta) = \mathsf{a}_{\mathrm{im},i}^{\star} - \tilde{\mathsf{c}}_{\mathrm{im},i}(\Delta), \quad \forall i = 0,\ldots,2n_{\mathsf{m}}, \tag{5.6.8}$$

where $\tilde{\mathsf{c}}_{\mathrm{im},i}$ are the coefficients of the polynomial

$$\begin{aligned}&(z-1)^{2n_{\mathsf{m}}+1} + \tilde{\mathsf{c}}_{\mathrm{im},2n_{\mathsf{m}}}(\Delta)(z-1)^{2n_{\mathsf{m}}} + \cdots + \tilde{\mathsf{c}}_{\mathrm{im},0}(\Delta) \\ &= (z-1)\prod_{i=1}^{n_{\mathsf{m}}}\Big(z^2 - 2\cos(\sigma_i\Delta)z + 1\Big) \\ &= (z-1)\prod_{i=1}^{n_{\mathsf{m}}}\Big((z-1)^2 + (2-2\cos(\sigma_i\Delta))(z-1) + (2-2\cos(\sigma_i\Delta))\Big)\end{aligned} \tag{5.6.9}$$

By definition, it follows that the desired equality (5.5.19) is satisfied. Note that all $\tilde{\mathsf{c}}_i(\Delta)$ converge to zero as Δ approaches 0, because the right-hand side of the equality becomes $(z-1)^{2n_{\mathsf{m}}+1}$ when $\Delta = 0$.

The remaining design freedom, lying in the selection of $\mathsf{a}_{\mathrm{im},i}^{\star}$, will be used to

make $\Psi^{\mathsf{d}}_{\rm fast}(z)$ and $\mathrm{D}^{\mathsf{d}}_{\mathsf{q},\rm im}(z;\Delta)$ Schur. Notice that $\Psi^{\mathsf{d}}_{\rm fast}(z)$ is now computed as

$$\Psi^{\mathsf{d}}_{\rm fast,im}(z) = z^{\nu}(z-1)^{n_{\mathsf{q}}} + \frac{g}{g_{\mathsf{n}}}\mathrm{M}^{\star}(z)\left(\mathsf{a}^{\star}_{\rm im,n_{\mathsf{q}}-1}(z-1)^{n_{\mathsf{q}}-1} + \cdots + \mathsf{a}^{\star}_{\rm im,0}\right) \tag{5.6.10}$$

in which $\mathrm{M}^{\star}_{\mathsf{n}}(z) = z^{\nu}$ is used. It is obtained from the bounded phase lemma [BCK95, Lemma 2.1] that $\Psi^{\mathsf{d}}_{\rm fast,im}(z)$ is Schur for all uncertain parameters $g \in [\underline{g}, \overline{g}]$ if and only if

(a) the polynomial is Schur for at least one g among $[\underline{g}, \overline{g}]$, and

(b) for the transfer function

$$\mathrm{L}^{\mathsf{d}}_{\rm im}(z) := \frac{\mathrm{M}^{\star}(z)\left(\mathsf{a}^{\star}_{\rm im,n_{\mathsf{q}}-1}(z-1)^{n_{\mathsf{q}}-1} + \cdots + \mathsf{a}^{\star}_{\rm im,0}\right)}{z^{\nu}(z-1)^{n_{\mathsf{q}}}}, \tag{5.6.11}$$

the Nyquist plot of

$$\mathrm{Z}^{\mathsf{d}}_{\rm im}(z) = \frac{1 + (\overline{g}/g_{\mathsf{n}})\mathrm{L}^{\mathsf{d}}_{\rm im}(z)}{1 + (\underline{g}/g_{\mathsf{n}})\mathrm{L}^{\mathsf{d}}_{\rm im}(z)} \tag{5.6.12}$$

does not cut the negative real axis in the complex plane.

In particular, the latter condition is equivalent to:

(b′) the Nyquist plot of $\mathrm{L}^{\mathsf{d}}_{\rm im}(z)$ does not touch the line $\mathcal{E}(\underline{g}/g_{\mathsf{n}}, \overline{g}/g_{\mathsf{n}})$.

To construct the coefficients in a recursive fashion, we define

$$\mathrm{p}^{\mathsf{d}}_{\rm im,i}(z) := \mathrm{M}^{\star}(z)\big(\mathsf{a}^{\star}_{\rm im,n_{\mathsf{q}}-1}(z-1)^{i-1} + \mathsf{a}^{\star}_{\rm im,n_{\mathsf{q}}-2}(z-1)^{i-2} + \cdots + \mathsf{a}^{\star}_{\rm im,n_{\mathsf{q}}-i}\big)$$

and also

$$\mathrm{h}^{\mathsf{d}}_{\mathsf{a},i}(z) := (z-1)^{i}z^{\nu} + \frac{\underline{g}}{g_{\mathsf{n}}}\mathrm{p}^{\mathsf{d}}_{\rm im,i}(z), \quad \mathrm{L}^{\mathsf{d}}_{\rm im,i}(z) := \frac{\mathrm{p}^{\mathsf{d}}_{\rm im,i}(z)}{(z-1)^{i}z^{\nu}}, \quad \text{and}$$
$$\mathrm{h}^{\mathsf{d}}_{\mathsf{b},i}(z) := (z-1)^{i} + \mathsf{a}^{\star}_{\rm im,n_{\mathsf{q}}-1}(z-1)^{i-1} + \mathsf{a}^{\star}_{\rm im,n_{\mathsf{q}}-2}(z-1)^{i-2} + \cdots + \mathsf{a}^{\star}_{\rm im,n_{\mathsf{q}}-i}$$

for $i = 1, \ldots, n_{\mathsf{q}}$. It is noted that $\mathrm{h}^{\mathsf{d}}_{\mathsf{a},n_{\mathsf{q}}}(z) = \Psi^{\mathsf{d}}_{\rm fast,im}(z)$, $\mathrm{h}^{\mathsf{d}}_{\mathsf{b},n_{\mathsf{q}}}(z) = \mathrm{D}^{\mathsf{d}}_{\mathsf{q},\rm im}(z;\Delta)$, and $\mathrm{L}^{\mathsf{d}}_{\rm im,n_{\mathsf{q}}}(z) = \mathrm{L}^{\mathsf{d}}_{\rm im}(z)$ by definition. We also observe that the following recursive

relations are satisfied:

$$\mathrm{h}^{\mathsf{d}}_{\mathsf{a},i+1}(z) = (z-1)\mathrm{h}^{\mathsf{d}}_{\mathsf{a},i}(z) + \frac{\underline{g}}{g_{\mathsf{n}}}\mathrm{M}^{\star}(z)\mathsf{a}^{\star}_{\mathrm{im},n_{\mathsf{q}}-(i+1)}, \tag{5.6.13a}$$

$$\mathrm{h}^{\mathsf{d}}_{\mathsf{b},i+1}(z) = (z-1)\mathrm{h}^{\mathsf{d}}_{\mathsf{b},i}(z) + \mathsf{a}^{\star}_{\mathrm{im},n_{\mathsf{q}}-(i+1)}, \tag{5.6.13b}$$

$$\mathrm{L}^{\mathsf{d}}_{\mathrm{im},i+1}(z) = \mathrm{L}^{\mathsf{d}}_{\mathrm{im},i}(z) + \mathsf{a}^{\star}_{\mathrm{im},n_{\mathsf{q}}-(i+1)}\frac{1}{(z-1)^{i+1}z^{\nu}} \tag{5.6.13c}$$

(for all $i = 1, \ldots, n_{\mathsf{q}} - 1$). Now, by applying Lemmas 5.6.1 and 5.6.2 recursively up to n_{q} steps, we obtain the following design guideline.

Procedure 5.6.5. (Design of DT-DOB-based controller to embed disturbance model)

STEP 0 Select a CT nominal model $\mathrm{P}_{\mathsf{n}}(s)$ and a CT baseline controller $\mathrm{C}(s)$ such that the CT nominal closed-loop system is stable and the nominal tracking performance is satisfactory. Discretize the components to satisfy Assumption 5.3.1, especially using the backward difference method for $\mathrm{P}_{\mathsf{n}}(s)$ as in (5.6.6). Choose $\mathsf{a}^{\star}_{\mathrm{im},n_{\mathsf{q}}-1}$ sufficiently small such that $\mathrm{h}^{\mathsf{d}}_{\mathsf{a},1}(z)$ and $\mathrm{h}^{\mathsf{d}}_{\mathsf{b},1}(z)$ are Schur and the Nyquist plot of $\mathrm{L}^{\mathsf{d}}_{\mathrm{im},1}(z)$ does not cut the line $\mathcal{E}(\underline{g}/g_{\mathsf{n}}, \overline{g}/g_{\mathsf{n}})$.

STEP j ($j = 1, \ldots, n_{\mathsf{q}} - 1$) Take $\overline{\mathsf{k}}_{1,n_{\mathsf{q}}-(j+1)} > 0$ satisfying that the polynomials $\mathrm{h}^{\mathsf{d}}_{\mathsf{a},j+1}(z)$ and $\mathrm{h}^{\mathsf{d}}_{\mathsf{b},j+1}(z)$ in (5.6.13a) and (5.6.13b) are Schur for all $\mathsf{a}^{\star}_{\mathrm{im},n_{\mathsf{q}}-(j+1)} \in (0, \overline{\mathsf{k}}_{1,n_{\mathsf{q}}-(j+1)})$ (by Lemma 5.6.1). Select $\overline{\mathsf{k}}_{2,n_{\mathsf{q}}-(j+1)} > 0$ satisfying that the Nyquist plot of $\mathrm{L}^{\mathsf{d}}_{\mathrm{im},j+1}(z)$ does not cut the line $\mathcal{E}(\underline{g}/g_{\mathsf{n}}, \overline{g}/g_{\mathsf{n}})$ for all $\mathsf{a}^{\star}_{\mathrm{im},n_{\mathsf{q}}-(j+1)} \in (0, \overline{\mathsf{k}}_{2,n_{\mathsf{q}}-(j+1)})$ (by Lemma 5.6.2). Finally, choose $0 < \mathsf{a}^{\star}_{\mathrm{im},n_{\mathsf{q}}-(j+1)} < \min\{\overline{\mathsf{k}}_{1,n_{\mathsf{q}}-(j+1)}, \overline{\mathsf{k}}_{2,n_{\mathsf{q}}-(j+1)}\}$

STEP n_{q} Construct the DT-DOB-based controller with the DT nominal model $\mathrm{P}^{\mathsf{d}}_{\mathsf{n}}(z;\Delta)$ and the DT baseline controller $\mathrm{C}^{\mathsf{d}}(z;\Delta)$ obtained in Step 0, and with the Q-filter $\mathrm{Q}^{\mathsf{d}}(z;\Delta) = \mathrm{Q}^{\mathsf{d}}_{\mathrm{im}}(z;\Delta)$ in (5.6.7) where the coefficients have the form (5.6.8)

$\Diamond$

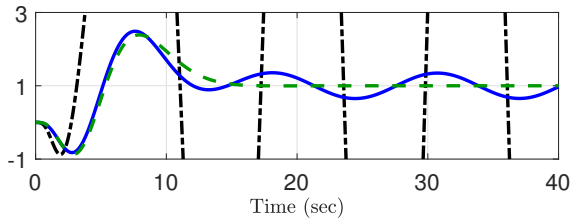

(a) CT outputs y and y_{n}

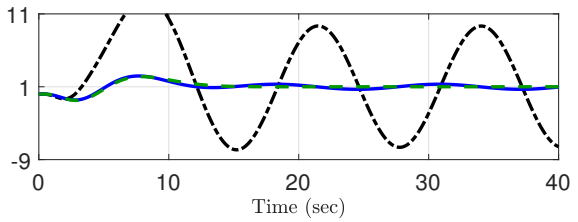

(b) Contraction

Figure 5.5: Simulation results for the proposed DT-DOB with simplest Q-filter (Procedure 5.6.3): Sampled-data systems with baseline controller $\mathrm{C}^{\mathsf{d}}_{\mathrm{fw}}$ only (black dash-dotted) and with the proposed DT-DOB-based controller $\left(\mathrm{P}^{\mathsf{d}}_{\mathsf{n},\mathrm{fw}}, \mathrm{C}^{\mathsf{d}}_{\mathrm{fw}}, \mathrm{Q}^{\mathsf{d}}_{\mathrm{simp,fw}}\right)$ (blue solid), and CT nominal closed-loop system (green dashed)

Theorem 5.6.6. Suppose that Assumption 5.4.1 holds. Then the DT-DOB-based controller obtained by Procedure 5.6.5 satisfies Item (c) of Theorem 5.4.5 and the equality (5.5.19). ◊

5.7 Simulation Results: Two-mass-spring System Revisited

In this section, we revisit the example in Section 5.1 to verify the validity of our stability analysis and design procedures.

For a fair comparison with the simulation results in Section 5.1, we set the DT nominal model $\mathrm{P}^{\mathsf{d}}_{\mathsf{n}}(z;\Delta)$ and $\mathrm{C}^{\mathsf{d}}(z;\Delta)$ as (5.1.6). In addition, by following Procedure 5.6.3, select the DT Q-filter $\mathrm{Q}^{\mathsf{d}}(z;\Delta)$ as

$$\mathrm{Q}^{\mathsf{d}}_{\mathrm{simp,fw}}(z;\Delta) = \frac{0.24}{z^4 - z^3 + 0.24} \tag{5.7.1}$$

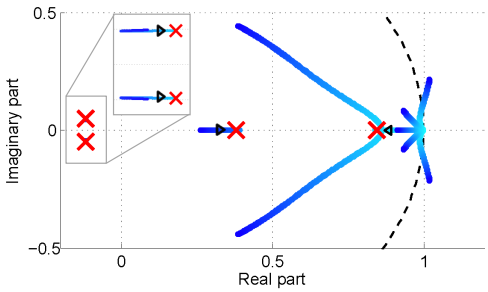

(a) Roots of $\mathbf{\Psi}^{\mathsf{d}}(z;\Delta)=0$ (blue) under variation of Δ and of $\Psi^{\mathsf{d}}_{\text{fast}}(z)=0$ (red) (in z-domain)

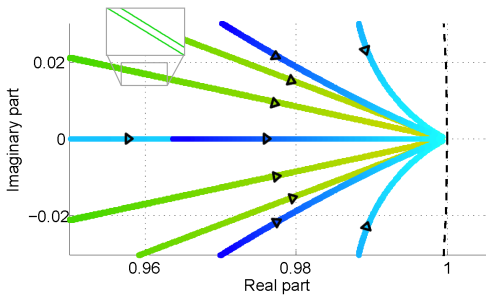

(b) Roots of $\mathbf{\Psi}^{\mathsf{d}}(z;\Delta)=0$ (blue) under variation of Δ and of $\Psi^{\mathsf{d}}_{\text{fast}}(z)=0$ (red) (in z-domain, enlargement)

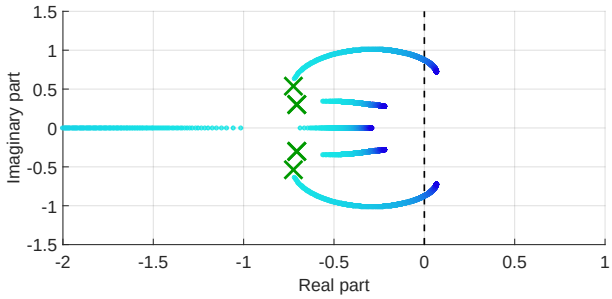

(c) Roots of $\mathbf{\Psi}^{\mathsf{i}}(s^{\mathsf{d}};\Delta)=0$ (blue) under variation of Δ and of $\Psi_{\text{slow}}(s^{\mathsf{d}})=0$ (green) (in s^{d}-domain)

Figure 5.6: Location of roots of $\mathbf{\Psi}^{\mathsf{d}}(z;\Delta)=0$ ((a) and (b)) and roots of $\mathbf{\Psi}^{\mathsf{i}}(s^{\mathsf{d}};\Delta)=0$ ((c)) with $\left(\mathrm{P}^{\mathsf{d}}_{\mathsf{n},\text{fw}},\mathrm{C}^{\mathsf{d}}_{\text{fw}},\mathrm{Q}^{\mathsf{d}}_{\text{simp,fw}}\right)$: the brighter the color is, the smaller Δ is; and black triangles represent direction of roots when Δ gets smaller.

so that $\Psi^{\mathsf{d}}_{\text{fast}}(z)$ is Schur for all uncertain parameters. The simulation results with $\mathsf{K}=2$, and $\mathsf{M}_1=\mathsf{M}_2=1$ are given in Figure 5.5. (For simplicity, for now we often represent a DT-DOB-based controller as the triplet $\left(\mathrm{P}^{\mathsf{d}}_{\mathsf{n}},\mathrm{C}^{\mathsf{d}},\mathrm{Q}^{\mathsf{d}}\right)$, and CT-DOB-based controller similarly as $\left(\mathrm{P}_{\mathsf{n}},\mathrm{C},\mathrm{Q}\right)$.) It is seen in the figure that the baseline controller $\mathrm{C}^{\mathsf{d}}_{\text{fw}}(z;\Delta)$ alone is insufficient to attenuate the disturbance, while the DT-DOB with the proposed Q-filter $\mathrm{Q}^{\mathsf{d}}_{\text{simp,fw}}(z;\Delta)$ recovers the nominal tracking performance in the presence of external disturbance and model uncertainty.

To discuss further on the limiting behavior of the DT-DOB controlled system with $\left(\mathrm{P}^{\mathsf{d}}_{\mathsf{n},\text{fw}},\mathrm{C}^{\mathsf{d}}_{\text{fw}},\mathrm{Q}^{\mathsf{d}}_{\text{simp,fw}}\right)$, we draw the location of the roots of $\mathbf{\Psi}^{\mathsf{d}}(z;\Delta)=0$

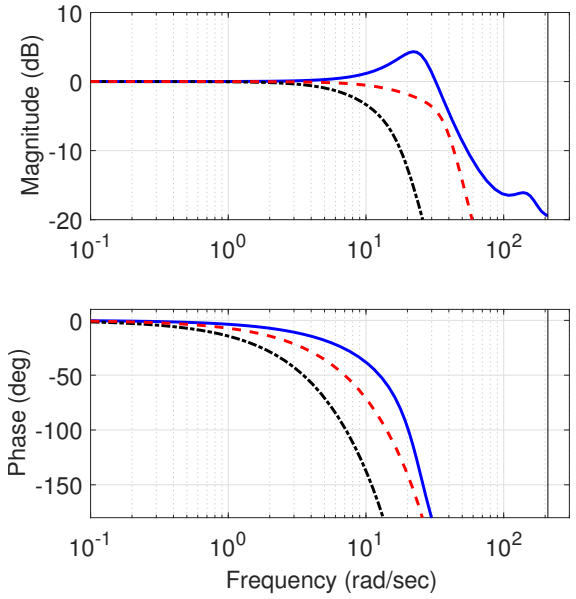

Figure 5.7: Bode plot of DT Q-filters $\mathsf{Q}^{\mathsf{d}}_{\mathrm{simp,fw}}$ (blue solid), $\mathsf{Q}^{\mathsf{d}}_{\mathrm{ind,fast}}$ (red dashed), and $\mathsf{Q}^{\mathsf{d}}_{\mathrm{ind,slow}}$ (black dash-dotted)

under variation of $\Delta \in [0.0001, 0.3]$ in Figure 5.6. As seen in the proof of Theorem 5.4.5, as $\Delta \to 0^+$, 4 roots of $\mathbf{\Psi}^{\mathsf{d}}(z;\Delta) = 0$ approach those of $\Psi^{\mathsf{d}}_{\mathrm{fast}}(z;\Delta) = 0$ (Figure 5.6-(a)), while the other 6 roots converge to the point $(1, 0)$ remaining inside the unit circle. Especially, each of the latter roots approaches $1+\Delta \mathsf{s}^{\star}_i$ where $s = \mathsf{s}^{\star}_i$ are the roots of $\Psi_{\mathrm{slow}}(s) = 0$ (Figure 5.6-(b)), which is seen more clearly in s^{d}-domain (Figure 5.6-(c)).

In what follows, we set $\mathsf{M}_1 = 0.8$, $\mathsf{M}_2 = 0.8$, and $\mathsf{K} = 2$ for the simulation purpose. We now draw a comparison between the direct and indirect DOB designs, studied in Subsection 5.4.4. For this purpose, consider a CT Q-filter

$$\mathrm{Q}_{\mathrm{ind}}(s;\tau) = \frac{\mathsf{a}_0}{(\tau s)^4 + \mathsf{a}_3(\tau s)^3 + \mathsf{a}_2(\tau s)^2 + \mathsf{a}_1(\tau s) + \mathsf{a}_0} \tag{5.7.2}$$

with a_i set as $[\mathsf{a}_3, \mathsf{a}_2, \mathsf{a}_1, \mathsf{a}_0] = [2, 2, 1, 0.3]$. From the selection, $\Psi_{\mathrm{fast,CT}}(s)$ in (5.4.17) is Hurwitz for all $\mathsf{M}_i \in [0.8, 1.2]$ and $\mathsf{K} \in [0.5, 2]$; this implies that the CT-DOB controlled system in Figure 1.2 is robustly stable with sufficiently small $\tau > 0$ [SJ09]. By discretizing the CT Q-filters (5.7.2) with $\tau = 0.05$ and $\tau = 0.025$

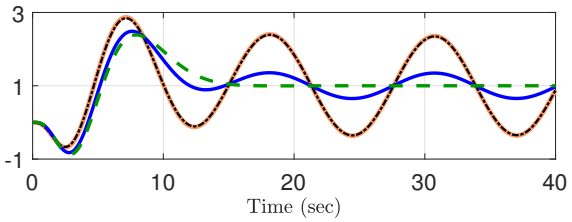

(a) Output $y(t)$ of CT-DOB controlled system with $\left(\mathrm{P_n}, \mathrm{C}, \mathrm{Q_{ind}}(s; 0.05)\right)$ (orange) and DT-DOB controlled system with $\left(\mathrm{P}^{\mathsf{d}}_{\mathrm{n,fw}}, \mathrm{C}^{\mathsf{d}}_{\mathrm{fw}}, \mathrm{Q}^{\mathsf{d}}_{\mathrm{ind,slow}}\right)$ (black) and with $\left(\mathrm{P}^{\mathsf{d}}_{\mathrm{n,fw}}, \mathrm{C}^{\mathsf{d}}_{\mathrm{fw}}, \mathrm{Q}^{\mathsf{d}}_{\mathrm{simp,fw}}\right)$ (blue)

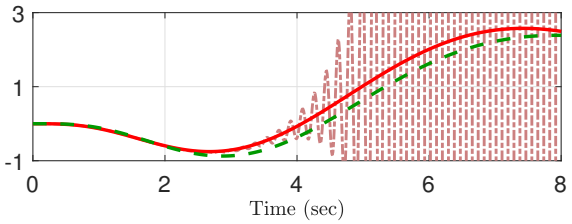

(b) Output $y(t)$ of CT-DOB controlled system with $\left(\mathrm{P_n}, \mathrm{C}, \mathrm{Q_{ind}}(s; 0.025)\right)$ (red) and DT-DOB controlled system with $\left(\mathrm{P}^{\mathsf{d}}_{\mathrm{n,fw}}, \mathrm{C}^{\mathsf{d}}_{\mathrm{fw}}, \mathrm{Q}^{\mathsf{d}}_{\mathrm{ind,fast}}\right)$ (bright red)

Figure 5.8: Simulation results for direct and indirect DT-DOB designs: CT-DOB controlled systems (Figure 1.2, dash-dotted), DT-DOB controlled systems (Figure 5.2, solid), and CT nominal closed-loop system (green dashed)

via the forward difference method, we obtain the following two DT Q-filters (in an indirect way)

$$\mathrm{Q}^{\mathsf{d}}_{\mathrm{ind,fast}}(z; \Delta) = \mathrm{Q_{ind}}\left(\frac{z-1}{\Delta}; 0.025\right), \quad \mathrm{Q}^{\mathsf{d}}_{\mathrm{ind,slow}}(z; \Delta) = \mathrm{Q_{ind}}\left(\frac{z-1}{\Delta}; 0.05\right).$$

We remind that the smaller τ is, the larger the bandwidth of $\mathrm{Q_{ind}}(s; \tau)$ (and thus that of its discretization) is (Figure 5.7). Figure 5.8 shows the simulation results in time domain with the DT Q-filters $\mathrm{Q}^{\mathsf{d}}_{\mathrm{simp,fw}}$, $\mathrm{Q}^{\mathsf{d}}_{\mathrm{ind,fast}}$, and $\mathrm{Q}^{\mathsf{d}}_{\mathrm{ind,slow}}$ (where the latter two ones are obtained by the indirected design method). In the figure, one can observe that too large bandwidth of the CT-DOB (even though it is stable in the CT domain). One can obtain the same conclusion by the frequency domain analysis with Figure 5.9.

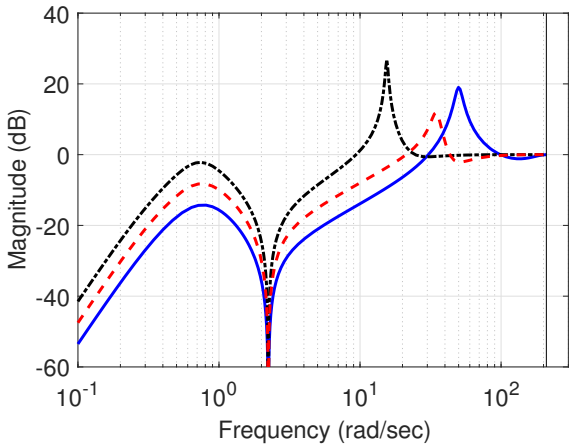

Figure 5.9: Sensitivity functions of DT-DOB controlled systems with DT Q-filters $\mathrm{Q}^{\mathsf{d}}_{\mathrm{simp,fw}}$ (blue solid), $\mathrm{Q}^{\mathsf{d}}_{\mathrm{ind,fast}}$ (red dashed), and $\mathrm{Q}^{\mathsf{d}}_{\mathrm{ind,slow}}$ (black dash-dotted)

The following two simulations are made to show the relation between stability and the discretization methods of $\mathrm{P}^{\mathsf{d}}_{\mathsf{n}}$ and C^{d}. In particular, for the former we introduce additional two DT nominal models

$$\mathrm{P}^{\mathsf{d}}_{\mathsf{n},\mathrm{bw}}(z;\Delta) = \mathrm{P}_{\mathsf{n}}\left(\frac{z-1}{z\Delta}\right), \qquad \mathrm{P}^{\mathsf{d}}_{\mathsf{n},\mathrm{bt}}(z;\Delta) = \mathrm{P}_{\mathsf{n}}\left(\frac{2}{\Delta}\frac{z-1}{z+1}\right)$$

(each of which is the consequence of the backward difference method and the bilinear transformation). After that, by applying Procedure 5.6.3 again to $\mathrm{P}^{\mathsf{d}}_{\mathsf{n},\mathrm{bw}}(z;\Delta)$, one can obtain a (first-order) DT Q-filter

$$\mathrm{Q}^{\mathsf{d}}_{\mathrm{simp,bw}}(z;\Delta) = \frac{0.15}{(z-1)+0.15}$$

(so that the DT-DOB with $\mathrm{P}^{\mathsf{d}}_{\mathsf{n},\mathrm{bw}}(z;\Delta)$ and $\mathrm{Q}^{\mathsf{d}}_{\mathrm{simp,bw}}(z;\Delta)$ satisfies Item (c) of Theorem 5.4.5). We point out that unlike the backward difference method case, $\mathrm{P}^{\mathsf{d}}_{\mathsf{n},\mathrm{bt}}(z;\Delta)$ cannot allow "any" first-order DT Q-filter to make $\Psi^{\mathsf{d}}_{\mathrm{fast}}(z)$ Schur (even if there is no uncertainty on the CT plant). The simulation results for the DT-DOB-based controllers with different $\mathrm{P}^{\mathsf{d}}_{\mathsf{n}}(z;\Delta)$ are provided in Figure 5.10. By comparing the results of $\left(\mathrm{P}^{\mathsf{d}}_{\mathsf{n},\mathrm{bw}}, \mathrm{C}^{\mathsf{d}}_{\mathrm{bw}}, \mathrm{Q}^{\mathsf{d}}_{\mathrm{bw}}\right)$ and $\left(\mathrm{P}^{\mathsf{d}}_{\mathsf{n},\mathrm{bt}}, \mathrm{C}^{\mathsf{d}}_{\mathrm{bt}}, \mathrm{Q}^{\mathsf{d}}_{\mathrm{bw}}\right)$, it can be concluded that the way of discretizing the nominal model $\mathrm{P}_{\mathsf{n}}(s)$ is also important

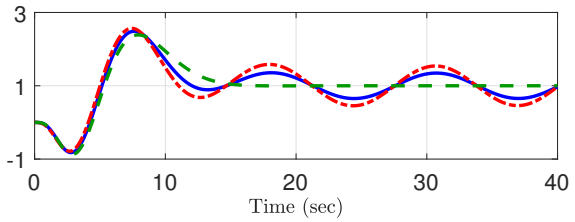

(a) Output $y(t)$

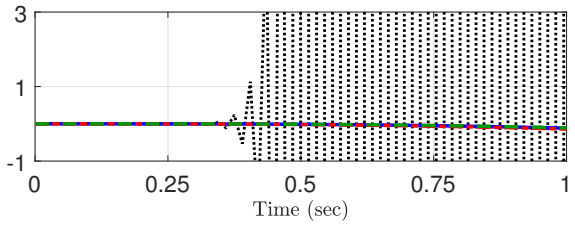

(b) Enlargement

Figure 5.10: Simulation results with different discretization methods for P_n: DT-DOB controlled systems with $\left(\mathsf{P}^\mathsf{d}_{\mathsf{n},\mathrm{fw}}, \mathsf{C}^\mathsf{d}_{\mathrm{fw}}, \mathsf{Q}^\mathsf{d}_{\mathrm{fw}}\right)$ (blue solid), $\left(\mathsf{P}^\mathsf{d}_{\mathsf{n},\mathrm{bw}}, \mathsf{C}^\mathsf{d}_{\mathrm{bw}}, \mathsf{Q}^\mathsf{d}_{\mathrm{bw}}\right)$ (red dash-dotted), and $\left(\mathsf{P}^\mathsf{d}_{\mathsf{n},\mathrm{bt}}, \mathsf{C}^\mathsf{d}_{\mathrm{bt}}, \mathsf{Q}^\mathsf{d}_{\mathrm{bw}}\right)$ (black dotted), and CT nominal closed-loop system (green dashed)

for the robust stabilization. However, this is not the case for the DT baseline controller C^d, as seen in Figure 5.11 where the three discretization results $\mathsf{C}^\mathsf{d}_{\mathrm{fw}}$,

$$\mathsf{C}^\mathsf{d}_{\mathrm{bw}}(z;\Delta) := \mathsf{C}\left(\frac{z-1}{z\Delta}\right), \qquad \mathsf{C}^\mathsf{d}_{\mathrm{bt}}(z;\Delta) := \mathsf{C}\left(\frac{2}{\Delta}\frac{z-1}{z+1}\right)$$

are dealt with.

Now assume that the frequency $\sigma = 0.5$ of the CT sinusoidal disturbance is available in the DT-DOB design. Then by following Procedure 5.6.5 we can construct another type of DT-DOB-based controller, as $\left(\mathsf{P}^\mathsf{d}_{\mathsf{n},\mathrm{bw}}, \mathsf{C}^\mathsf{d}_{\mathrm{bw}}, \mathsf{Q}^\mathsf{d}_{\mathrm{im}}\right)$ with the 3rd-order Q-filter

$$\mathsf{Q}^\mathsf{d}_{\mathrm{im}}(z;\Delta) \tag{5.7.3}$$
$$= \frac{\left(\mathsf{a}^\star_{\mathrm{im},2} - 2(1-\cos(\sigma\Delta))\right)(z-1)^2 + \left(\mathsf{a}^\star_{\mathrm{im},1} - 2(1-\cos(\sigma\Delta))\right)(z-1) + \mathsf{a}^\star_{\mathrm{im},0}}{(z-1)^3 + \mathsf{a}^\star_{\mathrm{im},2}(z-1)^2 + \mathsf{a}^\star_{\mathrm{im},1}(z-1) + \mathsf{a}^\star_{\mathrm{im},0}}$$

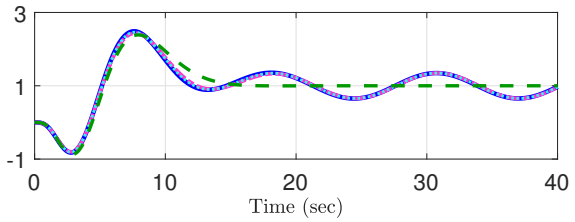

Figure 5.11: Simulation results with various discretized baseline controller C^{d}: DT-DOB controlled systems with $\left(\mathsf{P}^{\mathsf{d}}_{\mathsf{n},\mathrm{fw}}, \mathsf{C}^{\mathsf{d}}_{\mathrm{fw}}, \mathsf{Q}^{\mathsf{d}}_{\mathrm{fw}}\right)$ (blue solid), $\left(\mathsf{P}^{\mathsf{d}}_{\mathsf{n},\mathrm{fw}}, \mathsf{C}^{\mathsf{d}}_{\mathrm{bw}}, \mathsf{Q}^{\mathsf{d}}_{\mathrm{fw}}\right)$ (pink dashed), and $\left(\mathsf{P}^{\mathsf{d}}_{\mathsf{n},\mathrm{fw}}, \mathsf{C}^{\mathsf{d}}_{\mathrm{bt}}, \mathsf{Q}^{\mathsf{d}}_{\mathrm{fw}}\right)$ (ivory dotted), and CT nominal closed-loop system (green dashed)

and the coefficients $[\mathsf{a}^{\star}_{\mathrm{im},2}; \mathsf{a}^{\star}_{\mathrm{im},1}; \mathsf{a}^{\star}_{\mathrm{im},0}] = [0.12; 0.01; 0.0002]$. It is remarked that with the coefficients of $\mathrm{Q}^{\mathsf{d}}_{\mathrm{im}}(z;\Delta)$ above, the Nyquist plots of the transfer functions $\mathrm{L}^{\mathsf{d}}_{\mathrm{im},i}(z)$, $i = 1, 2$, do not cut the line $\mathcal{E}(\underline{g}/g_{\mathsf{n}}, \overline{g}/g_{\mathsf{n}})$ (as desired in Procedure 5.6.5). We perform the time-domain simulation with the DT-DOB-based controller as in Figure 5.12, which shows that the DT-DOB derived by Procedure 5.6.5 completely eliminates the sinusoidal disturbance in the steady state period.

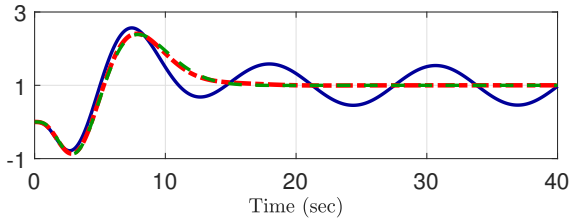

(a) Output $y(t)$

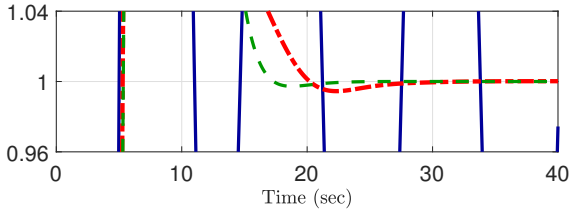

(b) Enlargement

Figure 5.12: Simulation results for the proposed DT-DOB with simplest Q-filter (Procedure 5.6.5): DT-DOB controlled systems with $\left(\mathsf{P}^{\mathsf{d}}_{\mathsf{n,bw}}, \mathsf{C}^{\mathsf{d}}_{\mathsf{bw}}, \mathsf{Q}^{\mathsf{d}}_{\mathsf{im}}\right)$ (red dash-dotted) and with $\left(\mathsf{P}^{\mathsf{d}}_{\mathsf{n,bw}}, \mathsf{C}^{\mathsf{d}}_{\mathsf{bw}}, \mathsf{Q}^{\mathsf{d}}_{\mathsf{bw}}\right)$ (dark blue solid), and CT nominal closed-loop system (green dashed)

Chapter 6

Robust Zero-dynamics Attack on Uncertain Cyber-physical Systems: Malicious Use of Disturbance Observer

Modern control systems often have complex structures integrating physical plants and digital devices, which are linked through communication networks. These CPS offer great opportunities to achieve high cost efficiency and productivity over traditional control systems [Lee08, LBK15]. Yet at the same time, CPS are vulnerable to malicious attackers, as nowadays the data networks are easier to access by anonymous users. Serious cyber threats to CPS already have taken place in recent years, such as the attacks on the U.S. electric grid [Gor09] and the Stuxnet malware [Rid12]. In this context, it is not surprising that security of the CPS has attracted widespread attention with emerging resilient control and secure estimation schemes [FTD14, TSSJ15b, PDB13, TSSJ15a, SNP+17, LSE15]. (See Figure 6.1 where an overall configuration of the cyber-physical system is shown.)

With the increased interest, a variety of cyber attack scenarios have been studied from a "control-theoretic" perspective; e.g., denial-of-service (DoS) attack, replay attack [MS09], zero-dynamics attack [PDB13, TSSJ15b, TSSJ12], bias injection attack [TSSJ15b], optimal linear attack [GSJS17], switching location attack [LWLW17], multi-rate sampling attack [KPSE16], to name just a few. Among various purposes of these attacks, "stealthiness" is of utter importance to most adversaries: i.e., when an attack signal enters CPS, its impact should not be detected by any anomaly detector. In view of the adversary, one approach

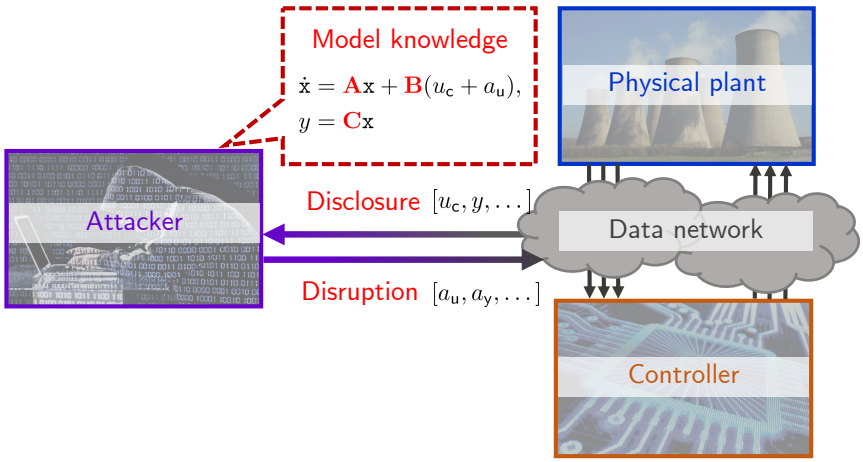

Figure 6.1: Overall configuration of cyber-physical system with malicious attacker

for achieving stealthiness is to employ structural information of the plant in the attack design. For instance, zero-dynamics attack is known as a model-based attack strategy that remains stealthy [PDB13, TSSJ15b, TSSJ12]. In this attack scenario, the adversary duplicates exactly the real unstable zero-dynamics of non-minimum phase plants. As a result, the attack signal conceals itself in the so-called output-nulling space, even if a large amount of false data are injected into the plant [TSSJ15b, TSSJ12].

Model-based attacks may easily lose their stealthiness when the model knowledge is not perfect. Indeed, even small mismatch between the real and estimated models leaves the zero-dynamics attack detectable [TSSJ12]. This fundamental limitation of model-based attacks has led to recent developments of attack prevention strategies, such as structural modification schemes [TSSJ12, HZ16]. Furthermore, exact model knowledge is not obtainable in many industrial problems, which is another hurdle to the attacker. If so, are CPS be safe from these lethal stealthy attacks thanks to model uncertainty?

Interestingly, we will show in this chapter that it may not be the case when the attacker employs the DOB technique in their attack designs. Specifically, we address the problem of constructing a "robust zero-dynamics attack" that is

stealthy for "uncertain" non-minimum phase plants. Moving away from the traditional methods to construct the stealthy attack, our key idea is (a) to eliminate the effect of model uncertainty and the real zero-dynamics from the input-output relation in the plant's dynamics, and (b) to build up an "auxiliary" nominal zero-dynamics which replaces the role of the real counterpart. Then the actual zero-dynamics is left alone while being unstable, and thus its state trajectory will diverge without being detected in a sense. Actually, all these features can be achieved by applying a high gain-based DOB to non-minimum phase systems, which allows the adversary to use the DOB as an attack generator maliciously.

Since the proposed attack policy is oriented from a feedback control scheme, it is of necessity to utilize the control input and the plant's output information in the attack design. This is in fact the price to pay for robustness on the model uncertainty. In other words, in view of the "cyber-physical attack space" in Figure 6.2, the proposed robust zero-dynamics attack requires more "disclosure resources" [TSSJ15a][1]. It is also worth mentioning that the robust zero-dynamics attack is at entirely new location in the cyber-physical attack space.

6.1 Normal Form-based Interpretation of Zero-dynamics Attack

Zero-dynamics attack is a systematic methodology to compromise a class of CPS whose physical plants are of non-minimum phase [FTD14, TSSJ12, TSSJ15b]. The basic concept of the attack is that the attack generator produces a signal based on the unstable zero-dynamics of the physical plant and injects its diverging output into the actuator channel. This consequently leads to two important

[1] Consider a linear system under actuator and sensor attacks, a_{u} and a_{y},

$$\dot{\mathbf{x}} = \mathbf{A}\mathbf{x} + \mathbf{B}(u_{\mathsf{c}} + a_{\mathsf{u}}), \quad y = \mathbf{C}\mathbf{x} + a_{\mathsf{y}}.$$

Then the resources used in the attack design can be classified into the following three items:

- *model knowledge* indicates the knowledge on the triplet $(\mathbf{A}, \mathbf{B}, \mathbf{C})$ of the plant.
- *disclosure resource* means the availability of the signals $\mathbf{x}(t)$, $u_{\mathsf{c}}(t)$, and $y(t)$.
- *disruption resource* stands for the ability to inject the attack signals $a_{\mathsf{u}}(t)$ and $a_{\mathsf{y}}(t)$.

A more detailed explanation on the classification can be found in [TSSJ15a].

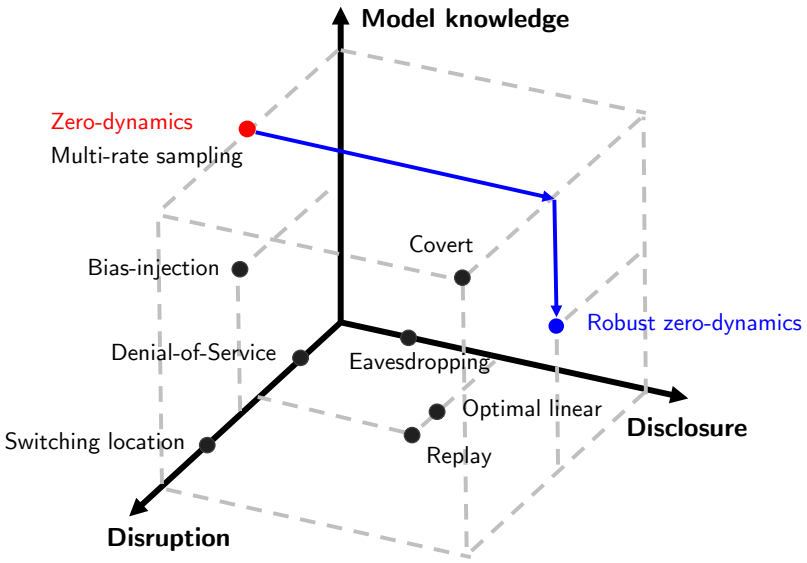

Figure 6.2: Cyber-physical attack space [TSSJ15a] with model knowledge, disruption, and disclosure resources: The robust zero-dynamics attack is at entirely new location.

features: (a) the actual (zero-dynamics) state diverges as time elapses, and (b) the plant's state remains close to the output-nulling space so that the corresponding output is almost zero. By the latter property, the zero-dynamics attack has been known as a "stealthy attack".

In this section, we re-interpret the conventional zero-dynamics attack first. In particular, while the geometric control theory [TSSJ15b] usually has been employed as a tool for the analysis in the literature, we here present another way to analyze the attack, based on the Byrnes-Isidori normal form [Kha96, Chapter 13]. This new approach will allow us to gain further insight on the attack, especially on its fundamental limitation against model uncertainty.

6.1.1 System Description

Consider a linear SISO plant under an actuator attack, denoted by $a(t)$, especially represented in the Byrnes-Isidori normal form

$$\dot{z} = Sz + Gy, \tag{6.1.1a}$$

$$\dot{x} = A_\nu x + B_\nu\big(\psi^\top z + \phi^\top x + g(u_{\mathsf{c}} + a)\big), \qquad y = C_\nu x \tag{6.1.1b}$$

where $z \in \mathbb{R}^l$ and $x \in \mathbb{R}^{n-l}$ are the states with the relative degree $\nu := n - l \geq 1$, $y \in \mathbb{R}$ is the output, $u \in \mathbb{R}$ is the control input, and $a \in \mathbb{R}$ is the attack signal that enters the actuator channel. For an integer $i \geq 1$, the matrices A_i, B_i, and C_i are given by

$$A_i := \begin{bmatrix} 0_{i-1} & I_{i-1} \\ 0 & 0_{i-1}^\top \end{bmatrix}, \quad B_i := \begin{bmatrix} 0_{i-1} \\ 1 \end{bmatrix}, \quad C_i := \begin{bmatrix} 1 & 0_{i-1}^\top \end{bmatrix}.$$

The matrices S, G, ψ and ϕ, and the scalar g are with suitable dimensions. Without loss of generality, it is supposed that (6.1.1) is controllable and observable, and the high-frequency gain g is positive.

For now, it is assumed that at least one of the eigenvalues of S lies in the open right half-plane (so that the plant (6.1.1) is of non-minimum phase). Then without loss of generality, the z-dynamics (6.1.1a) can be rewritten (by applying a suitable coordinate change for z) as

$$\begin{bmatrix} \dot{z}_{\mathsf{u}} \\ \dot{z}_{\mathsf{s}} \end{bmatrix} = \begin{bmatrix} S_{\mathsf{u}} & 0 \\ 0 & S_{\mathsf{s}} \end{bmatrix} \begin{bmatrix} z_{\mathsf{u}} \\ z_{\mathsf{s}} \end{bmatrix} + \begin{bmatrix} G_{\mathsf{u}} \\ G_{\mathsf{s}} \end{bmatrix} y \tag{6.1.2}$$

where $S_{\mathsf{u}} \in \mathbb{R}^{l_{\mathsf{u}} \times l_{\mathsf{u}}}$ and $S_{\mathsf{s}} \in \mathbb{R}^{l_{\mathsf{s}} \times l_{\mathsf{s}}}$ are square matrices with $l_{\mathsf{u}} \geq 1$ and $l_{\mathsf{s}} := l - l_{\mathsf{u}}$, such that all the eigenvalues of S_{u} and S_{s} are located in the open right half-plane and the closed left half-plane, respectively. The matrices G_{u} and G_{s} are constant and satisfy $G = [G_{\mathsf{u}}; G_{\mathsf{s}}]$.

The control input u_{c} in (6.1.1) is supposed to be generated by an output feedback controller

$$\dot{c} = Ec + L(r - y), \qquad u_{\mathsf{c}} = Jc + K(r - y). \tag{6.1.3}$$

Here $c \in \mathbb{R}^{n_{\mathsf{c}}}$ is the controller state, and $r \in \mathbb{R}$ is the reference signal, which is bounded and sufficiently smooth with bounded time derivatives, and E, L, J, and K are some constant matrices. We assume that without the attack (i.e., $a(t) \equiv 0$), the closed-loop system (6.1.1) and (6.1.3) is stable.

As introduced in the previous works [TSSJ15b, TSSJ12], the zero-dynamics attack is usually constructed by duplicating the zero-dynamics of the plant (6.1.1). In particular, with the help of the normal form representation, one can express the attack as

$$\dot{z}^{\mathsf{a}} = Sz^{\mathsf{a}}, \qquad a_{\mathrm{za}} = -\frac{1}{g}\psi^{\top} z^{\mathsf{a}} \tag{6.1.4}$$

where $z^{\mathsf{a}} =: [z_{\mathsf{u}}^{\mathsf{a}}; z_{\mathsf{s}}^{\mathsf{a}}] \in \mathbb{R}^{l_{\mathsf{u}}+l_{\mathsf{s}}}$ is the attacker's state. (In what follows, the superscript 'a' is used to indicate signals generated by the adversary.) To activate the unstable mode of the z^{a}-dynamics (6.1.4), the initial condition $z_{\mathsf{u}}^{\mathsf{a}}(t_0)$ of the unstable part is selected as a nonzero vector. (Hereinafter, we denote the moment when the attack $a(t)$ enters the system as $t = t_0$.)

6.1.2 Performance of Zero-dynamics Attack

We start the analysis of the attack (6.1.4) with a new variable $\chi := [x; c] \in \mathbb{R}^{\nu+n_{\mathsf{c}}}$.[2] Then the actual stable closed-loop system (6.1.1) and (6.1.3) can be rewritten in a more compact form

$$\dot{z} = Sz + G\mathsf{C}\chi, \tag{6.1.5a}$$

$$\dot{\chi} = \mathsf{A}\chi + \mathsf{B}_1 r + \mathsf{B}_2\left(ga + \psi^{\top} z\right), \qquad y = \mathsf{C}\chi \tag{6.1.5b}$$

where the matrices A, B, and C are given by

$$\mathsf{A} := \begin{bmatrix} A_\nu + B_\nu\left(\phi^{\top} - gKC_\nu\right) & gB_\nu J \\ -LC_\nu & E \end{bmatrix}, \tag{6.1.6a}$$

$$\mathsf{B}_1 := \begin{bmatrix} gB_\nu K \\ L \end{bmatrix}, \quad \mathsf{B}_2 := \begin{bmatrix} B_\nu \\ 0_{n_{\mathsf{c}}} \end{bmatrix}, \quad \mathsf{C} := \begin{bmatrix} C_\nu & 0_{n_{\mathsf{c}}}^{\top} \end{bmatrix}. \tag{6.1.6b}$$

For comparison, by putting $a(t) \equiv 0$ into (6.1.5) we obtain an (auxiliary) "attack-free" closed-loop system

$$\dot{z}_{\mathsf{o}} = Sz_{\mathsf{o}} + G\mathsf{C}\chi_{\mathsf{o}}, \tag{6.1.7a}$$

[2] To take a closer look at the behavior of the nominal zero-dynamics state $z_{\mathsf{n}}^{\mathsf{a}}$ (to be presented shortly), the stacked variable χ is defined in a reduced form $[x; c]$ (rather than a larger one $[z_{\mathsf{n}}^{\mathsf{a}}; x; c]$ as in the previous chapters).

$$\dot{\chi}_{\mathsf{o}} = \mathsf{A}\chi_{\mathsf{o}} + \mathsf{B}_1 r + \mathsf{B}_2 \psi^\top z_{\mathsf{o}}, \qquad y_{\mathsf{o}} = \mathsf{C}\chi_{\mathsf{o}} \tag{6.1.7b}$$

where $\chi_{\mathsf{o}} =: [x_{\mathsf{o}}; c_{\mathsf{o}}]$ is the attack-free counterpart of χ.

Now, the nature of the zero-dynamics attack (6.1.4) is introduced in the following proposition.

Proposition 6.1.1. The solution $[z^{\mathsf{a}}(t); z(t); \chi(t)]$ of the closed-loop system (6.1.5) under the attack $a = a_{\mathrm{za}}$ in (6.1.4), initiated in $\mathbb{R}^l \times \mathbb{R}^l \times \mathbb{R}^{\nu+n_{\mathsf{c}}}$, satisfies the following statements:

(a) For any $z^{\mathsf{a}}(t_0) \in \mathbb{R}^l$ such that $z^{\mathsf{a}}_{\mathsf{u}}(t_0) \neq 0$,

$$\|z_{\mathsf{u}}(t)\| \to \infty \quad \text{as} \quad t \to \infty; \tag{6.1.8}$$

(b) For the solution $[z_{\mathsf{o}}(t); \chi_{\mathsf{o}}(t)]$ of the attack-free system (6.1.7) initiated at $[z_{\mathsf{o}}(t_0); \chi_{\mathsf{o}}(t_0)] = [z(t_0); \chi(t_0)]$,

$$\big\|\chi(t) - \chi_{\mathsf{o}}(t)\big\| \leq \mathsf{k}_{\mathrm{za}} e^{-\mathsf{h}_{\mathrm{za}}(t-t_0)} \|z^{\mathsf{a}}(t_0)\|, \quad \forall t \geq t_0$$

where $\mathsf{k}_{\mathrm{za}} > 0$ and $\mathsf{h}_{\mathrm{za}} > 0$ are constant.

$\Diamond$

Proposition 6.1.1 explicitly points out that the zero-dynamics attack (6.1.4) is capable of damaging the internal state $z_{\mathsf{u}}(t)$ of the plant. We also note that just a small non-zero initial condition $\|z^{\mathsf{a}}_{\mathsf{u}}(t_0)\|$ of the attack generator (6.1.4) will do the job, while maintaining stealthiness in the sense that

$$\|y(t) - y_{\mathsf{o}}(t)\| = \|\mathsf{C}\chi(t) - \mathsf{C}\chi_{\mathsf{o}}(t)\| < \epsilon, \quad \forall t \geq t_0 \tag{6.1.9}$$

with a given threshold $\epsilon > 0$.

Proof. Let us define an error variable $\tilde{z} := z - z^{\mathsf{a}}$. It is trivial that $ga + \psi^\top z = \psi^\top \tilde{z}$. It then follows that the closed-loop system (6.1.5) is transformed into

$$\dot{\tilde{z}} = \dot{z} - \dot{z}^{\mathsf{a}} = S(z - z^{\mathsf{a}}) + G\mathsf{C}\chi = S\tilde{z} + G\mathsf{C}\chi, \tag{6.1.10a}$$

$$\dot{\chi} = \mathsf{A}\chi + \mathsf{B}_1 r + \mathsf{B}_2 \psi^\top \tilde{z} \tag{6.1.10b}$$

which has exactly the same (stable) dynamics as the attack-free one (6.1.7). Thus for some positive constants k_{za} and h_{za},

$$\begin{aligned}
&\big\|[\tilde{z}(t);\chi(t)] - [z_{\mathsf{o}}(t);\chi_{\mathsf{o}}(t)]\big\| \\
&\qquad \le \mathsf{k}_{\mathrm{za}} e^{-\mathsf{h}_{\mathrm{za}}(t-t_0)} \big\|[\tilde{z}(t_0);\chi(t_0)] - [z_{\mathsf{o}}(t_0);\chi_{\mathsf{o}}(t_0)]\big\| \\
&\qquad = \mathsf{k}_{\mathrm{za}} e^{-\mathsf{h}_{\mathrm{za}}(t-t_0)} \|z^{\mathsf{a}}(t_0)\|
\end{aligned}$$

where the last equality results from $z(t_0) = z_{\mathsf{o}}(t_0)$ and $\chi(t_0) = \chi_{\mathsf{o}}(t_0)$. This directly implies the item (b). On the other hand, the attacker's state $z^{\mathsf{a}}(t)$ generated by (6.1.4) with nonzero $z^{\mathsf{a}}_{\mathsf{u}}(t_0)$ must diverge as time goes on. It means that $z(t) = z^{\mathsf{a}}(t) + \tilde{z}(t)$ also diverges, because the state $\tilde{z}(t)$ of the stable system (6.1.10) remains bounded. This completes the proof. □

Remark 6.1.1. From the analysis, it is clear that the lower-order dynamics $\dot{z}^{\mathsf{a}}_{\mathsf{u}} = S_{\mathsf{u}} z^{\mathsf{a}}_{\mathsf{u}}$ and $a_{\mathrm{za}} = -(1/g)\psi_{\mathsf{u}}^\top z^{\mathsf{a}}_{\mathsf{u}}$ (where ψ_{u} is a suitable partition of ψ) is enough to realize the zero-dynamics attack. ◊

6.1.3 Limitation of Zero-dynamics Attack against Model Uncertainty

It is important to note that exact model knowledge on the plant (6.1.1) is of necessity in the design of the zero-dynamics attack (6.1.4). However, such a requirement is quite unrealistic. This is because in most industrial systems, it is not always possible for the attacker (nor for the defender) to obtain the exact plant model. In other words, it is natural to assume that the physical plant (6.1.1) has model uncertainty.

Assumption 6.1.1. The parameters S, G, ψ, ϕ, and g of the plant (6.1.1) are uncertain, while the uncertain quantities are bounded and their bounds are known to the attacker.[3] In particular, $0 < \underline{g} \le g \le \overline{g}$ for some constants $\underline{g}$ and $\overline{g}$. ◊

[3]The attacker need not know exact bounds of uncertainties. Overestimate would work.

We assume that the controller (6.1.3) is appropriately designed to robustly stabilize the uncertain plant satisfying Assumption 6.1.1.

From now on, we take a glance at the situation when the attacker tries to design a zero-dynamics attack, in the presence of the model uncertainty in Assumption 6.1.1. Since the ideal structure (6.1.4) is not available at this stage, a possible alternative would be

$$\dot{z}^{\mathsf{a}} = S_{\mathsf{n}} z^{\mathsf{a}}, \quad a_{\mathrm{za}} = -\frac{1}{g_{\mathsf{n}}} \psi_{\mathsf{n}}^{\top} z^{\mathsf{a}} \tag{6.1.11}$$

where S_{n}, ψ_{n}, and $g_{\mathsf{n}} > 0$ are selected as some nominal counterparts of S, ψ, and g, respectively. Then, the attack signal $a_{\mathrm{za}}(t)$ is exponentially diverging with rate determined by the unstable modes of S_{n}. If these modes are different from the zeros of (6.1.5) (i.e., the eigenvalues of S), then the output $y(t)$ should diverge with the same exponential rate as those modes. In fact, even arbitrarily small differences will lead to a diverging output with fixed rate.

From the discussion so far, it may seem that CPS are safe from those stealthy attacks because model uncertainty exists in practice. Unfortunately, we find in the next section that there is another type of stealthy attack which is "robust against model uncertainty".

6.2 Robust Zero-dynamics Attack for Uncertain Cyber-Physical Systems

6.2.1 Problem Revisited with Model Uncertainty

In what follows, we consider the closed-loop system (6.1.1) and (6.1.3) (or equivalently, (6.1.5)) where the plant (6.1.1) of interest has parametric uncertainty as in Assumption 6.1.1. Also, we suppose that the initial conditions $z(t_0)$ and $\chi(t_0)$ of the closed-loop system (6.1.5) belong to some compact sets $\mathcal{Z}^0 \subset \mathbb{R}^l$ and $\mathcal{X}^0 \times \mathcal{C}^0 \subset \mathbb{R}^{\nu+n_{\mathsf{c}}}$, respectively.

The following (attack-free) "nominal" plant of (6.1.1) is taken into account:

$$\begin{aligned} \dot{z}_{\mathsf{n}} &= S_{\mathsf{n}} z_{\mathsf{n}} + G_{\mathsf{n}} y_{\mathsf{n}}, \\ \dot{x}_{\mathsf{n}} &= A_\nu x_{\mathsf{n}} + B_\nu \left(\psi_{\mathsf{n}}^\top z_{\mathsf{n}} + \phi_{\mathsf{n}}^\top x_{\mathsf{n}} + g_{\mathsf{n}} u_{\mathsf{n}} \right), \qquad y_{\mathsf{n}} = C_\nu x_{\mathsf{n}} \end{aligned} \tag{6.2.1}$$

where $z_{\mathsf{n}} \in \mathbb{R}^l$ and $x_{\mathsf{n}} \in \mathbb{R}^\nu$ are the nominal states, $y_{\mathsf{n}} \in \mathbb{R}$ is the nominal output, and $u_{\mathsf{n}} \in \mathbb{R}$ is the nominal input, which is generated by the existing control law (6.1.3) as

$$\dot{c}_{\mathsf{n}} = E c_{\mathsf{n}} + L(r - y_{\mathsf{n}}), \qquad u_{\mathsf{n}} = J c_{\mathsf{n}} + K(r - y_{\mathsf{n}}) \tag{6.2.2}$$

where c_{n} represents the nominal state of the controller. The parameters S_{n}, G_{n}, ψ_{n}, ϕ_{n}, and $g_{\mathsf{n}} > 0$ are nominal counterparts of the actual (uncertain) S, G, ψ, ϕ, and $g > 0$, respectively, and these are the attacker's selection. The nominal model (6.2.1) is of course different from the real plant (6.1.1), but it is assumed that the parameters of (6.2.1) are within the uncertainty bounds of Assumption 6.1.1, so that both (6.1.1) and (6.2.1) have the same relative degree and the same sign of high-frequency gains g and g_{n}. It will be seen that the plant (6.1.1) behaves like the nominal model (6.2.1) by the initiation of the proposed attack. In this context, it may be better for stealthiness if the nominal model (6.2.1) coincides with a design model used for designing the controller (6.1.3) (which, however, requires that the design model is leaked to the attacker "a priori"). For brevity, we often express the nominal closed-loop system (6.2.1) and (6.2.2) with $\chi_{\mathsf{n}} := [x_{\mathsf{n}}; c_{\mathsf{n}}]$ as

$$\dot{z}_{\mathsf{n}} = S_{\mathsf{n}} z_{\mathsf{n}} + G_{\mathsf{n}} \mathsf{C} \chi_{\mathsf{n}}, \tag{6.2.3a}$$

$$\dot{\chi}_{\mathsf{n}} = \mathsf{A}_{\mathsf{n}} \chi_{\mathsf{n}} + \mathsf{B}_{\mathsf{n},1} r + \mathsf{B}_{\mathsf{n},2} \psi_{\mathsf{n}}^\top z_{\mathsf{n}}, \qquad y_{\mathsf{n}} = \mathsf{C} \chi_{\mathsf{n}} \tag{6.2.3b}$$

where A_{n}, $\mathsf{B}_{\mathsf{n},1}$, and $\mathsf{B}_{\mathsf{n},2}$ are the same as A, B_1, and B_2 defined in (6.1.6), with S, G, ψ, ϕ, and g being replaced by their nominal counterparts.

We note in advance that similar to (6.1.7), the nominal closed-loop system (6.2.3) (or equivalently (6.2.1) and (6.2.2)) will play the role of a reference system in the attack design. For this, the nominal closed-loop system (6.2.3) is supposed

to be stable; i.e., the matrix

$$\begin{bmatrix} S_{\mathsf{n}} & G_{\mathsf{n}}\mathsf{C} \\ \mathsf{B}_{\mathsf{n},2}\psi_{\mathsf{n}}^{\top} & \mathsf{A}_{\mathsf{n}} \end{bmatrix} \tag{6.2.4}$$

is Hurwitz.

Now, motivated by Proposition 6.1.1, we formulate the problem of our interest with respect to the uncertain plant.

Problem of Chapter 6: For given $\underline{z}_{\mathsf{u}} > 0$ and $\epsilon > 0$, to construct a "robust" attack generator

$$\dot{\varrho}^{\mathsf{a}} = f(\varrho^{\mathsf{a}}, u_{\mathsf{c}}, y), \quad a = h(\varrho^{\mathsf{a}}, u_{\mathsf{c}}, y) \tag{6.2.5}$$

that achieves the following properties simultaneously for all admissible model uncertainties in Assumption 6.1.1:

(a) $\|z_{\mathsf{u}}(t)\|$ becomes eventually larger than $\underline{z}_{\mathsf{u}} > 0$ within a finite time $t = t_{\text{fin}} \geq t_0$;

(b) $\|y(t) - y_{\mathsf{n}}(t)\|$ is smaller than the threshold $\epsilon > 0$ until the attack succeeds (i.e., for all $t_0 \leq t \leq t_{\text{fin}}$). □

The items in Problem Statement can be interpreted as some refinements of those in Proposition 6.1.1. On one hand, item (a) indicates the capability of the attack (6.2.5) to damage the plant's internal state $z(t)$. Here, $\underline{z}_{\mathsf{u}}$ is one of the attacker's design specifications. On the other hand, a "new" notion of stealthiness is introduced in item (b). Indeed, the actual output $y(t)$ under attack is compared with the output $y_{\mathsf{n}}(t)$ of the "nominal" system (6.2.3), rather than with $y_{\mathsf{o}}(t)$ of the (attack-free) "uncertain" system (6.1.5) as in Proposition 6.1.1. At first glance, it may seem that item (b) easily fails if the model uncertainty is large. However, this is often not the case even for large model uncertainty, as long as the existing controller (6.1.3) is robust against the parametric uncertainties of Assumption 6.1.1. In fact, when a tracking or regulating problem is (robustly) solved by (6.1.3) for both actual and nominal systems (with no attack), their outputs $y_{\mathsf{n}}(t)$ and $y_{\mathsf{o}}(t)$ reach the same reference $r(t)$ in the end. It means that

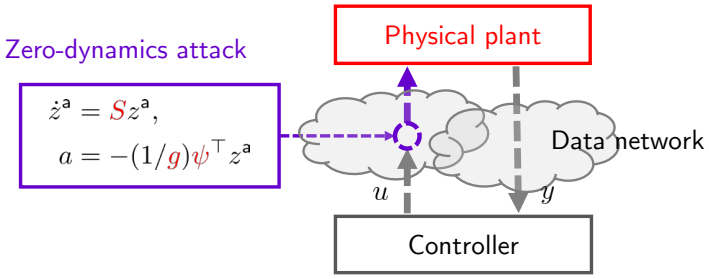

(a) Conventional zero-dynamics attack (6.1.4)

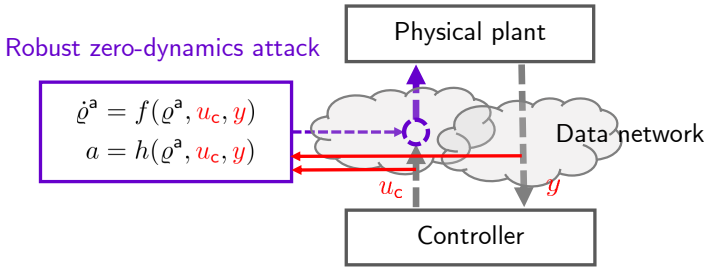

(b) Robust zero-dynamics attack (6.2.5)

Figure 6.3: Configurations of two different attack scenarios: The zero-dynamics attack (6.1.4) requires the exact model knowledge, while the robust zero-dynamics attack (6.2.5) instead utilizes the disclosure resources (i.e., u_{c} and y).

$y_{\mathsf{n}}(t) \approx y_{\mathsf{o}}(t)$ during the steady-state operation of the system when the attack is usually initiated. In summary, we claim in this paper that the new stealthiness is also valid if the uncertainty is not large or if the attack (6.2.5) enters the system in the steady state.

We further remark that, different from traditional zero-dynamics attack (6.1.4), the attack generator (6.2.5) explicitly makes use of the signals u_{c} and y. This is in fact the price to pay for the "robustness" against model uncertainty; i.e., instead of using less model knowledge, the attacker relies more on the input and output information of the plant to adjust to uncertain environment on-line. In short, more disclosure resources are needed as follows.

Assumption 6.2.1. The plant output $y(t)$ and the control input $u(t)$ are avail-

able to attackers. ◊

In addition, for a technical reason, we restrict our attention on the non-minimum phase systems with "hyperbolic" zero-dynamics.

Assumption 6.2.2. At least one of the eigenvalues of S lies in the open right half-plane, and none of the eigenvalues are located on the imaginary axis of the complex plane. ◊

To distinguish (6.2.5) from the (non-robust) zero-dynamics attack (6.1.4), we call (6.2.5) a *robust zero-dynamics attack*. Overall configurations of these attack scenarios are depicted in Figure 6.3.

6.2.2 Yet Another Attack Policy on Unstable Zero-dynamics: Ideal Strategy

As an intermediate step, in this subsection we provide a new attack strategy on the non-minimum phase plant (6.1.1). It is noted in advance that the method to be provided here is not realizable yet, but we will shortly make it feasible in the next subsection.

The first task is, using the information of the output y, to duplicate the nominal z_{n}-dynamics (6.2.6) as the form

$$\dot{z}_{\mathsf{n}}^{\mathsf{a}} = S_{\mathsf{n}} z_{\mathsf{n}}^{\mathsf{a}} + G_{\mathsf{n}} y \tag{6.2.6}$$

where $z_{\mathsf{n}}^{\mathsf{a}}(t_0)$ is chosen in $\mathcal{Z}_0$. With the auxiliary state $z_{\mathsf{n}}^{\mathsf{a}}$ and the nominal components ψ_{n}, ϕ_{n}, and g_{n}, one can rewrite the time derivative of x_ν in (6.1.1b) as

$$\begin{aligned} \dot{x}_\nu &= \psi^\top z + \phi^\top x + g(u_{\mathsf{c}} + a) && \text{(6.2.7a)} \\ &= \psi_{\mathsf{n}}^\top z_{\mathsf{n}}^{\mathsf{a}} + \phi_{\mathsf{n}}^\top x + g_{\mathsf{n}} u + g(a - a^\star) && \text{(6.2.7b)} \end{aligned}$$

where $a^\star \in \mathbb{R}$ is defined as

$$a^\star := \frac{1}{g}\big(- \psi^\top z + \psi_{\mathsf{n}}^\top z_{\mathsf{n}}^{\mathsf{a}} + (\phi_{\mathsf{n}}^\top - \phi^\top)x + (g_{\mathsf{n}} - g)u_{\mathsf{c}}\big). \tag{6.2.8}$$

Then the actual closed-loop system (6.1.5) (i.e., (6.1.1)–(6.1.3)) with the auxiliary dynamics (6.2.6) can be equivalently represented using (6.2.8) by

$$\dot{z} = Sz + G\mathsf{C}\chi \quad \text{(same as (6.1.2))}, \tag{6.2.9a}$$

$$\dot{z}_{\mathsf{n}}^{\mathsf{a}} = S_{\mathsf{n}} z_{\mathsf{n}}^{\mathsf{a}} + G_{\mathsf{n}}\mathsf{C}\chi, \tag{6.2.9b}$$

$$\dot{\chi} = \mathsf{A}_{\mathsf{n}}\chi + \mathsf{B}_{\mathsf{n},1} r + \mathsf{B}_{\mathsf{n},2}\left(g(a - a^\star) + \psi_{\mathsf{n}}^\top z_{\mathsf{n}}^{\mathsf{a}}\right), \qquad y = \mathsf{C}\chi. \tag{6.2.9c}$$

For now, we suppose that $a^\star$ is available to the attacker, from which the attack signal a is constructed as

$$a(t) = a^\star(t), \quad \forall t \geq t_0. \tag{6.2.10}$$

It should be emphasized that under the attack $a = a^\star$, the $(z_{\mathsf{n}}^{\mathsf{a}}, \chi)$-dynamics (6.2.9b)–(6.2.9c) is exactly the same as the nominal closed-loop system (6.2.3) where the auxiliary $z_{\mathsf{n}}^{\mathsf{a}}$-dynamics disguises as the plant's internal dynamics. At the same time, the attack $a = a^\star$ in (6.2.10) leaves the real (unstable) z-dynamics (6.2.9a) decoupled from (6.2.9b)–(6.2.9c) so that the real internal state $z(t)$ possibly diverges. The discussion so far is summarized in the following proposition.

Proposition 6.2.1. The solution $[z(t); z_{\mathsf{n}}^{\mathsf{a}}(t); \chi(t)]$ of the closed-loop system (6.1.5) under the attack (6.2.6), (6.2.8), and (6.2.10), initiated in $\mathcal{Z}^0 \times \mathcal{Z}^0 \times \mathcal{X}^0 \times \mathcal{C}^0$, satisfies the following statements:

(a) For almost every $[z(t_0); z_{\mathsf{n}}^{\mathsf{a}}(t_0); \chi(t_0)]$,

$$\|z_{\mathsf{u}}(t)\| \to \infty \ \text{ as } \ t \to \infty; \tag{6.2.11}$$

(b) For the solution $[z_{\mathsf{n}}(t); \chi_{\mathsf{n}}(t)]$ of the nominal system (6.2.3) initiated at $[z_{\mathsf{n}}(t_0); \chi_{\mathsf{n}}(t_0)] = [z_{\mathsf{n}}^{\mathsf{a}}(t_0); \chi(t_0)]$,

$$\begin{bmatrix} z_{\mathsf{n}}^{\mathsf{a}}(t) \\ \chi(t) \end{bmatrix} = \begin{bmatrix} z_{\mathsf{n}}(t) \\ \chi_{\mathsf{n}}(t) \end{bmatrix}, \quad \forall t \geq t_0.$$

Moreover, $[z_{\mathsf{s}}(t); z_{\mathsf{n}}^{\mathsf{a}}(t); \chi(t)] \in \mathcal{Z}_{\mathsf{s}} \times \mathcal{Z}_{\mathsf{n}} \times \mathcal{X} \times \mathcal{C}$ for all $t \geq t_0$ where $\mathcal{Z}_{\mathsf{s}} \subset \mathbb{R}^{l_{\mathsf{s}}}$, $\mathcal{Z}_{\mathsf{n}} \subset \mathbb{R}^{l}$, $\mathcal{X} \subset \mathbb{R}^{\nu}$, $\mathcal{C} \subset \mathbb{R}^{n_{\mathsf{c}}}$ are some compact sets. $\lozenge$

Proof. The item (b) is trivial and omitted. From (b), the last statement also follows straightforwardly since $r(t)$ is uniformly bounded. Now, for (a), let us define some matrices

$$\mathsf{P}_\mathsf{s} := \begin{bmatrix} S_\mathsf{s} & 0 & G_\mathsf{s}\mathsf{C} \\ 0 & S_\mathsf{n} & G_\mathsf{n}\mathsf{C} \\ 0 & \mathsf{B}_{\mathsf{n},2}\psi_\mathsf{n}^\top & \mathsf{A}_\mathsf{n} \end{bmatrix}, \quad \mathsf{R}_\mathsf{s} := \begin{bmatrix} 0_{l_\mathsf{s}}^\top & 0_l^\top & \mathsf{C} \end{bmatrix},$$
$$\mathsf{Q}_{\mathsf{s},1} := \begin{bmatrix} 0_{l_\mathsf{s}} \\ 0_l \\ \mathsf{B}_{\mathsf{n},1} \end{bmatrix}, \quad \mathsf{Q}_{\mathsf{s},2} := \begin{bmatrix} 0_{l_\mathsf{s}} \\ 0_l \\ g\mathsf{B}_{\mathsf{n},2} \end{bmatrix}. \tag{6.2.12}$$

Notice that P_s is Hurwitz. By this, one obtains the "unique" solution $\mathsf{T} \in \mathbb{R}^{l_\mathsf{u} \times (l_\mathsf{s}+l+\nu+m)}$ of the Sylvester equation

$$\mathsf{T}\mathsf{P}_\mathsf{s} - S_\mathsf{u}\mathsf{T} + G_\mathsf{u}\mathsf{R}_\mathsf{s} = 0. \tag{6.2.13}$$

With these symbols and the coordination transformations

$$\boldsymbol{\chi}_\mathsf{s} := \begin{bmatrix} z_\mathsf{s} \\ z_\mathsf{n}^\mathsf{a} \\ \chi \end{bmatrix} \quad \text{and} \quad \boldsymbol{\chi}_\mathsf{u} := z_\mathsf{u} + \mathsf{T}\boldsymbol{\chi}_\mathsf{s}, \tag{6.2.14}$$

we newly represent the overall system (6.2.9) as

$$\dot{z}_\mathsf{u} = S_\mathsf{u} z_\mathsf{u} + G_\mathsf{u}\mathsf{R}_\mathsf{s}\boldsymbol{\chi}_\mathsf{s} \tag{6.2.15}$$
$$\dot{\boldsymbol{\chi}}_\mathsf{s} = \mathsf{P}_\mathsf{s}\boldsymbol{\chi}_\mathsf{s} + \mathsf{Q}_{\mathsf{s},1} r + \mathsf{Q}_{\mathsf{s},2}(a - a^\star). \tag{6.2.16}$$

Differentiating $\boldsymbol{\chi}_\mathsf{u}$ along with these two dynamics gives

$$\begin{aligned} \dot{\boldsymbol{\chi}}_\mathsf{u} &= \dot{z}_\mathsf{u} + \mathsf{T}\dot{\boldsymbol{\chi}}_\mathsf{s} \\ &= (S_\mathsf{u} z_\mathsf{u} + G_\mathsf{u}\mathsf{R}_\mathsf{s}\boldsymbol{\chi}_\mathsf{s}) + \mathsf{T}\left(\mathsf{P}_\mathsf{s}\boldsymbol{\chi}_\mathsf{s} + \mathsf{Q}_{\mathsf{s},1} r + \mathsf{Q}_{\mathsf{s},2}(a - a^\star)\right) \\ &= S_\mathsf{u}\boldsymbol{\chi}_\mathsf{u} + \mathsf{T}\mathsf{Q}_{\mathsf{s},1} r + \mathsf{T}\mathsf{Q}_{\mathsf{s},2}(a - a^\star). \end{aligned} \tag{6.2.17}$$

It is then clear that under $a(t) \equiv a^\star(t)$, the above $\boldsymbol{\chi}_{\mathsf{u}}$- and $\boldsymbol{\chi}_{\mathsf{s}}$-dynamics become

$$\dot{\boldsymbol{\chi}}_{\mathsf{s}} = \mathsf{P}_{\mathsf{s}}\boldsymbol{\chi}_{\mathsf{s}} + \mathsf{Q}_{\mathsf{s},1} r, \quad \text{and} \quad \dot{\boldsymbol{\chi}}_{\mathsf{u}} = S_{\mathsf{u}}\boldsymbol{\chi}_{\mathsf{u}} + \mathsf{T}\mathsf{Q}_{\mathsf{s},1} r, \tag{6.2.18}$$

respectively, so that both are decoupled from each other. Among them, the $\boldsymbol{\chi}_{\mathsf{u}}$-dynamics is anti-stable (i.e., S_{u} is anti-Hurwitz) and the external signal $r(t)$ is bounded. Then, "almost all" trajectories $\boldsymbol{\chi}_{\mathsf{u}}(t)$ diverge as time goes on: more precisely, the divergence of $\boldsymbol{\chi}_{\mathsf{u}}(t)$ occurs for all admissible initial condition $\boldsymbol{\chi}_{\mathsf{u}}(t_0)$ except only one point

$$\boldsymbol{\chi}_{\mathsf{u}}(t_0) = -\int_{t_0}^{\infty} e^{-S_{\mathsf{u}}(\rho - t_0)} \mathsf{T}\mathsf{Q}_{\mathsf{s},1} r(\rho) \mathrm{d}\rho =: \boldsymbol{\chi}^\star_{\mathsf{u},0} \tag{6.2.19}$$

(which is well-defined because $-S_{\mathsf{u}}$ is Hurwitz). This exceptional initial condition generates the "bounded" solution of (6.2.17)

$$\boldsymbol{\chi}^\star_{\mathsf{u}}(t) = -\int_{t}^{\infty} e^{-S_{\mathsf{u}}(\rho - t)} \mathsf{T}\mathsf{Q}_{\mathsf{s},1} r(\rho) \mathrm{d}\rho, \quad t \geq t_0. \tag{6.2.20}$$

(The readers are referred to [HMS96, JD99] for more details on the bounded solution $\boldsymbol{\chi}^\star_{\mathsf{u}}(t)$ for anti-stable system.)

Once $\boldsymbol{\chi}_{\mathsf{u}}(t)$ diverges as time goes on, $z_{\mathsf{u}}(t) = \boldsymbol{\chi}_{\mathsf{u}}(t) - \mathsf{T}\boldsymbol{\chi}_{\mathsf{s}}(t)$ also does because $\boldsymbol{\chi}_{\mathsf{s}}(t)$ is bounded. Finally, one can summarize the above arguments that (6.2.11) holds if $[z(t_0); z^{\mathsf{a}}_{\mathsf{n}}(t_0); \chi(t_0)] \in \big(\mathcal{Z}^0 \times \mathcal{Z}^0 \times \mathcal{X}^0 \times \mathcal{C}^0\big) \setminus \mathcal{L}^0_{\mathrm{za}}$ with the set

$$\mathcal{L}^0_{\mathrm{za}} := \Big\{ \big[z(t_0); z^{\mathsf{a}}_{\mathsf{n}}(t_0); \chi(t_0)\big] : \ z_{\mathsf{u}}(t_0) + \mathsf{T}\big[z_{\mathsf{s}}(t_0); z^{\mathsf{a}}_{\mathsf{n}}(t_0); \chi(t_0)\big] = \boldsymbol{\chi}^\star_{\mathsf{u},0} \Big\},$$

which concludes the proof. □

Remark 6.2.1. Item (a) of Proposition 6.2.1 highlights that unlike the conventional attack (6.1.4), the present one (6.2.10) might fail to damage the internal state $z_{\mathsf{u}}(t)$ for the specific initial conditions $[z(t_0); z^{\mathsf{a}}_{\mathsf{n}}(t_0); \chi(t_0)] \in \mathcal{L}^0_{\mathrm{za}}$, defined in the proof above. Worse yet, it is rarely possible to compute $\mathcal{L}^0_{\mathrm{za}}$ "a priori", since $\boldsymbol{\chi}^\star_{\mathsf{u},0}$ is determined by the "future" information of the external input $r(t)$ (so $\boldsymbol{\chi}^\star_{\mathsf{u}}(t)$ is "non-causal"). Nonetheless, this may not be a big problem to the adversary. Indeed, the Lebesgue measure of $\mathcal{L}^0_{\mathrm{za}}$ is zero, which means that this unwanted

scenario hardly occurs. ◊

Remark 6.2.2. The effect of the attack (6.2.8) at time t_0 is to replace the uncertain parameters and the state z in (6.2.7a) with the nominal ones and the state $z_{\mathsf{n}}^{\mathsf{a}}$ as in (6.2.7b). As a result, it is like replacing the zero-dynamics (6.2.9a) with (6.2.9b) at time t_0. In order to make this abrupt change as invisible as possible from the output response, it would be better to have $z_{\mathsf{n}}^{\mathsf{a}}(t_0) \approx z(t_0)$. This is possible in some situations: (a) the overall system is already in the steady state (i.e., $y(t) \approx r(t)$) before the attack is injected so that the value of z is easily guessed (at least approximately); or (b) the model uncertainty is not too large to run a state observer before the initiation of the attack using the information of y and u. If the attacker is not able to set $z_{\mathsf{n}}^{\mathsf{a}}(t_0)$ close to $z(t_0)$, then a control action of (6.1.3) may cause a transient from $t = t_0$. More discussion can be found in Section 6.3 with some simulations. ◊

Even though the new attack policy (6.2.10) seems to resolve the considered problem directly (as in Proposition 6.2.1), there is still a huge gap between (6.2.10) and the desired attack generator (6.2.5). This is because $a^\star$ used in (6.2.10) is composed of uncertain parameters and unmeasured states and thus it is not obtainable in general. Yet, surprisingly, we observe that the considered situation is analogous to one in robust control theory. Indeed, $a^\star(t)$ represents the discrepancy between the actual and nominal plants, which has been known in the literature under the name of "total disturbance" [SPJ+16, Han09]. From this viewpoint, the problem of our interest can be converted into how to design a robust controller that estimates and compensates the lumped disturbance $a^\star$. Motivated by this, in the next subsection we will construct a DOB [SPJ+16, BS08] as the robust attack generator (6.2.5). We note in advance that the disturbance observer to be presented will estimate and compensate the lumped disturbance $a^\star(t)$ quickly, from which the ideal attack policy (6.2.10) will be recovered in a practical sense.

6.2.3 Design of Robust Zero-dynamics Attack: Practical Implementation of New Attack Policy via Disturbance Observer

For the design of the attack generator (6.2.5), we first compute some bounds for the state variables of the overall system. Take compact sets $\overline{\mathcal{Z}}_{\mathsf{n}} \overset{\epsilon}{\supset} \mathcal{Z}_{\mathsf{n}}$, $\overline{\mathcal{X}} \overset{\epsilon}{\supset} \mathcal{X}$, and $\overline{\mathcal{C}} \overset{\epsilon}{\supset} \mathcal{C}$ where $\mathcal{Z}_{\mathsf{n}}$, $\mathcal{X}$, and $\mathcal{C}$ are presented in Proposition 6.2.1, and ϵ is given in the problem of interest. We also choose a compact set $\overline{\mathcal{Z}}_{\mathsf{s}} \supset \mathcal{Z}_{\mathsf{s}}$ such that the state trajectory $z_{\mathsf{s}}(t)$ of (6.1.1a) belongs to $\overline{\mathcal{Z}}_{\mathsf{s}}$ for all initial condition $z(t_0) \in \mathcal{Z}_0$ and for all $\chi(t) \in \overline{\mathcal{X}}$. In addition, select a positive constant $\overline{z}_{\mathsf{u}}$ to be larger than the attack specification $\underline{z}_{\mathsf{u}}$ in the problem formulation. It will be shown shortly that the state variable remains bounded as

$$\|z_{\mathsf{u}}(t)\| \leq \overline{z}_{\mathsf{u}} \quad \text{and} \quad \left[z_{\mathsf{s}}(t); z_{\mathsf{n}}^{\mathsf{a}}(t); \chi(t)\right] \in \overline{\mathcal{Z}}_{\mathsf{s}} \times \overline{\mathcal{Z}}_{\mathsf{n}} \times \overline{\mathcal{X}} \times \overline{C} \tag{6.2.21}$$

until the attack (6.2.5) succeeds (in the sense of item (a) in the problem formulation).

With these bounds, we consider the set

$$\mathcal{A} := \left\{ a^\star \text{ in (6.2.8)} : \ \left[z_{\mathsf{u}}; z_{\mathsf{s}}; z_{\mathsf{n}}^{\mathsf{a}}; \chi\right] \text{ is bounded as (6.2.21)} \right\}$$

which contains all possible values of $a^\star$ of (6.2.8) with respect to the model uncertainty, the (bounded) state variables, and the values of $r(t)$. The set $\mathcal{A}$ is clearly bounded under the assumptions. Since computing the exact $\mathcal{A}$ can be a difficult task, we instead choose any compact set $\overline{\mathcal{A}}$ strictly larger than $\mathcal{A}$, which is enough for the design of the attack generator.

On top of that, some components to be used in the DOB design are introduced below. First, let us choose a saturation function $\bar{s}_{\mathsf{a}} : \mathbb{R} \to \mathbb{R}$ that is $\mathfrak{C}^1$ and bounded, and satisfies[4]

$$\bar{s}_{\mathsf{a}}(\hat{a}) = \hat{a}, \quad \forall \hat{a} \in \overline{\mathcal{A}} \quad \text{and} \quad 0 \leq \frac{\partial \bar{s}_{\mathsf{a}}}{\partial \hat{a}}(\hat{a}) \leq 1, \quad \forall \hat{a} \in \mathbb{R}. \tag{6.2.22}$$

Also, for a positive integer i, define a diagonal matrix $\underline{\Upsilon}_i(\tau) := \operatorname{diag}(\tau, \tau^2, \ldots, \tau^i) \in$

[4] In other words, $\bar{s}_{\mathsf{a}}$ is any smooth bounded function whose slope is limited by one and which is identity on $\hat{\mathcal{A}}$.

$\mathbb{R}^{i\times i}$ which is invertible for any positive constant τ. (Here, τ is a design parameter to be determined in Theorem 6.2.2.) Next, by using the design guidelines in Appendix A.1, choose a_i, $i = 0, \dots, \nu-1$, such that the transfer function

$$\mathrm{Z}_{\nu,0}(s) = \frac{s^\nu + \mathsf{a}_{\nu-1}s^{\nu-1} + \cdots + \mathsf{a}_1 s + (\overline{g}/g_{\mathsf{n}})\mathsf{a}_0}{s^\nu + \mathsf{a}_{\nu-1}s^{\nu-1} + \cdots + \mathsf{a}_1 s + (\underline{g}/g_{\mathsf{n}})\mathsf{a}_0} \tag{6.2.23}$$

is SPR where $\underline{g}$ and $\overline{g}$ are the bounds of g in Assumption 6.1.1.

Finally, by following the design methodology of [BS14] (or that of Chapter 2 with $l_{\mathsf{q}} = 0$), we propose the robust zero-dynamics attack (6.2.5) as the $z^{\mathsf{a}}_{\mathsf{n}}$-dynamics (6.2.6) and

$$\begin{aligned}\dot{p}^{\mathsf{a}} &= \left(A_\nu - \underline{\Upsilon}_\nu^{-1}\overline{\alpha}C_\nu\right)p^{\mathsf{a}} + \frac{\mathsf{a}_0}{\tau^\nu}B_\nu\left(u_{\mathsf{c}} + a_{\mathrm{rza}} + \frac{1}{g_{\mathsf{n}}}\psi_{\mathsf{n}}^\top z^{\mathsf{a}}_{\mathsf{n}}\right)\\ &\quad + \frac{\mathsf{a}_0}{\tau^\nu}\frac{1}{g_{\mathsf{n}}}\left(\overline{\phi}_{\mathsf{n}} + \underline{\Upsilon}_\nu^{-1}\overline{\alpha}\right)y, \end{aligned}\tag{6.2.24a}$$

$$a_{\mathrm{rza}} = \bar{s}_{\mathsf{a}}\left(C_\nu p^{\mathsf{a}} - \frac{\mathsf{a}_0}{\tau^\nu}\frac{1}{g_{\mathsf{n}}}y\right) \tag{6.2.24b}$$

where $p^{\mathsf{a}} \in \mathbb{R}^\nu$ and $z^{\mathsf{a}}_{\mathsf{n}} \in \mathbb{R}^l$ are the states of the attack generator, $\overline{\phi}_{\mathsf{n}} := [\phi_{\mathsf{n},\nu}; \cdots; \phi_{\mathsf{n},1}] \in \mathbb{R}^\nu$ and $\overline{\alpha} := [\mathsf{a}_{\nu-1}; \cdots; \mathsf{a}_0] \in \mathbb{R}^\nu$. It is noted that the output $a_{\mathrm{rza}} \in \mathbb{R}$ will serve as an estimate of $a^\star$. We take $p^{\mathsf{a}}(t_0)$ in a compact set $\mathcal{F}^0_{\mathsf{p}} \subset \mathbb{R}^\nu$ while $z^{\mathsf{a}}_{\mathsf{n}}(t_0)$ belongs to $\mathcal{Z}^0$. (While $\mathcal{F}^0_{\mathsf{p}} \subset \mathbb{R}^\nu$ can be any compact set, for example, $\mathcal{F}^0_{\mathsf{p}} = \{0\}$ would work, it is preferred to have $z^{\mathsf{a}}_{\mathsf{n}}(t_0) \approx z(t_0)$ as discussed in Remark 6.2.2.)

The following theorem describes our main result that the proposed attack (6.2.6) and (6.2.24) recovers the attack performance of the ideal attack policy (6.2.10) in a practical sense, while being robustly stealthy against model uncertainty.

Theorem 6.2.2. Suppose that Assumptions 6.1.1–6.2.2 hold. Then for given $\underline{z}_{\mathsf{u}} > 0$ and $\epsilon > 0$, there exists $\overline{\tau} > 0$ such that the solution $[z(t); z^{\mathsf{a}}_{\mathsf{n}}(t); \chi(t); p^{\mathsf{a}}(t)]$ of the closed-loop system (6.1.5) under the robust zero-dynamics attack $a = a_{\mathrm{rza}}$ in (6.2.6) and (6.2.24) with $\tau \in (0, \overline{\tau})$, initiated in $\mathcal{Z}^0 \times \mathcal{Z}^0 \times \mathcal{X}^0 \times \mathcal{F}^0_{\mathsf{p}}$, satisfies the following statements:

(a) For almost every $[z(t_0); z_{\mathsf{n}}^{\mathsf{a}}(t_0); \chi(t_0); p^{\mathsf{a}}(t_0)]$, there exists $t_{\text{fin}} \geq t_0$ such that

$$\|z_{\mathsf{u}}(t_{\text{fin}})\| > \underline{z}_{\mathsf{u}}; \tag{6.2.25}$$

(b) For the solution $[z_{\mathsf{n}}(t); \chi_{\mathsf{n}}(t)]$ of the nominal system (6.2.3) initiated at $[z_{\mathsf{n}}(t_0); \chi_{\mathsf{n}}(t_0)] = [z_{\mathsf{n}}^{\mathsf{a}}(t_0); \chi(t_0)]$,

$$\left\| \begin{bmatrix} z_{\mathsf{n}}^{\mathsf{a}}(t) \\ \chi(t) \end{bmatrix} - \begin{bmatrix} z_{\mathsf{n}}(t) \\ \chi_{\mathsf{n}} \end{bmatrix} \right\| < \epsilon \tag{6.2.26}$$

for $t_0 \leq t \leq t_{\text{fin}}$.

$\Diamond$

6.2.4 Proof of Main Result

The rest of this section is devoted to the proof of Theorem 6.2.2. To this end, we represent the attacked closed-loop system into the singular perturbation form [Kha96].

Lemma 6.2.3. With the coordinate changes (6.2.14) and

$$\tilde{\eta}_1 = p_1^{\mathsf{a}} - \frac{\mathsf{a}_0}{\tau^\nu} \frac{1}{g_{\mathsf{n}}} y - a^\star, \tag{6.2.27a}$$

$$\tilde{\eta}_i = \tau^{i-1} \left(p_1^{\mathsf{a}(i-1)} - \frac{\mathsf{a}_0}{\tau^\nu} \frac{1}{g_{\mathsf{n}}} y^{(i-1)} \right), \quad i = 2, \ldots, \nu, \tag{6.2.27b}$$

the overall system (6.1.5), (6.2.6), (6.2.24), and $a = a_{\text{rza}}$ is transformed into the standard singular perturbation form:

(6.2.16), (6.2.17), and

$$\tau \dot{\tilde{\eta}} = \big(A_\nu - B_\nu \underline{\alpha}^\top\big)\tilde{\eta} + \mathsf{a}_0 B_\nu \left(\frac{g - g_{\mathsf{n}}}{g_{\mathsf{n}}} \right) \tilde{a} - \tau \begin{bmatrix} \dot{a}^\star \\ 0_{\nu-1} \end{bmatrix} \tag{6.2.28}$$

where $\underline{\alpha} := [\mathsf{a}_0; \cdots; \mathsf{a}_{\nu-1}] \in \mathbb{R}^\nu$ and

$$\tilde{a} := -a_{\text{rza}} + a^\star = -\bar{s}_{\mathsf{a}}\big(C_\nu \tilde{\eta} + a^\star\big) + a^\star. \tag{6.2.29}$$

$\Diamond$

The proof of Lemma 6.2.3 is largely similar to that of Lemma 2.3.2, and thus we skip the detailed proof.

With τ regarded as a perturbation parameter, from now on we call $\tilde{\eta}$ the *fast* variable, while the other states the *slow* variables. The following lemma indicates that as long as the slow variables remain in the region of interest, the fast variable $\tilde{\eta}$ approaches the *boundary layer* $\tilde{\eta} = 0$ during transient period.

Lemma 6.2.4. Suppose that $[z(t); z_{\mathsf{n}}^{\mathsf{a}}(t); \chi(t)]$ is bounded as in (6.2.21) for $t \geq t_0$. Then $\tilde{\eta}(t)$ satisfies

$$\|\tilde{\eta}(t)\| \leq \mathsf{k}_\eta e^{-\mathsf{h}_\eta((t-t_0)/\tau)}\|\tilde{\eta}(t_0)\| + \kappa_\eta(\tau), \quad \forall t \geq t_0, \tag{6.2.30}$$

for some positive constants k_η and h_η, and a class-$\mathcal{K}$ function $\kappa_\eta : \mathbb{R} \to \mathbb{R}$. $\Diamond$

Proof. The lemma can be derived in a similar way of Lemma 2.3.4. $\square$

For further analysis, we define an error variable

$$\tilde{z}_{\mathsf{n}}^{\mathsf{a}} := z_{\mathsf{n}}^{\mathsf{a}} - z_{\mathsf{n}}, \quad \tilde{\chi} := \chi - \chi_{\mathsf{n}} \tag{6.2.31}$$

on the slow variables, whose time derivative is given (from (6.2.3) and (6.2.9)) by

$$\begin{bmatrix} \dot{\tilde{z}}_{\mathsf{n}}^{\mathsf{a}} \\ \dot{\tilde{\chi}} \end{bmatrix} = \begin{bmatrix} S_{\mathsf{n}} & G_{\mathsf{n}}\mathsf{C} \\ \mathsf{B}_{\mathsf{n},2}\psi_{\mathsf{n}}^\top & \mathsf{A}_{\mathsf{n}} \end{bmatrix} \begin{bmatrix} \tilde{z}_{\mathsf{n}}^{\mathsf{a}} \\ \tilde{\chi} \end{bmatrix} - \begin{bmatrix} 0 \\ \mathsf{B}_{\mathsf{n},2} g \end{bmatrix} \tilde{a}. \tag{6.2.32}$$

We remark that (6.2.32) is a stable linear system with an additional external signal $\tilde{a}(t)$. In particular, one has a Lyapunov function $V_{\mathsf{s}}(\tilde{z}_{\mathsf{n}}^{\mathsf{a}}, \tilde{\chi}) := [\tilde{z}_{\mathsf{n}}^{\mathsf{a}}; \tilde{\chi}]^\top P_{\mathsf{s}} [\tilde{z}_{\mathsf{n}}^{\mathsf{a}}; \tilde{\chi}]$ where $P_{\mathsf{s}} = P_{\mathsf{s}}^\top > 0$ satisfies

$$P_{\mathsf{s}} \begin{bmatrix} S_{\mathsf{n}} & G_{\mathsf{n}}\mathsf{C} \\ \mathsf{B}_{\mathsf{n},2}\psi_{\mathsf{n}}^\top & \mathsf{A}_{\mathsf{n}} \end{bmatrix} + \begin{bmatrix} S_{\mathsf{n}} & G_{\mathsf{n}}\mathsf{C} \\ \mathsf{B}_{\mathsf{n},2}\psi_{\mathsf{n}}^\top & \mathsf{A}_{\mathsf{n}} \end{bmatrix}^\top P_{\mathsf{s}} = -I.$$

By differentiating V_{s} along with (6.2.32), we readily have

$$\dot{V}_{\mathsf{s}} < -\mathsf{h}_{\mathsf{s}} V_{\mathsf{s}} + \mathsf{k}_{\mathsf{s}} \|\tilde{a}\| \tag{6.2.33}$$

where $\mathsf{h_s}$ and $\mathsf{k_s}$ are some positive constants. We note that the initial value of V_s is zero, because the nominal trajectory $[z_\mathsf{n}(t); \chi_\mathsf{n}(t)]$ of interest is initiated at the same point as the real one $[z_\mathsf{n}^\mathsf{a}(t); \chi(t)]$. In addition, due to the saturation function $\bar{s}_\mathsf{a}$, $\tilde{a}$ has a bounded value at $t = t_0$ independent of $\tilde{\eta}$. From these facts, one can select $t_{\rm tr} > t_0$ sufficiently small such that

$$V_\mathsf{s}\big(\tilde{z}_\mathsf{n}^\mathsf{a}(t), \tilde{\chi}(t)\big) < \frac{\epsilon^2}{2}\underline{\lambda}(P_\mathsf{s}), \quad \forall t_0 \le t \le t_{\rm tr}. \tag{6.2.34}$$

Then the inclusions in (6.2.21) are satisfied for $t_0 \le t \le t_{\rm tr}$. Notice that the inequality (6.2.26) in Theorem 6.2.2 naturally holds during the transient period $t_0 \le t \le t_{\rm tr}$. Keeping this in mind, in what follows we focus on the reduced time period $t \ge t_{\rm tr}$.

Firstly, we claim that if the slow variables are bounded as in (6.2.21) for $t \ge t_{\rm tr}$, then the fast variable $\tilde{\eta}(t)$ with small τ remains around the boundary layer $\tilde{\eta} = 0$ for that time period. Indeed, it follows from (6.2.27) that $\tilde{\eta}(t_0)$ has the form of a polynomial of $1/\tau$ whose coefficients are determined by the initial conditions of the state variables. In particular, with $\tau \in (0, 1)$ we have $\|\tilde{\eta}(t_0)\| \le \sum_{j=0}^{\nu} \mathsf{v}_{\eta,j}/\tau^j$ where positive constants $\mathsf{v}_{\eta,j}$, $j = 0, \ldots, \nu$, are independent of τ. Lemma 6.2.4 implies that

$$\|\tilde{\eta}(t)\| \le \mathsf{k}_\eta e^{-\mathsf{h}_\eta((t_{\rm tr}-t_0)/\tau)} \sum_{j=0}^{\nu} \frac{\mathsf{v}_{\eta,j}}{\tau^j} + \kappa_\eta(\tau) =: \overline{\kappa}_\eta(\tau), \quad \forall t \ge t_{\rm tr} \tag{6.2.35}$$

where $\overline{\kappa} : \mathbb{R}_{>0} \to \mathbb{R}_{>0}$ is continuous on τ and satisfies $\overline{\kappa}(\tau) \to 0$ as $\tau \to 0$ (because $t_{\rm tr} - t_0 > 0$). This concludes the claim. For further analysis, we particularly choose $0 < \overline{\tau}_1 < 1$ such that for all $0 < \tau < \overline{\tau}_1$, the function $\overline{\kappa}_\eta(\tau)$ satisfies

$$\overline{\kappa}_\eta(\tau) \le \min\left\{\epsilon_\eta, \frac{\mathsf{h_s}}{\mathsf{k_s}}\epsilon^2\underline{\lambda}(P_\mathsf{s})\right\} \tag{6.2.36}$$

where $\epsilon_\eta > 0$ is a small constant such that

$$a^\star \in \mathcal{A} \ \text{ and } \ \|\tilde{\eta}\| < \epsilon_\eta \quad \Rightarrow \quad \bar{s}_\mathsf{a}\big(a^\star + C_\nu\tilde{\eta}\big) = a^\star + C_\nu\tilde{\eta}.$$

Note that such ϵ_η always exists, since the saturation level set $\overline{\mathcal{A}}$ of $\bar{s}_\mathsf{a}$ is selected

strictly larger than $\mathcal{A}$.

Next, we argue that for each $0 < \tau < \overline{\tau}_1$, the inequality (6.2.26) holds (and thus $a^\star(t)$ belongs to $\mathcal{A}$) until $\|z_{\mathsf{u}}(t)\| \leq \overline{z}_{\mathsf{u}}$ is violated. To see this, it should be noted that if (6.2.21) holds for $t \geq t_{\rm tr}$, then it follows from (6.2.33), (6.2.35), and (6.2.36) that

$$\dot{V}_{\mathsf{s}} < -\mathsf{h}_{\mathsf{s}} \left(V_{\mathsf{s}} - \epsilon^2 \underline{\lambda}(P_{\mathsf{s}}) \right).$$

This implies that the set

$$\mathcal{V} := \left\{ [\tilde{z}^{\mathsf{a}}_{\mathsf{n}}; \tilde{\chi}] : \ V_{\mathsf{s}}(\tilde{z}^{\mathsf{a}}_{\mathsf{n}}, \tilde{\chi}) \leq \epsilon^2 \underline{\lambda}(P_{\mathsf{s}}) \right\}$$

is positively invariant. The proof of the argument is complete by noting that the error variable $[\tilde{z}^{\mathsf{a}}_{\mathsf{n}}(t); \tilde{\chi}(t)]$ is located inside $\mathcal{V}$ at $t = t_{\rm tr}$, and that

$$\left\| \begin{bmatrix} \tilde{z}^{\mathsf{a}}_{\mathsf{n}} \\ \tilde{\chi} \end{bmatrix} \right\| < \epsilon \ \Rightarrow \ \begin{bmatrix} z^{\mathsf{a}}_{\mathsf{n}} \\ \chi \end{bmatrix} = \begin{bmatrix} z_{\mathsf{n}} \\ \chi_{\mathsf{n}} \end{bmatrix} + \begin{bmatrix} \tilde{z}^{\mathsf{a}}_{\mathsf{n}} \\ \tilde{\chi} \end{bmatrix} \in \overline{\mathcal{Z}}_{\mathsf{n}} \times \overline{\mathcal{X}} \times \overline{\mathcal{C}}.$$

At last, we complete the proof of the theorem by showing that with sufficiently small τ, there exists a finite time $t = t_{\rm fin}$ such that the partial state $z_{\mathsf{u}}(t)$ satisfies (6.2.25) for almost every $[z(t_0); z^{\mathsf{a}}_{\mathsf{n}}(t_0); \chi(t_0); p^{\mathsf{a}}(t_0)]$ in $\mathcal{Z}^0 \times \mathcal{Z}^0 \times \mathcal{X}^0 \times \mathcal{C} \times \mathcal{F}^0_{\mathsf{p}}$. It is obvious from the arguments so far that as long as $\|z_{\mathsf{u}}(t)\| \leq \overline{z}_{\mathsf{u}}$ and $0 < \tau < \overline{\tau}_1$, the saturation function $\bar{s}_{\mathsf{a}}$ is inactive for $t \geq t_{\rm tr}$. Then one has $\tilde{a} = -C_\nu \tilde{\eta}$ and $\dot{a}^\star = \mathsf{E}_{\mathsf{a},1}\tilde{\eta} + \mathsf{E}_{\mathsf{a},2}[\boldsymbol{\chi}_{\mathsf{u}}; \boldsymbol{\chi}_{\mathsf{s}}] + \mathsf{E}_{\mathsf{a},3}[r; \dot{r}]$ for some constant matrices $\mathsf{E}_{\mathsf{a},i}$, $i = 1, 2, 3$. It follows that the overall (transformed) system (6.2.16), (6.2.17), and (6.2.28) turns out to be "linear"; in particular,

$$\tau \dot{\tilde{\eta}} = \left(A_\nu - B_\nu \underline{\alpha}_{\mathsf{g}}^\top + \tau \mathsf{E}_{\mathsf{a},1} \right) \tilde{\eta} + \tau \mathsf{E}_{\mathsf{a},2} \begin{bmatrix} \boldsymbol{\chi}_{\mathsf{u}} \\ \boldsymbol{\chi}_{\mathsf{s}} \end{bmatrix} + \tau \mathsf{E}_{\mathsf{a},3} \begin{bmatrix} r \\ \dot{r} \end{bmatrix} \tag{6.2.37}$$

where

$$\underline{\alpha}_{\mathsf{g}} := \underline{\alpha} + \frac{g - g_{\mathsf{n}}}{g_{\mathsf{n}}} \mathsf{a}_0 C_\nu = [(g/g_{\mathsf{n}})\mathsf{a}_0; \mathsf{a}_1; \cdots; \mathsf{a}_{\nu-1}] \in \mathbb{R}^\nu.$$

For further analysis, let us consider the non-symmetric algebraic Riccati equation

$$\begin{bmatrix} \mathsf{Q}_{\mathsf{s},2} \\ 0 \end{bmatrix} + \mathsf{L}\big(A_\nu - B_\nu \underline{\alpha}_{\mathsf{g}}^\top + \tau \mathsf{E}_{\mathsf{a},1}\big) - \tau \begin{bmatrix} S_{\mathsf{u}} & 0 \\ 0 & \mathsf{P}_{\mathsf{s}} \end{bmatrix} \mathsf{L} - \tau \mathsf{L} \mathsf{E}_{\mathsf{a},2} \mathsf{L} = 0. \tag{6.2.38}$$

Here, since the matrix $A_\nu - B_\nu \underline{\alpha}_{\mathsf{g}}^\top$ is Hurwitz, it follows from [KKO99, Subsection 2.2] that there exists $0 < \overline{\tau} \le \overline{\tau}_1$ such that for fixed $\tau \in (0, \overline{\tau})$, the solution $\mathsf{L} = \mathsf{L}(\tau)$ of (6.2.38) is uniquely determined and its norm is bounded. Using this, we now take $\tau \in (0, \overline{\tau})$ and define a coordinate change

$$\begin{bmatrix} \hat{\boldsymbol{\chi}}_{\mathsf{u}} \\ \hat{\boldsymbol{\chi}}_{\mathsf{s}} \end{bmatrix} := \begin{bmatrix} \boldsymbol{\chi}_{\mathsf{u}} \\ \boldsymbol{\chi}_{\mathsf{s}} \end{bmatrix} + \tau \mathsf{L} \tilde{\eta}$$

Then with $\mathsf{L} =: [\mathsf{L}_{\mathsf{u}}; \mathsf{L}_{\mathsf{s}}] \in \mathbb{R}^{l_{\mathsf{u}} \times \nu} \times \mathbb{R}^{(l_{\mathsf{s}}+n+m)\times \nu}$, it is easy to see that for $t \ge t_{\mathrm{tr}}$,

$$\begin{bmatrix} \dot{\hat{\boldsymbol{\chi}}}_{\mathsf{u}} \\ \dot{\hat{\boldsymbol{\chi}}}_{\mathsf{s}} \end{bmatrix} = \begin{bmatrix} S_{\mathsf{u}} & 0 \\ 0 & \mathsf{P}_{\mathsf{s}} \end{bmatrix} \begin{bmatrix} \hat{\boldsymbol{\chi}}_{\mathsf{u}} \\ \hat{\boldsymbol{\chi}}_{\mathsf{s}} \end{bmatrix} + \begin{bmatrix} \mathsf{T}\mathsf{Q}_{\mathsf{s},1} \\ \mathsf{Q}_{\mathsf{s},1} \end{bmatrix} r + \begin{bmatrix} \tau \mathsf{L}_{\mathsf{u}} \mathsf{E}_3 \\ \tau \mathsf{L}_{\mathsf{s}} \mathsf{E}_3 \end{bmatrix} \begin{bmatrix} r \\ \dot{r} \end{bmatrix}. \tag{6.2.39}$$

Observe that the above $\hat{\boldsymbol{\chi}}_{\mathsf{u}}$-dynamics is an anti-stable linear system with the bounded external signal r. Thus similar to the case of Proposition 6.2.1, one has

$$z_{\mathsf{u}}(t) = \hat{\boldsymbol{\chi}}_{\mathsf{u}}(t) - \mathsf{T}\boldsymbol{\chi}_{\mathsf{s}}(t) - \tau \mathsf{L}_{\mathsf{u}} \tilde{\eta}(t)$$

diverges as time goes on, as long as

$$\begin{aligned} \hat{\boldsymbol{\chi}}_{\mathsf{u}}(t_{\mathrm{tr}}) &\neq -\int_{t_{\mathrm{tr}}}^{\infty} e^{-S_{\mathsf{u}}(v-t)} \left(\mathsf{T}\mathsf{Q}_{\mathsf{s},1} r(v) + \tau \mathsf{L}_{\mathsf{u}} \mathsf{E}_3 \begin{bmatrix} r(v) \\ \dot{r}(v) \end{bmatrix} \right) dv \\ &=: \hat{\boldsymbol{\chi}}^\star_{\mathsf{u},\mathrm{tr}}. \end{aligned}$$

To find out the exceptional case at the initial time $t = t_0$ (rather than at $t = t_{\mathrm{tr}}$), let us consider the " backward" solution of the $\hat{\boldsymbol{\chi}}_{\mathsf{u}}$-dynamics in (6.2.39). If the solution is initiated at $\hat{\boldsymbol{\chi}}_{\mathsf{u}}(t_{\mathrm{tr}}) = \hat{\boldsymbol{\chi}}^\star_{\mathsf{u},\mathrm{tr}}$, the corresponding value $\hat{\boldsymbol{\chi}}_{\mathsf{u}}(t_0)$, denoted by $\hat{\boldsymbol{\chi}}^\star_{\mathsf{u},0}$, is uniquely determined. Using this, we can summarize that $z_{\mathsf{u}}(t)$ must diverge if $[z(t_0); z^{\mathsf{a}}_{\mathsf{n}}(t_0); \chi(t_0); p^{\mathsf{a}}(t_0)]$ is not located in a Lebesgue measure zero set $\mathcal{L}^0_{\mathrm{rza}}$ on which $\hat{\boldsymbol{\chi}}_{\mathsf{u}}(t_0) = \hat{\boldsymbol{\chi}}^\star_{\mathsf{u},0}$ holds.

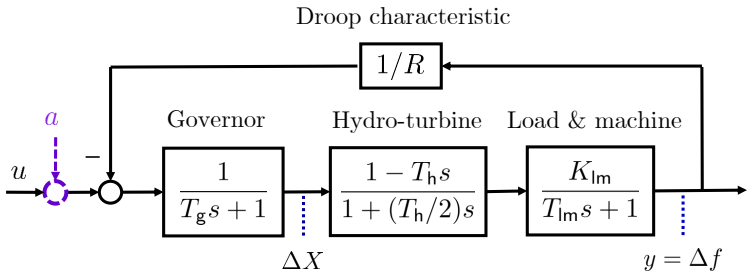

Figure 6.4: Configuration of a power generating system with a hydro turbine [Tan10]

6.3 Simulation: Power Generating Systems

We consider the scenario when a malicious attack enters a power generating system with a hydro turbine [Kun94], [Tan10], as depicted in Figure 6.4. A state-space representation of the plant is given by

$$\dot{\mathtt{x}}_1 = -(1/T_{\mathsf{lm}})\mathtt{x}_1 + (K_{\mathsf{lm}}/T_{\mathsf{lm}})(\mathtt{x}_2 - 2\mathtt{x}_3), \tag{6.3.1a}$$

$$\dot{\mathtt{x}}_2 = -(2/T_{\mathsf{h}})\mathtt{x}_2 + (6/T_{\mathsf{h}})\mathtt{x}_3, \tag{6.3.1b}$$

$$\dot{\mathtt{x}}_3 = -(1/T_{\mathsf{g}})\mathtt{x}_3 + (1/T_{\mathsf{g}})\big(u + a - (1/R)\mathtt{x}_1\big), \tag{6.3.1c}$$

where u is the input, $y = \mathtt{x}_1$ is the output, and $\mathtt{x} := [\mathtt{x}_1; \mathtt{x}_2; \mathtt{x}_3] := [\Delta f; \Delta P + 2\Delta X; \Delta X]$ is the state consisting of the frequency deviation Δf (Hz), the change in generator output ΔP (p.u.), and the change in governor valve position ΔX (p.u.). The constants T_{lm}, T_{h}, and T_{g} indicate time constants of load and machine, hydro turbine, and governor, respectively, and R (Hz/p.u.) is the speed regulation due to the governor action. The detailed parameters of the plants are given by $K_{\mathsf{lm}} = 1$, $T_{\mathsf{lm}} = 6$, $T_{\mathsf{g}} = 0.2$, and $R = 0.05$, while $T_{\mathsf{h}} \in [4, 6]$ is uncertain [Tan10]. To robustly regulate the output of the uncertain plant, the control input u is generated by a (band-limited) PID-type controller $K(s) = (1.8124s^2 - 18.8558s + 0.1523)/(0.01s^2 + s)$.

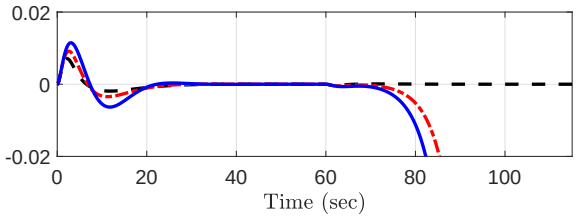

(a) Frequency deviation Δf (Hz)

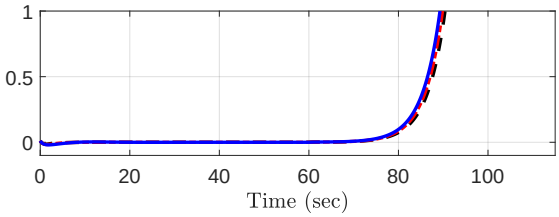

(b) Change in valve position ΔX (p.u.)

Figure 6.5: Simulation results with the conventional zero-dynamics attack (6.1.11) when $T_{\mathsf{h}} = 4 = T_{\mathsf{h,n}}$ (black dashed), $T_{\mathsf{h}} = 5$ (red dash-dotted), and $T_{\mathsf{h}} = 6$ (blue solid)

For the attack design, with a suitable coordinate change

$$\begin{aligned} x_1 &:= \mathtt{x}_1, \\ x_2 &:= -(1/T_{\mathsf{lm}})\mathtt{x}_1 + (K_{\mathsf{lm}}/T_{\mathsf{lm}})\mathtt{x}_2 - (2K_{\mathsf{lm}}/T_{\mathsf{lm}})\mathtt{x}_3, \\ z &:= \mathtt{x}_2 + (3T_{\mathsf{lm}}/T_{\mathsf{h}})(1/K_{\mathsf{lm}})\mathtt{x}_1, \end{aligned}$$

we transform (6.3.1) into the Byrnes-Isidori normal form (6.1.1). We omit the description of the system in the normal form due to the page limit, but one can verify that the resulting parameters ϕ, ψ, G, and S depend on T_{h}, and thus, are all uncertain, and that $S = 1/T_{\mathsf{h}} > 0$ so that the power generating system (6.3.1) is of non-minimum phase. It can also be seen that $\Delta f = x_1$, ΔP is a linear function of x_1 and x_2, and ΔX is a linear function of x_1, x_2, and z. Hence, with diverging $z(t)$, only $\Delta X(t)$ diverges when $x_1(t)$ and $x_2(t)$ are bounded. So, the goal of the adversary is set to enforce the valve position ΔX to become larger than 1 (p.u.) eventually, while the frequency deviation $\Delta f = y$ remains small as $|\Delta f| \leq 0.02$ (Hz). As a result, the attack leads to overuse of water in a forebay

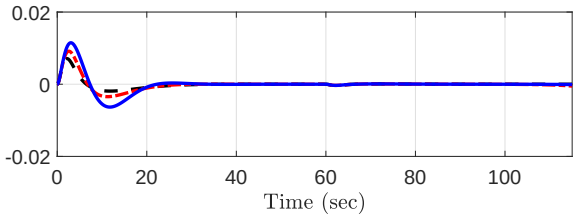

(a) Frequency deviation Δf (Hz)

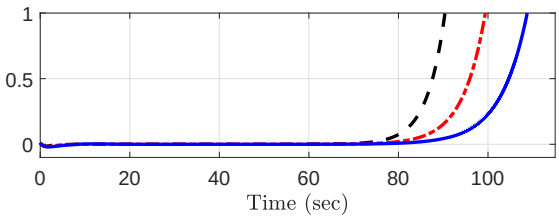

(b) Change in valve position ΔX (p.u.)

Figure 6.6: Simulation results with the proposed robust zero-dynamics attack (6.2.6) and (6.2.24) when $\tau = 0.001$, $T_{\mathsf{h}} = 4 = T_{\mathsf{h,n}}$ (black dashed), $T_{\mathsf{h}} = 5$ (red dash-dotted), and $T_{\mathsf{h}} = 6$ (blue solid)

for generating the same amount of power.

For comparison, we now construct two types of attack generator without knowledge on the value of T_{h}. One is the conventional zero-dynamics attack (6.1.11) with a nominal value $T_{\mathsf{h,n}} = 4$. The other is the proposed robust zero-dynamics attack (6.2.6) and (6.2.24) designed with the same $T_{\mathsf{h,n}}$, $\overline{z}_{\mathsf{u}} = 1.6$, and a saturation function $\bar{s}_{\mathsf{a}}(\hat{a})$ whose inactive region $\overline{\mathcal{A}}$ is selected as $\{\hat{a} : |\hat{a}| \leq 20000\}$. Initial conditions are set $z^{\mathsf{a}}(t_0) = 0.001$ for (6.1.11), $z^{\mathsf{a}}_{\mathsf{n}}(t_0) = -0.001$ for (6.2.6), and $p^{\mathsf{a}}(t_0) = [0; 0]$ for (6.2.24). Selection for $z^{\mathsf{a}}_{\mathsf{n}}(t_0)$ is motivated by the fact that, in the steady state, the regulated output $\Delta f = y = 0$ so that the steady state values for $\mathtt{x}$ and z are zero. (The effect of small mismatch between $z(t_0)$ and $z^{\mathsf{a}}_{\mathsf{n}}(t_0)$ will be observed as a small transient of $y(t)$ in the simulation result around $t = t_0$.)

Figure 6.5 and 6.6 depict the simulation results of applying the conventional attack (6.1.11) and the proposed attacks (6.2.6) and (6.2.24) with $\tau = 0.001$ to the uncertain plant (6.3.1) at the time instant $t = t_0 := 60$ (sec). As shown in these figures, when there is no uncertainty, both attacks work as desired and successfully

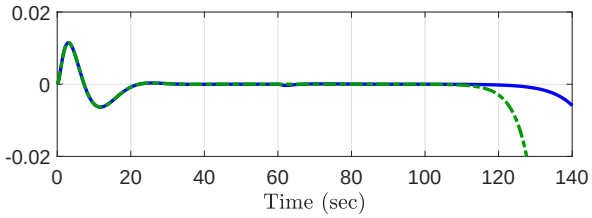

(a) Frequency deviation Δf (Hz)

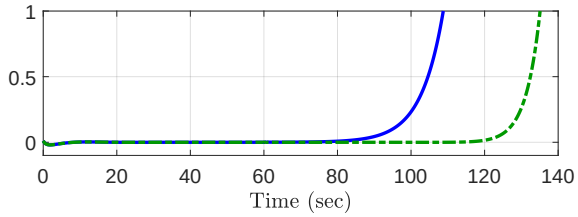

(b) Change in valve position ΔX (p.u.)

Figure 6.7: Simulation results with the robust zero-dynamics attack (6.2.6) and (6.2.24) where $T_{\mathsf{h}} = 6$ and $\tau = 0.005$ (green dash-dotted) and $\tau = 0.001$ (blue solid)

spoils the plant. However, the conventional scheme (6.1.4) immediately fails to be stealthy if it encounters the uncertain plant (Fig. 6.5), while the proposed attack (6.2.6) and (6.2.24) remains robust against model uncertainty (Figure 6.6). It is worth noting that ΔX with the robust zero-dynamics attack diverges at different paces dependent on the value of T_{h}. Indeed, this results from the fact that the real z-dynamics under the robust zero-dynamics attack is left alone, so that the divergence of $z(t)$ depends on the unstable mode of its dynamics (i.e., $S = 1/T_{\mathsf{h}}$).

On the other hand, Figure 6.7 depicts the plant's output y under the robust zero-dynamics attacks with different τ. The figure points out that for success of the attack, it is necessary for the adversary to take sufficiently small τ.

To investigate the presented attack further, we perform the same simulation of Fig. 6.6 again, with $T_{\mathsf{h}} = 6$ and a "noisy" measurement $y = C_2 x + n_{\mathsf{y}}$. Here, $n_{\mathsf{y}}(t)$ is selected to have the maximum magnitude as 2×10^{-3} (Hz) and have the uniform distribution. The simulation result is depicted in Figure 6.8, which indicates that the robust zero-dynamics attack still remains stealthy even in the

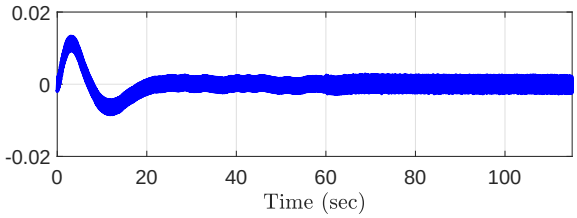

Figure 6.8: Frequency deviation Δf under the robust zero-dynamics attack (6.2.6) and (6.2.24) with noisy measurement

presence of measurement noise.

Chapter 7

Conclusion of Dissertation

The main objective of this dissertation is to bring new perspectives on the inverse model-based disturbance observer, which allows to resolve several problems modern control systems often encountered. The details are listed as follows.

i) In Chapter 2, we addressed the problem of recovering the (pre-defined) nominal tracking performance in an "asymptotic" sense for uncertain and minimum-phase linear systems. Motivated by the internal model principle, a standing assumption was that a part of external inputs are generated by an exogenous system. Under the hypothesis, we proposed a high-gain disturbance observer, into which the internal model of the external inputs is implicitly embedded. From the viewpoint of the singular perturbation theory with a modified notion of the quasi-steady-state, we showed that the proposed disturbance observer can capture the total disturbance quickly in transient and exactly in the steady-state; from this the asymptotic recovery of nominal performance is carried out.

ii) In Chapter 3, we extended the result of Chapter 2 (for linear mechanical systems) with no information on the frequency of the sinusoidal external input. Instead of utilizing the frequency explicitly in the disturbance observer design, in this work we employed an additional frequency identifier to adjust the unknown frequency of the external input in the steady state. By implementing the disturbance observer in Chapter 2 with the frequency estimate, we presented an adaptive robust controller that includes an "adaptive

internal model" into its structure. It was observed through simulation and experiments that the proposed controller can serve as an effective solution for the track-following problem of the optical disk drives.

iii) In Chapter 4, we dealt with the problem of constructing a output-feedback fault tolerant controller that guarantees "fault-free" tracking performance under actuator faults. Provided that the plant has redundant inputs and is of minimum-phase in an input-wise sense, the central idea was to allocate a virtual scalar input appropriately such that the minimum phaseness (in view of the scalar input) is maintained under any patterns of the faults. We presented a systematic design procedure of the control allocation law available under arbitrarily large (but bounded) model uncertainty. On top of that, a disturbance observer-based controller was constructed for the virtual scalar input, especially by taking into account the fact that the total disturbance (to be compensated by the disturbance observer) may experience abrupt jumps in the presence of faults.

iv) In Chapter 5, we presented a new "almost necessary and sufficient" condition for robust stability of the discrete-time disturbance observer controlled systems in sampled-data setting, under fast sampling. In particular, this work provided a "generalized" framework for robust stability analysis in the sense that it is available (a) "in whichever way" the nominal model and the baseline controller are discretized, and (b) no matter how the plant has "arbitrarily large" parametric uncertainty. Our stability analysis revealed an explicit constraint on the discrete-time disturbance observers, which may be violated when the disturbance observer is designed without consideration of the (unstable) sampling zeros. In this regard, we introduced new design methodologies for the discrete-time disturbance observers in order to handle the stability constraint under large parametric uncertainty. Moreover, a systematic design method to embed a disturbance model into the discrete-time disturbance observer was also proposed.

v) In Chapter 6, we addressed the problem of constructing a "robust" stealthy attack that compromises "uncertain" cyber-physical systems having unstable

zeros. Different from the conventional strategy, our key idea was to isolate the real zero-dynamics from the plant's input-output relation and to replace it with an auxiliary nominal zero-dynamics. It was shown that this idea can be realized in a practical sense, when the adversary maliciously uses the disturbance observer technique in the design of the attack signal.

APPENDIX

A.1 Design Guidelines of a_i for CT-DOBs

In this section, we will present two ways of constructing the coefficients a_i such that the associated $\mathrm{Z}_{k,j}(s)$ in (2.2.23) is SPR for given constants $\underline{g}$, $\overline{g}$, and g_{n}.

A.1.1 Recursive Design Algorithm

We start by introducing two technical lemmas which will play an important role in the main proof.

Lemma A.1.1. For given Hurwitz polynomial $\mathrm{h}(s)$, there exists $\overline{\mathsf{k}}_1 > 0$ such that the polynomial $\mathrm{h}'(s) := s\mathrm{h}(s) + \mathsf{k}$ is Hurwitz for all $\mathsf{k} \in (0, \overline{\mathsf{k}}_1)$. $\Diamond$

Proof. The proof of the lemma is provided in [BS08]. $\square$

Lemma A.1.2. Suppose that the Nyquist plot of a transfer function

$$\mathrm{L}(s) = \frac{\mathrm{p}(s)}{s^k \mathrm{q}(s)} \tag{A.1.1}$$

does not enter the disk $\mathcal{D}(\underline{g}/g_{\mathsf{n}}, \overline{g}/g_{\mathsf{n}})$ where k is a positive integer, $\mathrm{p}(s)$ is a polynomial satisfying $\mathrm{p}(0) > 0$, $\mathrm{q}(s)$ is a Hurwitz polynomial. Then there exists $\overline{\mathsf{k}}_2 > 0$ such that the Nyquist plot of

$$\mathrm{L}'(s) := \frac{\mathrm{p}(s)}{s^k \mathrm{q}(s)} + \mathsf{k}\frac{1}{s^{k+1}\mathrm{q}(s)} \tag{A.1.2}$$

also does not enter the disk $\mathcal{D}(\underline{g}/g_{\mathsf{n}}, \overline{g}/g_{\mathsf{n}})$ for all $\mathsf{k} \in (0, \overline{\mathsf{k}}_2)$. $\Diamond$

To obtain Lemma A.1.2, we need to prove the following property first.

Lemma A.1.3. Assume that the hypothesis of Lemma (A.1.2) holds. Then for given $\epsilon' > 0$, there exists $\overline{\omega} > 0$ such that the Nyquist plot $\mathrm{L}'(j\omega)$ of (A.1.2) satisfies

$$\left|\mathrm{L}'(j\omega)\right| = \left|\frac{\mathrm{p}(j\omega)}{(j\omega)^k \mathrm{q}(j\omega)} + \mathsf{k}\frac{1}{(j\omega)^{k+1}\mathrm{q}(j\omega)}\right| > \epsilon' \tag{A.1.3}$$

for all $\mathsf{k} > 0$ and for all $\omega \in [0, \overline{\omega}]$. $\Diamond$

Proof. Without loss of generality, one can express the frequency response $\mathrm{p}(j\omega)$ of $\mathrm{p}(s)$ as $\mathrm{p}(j\omega) = \mathrm{p}_{\mathrm{even}}(\omega) + j\mathrm{p}_{\mathrm{odd}}(\omega)$ where $\mathrm{p}_{\mathrm{even}}(\omega)$ and $\mathrm{p}_{\mathrm{odd}}(\omega)$ are some even and odd polynomials of ω, respectively. Then the frequency response of the "inverse" transfer function $1/\mathrm{L}'(s)$ is computed by

$$\begin{aligned}\left|\frac{1}{\mathrm{L}'(j\omega)}\right| &= \left|\frac{(j\omega)^{k+1}\mathrm{q}(j\omega)}{j\omega\mathrm{p}(j\omega) + \mathsf{k}}\right| = \left|\frac{(j\omega)^{k+1}\mathrm{q}(j\omega)}{j\omega\left(\mathrm{p}_{\mathrm{even}}(\omega) + j\mathrm{p}_{\mathrm{odd}}(\omega)\right) + \mathsf{k}}\right| \\ &= \frac{\omega^{k+1}|\mathrm{q}(j\omega)|}{\sqrt{\left(\mathsf{k} - \omega\mathrm{p}_{\mathrm{odd}}(\omega)\right)^2 + \left(\omega\mathrm{p}_{\mathrm{even}}(\omega)\right)^2}} \\ &\leq \frac{\omega^{k+1}|\mathrm{q}(j\omega)|}{\sqrt{\left(\omega\mathrm{p}_{\mathrm{even}}(\omega)\right)^2}} = \frac{\omega^k|\mathrm{q}(j\omega)|}{|\mathrm{p}_{\mathrm{even}}(\omega)|}\end{aligned} \tag{A.1.4}$$

where the inequality holds for all $\omega \geq 0$ regardless of k. We note that $\mathrm{p}(0) = \mathrm{p}_{\mathrm{even}}(0) > 0$ by the assumption. In addition, both $|\mathrm{q}(j\omega)|$ and $|\mathrm{p}_{\mathrm{even}}(\omega)|$ are continuous on $\omega \in [0, \infty)$. Therefore, there exists $\overline{\omega} > 0$ such that

$$\frac{\omega^k|\mathrm{q}(j\omega)|}{|\mathrm{p}_{\mathrm{even}}(\omega)|} \leq \frac{1}{\epsilon'} \quad \text{for all } \omega \in [0, \overline{\omega}], \tag{A.1.5}$$

from which the lemma is proved. $\square$

With the above lemma, we are ready to derive Lemma A.1.2.

Proof of Lemma A.1.2. Let ϵ' be $\epsilon' > |-1/\underline{\kappa}| > 0$. Then Lemma A.1.3 implies that there is $\overline{\omega} > 0$ such that (A.1.3) holds for all $\omega \in [0, \overline{\omega}]$ and for all $\mathsf{k} > 0$. Notice that the inequality results in that $\mathrm{L}'(j\omega)$ does not meet with the disk $\mathcal{D}(\underline{g}/g_{\mathsf{n}}, \overline{g}/g_{\mathsf{n}})$ at least for a partial frequency range $\omega \in [0, \overline{\omega}]$ regardless of $\mathsf{k} > 0$.

To see the situation on the remaining frequency range $\omega \in [\overline{\omega}, \infty)$, let us denote the center and the radius of the disk $\mathcal{D}(\underline{g}/g_{\mathsf{n}}, \overline{g}/g_{\mathsf{n}})$ as as $c_{\text{disk}} + j0$ (with a real number c_{disk}) and r_{disk}, respectively. Then a lower bound of the distance between $L'(j\omega)$ and $\mathcal{D}(\underline{g}/g_{\mathsf{n}}, \overline{g}/g_{\mathsf{n}})$ is computed by

$$\begin{aligned}
&\inf_{\omega\in[\overline{\omega},\infty)} \left|\mathrm{L}'(j\omega) - c_{\text{disk}}\right| - r_{\text{disk}} \\
&= \inf_{\omega\in[\overline{\omega},\infty)} \left|\mathrm{L}(j\omega) + \mathsf{k}\frac{1}{s^{k+1}\mathrm{q}(j\omega)} - c_{\text{disk}}\right| - r_{\text{disk}} \\
&\geq \left(\inf_{\omega\in[\overline{\omega},\infty)} |\mathrm{L}(j\omega) - c_{\text{disk}}| - r_{\text{disk}}\right) - \mathsf{k}\left(\sup_{\omega\in[\overline{\omega},\infty)} \left|\frac{1}{s^{k+1}\mathrm{q}(j\omega)}\right|\right). \qquad \text{(A.1.6)}
\end{aligned}$$

By the assumption, one has

$$\begin{aligned}
\inf_{\omega\in[\overline{\omega},\infty)} |\mathrm{L}(j\omega) - c_{\text{disk}}| - r_{\text{disk}} &\geq \inf_{\omega\in(-\infty,\infty)} |\mathrm{L}(j\omega) - c_{\text{disk}}| - r_{\text{disk}} \\
&=: \epsilon'' > 0. \qquad \text{(A.1.7)}
\end{aligned}$$

Moreover, since $|1/\big((j\omega)^{k+1}\mathrm{q}(j\omega)\big)|$ approaches zero as ω goes to infinity and $1/\big(s^{k+1}\mathrm{q}(s)\big)$ has no pole on the imaginary axis except the origin, $|1/\big((j\omega)^{k+1}\mathrm{q}(j\omega)\big)|$ is bounded for all $\omega \in [\overline{\omega}, \infty)$. Then it follows that there exists $\overline{\mathsf{k}}_2 > 0$ such that

$$\mathsf{k}\left(\sup_{\omega\in[\overline{\omega},\infty)} \left|\frac{1}{s^{k+1}\mathrm{q}(j\omega)}\right|\right) < \frac{h}{2} \qquad \text{(A.1.8)}$$

for all $\mathsf{k} \in (0, \overline{\mathsf{k}}_2)$. Applying two inequalities (A.1.7) and (A.1.8) into (A.1.6) then brings

$$\inf_{\omega\in[\overline{\omega},\infty)} \left|\mathrm{L}'(j\omega) - c_{\text{disk}}\right| - r_{\text{disk}} > \frac{\epsilon''}{2} > 0 \qquad \text{(A.1.9)}$$

for $\mathsf{k} \in (0, \overline{\mathsf{k}}_2)$, which means that the minimum distance between the Nyquist plot $\mathrm{L}'(j\omega)$ and the disk $D(\underline{\kappa}, \overline{\kappa})$ for the remaining frequency range $\omega \in [\overline{\omega}, \infty)$ is also nonnegative. □

Based on Lemmas A.1.1 and A.1.2, we now present a recursive design method

for a_i below. For this, let us define

$$\mathrm{p}_{\mathrm{spr}}(s) := \mathsf{a}_j s^j + \cdots + \mathsf{a}_0, \tag{A.1.10a}$$

$$\mathrm{q}_{\mathrm{spr}}(s) := s^{k-1} + \mathsf{a}_{k+j-1} s^{k-2} + \cdots + \mathsf{a}_{j+1} \tag{A.1.10b}$$

with which the transfer function $\mathrm{Z}_{k,j}(s)$ in (2.2.23) is rewritten as follows:

$$\mathrm{Z}_{k,j}(s) = \frac{1 + (\overline{g}/g_{\mathsf{n}})\mathrm{L}(s)}{1 + (\underline{g}/g_{\mathsf{n}})\mathrm{L}(s)} \tag{A.1.11}$$

where

$$\mathrm{L}(s) := \frac{\mathsf{a}_j s^j + \cdots + \mathsf{a}_0}{s^{k+j} + \mathsf{a}_{k+j} s^{k+j-1} + \cdots + \mathsf{a}_{j+1} s^{j+1}} = \frac{\mathrm{p}_{\mathrm{spr}}(s)}{s^{j+1}\mathrm{q}_{\mathrm{spr}}(s)}. \tag{A.1.12}$$

Notice that the SISO transfer function $\mathrm{Z}_{k,j}(s)$ is SPR if the following two statements hold:

(a) its denominator

$$\mathrm{h}(s) := s^{j+1}\mathrm{q}_{\mathrm{spr}}(s) + \frac{\underline{g}}{g_{\mathsf{n}}}\mathrm{p}_{\mathrm{spr}}(s) \tag{A.1.13}$$

is Hurwitz, and

(b) the Nyquist plot $\mathrm{L}(j\omega)$ of (A.1.12) does not enter the disk $\mathcal{D}((\underline{g}/g_{\mathsf{n}}), \overline{g}/g_{\mathsf{n}})$.

For $i = 1, \ldots, j+1$, let

$$\mathrm{p}_{\mathrm{spr},i}(s) := \mathsf{a}_j s^{i-1} + \mathsf{a}_{j-1} s^{i-2} + \cdots + \mathsf{a}_{j+1-i}, \tag{A.1.14a}$$

$$\mathrm{h}_i(s) := s^i \mathrm{q}_{\mathrm{spr}}(s) + \frac{\underline{g}}{g_{\mathsf{n}}}\mathrm{p}_{\mathrm{spr},i}(s) \quad \text{and} \quad \mathrm{L}_i(s) := \frac{\mathrm{p}_{\mathrm{spr},i}(s)}{s^i \mathrm{q}_{\mathrm{spr}}(s)}. \tag{A.1.14b}$$

so that $\mathrm{h}_{j+1}(s) = \mathrm{h}(s)$ and $\mathrm{L}_{j+1}(s) = \mathrm{L}(s)$.

Now, a recursive design procedure for the coefficients is introduced below.

Procedure A.1.4. (Recursive algorithm for a_i)

STEP 0 Choose $\mathsf{a}_{k+j-1}, \ldots, \mathsf{a}_{j+1}$ such that $\mathrm{q}_{\mathrm{spr}}(s)$ in (A.1.10) is Hurwitz. Then select a small $\mathsf{a}_j > 0$ satisfying that $\mathrm{h}_1(s)$ is Hurwitz and the Nyquist plot $\mathrm{L}_1(j\omega)$ does not enter the disk $\mathcal{D}(\underline{g}/g_{\mathsf{n}}, \overline{g}/g_{\mathsf{n}})$.

STEP i $(i = 1, \dots, j)$ Choose $\overline{\mathsf{k}}_{j-i,1} > 0$ such that $\mathrm{h}_{i+1}(s)$ is Hurwitz for all $\mathsf{a}_{j-i} \in (0, \overline{\mathsf{k}}_{j-i,1})$ (by Lemma A.1.1), and take $\overline{\mathsf{k}}_{j-i,2} > 0$ satisfying that the Nyquist plot of $\mathrm{L}_{i+1}(s)$ does not enter the disk $\mathcal{D}(\underline{g}/g_{\mathsf{n}}, \overline{g}/g_{\mathsf{n}})$ for all $\mathsf{a}_{j-i} \in (0, \overline{\mathsf{k}}_{j-i,2})$ (by Lemma A.1.2). Select $0 < \mathsf{a}_{j-i} < \min\{\overline{\mathsf{k}}_{j-i,1}, \overline{\mathsf{k}}_{j-i,2}\}$.

$\Diamond$

It is further noted that the discussions so far in this subsection (and Procedure A.1.4) serves as the proof of Theorem 2.2.1.

A.1.2 Bilinear Matrix Inequality-based Design

The recursive design procedure above is of particular importance, because it guarantees the existence of the coefficients a_i. At the same time, however, this method is somewhat complicated in a sense and may bring a conservative value as the coefficients are selected one by one (see also [KBP14] for a similar discussion for the linear DOB case).

To overcome such drawbacks, we here present an optimization-based design method. This alternative way relies on the well-known Kalman-Yakubovich-Popov (KYP) lemma [Kha96], which implies that $\mathrm{Z}_{k,j}(s)$ in (2.2.1) is SPR if and only if there are a constant $\epsilon_{\mathsf{z}} \in \mathbb{R}$ and a square matrix $P_{\mathsf{z}} \in \mathbb{R}^{(k+j)\times(k+j)}$ such that the following matrix inequalities are satisfied at once:

$$\epsilon_{\mathsf{z}} > 0, \quad P_{\mathsf{z}} = P_{\mathsf{z}}^{\top} > 0, \tag{A.1.15a}$$

$$\begin{bmatrix} P_{\mathsf{z}}A_{\mathsf{z}} + A_{\mathsf{z}}^{\top}P_{\mathsf{z}} + \epsilon_{\mathsf{z}}P_{\mathsf{z}} & P_{\mathsf{z}}B_{\mathsf{z}} - C_{\mathsf{z}}^{\top} \\ B_{\mathsf{z}}^{\top}P_{\mathsf{z}} - C_{\mathsf{z}} & -D_{\mathsf{z}} - D_{\mathsf{z}}^{\top} \end{bmatrix} \leq 0 \tag{A.1.15b}$$

where the quadruple $(A_{\mathsf{z}}, B_{\mathsf{z}}, C_{\mathsf{z}}, D_{\mathsf{z}})$ is a minimal realization of

$$\begin{aligned} \mathrm{Z}_{k,j}(s) &= \frac{s^{k+j} + \mathsf{a}_{k+j-1}s^{k+j-1} + \mathsf{a}_{j+1}s^{j+1} + \dfrac{\overline{g}}{g_{\mathsf{n}}}\mathsf{a}_j s^j + \cdots + \dfrac{\overline{g}}{g_{\mathsf{n}}}\mathsf{a}_0}{s^{k+j} + \mathsf{a}_{k+j-1}s^{k+j-1} + \mathsf{a}_{j+1}s^{j+1} + \dfrac{\underline{g}}{g_{\mathsf{n}}}\mathsf{a}_j s^j + \cdots + \dfrac{\underline{g}}{g_{\mathsf{n}}}\mathsf{a}_0} \\ &= 1 + \frac{\dfrac{\overline{g}-\underline{g}}{g_{\mathsf{n}}}\mathsf{a}_j s^j + \cdots + \dfrac{\overline{g}-\underline{g}}{g_{\mathsf{n}}}\mathsf{a}_0}{s^{k+j} + \mathsf{a}_{k+j-1}s^{k+j-1} + \mathsf{a}_{j+1}s^{j+1} + \dfrac{\underline{g}}{g_{\mathsf{n}}}\mathsf{a}_j s^j + \cdots + \dfrac{\underline{g}}{g_{\mathsf{n}}}\mathsf{a}_0}. \end{aligned}$$

Without lose of generality, let $(A_{\mathsf{z}}, B_{\mathsf{z}}, C_{\mathsf{z}}, D_{\mathsf{z}})$ be the observable canonical form of $\mathrm{Z}_{k,j}(s)$; i.e.,

$$A_{\mathsf{z}} = A_{k+j} - \mathrm{blockdiag}\left(I_{k-1}, \frac{g}{g_{\mathsf{n}}} I_{j+1}\right) \overline{\alpha} C_{k+j}, \tag{A.1.16a}$$

$$B_{\mathsf{z}} = \frac{\overline{g} - g}{g_{\mathsf{n}}} \mathrm{blockdiag}\left(O_{k-1}, I_{j+1}\right) \overline{\alpha}, \quad C_{\mathsf{z}} = C_{k+j}, \quad D_{\mathsf{z}} = 1. \tag{A.1.16b}$$

It is important to note that the matrix inequalities in (A.1.15b) are not linear but "bilinear" with respect to the matrix P_{z} and the vector $\overline{\alpha} = [\mathsf{a}_{k+j-1}; \cdots; \mathsf{a}_0]$. Therefore the problem of constructing a_i can be recast as finding a solution of the bilinear matrix inequalities (A.1.15b), which is enabled via some optimization solvers (for instance, PENLAB [KBP14, FKS13]). We emphasize again that the feasibility of this optimization problem is readily ensured by the theoretical result in Theorem 2.2.1.

A.2 Properties of δ in (3.3.19)

For ease of explanation, we rewrite δ as

$$\delta = \delta_1 + \delta_2 + \delta_3 + \delta_4$$

with the four sub-components

$$\begin{aligned}
\delta_1 &:= \left(1 - \frac{g}{g_{\mathsf{n}}}\right) \left(\overline{\gamma}(\hat{\theta}; \tau) - \overline{\gamma}(\theta; \tau)\right) \bar{s}_{\mathsf{w}}(C_4 \eta) + \frac{g}{g_{\mathsf{n}}} \left(\overline{\gamma}(\hat{\theta}; \tau) - \overline{\gamma}(\theta; \tau)\right) C_4 \eta^{\star}_{\mathrm{ext}}, \\
\delta_2 &:= \left(1 - \frac{g}{g_{\mathsf{n}}}\right) \left(\overline{\gamma}(\theta; \tau) - \overline{\gamma}(\theta; 0)\right) \bar{s}_{\mathsf{w}}(C_4 \eta) + \frac{g}{g_{\mathsf{n}}} \left(\overline{\gamma}(\theta; \tau) - \overline{\gamma}(\theta; 0)\right) C_4 \eta^{\star}_{\mathrm{ext}} \\
&\quad + \overline{\gamma}(\theta; 0) C_4 \eta^{\star}_{\mathrm{ext}} - \overline{\gamma}(\theta; \tau) C_4 \eta^{\star}_{\mathrm{ext}}, \\
\delta_3 &:= \underline{\Upsilon}(\tau) \frac{\partial \Gamma}{\partial \hat{\theta}} \dot{\hat{\theta}} \Phi_{\mathsf{n}} \frac{1}{g_{\mathsf{n}}} x, \\
\delta_4 &:= \overline{\gamma}(\theta; \tau) C_4 \eta^{\star}_{\mathrm{ext}} + (A_4 - \overline{\alpha} C_4) \eta^{\star}_{\mathrm{ext}} - \tau \dot{\eta}^{\star}_{\mathrm{ext}}.
\end{aligned}$$

We now show that each sub-component δ_i, $i = 1, \ldots, 4$, is a continuous function of the time t, the state variables, and the parameter τ such that (3.3.12) holds for

all $t \geq 0$; thus, their linear combination δ also does. Some useful equalities are

$$\overline{\gamma}(\hat{\theta};\tau) - \overline{\gamma}(\theta;\tau) = -\tau^2 \begin{bmatrix} 0 \\ 1 \\ \mathsf{a}_3 \\ 0 \end{bmatrix} \tilde{\theta} = -\tau^2 A_4 \overline{\alpha}^\star \tilde{\theta},$$

$$\overline{\gamma}(\theta;\tau) - \overline{\gamma}(\theta;0) = -\tau^2 \begin{bmatrix} 0 \\ 1 \\ \mathsf{a}_3 \\ 0 \end{bmatrix} \theta = -\tau^2 A_4 \overline{\alpha}^\star \theta,$$

$$\underline{\Upsilon}(\tau) \frac{\partial \Gamma}{\partial \hat{\theta}} = \begin{bmatrix} -\tau & 0 \\ -\mathsf{a}_3\tau & -\tau^2 \\ 0 & -\mathsf{a}_3\tau^2 \\ 0 & 0 \end{bmatrix} = -\begin{bmatrix} \tau\overline{\alpha}^\star & \tau^2 A_4 \overline{\alpha}^\star \end{bmatrix}.$$

After some computations, one has

$$\begin{aligned} &\delta_1\big(t, \tilde{\theta}, \tilde{\chi}, \tilde{\eta}_{\text{ext}}; \tau\big) \qquad \text{(A.2.1)} \\ &= \Big(\overline{\gamma}(\hat{\theta};\tau) - \overline{\gamma}(\theta;\tau)\Big) \left(\left(1 - \frac{g}{g_{\mathsf{n}}}\right) \bar{s}(C_4\eta) + \frac{g}{g_{\mathsf{n}}} C_4 \eta^\star_{\text{ext}} \right) \\ &= -\tau^2 A_4 \overline{\alpha}^\star \tilde{\theta} \Bigg(\left(1 - \frac{g}{g_{\mathsf{n}}}\right) \bar{s}_{\mathsf{w}}\big(C_4\tilde{\eta}_{\text{ext}} + \mathsf{C}_{\text{total}}\tilde{\chi} + d_{\text{total},\mathsf{n}}(t)\big) \\ &\qquad\qquad + \frac{g}{g_{\mathsf{n}}} \left(\mathsf{C}_{\text{total}}\tilde{\chi} + d_{\text{total},\mathsf{n}}(t)\right) \Bigg), \\ &\delta_2\big(t, \tilde{\chi}, \tilde{\eta}_{\text{ext}}; \tau\big) \qquad \text{(A.2.2)} \\ &= \Big(\overline{\gamma}(\theta;\tau) - \overline{\gamma}(\theta;0)\Big) \left(1 - \frac{g}{g_{\mathsf{n}}}\right) \left(\bar{s}_{\mathsf{w}}(C_4\eta) - C_4\eta^\star_{\text{ext}}\right) \\ &= -\tau^2 A_4 \overline{\alpha}^\star \theta \left(1 - \frac{g}{g_{\mathsf{n}}}\right) \\ &\qquad \times \left(\bar{s}_{\mathsf{w}}\Big(C_4\tilde{\eta} + \mathsf{C}_{\text{total}}\tilde{\chi} + d_{\text{total},\mathsf{n}}(t)\Big) - \Big(\mathsf{C}_{\text{total}}\tilde{\chi} + d_{\text{total},\mathsf{n}}(t)\Big) \right) \\ &= -\tau^2 A_4 \overline{\alpha}^\star \theta \left(1 - \frac{g}{g_{\mathsf{n}}}\right) \Omega(t, \tilde{\chi}, C_4\tilde{\eta}_{\text{ext}}), \\ &\delta_3\big(t, \tilde{\theta}, \tilde{\chi}, \tilde{\chi}_{\mathsf{n}}, \tilde{\zeta}, \tilde{\eta}_{\text{ext}}; \tau\big) \qquad \text{(A.2.3)} \end{aligned}$$

$$
\begin{aligned}
&= -\begin{bmatrix} \tau\overline{\alpha}^\star & \tau^2 A_4 \overline{\alpha}^\star \end{bmatrix} \dot{\tilde{\theta}} \Phi_{\mathsf{n}} \frac{1}{g_{\mathsf{n}}} \Big((x - x_{\mathsf{n}}(t)) + x_{\mathsf{n}}(t) \Big) \\
&= -\begin{bmatrix} \tau\overline{\alpha}^\star & \tau^2 A_4 \overline{\alpha}^\star \end{bmatrix} \kappa \\
&\quad \times \Big(-\Xi^\top(t) C_3^\top C_3 \Xi(t) \tilde{\theta} + \Xi^\top(t) \Big(\mathsf{M}_{\theta,1} \tilde{\chi} + \mathsf{M}_{\theta,2} \tilde{\chi}_{\mathsf{n}} + \mathsf{M}_{\theta,3} \tilde{\zeta} + \mathsf{E}_\theta \Omega(t, \tilde{\chi}, C_4 \tilde{\eta}_{\text{ext}}) \Big) \Big) \\
&\quad \times \Phi_{\mathsf{n}} \frac{1}{g_{\mathsf{n}}} \Big(\begin{bmatrix} I & O \end{bmatrix} \tilde{\chi} + x_{\mathsf{n}}(t) \Big).
\end{aligned}
$$

From this, the arguments on the first three sub-components δ_1, δ_2, and δ_3 are readily obtained. For the last term, we first note that

$$
\begin{aligned}
d_{\text{total}} - d^\star_{\text{total},\mathsf{n}} &= \mathsf{C}_{\text{total}} \tilde{\chi} + \mathsf{C}_{\text{total}} \tilde{\chi}_{\mathsf{n}}, \\
\dot{d}_{\text{total}} - \dot{d}^\star_{\text{total},\mathsf{n}} &= \mathsf{C}_{\text{total}} \dot{\tilde{\chi}} + \mathsf{C}_{\text{total}} \dot{\tilde{\chi}}_{\mathsf{n}} \\
&= \mathsf{C}_{\text{total}} \mathsf{A}_{\mathsf{n}} \tilde{\chi} + \mathsf{C}_{\text{total}} \mathsf{E}_\chi \Omega(t, \tilde{\chi}, C_4 \tilde{\eta}_{\text{ext}}) + \mathsf{C}_{\text{total}} \mathsf{A}_{\mathsf{n}} \tilde{\chi}_{\mathsf{n}}.
\end{aligned}
$$

Using these equalities, δ_4 can be expressed as

$$
\begin{aligned}
&\delta_4\big(t, \tilde{\chi}, \tilde{\chi}_{\mathsf{n}}, \tilde{\eta}_{\text{ext}}; \tau\big) \\
&= \begin{bmatrix} 0 \\ \mathsf{a}_2 - \tau^2\theta \\ \mathsf{a}_1 - \tau^2 \mathsf{a}_3 \theta \\ \mathsf{a}_0 \end{bmatrix} C_4 \eta^\star_{\text{ext}} + A_4 \eta^\star_{\text{ext}} - \begin{bmatrix} \mathsf{a}_3 \\ \mathsf{a}_2 \\ \mathsf{a}_1 \\ \mathsf{a}_0 \end{bmatrix} C_4 \eta^\star_{\text{ext}} - \tau \dot{\eta}^\star_{\text{ext}} \\
&= \begin{bmatrix} 0 \\ \mathsf{a}_2 \\ \mathsf{a}_1 \\ \mathsf{a}_0 \end{bmatrix} d_{\text{total}} - \begin{bmatrix} 0 \\ \tau^2\theta \\ \tau^2 \mathsf{a}_3 \theta \\ 0 \end{bmatrix} d_{\text{total}} + \begin{bmatrix} \mathsf{a}_3 \\ 0 \\ 0 \\ 0 \end{bmatrix} d_{\text{total}} - \begin{bmatrix} \mathsf{a}_3 \\ \mathsf{a}_2 \\ \mathsf{a}_1 \\ \mathsf{a}_0 \end{bmatrix} d_{\text{total}} \\
&\quad + \begin{bmatrix} \tau {d^\star_{\text{total},\mathsf{n}}}^{(1)} \\ \tau^2 {d^\star_{\text{total},\mathsf{n}}}^{(2)} + \tau \mathsf{a}_3 {d^\star_{\text{total},\mathsf{n}}}^{(1)} + \tau^2 \theta d^\star_{\text{total},\mathsf{n}} \\ \tau^3 {d^\star_{\text{total},\mathsf{n}}}^{(3)} + \tau^2 \mathsf{a}_3 {d^\star_{\text{total},\mathsf{n}}}^{(2)} + \tau^3 \theta {d^\star_{\text{total},\mathsf{n}}}^{(1)} + \tau^2 \mathsf{a}_3 \theta d^\star_{\text{total},\mathsf{n}} \\ 0 \end{bmatrix} - \tau \begin{bmatrix} 1 \\ \mathsf{a}_3 \\ 0 \\ 0 \end{bmatrix} \dot{d}_{\text{total}}
\end{aligned}
$$

$$
\begin{aligned}
&- \tau \begin{bmatrix} 0 \\ \tau {d^\star_{\text{total},\mathsf{n}}}^{(2)} \\ \tau^2 {d^\star_{\text{total},\mathsf{n}}}^{(3)} + \tau \mathsf{a}_3 {d^\star_{\text{total},\mathsf{n}}}^{(2)} + \tau^2 \theta {d^\star_{\text{total},\mathsf{n}}}^{(1)} \\ \tau^3 {d^\star_{\text{total},\mathsf{n}}}^{(4)} + \tau^2 \mathsf{a}_3 {d^\star_{\text{total},\mathsf{n}}}^{(3)} + \tau^3 \theta {d^\star_{\text{total},\mathsf{n}}}^{(2)} + \tau^2 \mathsf{a}_3 \theta {d^\star_{\text{total},\mathsf{n}}}^{(1)} \end{bmatrix} \\
&= -\tau^2 \begin{bmatrix} 0 \\ \theta \\ \mathsf{a}_3 \theta \\ 0 \end{bmatrix} (d_{\text{total}} - d^\star_{\text{total},\mathsf{n}}) - \tau \begin{bmatrix} 1 \\ \mathsf{a}_3 \\ 0 \\ 0 \end{bmatrix} (\dot{d}_{\text{total}} - \dot{d}_{\text{total},\mathsf{n}}) \\
&\quad - \tau \begin{bmatrix} 0 \\ 0 \\ 0 \\ \tau^3 {d^\star_{\text{total},\mathsf{n}}}^{(4)} + \tau^2 \mathsf{a}_3 {d^\star_{\text{total},\mathsf{n}}}^{(3)} + \tau^3 \theta {d^\star_{\text{total},\mathsf{n}}}^{(2)} + \tau^2 \mathsf{a}_3 \theta {d^\star_{\text{total},\mathsf{n}}}^{(1)} \end{bmatrix} \\
&= -\tau^2 A_4 \overline{\alpha}^\star \theta \Big(\mathsf{C}_{\text{total}} \tilde{\chi} + \mathsf{C}_{\text{total}} \tilde{\chi}_{\mathsf{n}} \Big) \\
&\quad - \tau \overline{\alpha}^\star \Big(\mathsf{C}_{\text{total}} \mathsf{A}_{\mathsf{n}} \tilde{\chi} + \mathsf{C}_{\text{total}} \mathsf{E}_\chi \Omega\big(t, \tilde{\chi}, C_4 \tilde{\eta}_{\text{ext}}\big) + \mathsf{C}_{\text{total}} \mathsf{A}_{\mathsf{n}} \tilde{\chi}_{\mathsf{n}} \Big) \\
&\quad - B_4 \Big((\tau \mathfrak{s})^4 + \mathsf{a}_3 (\tau \mathfrak{s})^3 + \tau^2 \theta (\tau \mathfrak{s})^2 + \tau^2 \mathsf{a}_3 \theta (\tau \mathfrak{s}) \Big) d^\star_{\text{total},\mathsf{n}}(t).
\end{aligned}
$$

It is noted that the last term of the equality is identically zero. Indeed, by definition $d^\star_{\text{total},\mathsf{n}}(t)$ is a biased sinusoidal signal whose frequency is given by $\sigma > 0$. This implies that

$$
\begin{aligned}
&\Big((\tau \mathfrak{s})^4 + \mathsf{a}_3 (\tau \mathfrak{s})^3 + \tau^2 \theta (\tau \mathfrak{s})^2 + \tau^2 \mathsf{a}_3 \theta (\tau \mathfrak{s}) \Big) d^\star_{\text{total},\mathsf{n}}(t) \\
&= \tau^2 \Big(\mathfrak{s}^2 + \sigma^2 \Big) \Big(\tau \mathfrak{s} + \mathsf{a}_3 \Big) d^\star_{\text{total},\mathsf{n}}(t) \equiv 0.
\end{aligned} \tag{A.2.4}
$$

This completes the claim on δ_4 and thus on δ.

A.3 Derivation of Normal Form Representation (6.3.1) of Power Generating System

Let us consider a power generating system with a hybro turbine that consists of (see also [Kun94, Tan10])

- governor

$$\mathrm{G}_{\mathsf{g}}(s) = \frac{1}{T_{\mathsf{g}}s + 1}, \tag{A.3.1a}$$

- hydro turbine

$$\mathrm{G}_{\mathsf{h}}(s) = \frac{-T_{\mathsf{h}}s + 1}{0.5T_{\mathsf{h}}s + 1} = \frac{-2(0.5T_{\mathsf{h}}s + 1) + 3}{0.5T_{\mathsf{h}}s + 1} = -2 + \frac{3}{0.5T_{\mathsf{h}}s + 1} \tag{A.3.1b}$$

- load and machine

$$\mathrm{G}_{\mathsf{lm}}(s) = \frac{K_{\mathsf{lm}}}{T_{\mathsf{lm}}s + 1}. \tag{A.3.1c}$$

where the outputs of the components are given by the incremental frequency deviation Δf (Hz), the change in generator output ΔP (p.u.), and the change in governor valve position ΔX (p.u.). The overall configuration of the power generating system is depicted in Figure 6.4. With a coordinate transformation

$$\mathtt{x}_1 := \Delta f, \tag{A.3.2a}$$

$$\mathtt{x}_2 := \Delta P + 2\Delta X, \tag{A.3.2b}$$

$$\mathtt{x}_3 := \Delta X, \tag{A.3.2c}$$

one can easily represent the plant in the state space as:

$$\dot{\mathtt{x}}_1 = -\frac{1}{T_{\mathsf{lm}}}\mathtt{x}_1 + \frac{K_{\mathsf{lm}}}{T_{\mathsf{lm}}}\Delta P = -\frac{1}{T_{\mathsf{lm}}}\mathtt{x}_1 + \frac{K_{\mathsf{lm}}}{T_{\mathsf{lm}}}(\mathtt{x}_2 - 2\mathtt{x}_3), \qquad \Delta f = \mathtt{x}_1, \tag{A.3.3a}$$

$$\dot{\mathtt{x}}_2 = -\frac{2}{T_{\mathsf{h}}}\mathtt{x}_2 + \frac{6}{T_{\mathsf{h}}}\Delta X = -\frac{2}{T_{\mathsf{h}}}\mathtt{x}_2 + \frac{6}{T_{\mathsf{h}}}\mathtt{x}_3, \qquad \Delta P = \mathtt{x}_2 - 2\mathtt{x}_3, \tag{A.3.3b}$$

$$\dot{\mathtt{x}}_3 = -\frac{1}{T_{\mathsf{g}}}\mathtt{x}_3 + \frac{1}{T_{\mathsf{g}}}\left(u - \frac{1}{R}\Delta f\right) = -\frac{1}{T_{\mathsf{g}}}\mathtt{x}_3 + \frac{1}{T_{\mathsf{g}}}\left(u - \frac{1}{R}\mathtt{x}_1\right), \quad \Delta X = \mathtt{x}_3. \tag{A.3.3c}$$

To proceed further, we introduce an additional coordinate change

$$x_1 := \mathtt{x}_1, \tag{A.3.4a}$$

$$x_2 := -\frac{1}{T_{\mathsf{lm}}}\mathtt{x}_1 + \frac{K_{\mathsf{lm}}}{T_{\mathsf{lm}}}\mathtt{x}_2 - \frac{2K_{\mathsf{lm}}}{T_{\mathsf{lm}}}\mathtt{x}_3, \tag{A.3.4b}$$

$$z := \mathtt{x}_2 + \frac{3T_{\mathsf{lm}}}{K_{\mathsf{lm}}}\frac{1}{T_{\mathsf{h}}}\mathtt{x}_1. \tag{A.3.4c}$$

It is noted that in this coordinate, the state $\mathtt{x} = [\mathtt{x}_1; \mathtt{x}_2; \mathtt{x}_3]$ can be expressed as

$$\mathtt{x}_1 := x_1, \tag{A.3.5a}$$

$$\mathtt{x}_2 := z - \frac{3T_{\mathsf{lm}}}{T_{\mathsf{h}}}\frac{1}{K_{\mathsf{lm}}}\mathtt{x}_1 = z - \frac{3T_{\mathsf{lm}}}{K_{\mathsf{lm}}}\frac{1}{T_{\mathsf{h}}}x_1, \tag{A.3.5b}$$

$$\begin{aligned}\mathtt{x}_3 &:= \frac{T_{\mathsf{lm}}}{2K_{\mathsf{lm}}}\left(-x_2 - \frac{1}{T_{\mathsf{lm}}}\mathtt{x}_1 + \frac{K_{\mathsf{lm}}}{T_{\mathsf{lm}}}\mathtt{x}_2\right)\\ &= -\frac{T_{\mathsf{lm}}}{2K_{\mathsf{lm}}}x_2 - \frac{1}{2K_{\mathsf{lm}}}x_1 + \frac{1}{2}\left(z - \frac{3T_{\mathsf{lm}}}{K_{\mathsf{lm}}}\frac{1}{T_{\mathsf{h}}}x_1\right)\\ &= \left(-\frac{1}{2K_{\mathsf{lm}}} - \frac{3T_{\mathsf{lm}}}{2K_{\mathsf{lm}}}\frac{1}{T_{\mathsf{h}}}\right)x_1 - \frac{T_{\mathsf{lm}}}{2K_{\mathsf{lm}}}x_2 + \frac{1}{2}z.\end{aligned} \tag{A.3.5c}$$

By this, the time derivatives of $\mathtt{x}_i$ in (A.3.3) are rewritten as

$$\begin{aligned}\dot{\mathtt{x}}_1 &= -\frac{1}{T_{\mathsf{lm}}}\mathtt{x}_1 + \frac{K_{\mathsf{lm}}}{T_{\mathsf{lm}}}\mathtt{x}_2 - \frac{2K_{\mathsf{lm}}}{T_{\mathsf{lm}}}\mathtt{x}_3\\ &= -\frac{1}{T_{\mathsf{lm}}}x_1 + \frac{K_{\mathsf{lm}}}{T_{\mathsf{lm}}}\left(z - \frac{3T_{\mathsf{lm}}}{K_{\mathsf{lm}}}\frac{1}{T_{\mathsf{h}}}x_1\right)\\ &\quad - \frac{2K_{\mathsf{lm}}}{T_{\mathsf{lm}}}\left(\left(-\frac{1}{2K_{\mathsf{lm}}} - \frac{3T_{\mathsf{lm}}}{2K_{\mathsf{lm}}}\frac{1}{T_{\mathsf{h}}}\right)x_1 - \frac{T_{\mathsf{lm}}}{2K_{\mathsf{lm}}}x_2 + \frac{1}{2}z\right)\\ &= x_2,\end{aligned} \tag{A.3.6a}$$

$$\begin{aligned}\dot{\mathtt{x}}_2 &= -\frac{2}{T_{\mathsf{h}}}\mathtt{x}_2 + \frac{6}{T_{\mathsf{h}}}\mathtt{x}_3\\ &= -\frac{2}{T_{\mathsf{h}}}\left(z - \frac{3T_{\mathsf{lm}}}{K_{\mathsf{lm}}}\frac{1}{T_{\mathsf{h}}}x_1\right) + \frac{6}{T_{\mathsf{h}}}\left(\left(-\frac{1}{2K_{\mathsf{lm}}} - \frac{3T_{\mathsf{lm}}}{2K_{\mathsf{lm}}}\frac{1}{T_{\mathsf{h}}}\right)x_1 - \frac{T_{\mathsf{lm}}}{2K_{\mathsf{lm}}}x_2 + \frac{1}{2}z\right)\\ &= \left(-\frac{3}{K_{\mathsf{lm}}}\frac{1}{T_{\mathsf{h}}} - \frac{3T_{\mathsf{lm}}}{K_{\mathsf{lm}}}\frac{1}{T_{\mathsf{h}}^2}\right)x_1 - \frac{T_{\mathsf{lm}}}{K_{\mathsf{lm}}}\frac{3}{T_{\mathsf{h}}}x_2 + \frac{1}{T_{\mathsf{h}}}z,\end{aligned} \tag{A.3.6b}$$

$$\begin{aligned}\dot{\mathtt{x}}_3 &= -\frac{1}{T_{\mathsf{g}}}\mathtt{x}_3 - \frac{1}{R}\frac{1}{T_{\mathsf{g}}}\mathtt{x}_1 + \frac{1}{T_{\mathsf{g}}}u\\ &= -\frac{1}{T_{\mathsf{g}}}\left(\left(-\frac{1}{2K_{\mathsf{lm}}} - \frac{3T_{\mathsf{lm}}}{2K_{\mathsf{lm}}}\frac{1}{T_{\mathsf{h}}}\right)x_1 - \frac{T_{\mathsf{lm}}}{2K_{\mathsf{lm}}}x_2 + \frac{1}{2}z\right) - \frac{1}{R}\frac{1}{T_{\mathsf{g}}}x_1 + \frac{1}{T_{\mathsf{g}}}u\end{aligned}$$

$$= \left(\frac{1}{T_\mathsf{g}}\frac{1}{2K_\mathsf{lm}} + \frac{1}{T_\mathsf{g}}\frac{3T_\mathsf{lm}}{2K_\mathsf{lm}}\frac{1}{T_\mathsf{h}} - \frac{1}{R}\frac{1}{T_\mathsf{g}}\right)x_1 + \frac{1}{2T_\mathsf{g}}\frac{T_\mathsf{lm}}{K_\mathsf{lm}}x_2 - \frac{1}{2T_\mathsf{g}}z + \frac{1}{T_\mathsf{g}}u. \tag{A.3.6c}$$

By differentiating the variables in (A.3.4) along with the $\mathtt{x}$-dynamics (A.3.3), we have

$$\dot{x}_1 = \dot{\mathtt{x}}_1 = x_2 \tag{A.3.7a}$$

$$\begin{aligned}
\dot{x}_2 &= -\frac{1}{T_\mathsf{lm}}\dot{\mathtt{x}}_1 + \frac{K_\mathsf{lm}}{T_\mathsf{lm}}\dot{\mathtt{x}}_2 - \frac{2K_\mathsf{lm}}{T_\mathsf{lm}}\dot{\mathtt{x}}_3 \\
&= -\frac{1}{T_\mathsf{lm}}x_2 + \frac{K_\mathsf{lm}}{T_\mathsf{lm}}\left(\left(-\frac{3}{K_\mathsf{lm}}\frac{1}{T_\mathsf{h}} - \frac{3T_\mathsf{lm}}{K_\mathsf{lm}}\frac{1}{T_\mathsf{h}^2}\right)x_1 - \frac{T_\mathsf{lm}}{K_\mathsf{lm}}\frac{3}{T_\mathsf{h}}x_2 + \frac{1}{T_\mathsf{h}}z\right) \\
&\quad - \frac{2K_\mathsf{lm}}{T_\mathsf{lm}}\left(\left(\frac{1}{T_\mathsf{g}}\frac{1}{2K_\mathsf{lm}} + \frac{1}{T_\mathsf{g}}\frac{3T_\mathsf{lm}}{2K_\mathsf{lm}}\frac{1}{T_\mathsf{h}} - \frac{1}{R}\frac{1}{T_\mathsf{g}}\right)x_1 + \frac{1}{2T_\mathsf{g}}\frac{T_\mathsf{lm}}{K_\mathsf{lm}}x_2 - \frac{1}{2T_\mathsf{g}}z + \frac{1}{T_\mathsf{g}}u\right) \\
&= \phi_1 x_1 + \phi_2 x_2 + \psi z + g u,
\end{aligned} \tag{A.3.7b}$$

$$\begin{aligned}
\dot{z} &= \dot{\mathtt{x}}_2 + \frac{3T_\mathsf{lm}}{K_\mathsf{lm}}\frac{1}{T_\mathsf{h}}\dot{\mathtt{x}}_1 \\
&= \left(-\frac{3}{K_\mathsf{lm}}\frac{1}{T_\mathsf{h}} - \frac{3T_\mathsf{lm}}{K_\mathsf{lm}}\frac{1}{T_\mathsf{h}^2}\right)x_1 - \frac{T_\mathsf{lm}}{K_\mathsf{lm}}\frac{3}{T_\mathsf{h}}x_2 + \frac{1}{T_\mathsf{h}}z + \frac{3T_\mathsf{lm}}{K_\mathsf{lm}}\frac{1}{T_\mathsf{h}}x_2 \\
&= \left(-\frac{3}{K_\mathsf{lm}}\frac{1}{T_\mathsf{h}} - \frac{3T_\mathsf{lm}}{K_\mathsf{lm}}\frac{1}{T_\mathsf{h}^2}\right)x_1 + \frac{1}{T_\mathsf{h}}z \\
&= S z + G x_1
\end{aligned} \tag{A.3.7c}$$

where

$$\begin{aligned}
\phi_1 &:= -\frac{3}{T_\mathsf{lm}T_\mathsf{h}} - \frac{3}{T_\mathsf{h}^2} - \frac{2}{T_\mathsf{lm}T_\mathsf{g}} - \frac{3}{T_\mathsf{lm}T_\mathsf{h}} + \frac{1}{R}\frac{2K_\mathsf{lm}}{T_\mathsf{lm}}\frac{1}{T_\mathsf{g}}, \\
\phi_2 &:= -\frac{1}{T_\mathsf{lm}} - \frac{3}{T_\mathsf{h}} - \frac{1}{T_\mathsf{g}}, \\
\psi &:= \frac{K_\mathsf{lm}}{T_\mathsf{lm}}\frac{1}{T_\mathsf{h}} + \frac{K_\mathsf{lm}}{T_\mathsf{lm}}\frac{1}{T_\mathsf{g}}, \\
g &:= -\frac{2K_\mathsf{lm}}{T_\mathsf{lm}}\frac{1}{T_\mathsf{g}}, \quad S := \frac{1}{T_\mathsf{h}}, \quad G := -\frac{3}{K_\mathsf{lm}}\frac{1}{T_\mathsf{h}} - \frac{3T_\mathsf{lm}}{K_\mathsf{lm}}\frac{1}{T_\mathsf{h}^2}.
\end{aligned}$$

BIBLIOGRAPHY

[ÅHS84] K. J. Åström, P. Hagander, and J. Sternby. Zeros of sampled systems. *Automatica*, 20(1):31–38, 1984.

[ALWW16] H. An, J. Liu, C. Wang, and L. Wu. Disturbance observer-based antiwindup control for air-breathing hypersonic vehicles. *IEEE Transactions on Industrial Electronics*, 63(5):3038–3049, 2016.

[Ats10] T. Atsumi. Disturbance suppression beyond nyquist frequency in hard disk drives. *Mechatronics*, 20(1):67–73, 2010.

[BCK95] S. P. Bhattacharyya, H. Chapellat, and L. H. Keel. *Robust Control: The Parametric Approach*. Prentice-Hall, 1995.

[BFN+14] C. M. Belcastro, J. Foster, R. L. Newman, L. Groff, D. A. Crider, and D. H. Klyde. Preliminary analysis of aircraft loss of control accidents: Worst case precursor combinations and temporal sequencing. In *Proceedings of AIAA Guidance, Navigation, and Control Conference*, 2014.

[BHLO06] J. V. Burke, D. Henrion, A. S. Lewis, and M. L. Overton. HIFOO–a MATLAB package for fixed-order controller design and $\mathcal{H}_\infty$ optimization. In *Proceedings of IFAC Symposium on Robust Control Design*, 2006.

[Bro01] R. Brockett. New issue in the mathematics of control. *Mathematics Unlimited-2001 and beyond*, pages 189–220, 2001.

[BS08] J. Back and H. Shim. Adding robustness to nominal output-feedback controllers for uncertain nonlinear systems: A nonlinear version of disturbance observer. *Automatica*, 44(10):2528–2537, 2008.

[BS09] J. Back and H. Shim. An inner-loop controller guaranteeing robust transient performance for uncertain MIMO nonlinear systems. *IEEE Transactions on Automatic Control*, 54(7):1601–1607, 2009.

[BS14] J. Back and H. Shim. Reduced-order implementation of disturbance observers for robust tracking of non-linear systems. *IET Control Theory & Applications*, 8(17):1940–1948, 2014.

[BSP14] D. Bustan, S. K. H. Sani, and N. Pariz. Adaptive fault-tolerant spacecraft attitude control design with transient response control. *IEEE/ASME Transactions on Mechatronics*, 19(4):1404–1411, 2014.

[BT99] R. Bickel and M. Tomizuka. Passivity-based versus disturbance observer based robot control: Equivalence and stability. *Journal of Dynamic Systems, Measurement, and Control*, 121(1):41, 1999.

[BZ03] L. J. Brown and Q. Zhang. Identification of periodic signals with uncertain frequency. *IEEE Transactions on Signal Processing*, 51(6):1538–1545, 2003.

[CBGO00] W-H. Chen, D. J. Ballance, P. J. Gawthrop, and J. O'Reilly. A nonlinear disturbance observer for robotic manipulators. *IEEE Transactions on Industrial Electronics*, 47(4):932–938, 2000.

[CCKH16] J. Choi, H. Choi, K. Kong, and D. J. Hyun. An adaptive disturbance observer for precision control of time-varying systems. In *Proceedings of IFAC Symposium on Mechatronics Systems*, volume 49, pages 240–245, 2016.

[CCY96] Y. Choi, W. K. Chung, and Y. Youm. Disturbance observer in $\mathcal{H}_\infty$ frameworks. In *Proceedings of International Conference on Industrial Electronics, Control, and Instructution*, pages 1394–1400, 1996.

[CH08] C. Cao and N. Hovakimyan. Design and analysis of a novel $\mathcal{L}_1$ adaptive control architecture with guaranteed transient performance. *IEEE Transactions on Automatic Control*, 53(2):586–591, 2008.

[Che04] W-H. Chen. Disturbance observer based control for nonlinear systems. *IEEE/ASME Transactions on Mechatronics*, 9(4):706–710, 2004.

[CLTT17] S-L. Chen, X. Li, C. S. Teo, and K. K. Tan. Composite jerk feedforward and disturbance observer for robust tracking of flexible systems. *Automatica*, 80:253–260, 2017.

[CM15] A. Chakravarty and C. Mahanta. Actuator fault-tolerant control (FTC) design with post-fault transient improvement for application to aircraft control. *International Journal of Robust and Nonlinear Control*, 26(10):2049–2074, 2015.

[CT12] X. Chen and M. Tomizuka. A minimum parameter adaptive approach for rejecting multiple narrow-band disturbances with application to hard disk drives. *IEEE Transactions on Control Systems Technology*, 20(2):408–415, 2012.

[CT14] X. Chen and M. Tomizuka. Optimal decoupled disturbance observers for dual-input single-output systems. *Journal of Dynamic Systems, Measurement, and Control*, 136(5):051018, 2014.

[CYC+03] Y. Choi, K. Yang, W. K. Chung, H. R. Kim, and I. H. Suh. On the robustness and performance of disturbance observers for second-order systems. *IEEE Transactions on Automatic Control*, 48(2):315–320, 2003.

[CYGL15] W-H. Chen, J. Yang, L. Guo, and S. Li. Disturbance-observer-based control and related methods–An overview. *IEEE Transactions on Industrial Electronics*, 63(2):1083–1095, 2015.

[FG12] A. Feuer and G. C. Goodwin. *Sampling in Digital Signal Processing and Control*. Springer, 2012.

[FK08] L. B. Freidovich and H. K. Khalil. Performance recovery of feedback-linearization-based designs. *IEEE Transactions on Automatic Control*, 53(10):2324–2334, 2008.

[FKS13] J. Fiala, M. Kocvara, and M. Stingl. PENLAB-A MATLAB solver for nonlinear semidefinite optimization. 2013.

[Fla83] F. J. Flanigan. *Complex Variables*. Dover Publication, 1983.

[FPW98] G. F. Franklin, J. D. Powell, and M. L. Workman. *Digital Control of Dynamic Systems*. Addison-wesley, 1998.

[FTD14] H. Fawzi, P. Tabuada, and S. Diggavi. Secure estimation and control for cyber-physical systems under adversarial attacks. *IEEE Transactions on Automatic Control*, 59(6):1454–1467, 2014.

[FW76] B. A. Francis and W. M. Wonham. The internal model principle of control theory. *Automatica*, 12(5):457–465, 1976.

[Gao14] Zhiqiang Gao. On the centrality of disturbance rejection in automatic control. *ISA Transactions*, 53(4):850–857, 2014.

[GC05] L. Guo and W-H. Chen. Disturbance attenuation and rejection for systems with nonlinearity via DOBC approach. *International Journal of Robust and Nonlinear Control*, 15(3):109–125, 2005.

[GG01] B. A. Guvenc and L. Guvenc. Robustness of disturbance observers in the presence of structured real parametric uncertainty. In *Proceedings of American Control Conference*, pages 4222–4227, 2001.

[Gor09] S. Gorman. Electricity grid in U.S. penetrated by spies. *Wall Street Journal*, 2009.

[GSJS17] Z. Guo, D. Shi, K. H. Johansson, and L. Shi. Optimal linear cyber-attack on remote state estimation. *IEEE Transactions on Control of Network Systems*, 4(1):4–13, 2017.

[GY11] S. Gayaka and B. Yao. Accommodation of unknown actuator faults using output feedback-based adaptive robust control. *International Journal of Adaptive Control and Signal Processing*, 25(11):965–982, 2011.

[Han09] J. Han. From PID to active disturbance rejection control. *IEEE Transactions on Industrial Electronics*, 56(3):900–906, 2009.

[HMS96] L.R. Hunt, G. Meyer, and R. Su. Noncausal inverses for linear systems. *IEEE Transactions on Automatic Control*, 41(4):608–611, 1996.

[Hop66] F. C. Hoppensteadt. Singular perturbations on the infinite interval. *Transactions of the American Mathematical Society*, 123(2):521–521, feb 1966.

[Hua04] J. Huang. *Nonlinear Output Regulation: Theory and Applications*. Society for Industrial and Applied Mathematics, 2004.

[HYA93] T. Hagiwara, T. Yuasa, and M. Araki. Stability of the limiting zeros of sampled-data systems with zero-and first-order holds. *International Journal of Control*, 58(6):1325–1346, 1993.

[HZ16] A. Hoehn and P. Zhang. Detection of covert attacks and zero dynamics attacks in cyber-physical systems. In *Proceedings of American Control Conference*, pages 302–307, 2016.

[IS96] P. A. Iaonnou and J. Sun. *Robust Adaptive Control*. Prentice-Hall, 1996.

[JD99] Q. Jou and S. Devasia. Preview-based stable-inversion for output tracking. In *Proceedings of American Control Conference*, pages 3544–3548, 1999.

[JF13] T. A. Johansen and T. I. Fossen. Control allocation–A survey. *Automatica*, 49(5):1087–1103, 2013.

[JJS14] N. H. Jo, Y. Joo, and H. Shim. A study of disturbance observers with unknown relative degree of the plant. *Automatica*, 50(6):1730–1734, 2014.

[Joh71] C. Johnson. Accomodation of external disturbances in linear regulator and servomechanism problems. *IEEE Transactions on Automatic Control*, 16(6):635–644, 1971.

[Joh76] C.D. Johnson. Theory of disturbance-accommodating controllers. In *Control and Dynamic Systems*, pages 387–489. Elsevier, 1976.

[Joh08] C. D. Johnson. Real-time disturbance-observers: Origin and evolution of the idea - Part 1: The early years. In *Proceedings of Southeastern Symposium on System Theory*, pages 88–91, 2008.

[JPBS16] Y. Joo, G. Park, J. Back, and H. Shim. Embedding internal model in disturbance observer with robust stability. *IEEE Transactions on Automatatic Control*, 61(10):3128–3133, 2016.

[KBP14] J-S. Kim, J. Back, and G. Park. Design of Q-filters for disturbance observers via BMI approach. In *Proceedings of International Conference on Control, Automation, and Systems*, pages 1197–1200, 2014.

[KC03] B. K. Kim and W. K. Chung. Advanced disturbance observer design for mechanical positioning systems. *IEEE Transactions on Industrial Electronics*, 50(6):1207–1216, 2003.

[Kha96] H. K. Khalil. *Nonlinear Systems*. New Jersey: Prentice-Hall, 3rd edition, 1996.

[Kim05] K-S. Kim. Analysis of optical data storage systems—Tracking performance with eccentricity. *IEEE Transactions on Industrial Electronics*, 52(4):1056–1062, 2005.

[KK99] C. J. Kempf and S. Kobayashi. Disturbance observer and feedforward design for a high-speed direct-drive positioning table. *IEEE Transactions on Control Systems Technology*, 7(5):513–526, 1999.

[KKO99] P. Kokotovic, H. K. Khalil, and J. O'reilly. *Singular perturbation methods in control: Analysis and design*. Society for Industrial and Applied Mathematics, 1999.

[KKO07] H. Kobayashi, S. Katsura, and K. Ohnishi. An analysis of parameter variations of disturbance observer for motion control. *IEEE Transactions on Industrial Electronics*, 54(6):3413–3421, 2007.

[KPSE16] J. Kim, G. Park, H. Shim, and Y. Eun. Zero-stealthy attack for sampled-data control systems: The case of faster actuation than sensing. In *Proceedings of IEEE Conference on Decision and Control*, 2016.

[KPSJ16] H. Kim, G. Park, H. Shim, and N. H. Jo. Arbitrarily large gain/phase margin can be achieved by DOB-based controller. In *Proceedings of International Conference on Control, Automation and Systems*, pages 447–450, 2016.

[KR13] K-S. Kim and K-H. Rew. Reduced order disturbance observer for discrete-time linear systems. *Automatica*, 49(4):968–975, 2013.

[KRK10] K-S. Kim, K-H. Rew, and S. Kim. Disturbance observer for estimating higher order disturbances in time series expansion. *IEEE Transactions on Automatic Control*, 55(8):1905–1911, 2010.

[KSJ14] H. Kim, H. Shim, and N. H. Jo. Adaptive add-on output regulator for rejection of sinusoidal disturbances and application to optical disc drives. *IEEE Transactions on Industrial Electronics*, 61(10):5490–5499, 2014.

[KT13] K. Kong and M. Tomizuka. Nominal model manipulation for enhancement of stability robustness for disturbance observer-based control systems. *Proceedings of International Journal of Control, Automation and Systems*, 11(1):12–20, 2013.

[Kun94] P. Kundur. *Power System Stability and Control*. McGraw-Hill, 1994.

[Kwa93] H. Kwakernaak. Robust control and $\mathcal{H}_\infty$-optimization-Tutorial paper. *Automatica*, 29(2):255–273, 1993.

[LBK15] J. Lee, B. Bagheri, and H-A. Kao. A cyber-physical systems architecture for industry 4.0-based manufacturing systems. *Manufacturing Letters*, 3:18–23, 2015.

[Lee08] E. A. Lee. Cyber physical systems: Design challenges. In *Proceedings of IEEE International Symposium on Object and Component-Oriented Real-Time Distributed Computing*, pages 363–369, 2008.

[LJS12] C. Lee, Y. Joo, and H. Shim. Analysis of discrete-time disturbance observer and a new q-filter design using delay function. In *Proceedings of International Conference on Control, Automation and Systems*, pages 556–561, 2012.

[LLC+17] D-Y. Li, P. Li, W-C. Cai, Y-D. Song, and H-J. Chen. Adaptive fault tolerant control of wind turbines with guaranteed transient performance considering active power control of wind farms. *IEEE Transactions on Industrial Electronics*, 2017. available on-line.

[LMK16] J. Lee, R. Mukherjee, and H. K. Khalil. Output feedback performance recovery in the presence of uncertainties. *Systtem & Control Letters*, 90:31–37, 2016.

[LSE15] C. Lee, H. Shim, and Y. Eun. Secure and robust state estimation under sensor attacks, measurement noises, and process disturbances: Observer-based combinatorial approach. In *Proceedings of European Control Conference*, pages 1872–1877, 2015.

[Lu09] Y-S. Lu. Sliding-mode disturbance observer with switching-gain adaptation and its application to optical disk drives. *IEEE Transactions on Industrial Electronics*, 56(9):3743–3750, 2009.

[LWLW17] C. Liu, J. Wu, C. Long, and Y. Wang. Dynamic state recovery for cyber-physical systems under switching location attacks. *IEEE Transactions on Control of Network Systems*, 4(1):14–22, 2017.

[LY13] S. Li and J. Yang. Robust autopilot design for bank-to-turn missiles using disturbance observers. *IEEE Transactions on Aerospace and Electronic Systems*, 49(1):558–579, 2013.

[LYCC14] S. Li, J. Yang, W. H. Chen, and X. Chen. *Disturbance Observer-based Control: Methods and Applications*. CRC Press, 2014.

[MMT17] A. Mohammadi, H. J. Marquez, and M. Tavakoli. Nonlinear disturbance observers: Design and applications to euler-lagrange systems. *IEEE Control Systems*, 37(4):50–72, 2017.

[MS09] Y. Mo and B. Sinopoli. Secure control against replay attacks. In *Proceedings of Annual Allerton Conference on Communication, Control, and Computing*, pages 911–918, 2009.

[NOM87] M. Nakao, K. Ohnishi, and K. Miyachi. A robust decentralized joint control based on interference estimation. In *Proceedings of IEEE International Conference on Robotics and Automation*, pages 326–331, 1987.

[OC99] Y. Oh and W. K. Chung. Disturbance-observer-based motion control of redundant manipulators using inertially decoupled dynamics. *IEEE/ASME Transactions on Mechatronics*, 4(2):133–146, 1999.

[OMI+06] K. Ohishi, T. Miyazaki, K. Inomata, H. Yanagisawa, D. Koide, and H. Tokumaru. Robust tracking servo system considering force disturbance for the optical disk recording system. *IEEE Transactions on Industrial Electronics*, 53(3):838–847, 2006.

[OSM96] K. Ohnishi, M. Shibata, and T. Murakami. Motion control for advanced mechatronics. *IEEE/ASME Transactions on Mechatronics*, 1(1):56–67, 1996.

[PDB13] F. Pasqualetti, F. Dorfler, and F. Bullo. Attack detection and identification in cyber-physical systems. *IEEE Transactions on Automatic Control*, 58(11):2715–2729, 2013.

[PJLS15] G. Park, Y. Joo, C. Lee, and H. Shim. On robust stability of disturbance observer for sampled-data systems under fast sampling: An almost necessary and sufficient condition. In *Proceedings of IEEE Conference on Decision and Control*, pages 7536–7541, 2015.

[PJSB12] G. Park, Y. Joo, H. Shim, and J. Back. Rejection of polynomial-in-time disturbances via disturbance observer with guaranteed robust stability. In *Proceedings of IEEE Conference on Decision and Control*, pages 949–954, 2012.

[PK17] G. Park and H. Kim. Adaptive rejection to nominal response for uncertain mechanical systems and its application to optical disk drive. *IEEE Transactions on Industrial Electronics*, 2017. available on-line.

[PLS+] G. Park, C. Lee, H. Shim, Y. Eun, and K. H. Johansson. Stealthy adversaries against uncertain cyber-physical systems: Threat of robust zero-dynamics attack. under review, *IEEE Transactions on Automatic Control*.

[PN07] C. L. Phillips and H. T. Nagle. *Digital Control System Analysis and Design*. Prentice-Hall, 2007.

[PS] G. Park and H. Shim. Guaranteeing almost fault-free tracking performance from transient to steady-state: A disturbance observer approach. under review, *Science China Information Sciences*.

[PS15] G. Park and H. Shim. A generalized framework for robust stability analysis of discrete-time disturbance observer for sampled-data systems: A fast sampling approach. In *Proceedings of International Conference on Control, Automation and Systems*, pages 295–300, 2015.

[PSJ] G. Park, H. Shim, and Y. Joo. Recovering nominal tracking performance in asymptotic sense for uncertain linear systems. under review, *SIAM Journal on Control and Optimization*.

[PSL+16] G. Park, H. Shim, C. Lee, Y. Eun, and K. H. Johansson. When adversary encounters uncertain cyber-physical systems: Robust zero-

dynamics attack with disclosure resources. In *Proceedings of IEEE Conference on Decision and Control*, pages 5085–5090, 2016.

[PT14] I. Petersen and R. Tempo. Robust control of uncertain systems: Classical results and recent developments. *Automatica*, 50(5):1315–1335, 2014.

[PVM90] J.A. Profeta, W.G. Vogt, and M.H. Mickle. Disturbance estimation and compensation in linear systems. *IEEE Transactions on Aerospace and Electronic Systems*, 26(2):225–231, 1990.

[RDC04] J. R. Ryoo, T-Y. Doh, and M. J. Chung. Robust disturbance observer for the track-following control system of an optical disk drive. *Control Engineering Practice*, 12(5):577–585, 2004.

[Rid12] T. Rid. Cyber war will not take place. *Journal of Strategic Studies*, 35(1):5–32, 2012.

[Saf12] M. G. Safonov. Origins of robust cotrol: Early history and future speculations. *Annual Review in Control*, 36(2):173–181, 2012.

[SEFL14] Y. Shtessel, C. Edwards, L. Fridman, and A. Levant. *Sliding Mode Control and Observation*. Birkhäuser, 2014.

[SI00] A. Serrani and A. Isidori. Global robust output regulation for a class of nonlinear systems. *Systems & Control Letters*, 39(2):133–139, 2000.

[SJ07] H. Shim and Y. Joo. State space analysis of disturbance observer and a robust stability condition. In *Proceedings of IEEE Conference on Decision and Control*, pages 2193–2198, 2007.

[SJ09] H. Shim and N. H. Jo. An almost necessary and sufficient condition for robust stability of closed-loop systems with disturbance observer. *Automatica*, 45(1):296–299, 2009.

[SNP+17] Y. Shoukry, P. Nuzzo, A. Puggelli, A. L. Sangiovanni-Vincentelli, S. A. Seshia, and P. Tabuada. Secure state estimation for cyber-physical systems under sensor attacks: A satisfiability modulo theory

approach. *IEEE Transactions on Automatic Control*, 62(10):4917–4932, 2017.

[SO12] E. Sariyildiz and K. Ohnishi. Robust stability and performance analysis of the control systems with higher order disturbance observer: Frequency approach. In *Proceedings of International Conference on Human System Interactions*, pages 67–74, 2012.

[SO13a] E. Sariyildiz and K. Ohnishi. Bandwidth constraints of disturbance observer in the presence of real parametric uncertainties. *European Journal of Control*, 19(3):199–205, 2013.

[SO13b] E. Sariyildiz and K. Ohnishi. A guide to design disturbance observer. *Journal of Dynamic Systems, Measurement, and Control*, 136(2):021011, 2013.

[SO15] E. Sariyildiz and K. Ohnishi. Stability and robustness of disturbance-observer-based motion control systems. *IEEE Transactions on Industrial Electronics*, 62(1):414–422, 2015.

[SPJ+16] H. Shim, G. Park, Y. Joo, J. Back, and N. H. Jo. Yet another tutorial of disturbance observer: Robust stabilization and recovery of nominal performance. *Control Theory Technology*, 14(3):237–249, 2016.

[SvD02] E. Schrijver and J. van Dijk. Disturbance observers for rigid mechanical systems: Equivalence, stability, and design. *Journal of Dynamic Systems, Measurement, and Control*, 124(4):539–548, 2002.

[SWY14] J. Su, L. Wang, and J. N. Yun. A design of disturbance observer in standard $\langle$ control framework. *International Journal of Robust and Nonlinear Control*, 25(16):2894–2910, 2014.

[Tan10] W. Tan. Unified tuning of PID load frequency controller for power systems via IMC. *IEEE Transactions on Power Systems*, 25(1):341–350, 2010.

[TCJ02] G. Tao, S. Chen, and S.M. Joshi. An adaptive actuator failure compensation controller using output feedback. *IEEE Transactions on Automatic Control*, 47(3):506–511, 2002.

[TLT00] A. Tesfaye, H. S. Lee, and M. Tomizuka. A sensitivity optimization approach to design of a disturbance observer in digital motion control systems. *IEEE/ASME Transactions on Mechatronics*, 5(1):32–38, 2000.

[TSSJ12] A. Teixeira, I. Shames, H. Sandberg, and K. H. Johansson. Revealing stealthy attacks in control systems. In *Proceedings of Annual Allerton Conference on Communication, Control, and Computing*, pages 1806–1813, 2012.

[TSSJ15a] A. Teixeira, I. Shames, H. Sandberg, and K. H. Johansson. A secure control framework for resource-limited adversaries. *Automatica*, 51:135–148, 2015.

[TSSJ15b] A. Teixeira, K. C. Sou, H. Sandberg, and K. H. Johansson. Secure control systems: A quantitative risk management approach. *IEEE Control Systems*, 35(1):24–45, 2015.

[UH91] T. Umeno and Y. Hori. Robust speed control of DC servomotors using modern two degrees-of-freedom controller design. *IEEE Transactions on Industrial Electronics*, 38(5):363–368, 1991.

[Utk92] V. I. Utkin. *Sliding Modes in Control and Optimization*. Springer-Verlag, 1992.

[WB92] B. Wie and D. S. Bernstein. Benchmark problems for robust control design. *Journal of Guidance, Control, and Dynamics*, 15(5):1057–1059, 1992.

[WT04] C-C. Wang and M. Tomizuka. Design of robustly stable disturbance observers based on closed loop consideration using $\mathcal{H}_\infty$ optimization and its applications to motion control system. In *Proceedings of American Control Conference*, pages 3764–3769, 2004.

[WTS00] M.T. White, M. Tomizuka, and C. Smith. Improved track following in magnetic disk drives using a disturbance observer. *IEEE/ASME Transactions on Mechatronics*, 5(1):3–11, 2000.

[XH15] W. Xue and Y. Huang. Performance analysis of active disturbance rejection tracking control for a class of uncertain LTI systems. *ISA Transactions*, 58:133–154, 2015.

[Xie10] W. Xie. High frequency measurement noise rejection based on disturbance observer. *Journal of the Franklin Institute*, 347(10):1825–1836, 2010.

[YCC03] K. Yang, Y. Choi, and W. K. Chung. Performance analysis of discrete-time disturbance observer for second-order systems. In *Proceedings of IEEE Conference on Decision and Control*, pages 4877–4882, 2003.

[YCC05] K. Yang, Y. Choi, and W.K. Chung. On the tracking performance improvement of optical disk drive servo systems using error-based disturbance observer. *IEEE Transactions on Industrial Electronics*, 52(1):270–279, 2005.

[YCL+17] J. Yang, W-H. Chen, S. Li, L. Guo, and Y. Yan. Disturbance/uncertainty estimation and attenuation techniques in PMSM drives-A survey. *IEEE Transactions on Industrial Electronics*, 64(4):3273–3285, 2017.

[YG14] J. I. Yuz and G. C. Goodwin. *Sampled-data Models for Linear and Nonlinear Systems*. Springer, 2014.

[YJ15] X. Yu and J. Jiang. A survey of fault-tolerant controllers based on safety-related issues. *Annual Reviews in Control*, 39:46–57, 2015.

[YKIH97] K. Yamada, S. Komada, M. Ishida, and T. Hori. Analysis and classical control design of servo system using high order disturbance observer. In *Proceedings of International Conference on Industrial Electronics, Control, and Instrumentation*, pages 4–9, 1997.

[YLC12] J. Yang, S. Li, and W-H. Chen. Nonlinear disturbance observer-based control for multi-input multi-output nonlinear systems subject to mismatching condition. *International Journal of Control*, 85(8):1071–1082, 2012.

[ZD96] K. Zhou and J. C. Doyle. *Robust and Optimal Control*. New Jersey: Prentice-Hall, 1996.

[ZJ08] Y. Zhang and J. Jiang. Bibliographical review on reconfigurable fault-tolerant control systems. *Annual Reviews in Control*, 32(2):229–252, 2008.

국문초록

Theory of Disturbance Observers: A New Perspective on Inverse Model-based Design

외란 관측기 이론 : 역동역학 기반 설계에 대한 새로운 관점

외란 관측기(disturbance observer)는 직관적인 원리를 바탕으로 산업계에서 널리 사용되는 강인 제어 기법들 중 하나이다. 기존 문헌에서 제시된 다양한 설계법들 중, 공칭 시스템(nominal system)의 역동역학(inverse dynamics)를 기반으로 한 접근법은 외란(disturbance) 및 모델 불확실성(model uncertainty)에도 간단히 공칭 모델의 추종 성능을 복원해내는 장점을 지닌다. 하지만 설계의 단순함으로 인해 공칭 성능의 복원은 일반적으로 근사적(approximate)이고, 시스템의 특성(예를 들면 최소위상(minimum phase))에 따라 활용이 제한적이다. 본 논문은 역동역학 기반 외란 관측기 기법의 성능에서의 한계점을 개선하고, 제어 시스템이 처한 다양한 문제들에 대한 외란 관측기의 해석 및 활용 방안을 고찰하며 새로운 설계법을 이론적으로 제시한다.

구체적으로 본 논문에서는 다음의 다섯 가지 주제들을 다룬다. 첫 번째로, 본 논문은 외부 입력들의 생성 모델을 설계에 활용하여, 공칭 성능 복원(nominal performance recovery)을 정상 상태에서 완벽하게 이뤄내는 새로운 외란 관측기 설계 방법을 제시한다. 이에 대한 확장으로, 외부 입력들의 주파수 성분이 정확히 알려져 있지 않은 경우에도 주파수 추정(frequency identification) 알고리듬을 도입하면 공칭 성능의 점근적인(asymptotic) 복원이 이뤄질 수 있음을 이론적으로 밝힌다. 또한 외란 관측기 기법에 제어 분배(control allocation) 법칙을 접목하여, 잉여성(redundancy)이 존재하는 액츄에이터 중 일부가 고장(fault)이 발생할 수 있는 제어 시스템에 대해, 고장 직후에도 원하는 추종 성능을 유지하면서 구동할 수 있도록 하는 새로운 고장 허용 제어(fault tolerant control) 기법을 제안한다. 한편 이산 시간(discrete-time)에서 구현된 외란 관측기가 샘플링 주기가 충분히 빠른 샘플치 제어 시스템(sampled-data control system)에 적용된 상황에서, 모델 불확실성에 강인 안정할 필요 충분 조건을 찾고, 이를 활용한 이산 시간 외란 관측기의 새로운 설계법들을 제안한다. 마지막으로, 큰 대역폭의 Q-필터로 설계된

역동역학 기반 외란 관측기가 필연적으로 비 최소위상 시스템을 불안정하게 만듬에 주목하여, 불확실성이 있는 가상 물리 시스템(cyber-physical system)에 검출 불가능한(stealthy) 악의적인 공격 방법으로 활용 가능함을 이론적으로 밝힌다.

주요어: 외란 관측기, 공칭 성능 복원, 샘플치 제어 시스템, 강인 제어, 가상 물리 시스템

학 번: 2013–30235